

Mechanisms of developmental neuronal remodeling in dorsal root ganglia sensory neurons

by

Andrés de León
Integrated Program in Neuroscience
McGill University, Montreal

August 2020

A thesis submitted to McGill University in partial fulfillment
of the requirements of the degree of Doctor of Philosophy in Neuroscience

Table of Contents

Abstract	<i>i</i>
Résumé	<i>iii</i>
Acknowledgements	<i>v</i>
Contributions of Authors	<i>vi</i>
Abbreviations	<i>vii</i>
Chapter 1. Introductory literature review	13
1.1 The neurotrophin family and their receptors	13
1.1.1 Trk receptor signaling.....	13
1.1.2 p75NTR receptor signaling.....	17
1.2 Dorsal root ganglia sensory neurons	20
1.2.1 Development of sensory neurons and the role of neurotrophins.....	22
1.3 The diversity of neuronal cell death mechanisms	31
1.3.1 Classification of neuronal cell death.....	31
1.3.2 The apoptotic pathway.....	32
1.3.3 Necrotic pathways.....	35
1.3.4 Autophagy-mediated cell death.....	37
1.3.5 Calcium in neuronal cell death.....	38
1.3.6 Phosphatidylserine engulfment signal.....	42
1.4 Mechanisms of PCD in NGF-dependent embryonic DRG sensory neurons	43
1.5 The amyloid-precursor protein	52
1.5.1 The APP family.....	52
1.5.2 APP structure.....	53
1.5.3 Proteolytic processing of APP.....	54
1.5.4 APP trafficking and transportation.....	56
1.5.5 Biological functions of the APP family during neuronal development.....	57
1.6 Developmental cell death of BDNF-dependent DRG neurons	70
1.6.1 Supporting developmental survival of DRG neurons by BDNF.....	70
1.6.2 Dying in the absence of BDNF: from DRG neurons and beyond.....	74
1.7 Developmental axonal pruning and its modelling <i>in vitro</i>	78
1.7.1 Types of neurite pruning.....	78
1.7.2 <i>In vitro</i> models to mimic axonal pruning.....	83
1.7.3 Mechanisms of axonal pruning in DRG - and SCG - neurons.....	84
1.8 Aim of this thesis	93
Chapter 2. The role of the amyloid-precursor protein in the developmental remodeling of NGF-dependent DRG sensory neurons	94
2.1 Abstract	94
2.2 Introduction	96

2.3 Materials and methods	98
2.4 Results	105
2.5 Discussion	109
2.6 Figures and figure legends	114
Figure 2.1. APP and DR6 genetic deficiency protects DRG sensory neurons from degeneration induced by NGF deprivation.....	114
Figure 2.2. Hypertrophy phenotype in adult APP-null mice PNS	116
Figure 2.3. NGF-deprivation induces an early increase in full-length APP protein levels and of its phosphorylation state at threonine 668	118
Figure 2.4. Trk receptor inhibition protects axons from NGF deprivation and reduces levels of phosphorylated APP at threonine 668.....	120
Figure 2.5. PLC γ and PKC inhibitors protect axons from NGF deprivation, reduce the rise of axoplasmic Ca ²⁺ during degeneration and abolish the rise of APP phosphorylation at threonine 668 upon NGF withdrawal	122
Figure 2.6. APP genetic deficiency reduce axoplasmic Ca ²⁺ rise upon NGF deprivation and attenuates ER Ca ²⁺ content and SOCE in DRG neurons.....	125
Figure 2.7. DRG sensory neurons lacking APP have reduced functional mitochondria and increased TOM20 levels but do not have defects in caspase-3 activation upon NGF deprivation.....	127
Connecting text: Chapter 2 to 3	129
Chapter 3. NGF- and BDNF-dependent DRG sensory neurons deploy distinct degenerative signaling mechanisms	130
3.1 Abstract	130
3.2 Introduction	132
3.3 Materials and Methods	134
3.4 Results	138
3.5 Discussion	141
3.6 Figures and figure legends	146
Figure 3.1. Comparative growth of NGF- and BDNF-dependent DRG sensory neurons and their degeneration induced by trophic factor withdrawal.....	146
Figure 3.2. Axon growth of BDNF-dependent DRGs from the cervical, the thoracic or the lumbar region of the spinal cord with several concentration of BDNF	148
Figure 3.3. DRG sensory neurons undergoing BDNF deprivation display increased extracellular phosphatidylserine and increased axoplasmic Ca ²⁺	150
Figure 3.4. Trk receptor inhibition protects axons from NGF deprivation but not from BDNF-deprivation whereas p75NTR deficiency confers no protection to axons established in NGF or BDNF	152

Figure 3.5. PKC inhibitor Gö6976 and EGTA rescue degeneration induced by NGF deprivation but not BDNF deprivation	154
Figure 3.6. Translation, autophagy, necroptosis or Wallerian-like degeneration are not involved in BDNF deprivation-induced degeneration	156
Figure 3.7. NGF and BDNF deprivation-induced degeneration require BAX	160
Figure 3.8. pan-Caspase inhibition does not block degeneration induced by BDNF deprivation	162
Figure 3.9. Cleaved form of executioner caspase-3 does not increase during BDNF deprivation	164
Figure 3.10. Reactive oxygen species are required for axon degeneration induced by BDNF deprivation	166
Connecting text: Chapter 3 to 4	168
Chapter 4. Modelling developmental axonal pruning in vitro using compartmentalized microfluidic chambers	169
4.1 Abstract	169
4.2 Introduction	171
4.3 Materials and methods	173
4.4 Results	175
4.5 Discussion	179
4.6 Figures and figure legends	182
Figure 4.1. Establishment of dissociated DRG cultures in microfluidic devices	182
Figure 4.2. Serial Calcein-AM staining and imaging enable tracking of cellular changes induced by an axonal pruning protocol without altering the integrity of the cell culture	184
Figure 4.3. Progression of axonal pruning versus cell death in young DRG neurons maintained in microfluidic devices	186
Figure 4.4. Distal NGF deprivation in young DRG neurons induces a significant drop in the number of DRG cell bodies that is not observed in mature DRG neurons undergoing axonal pruning	188
Figure 4.5. Young DRG neurons only experience a minor loss of cell bodies if no distal NGF deprivation is applied during their culture in microfluidic devices	190
Figure 4.6. Graphic summary: the compartmentalization of NGF deprivation in axons of immature DRG neurons mimics a combination of developmental axonal pruning and cell death	192
Chapter 5. General Discussion	194
5.1 Study I: The role of APP in developmental remodelling of DRG sensory neurons	194
5.2 Study II: NGF- and BDNF-dependent DRG sensory neurons deploy distinct degenerative signaling mechanisms	200

5.3 Study III: Modelling developmental axonal pruning <i>in vitro</i> using compartmentalized microfluidic devices.....	205
5.4 Concluding remarks	209
5.5 Major original contributions.....	209
<i>References</i>	211

Abstract

Developmental neuronal cell death and axonal pruning are essential remodeling processes for the proper maturation and function of the nervous system. Dysregulation of developmental neuronal remodeling is associated with neuropsychiatric conditions such as autism and schizophrenia. Reactivation of similar degenerative mechanisms is suspected to contribute to the onset of neurodegenerative diseases. Understanding the mechanisms of degeneration during developmental neuronal remodeling could open new therapeutic strategies for the treatment of pathological neurodegeneration. Because of its accessibility, clear anatomical organization and the possibility to establish simple *in vitro* culture models, the sensory nervous system constitutes a convenient system for the study of developmental neuronal remodeling. This thesis explores different aspects of developmental neuronal remodeling in dorsal root ganglia (DRG) sensory neurons. Our first study, presented in Chapter 2, investigates the role of the amyloid-precursor protein (APP) in the developmental degeneration of NGF-dependent DRG neurons. Our results indicate that APP genetic deletion delays axonal degeneration and reduces the catastrophic axoplasmic Ca^{2+} rise triggered by NGF deprivation *in vitro*. We also observe an increase in the number of sciatic nerve axons in APP-null adult mice *in vivo*. We found evidence that APP regulates the amount of Ca^{2+} in the endoplasmic reticulum (ER), the store-operated Ca^{2+} entry (SOCE), and the mitochondrial membrane potential in DRG neurons. Interestingly, we observed that NGF deprivation triggers a transient increase in phosphorylated APP at threonine 668, a hallmark of APP pro-degenerative roles in other cellular models, and that the induction of this post-translational modification is modulated by TrkA receptor signaling through the phospholipase C gamma (PLC γ) and protein kinase C (PKC). Taken together, our findings support the hypothesis that APP plays a pro-degenerative role in developmental degeneration of DRG sensory neurons. Our second study presented in Chapter 3 investigates the mechanisms of developmental neuronal remodeling in a population of DRG neurons dependent on BDNF. Our results indicate differences and similarities between the molecular signaling pathways behind NGF and BDNF deprivation-induced degeneration. For instance, we observed that inhibitors of Trk receptors, PKC, protein translation or caspases protect DRG from NGF

deprivation but do not protect DRG from BDNF deprivation. Interestingly, degeneration of BDNF-dependent sensory neurons requires BAX and appears to rely on reactive oxygen species generation rather than caspases to induce degeneration. These results highlight the complexity and divergence of mechanisms regulating developmental sensory neuron death. Our last study presented in Chapter 4 explores if local deprivation of trophic support using microfluidic chamber is a suitable model to study the mechanisms of developmental axonal pruning in embryonic DRG neurons. Using microfluidic devices to establish compartmentalized cultures of DRG neurons, we followed the variations of the number of DRG soma and axons over the course of several trophic support protocols: 1) Global NGF supply, 2) Global NGF deprivation or 3) Local NGF deprivation in distal axons. Our results showed that NGF deprivation in distal axons induces a sharp drop in embryonic DRG cell bodies that is not seen in mature neurons or in embryonic neurons not deprived of NGF. Thus, local NGF deprivation in distal axons from developing neurons may not be mimicking just pruning but a mix of cell death and axonal pruning. These results suggest reconsidering whether the use of embryonic DRG neurons in compartmentalized chambers is a reliable way to model axonal pruning *in vitro*.

Résumé

Les processus de mort neuronale durant le développement embryonnaire ainsi que le raffinement des axones sont essentiels à la formation d'un système nerveux mature et fonctionnel. Des dérégulations de ces processus sont associées avec certaines conditions neuropsychiatriques telles que l'autisme et la schizophrénie. La réactivation de ces processus est aussi proposée comme origine de maladies neurodégénératives. Une meilleure compréhension des mécanismes de dégénération et de raffinement des neurones pendant le développement embryonnaire pourrait nous permettre de découvrir de nouveaux traitements contre ces neuropathologies. Le système nerveux sensoriel constitue un modèle de choix pour l'étude de ces mécanismes. En effet, il est simple à disséquer, son organisation est documentée et il est facile à maintenir en culture cellulaire. Cette thèse explore plusieurs aspects du raffinement neuronal en utilisant les neurones sensoriels des ganglions de la racine dorsale (DRG).

Notre première étude questionne le rôle de la protéine précurseur de l'amyloïde (APP) dans la dégénération développementale en utilisant les DRG dépendant au facteur de croissance nerveuse (NGF). Nos résultats montrent que l'ablation génétique de l'APP retarde la dégénérescence axonale et réduit l'augmentation du calcium dans les axones en réponse à une privation du NGF. *In vivo*, nous avons observé une augmentation du nombre d'axones dans le nerf sciatique chez les souris n'exprimant plus APP. Nos résultats montrent que l'APP régule la quantité de calcium dans le réticulum endoplasmique, l'entrée de calcium régulée par les stocks de calcium et le potentiel de membrane mitochondrial dans les neurones. De plus, nous avons observé que la privation de NGF induit une augmentation transitoire de la phosphorylation de l'APP sur l'acide aminé thréonine 668 (T668). T668 est reconnu pour être un marqueur du rôle pro-dégénératif de l'APP. Nos résultats supportent l'hypothèse que l'APP joue un rôle pro-dégénératif dans le développement des neurones ganglionnaires de la racine dorsale.

Notre seconde étude questionne les mécanismes de raffinement neuronal dans une population de DRG sensible au facteur neurotrophique dérivé du cerveau (BDNF). Nos résultats indiquent des différences et des similitudes avec les mécanismes de dégénération observés dans le modèle de privation du NGF. Par exemple, nous avons

observé que les inhibiteurs des récepteurs Trk, PKC, ou des caspases protègent les DRG de la privation de NGF mais pas de la privation de BDNF. La dégénération des neurones sensibles au BDNF requière la protéine BAX et implique les espèces réactives de l'oxygène. Ces nouveaux résultats démontrent la complexité des mécanismes qui régulent la mort cellulaire neuronale pendant le développement embryonnaire.

Notre dernière étude explore si la privation locale de support trophique en utilisant les chambres micro fluidiques comme mode de culture est un modèle adéquate pour l'étude des mécanismes de raffinement des axones chez les neurones sensoriels au stade embryonnaire. Nous avons suivi le nombre de corps cellulaires et la quantité d'axones des neurones ganglionnaires maintenus en culture dans des chambres micro fluidiques selon trois protocoles: 1) Du NGF était présent dans chaque compartiment, 2) une privation globale du NGF et 3) une privation locale du NGF. Nos résultats montrent que la privation de NGF au niveau des axones distaux chez les neurones embryonnaires provoque une forte diminution du nombre de corps cellulaires. Cet effet n'est pas observé chez les neurones matures ou chez les neurones embryonnaires maintenus avec du NGF. Il apparait donc que la privation locale du NGF en utilisant des neurones ganglionnaires embryonnaires ne reflète pas seulement le mécanisme de raffinement axonal mais plutôt un mélange entre mort cellulaire et raffinement axonal. Ces résultats suggèrent une reconsidération des modèles employés pour l'étude des mécanismes de raffinement.

Acknowledgements

I would first like to thank my mentor, Dr. Philip Barker, for accepting me as a student into his laboratory and providing me with an excellent training environment and the right combination of guidance and freedom to develop and enhance my strengths and limit my weakness during the course of this endeavour. Thanks for your generosity, teachings, patience and for checking that we were doing well in and out of science.

I want to thank to the members of my advisory committee for guiding me over the years: Dr. Lisa Münter, Dr. Alyson Fournier and Dr. Peter McPherson. They provided me invaluable advice as my project evolved.

To Dr. Nicolas Unsain and his family for their warm welcoming to the great city of Montreal, his guidance and teachings in the laboratory and for buffering the transition from South to North America.

To Dr. Julien Gibon who guided me with great predisposition, positive attitude and a sense of practicality to make my projects reach a good end.

To past and present Research technicians Dr. Genevieve Dorval, Mrs. Kathleen Dickson and M.Sc. Svetlana Simtchouk for their advice, help and tireless work keeping the laboratory gears oiled and in perfect order.

To my lab colleagues, especially Dr. Shannon Buckley, Dr. Aaron Johnstone, and Mr. Mark Cumming, for their teachings and significant impact on my project and everyday life.

I also want to thank all those who from academic and administrative positions work for making the Integrated Program in Neuroscience (IPN) possible. It is an honour for me to have been part of the IPN, the Montreal Neurological Institute and McGill University; Institutions of great history, present and future.

To the University of British Columbia - Okanagan Campus, for opening its doors so welcoming and efficient during my final years of study as a McGill exchange student. It was a pleasure to have been part of your community.

To Canada and its people for their warm welcome. To Christine, Susana and Nnedak.

I want to thank my family and friends for their overwhelming support and understanding.

To the Uruguayan scientific community, Fulbright Uruguay and Dr. Marcela Vilariño for their help and support to get here.

To Dr. Pablo Díaz-Amarilla: an example of hard work, innovative thinking and humility for those of us who had the privilege of working alongside him.

To π

Contributions of Authors

Chapter 2. The role of the amyloid-precursor protein in the developmental remodelling of NGF-dependent DRG sensory neurons.

Andrés de León planned and performed experiments, data analyses and wrote the text. Dr. Aaron Johnstone contributed to Figure 2.2. Dr. Julien Gibon contributed to essential discussion and edits to text, and Dr. Philip Barker directed experiments and edited the text.

Chapter 3. The mechanisms of developmental cell death in BDNF-dependent DRG sensory neurons.

Andrés de León planned and performed experiments, data analyses and wrote the text. Dr. Julien Gibon wrote the results section 3.4, contributed to essential discussion and edits to text, and Dr. Philip Barker directed experiments and edited the text.

Chapter 4. Modelling developmental axonal pruning *in vitro* using compartmentalized microfluidic chambers.

Andrés de León planned and performed experiments and wrote the text. Dr. Julien Gibon contributed to essential discussion and edits to text, and Dr. Philip Barker directed experiments and edited the text.

Abbreviations

$\Delta\Psi_m$	Mitochondrial membrane potential
A β	Amyloid-beta peptide
ACD	Autophagic cell death
AD	Alzheimer disease
AICD	APP intracellular C-terminal domain
AIF	Apoptosis inducing factor
Akt	Protein Kinase B
AMPK	Activation of AMP-protein kinase
Apaf-1	Apoptotic peptidase activating factor 1
APLP	APP-like protein
APP	Amyloid-precursor protein
ASK1	Apoptosis-signaling-kinase 1
ATF4	Activating transcription factor 4
BACE	β -secretase APP cleaving enzyme
BAX	Bcl-2-associated X protein
BDNF	Brain-derived trophic factor
CaM	Calmodulin-regulated protein kinase
Caspase	Cysteine-dependent aspartate-directed protease
CHOP	C/EBP homologous protein
CNS	Central nervous system
CGRP	Calcitonin gene-related peptide
CNTF	Ciliary neurotrophic factor
CPZ	Capsazepine
CREB	cAMP response element-binding protein
DAG	Diacylglycerol
DMSO	dimethylsulphoxide
DLK	Dual leucine-zipper kinase
DR6	Death receptor 6
DRG	Dorsal root ganglia
EDTA	Ethylenediaminetetraacetic acid
EGTA	Ethylene glycol-bis(β -aminoethyl ether)-N,N,N',N'-tetraacetic acid
eIF2 α	eukaryotic initiation factor 2 alpha
ER	Endoplasmic reticulum
FMRP	Fragile-X mental retardation protein
FoxO	Forkhead transcription factor
GAPs	Guanosine triphosphatease activation proteins
GEF	Guanine nucleotide exchange factors
GSK3	Glycogen synthase kinase 3
HBSS	Hank's balanced salt solution
IRES	internal ribosomal entry site
ISR	Integrated stress response
IP ₃ R	1,4,5-inositol triphosphate receptor
JNK	c-Jun kinase
LTP	Long-term potentiation
OMM	Outer mitochondrial membrane
MAPK	Mitogen-activated protein kinase
MB	Mushroom body

MMG	Mammary gland
MOMP	Mitochondrial outer membrane permeabilization
mPTP	Mitochondrial permeabilization transition pore
mTOR	Mammalian target of rapamycin
MSK1	Mitogen- and stress-activated protein kinase 1
NAC	N-acetylcysteine
NCC	Neural crest cells
NGF	Nerve growth factor
NMJ	Neuromuscular junction
NT	Neurotrophin
NT3	Neurotrophin 3
NT4	Neurotrophin 4
p75NTR	p75 neurotrophin receptor
PCD	Programmed cell death
PDMS	poly(dimethylsiloxane)
PERK	Protein kinase RNA-like ER kinase
PFA	Paraformaldehyde
PI3K	Phosphoinositide 3-kinase
PIP2	Phosphatidylinositol 4,5-bisphosphate
PKC	Protein kinase C
PLC	Phospholipase C
PMCA	Plasma membrane calcium ATPase
PNS	Peripheral nervous system
PS	Phosphatidylserine
PSN	Primary sensory neurons
PUMA	p53-upregulated modulator of apoptosis
RCD	Regulated cell death
RGC	Retinal ganglion cell
ROCCs	Receptor-operated calcium channels
ROS	Reactive oxygen species
RyR	Ryanodine receptors
SCG	Sympathetic cervical ganglia
SERCA	Sarco-endoplasmic calcium ATPase
SOCCs	Store-operated calcium channels
SOCE	Store-operated calcium entry
SVZ	Subventricular zone
TMRE	Tetramethylrhodamine, ethyl ester
TNFR	Tumor necrosis factor receptor
TOM	Translocase of the outer mitochondrial membrane
TRPC	Transient receptor potential channel
TRPV	Transient receptor potential vanilloid
Trk	Tropomyosin-kinase receptor
UPR	Unfolded protein response
VOCCs	Voltage-operated calcium channels
WD	Wallerian degeneration

Chapter 1

Introductory literature review

1.1 The neurotrophin family and their receptors

The neurotrophins (NTs) are structurally homologous secreted growth factors highly conserved across species. The NT family consist of four members in mammals: nerve growth factor (NGF), brain-derived growth factor (BDNF), neurotrophin-3 (NT3), and neurotrophin-4 (NT4). Functionally active NTs are noncovalent homodimers that originate as the cleavage product of immature - but active - pro-neurotrophins (proNTs). NTs and proNTs play important roles in many physiological events in the nervous system, including neuronal survival and death, neurite growth, axonal degeneration and synaptic plasticity [1, 2]. NTs functions will be discussed based on their relevance in the context of developmental neuronal remodelling.

NTs interact and exert their functions through four receptors: the low-affinity neurotrophin receptor p75 (p75NTR) and the family of high-affinity tropomyosin-kinase receptors (Trk) A, B and C. All four NTs, mature and immature, can bind and activate p75NTR, whereas only mature NTs selectively bind the Trk receptors [3]: NGF preferentially binds and activates TrkA, BDNF and NT4 preferentially bind and activate TrkB, and NT3 binds most specifically to TrkC, although it can also activate - with less efficiency and non-functional equivalency - TrkA and TrkB [4, 5]. Each of these receptors can function independently, but their co-expression in neurons substantially increases the complexity of their functions, altering the signaling properties of each other. The functional interaction between p75NTR and Trk receptors, increasing the ligand affinity and selectivity of the later, is well established [6, 7] but the mechanism for this effect is still debated.

1.1.1 Trk receptor signaling

Trk receptor family members are single-pass type I transmembrane glycoproteins with a ligand-binding extracellular domain, a transmembrane region and an intracellular tyrosine kinase domain. The binding of NTs to Trk receptors results in receptor homodimerization and subsequent transphosphorylation of tyrosine residues in the intracellular region. Phosphorylated tyrosine residues act as docking sites for a number of adaptor proteins that link downstream signaling to Trk receptor activation [8]. Differential splicing of the Trk receptor gene can also generate a truncated form of the receptor. Devoid of an intracellular tyrosine kinase domain, truncated isoforms were initially viewed as simple dominant negative receptors. Recent studies have challenged that view [9] (see below).

Among the signaling pathways activated by Trk receptors in response to NTs, the Shc-Ras-MAPK, MEK-ERK, PI3K-Akt and PLC γ -protein kinase C (PKC) pathways are most studied [10]. These pathways have been investigated preferentially in the context of NGF-TrkA signaling-mediated cell survival and differentiation, neurite growth and arborization, synapse formation and synaptic plasticity. Although a high degree of overlap is accepted with TrkB and TrkC, isoform-specific differences [11]. Ligand-independent signaling of Trk receptors is also an important part of their possible mechanism of action [12]. For its relevance in the field of developmental neuronal remodelling this aspect will be discussed more in detail later in this thesis (see section 1.4).

The small GTPase-binding protein Ras is a major target downstream of Trk receptor activation [13]. Numerous studies have demonstrated the importance of Ras activation for neuronal differentiation, survival and neurite outgrowth [14-16]. Ras proteins cycle between active GTP-bound and inactive GDP-bound states, the biological activity of these GTPases is controlled by guanine nucleotide exchange factors (GEFs) and guanosine triphosphatase activating proteins (GAPs). Upon neurotrophin stimulation of Trk receptors, tyrosine transphosphorylation at the intracellular domain recruits the adaptor proteins Shc and Gbr2 to activate GEFs, which then activate Ras. However, certain differences may exist between TrkA and TrkB. Although Ras stimulation by GTP binding is mediated by all neurotrophins, active Ras-GTP is lost in neurons exposed to BDNF for long periods of time. This neuronal desensitization to long-term BDNF treatments is not observed with NGF, nor when TrkB is expressed in non-neuronal cells.

It was suggested to be caused by a drastic loss in TrkB binding capacity [17] or by the proteasomal-dependent degradation of TrkB [18, 19]. However, proteasomal-dependent desensitization mechanisms have been reported only for TrkA but not for TrkB or TrkC. Upon NGF binding to TrkA, Nedd4-2, an E3 ubiquitin ligase, becomes phosphorylated and ubiquitinates the intracellular domain of TrkA, which leads to its turnover. Interestingly, this phenomenon does not occur when BDNF binds to TrkB, due to a lack of the consensus sequence P⁷⁸²PVY⁷⁸⁵ that is present only in the intracellular domain of TrkA. Nedd4-2 overexpression induces apoptosis of NGF-dependent DRG neurons but not in BDNF-dependent DRG neurons [11]. Sensory neurons within a knock-in mouse that expresses mutant TrkA with a single change in P782 have impaired TrkA ubiquitination upon NGF exposure and display increased number of sensory neurons [20].

Upon NT binding to Trk receptors, Ras activates the Raf mitogen activated protein kinase (MAPK). Subsequently, Raf phosphorylates MEK, which in turn phosphorylate and activate ERK (also known as the MEK-ERK pathway) [21]. Ultimately, ERK signaling leads the activation of several downstream targets that mediate gene transcription, such as Rsk and MSK1. These two kinases can phosphorylate and activate the cyclic adenosine monophosphate response element-binding protein (CREB). CREB controls the expression of genes essential for survival and differentiation of neurons, local axonal growth, memory and learning, and axon regeneration after injury [22, 23]. The regulation of BDNF expression by CREB suggests that a positive feedback loop may potentiate neurotrophin actions [24].

The PI3K-Akt pathway is one of the major signaling cascades downstream Trk receptors, regulating a wide variety of neuronal functions. Studies using both genetic and pharmacologically inhibitory approaches highlighted the crucial role of PI3K as a major survival protein in cultured neurons [16, 25-27]. PI3K could be activated by Ras upon neurotrophin stimulation [28] or it can be directly activated through the adaptor protein Gab-1 following tyrosine autophosphorylation of Trk receptor intracellular domain [29]. PI3K activation induces Akt translocation to the plasma membrane where it becomes active. Akt activity promotes neuronal survival by several mechanisms: 1) Akt inhibits the forkhead transcription factor (FKHRL1 or FoxO), which regulates expression of pro-

apoptotic genes [30], 2) Akt phosphorylates and inhibits the pro-apoptotic protein Bad [31] and 3) Akt phosphorylates and promotes the degradation of I κ B, an inhibitor of the NF κ B pro-survival pathway [32, 33]. Additionally, activation of Akt results in an increased protein translation via the mammalian target of rapamycin (mTOR)-p70S6 kinase and 4E-BP1 pathways and in an enhanced axonal growth through phosphorylation and inactivation of GSK-3 β leading to microtubule assembly [34-36].

Phosphorylation of Trk receptors also leads to recruitment and activation of PLC γ 1 which catalyze the hydrolysis of phosphatidylinositol (4, 5) biphosphate (PIP2) into diacylglycerol (DAG) and inositol tris-phosphate (IP $_3$). IP $_3$ induces intracellular Ca $^{2+}$ mobilization from the endoplasmic reticulum (ER) to the cytosol through the IP $_3$ receptor (IP $_3$ R), which in turn facilitates the activation of Ca $^{2+}$ -dependent enzymes such as Ca $^{2+}$ -calmodulin-regulated protein kinases (CaM kinases) and the phosphatase calcineurin. Additionally, the release of Ca $^{2+}$ into the cytosol and the production of DAG activate protein kinase C (PKC), which subsequently activates ERK signaling via Raf, the Ca $^{2+}$ channels TRPV1 [37], and the transient receptor potential channel (TRPC), which contributes to the BDNF-induced rise of Ca $^{2+}$ at growth cones and synapses [38]. Other activities affected by PLC γ include the formation of TrkB-postsynaptic density 95 (PSD95) complexes at synapses and CREB-dependent transcription. PLC γ signaling in response to both NGF and BDNF has been implicated in chemoattraction of axonal growth cones, and PLC γ prolonged activation in response to an NGF pulse induces the transcription of the peripheral nerve type 1 (PN1) sodium channel [39]. PLC γ may also be essential in mediating TrkB signaling induced long-term potentiation in the hippocampus [40] and structural plasticity in sensory neurons in response to BDNF [41].

In contrast to direct activation by NTs, Trk receptors can be transactivated intracellularly using alternative neurotrophin-independent pathways via G-protein coupled receptor signaling. Trk receptor transactivation is a relatively slow process in comparison with NT-direct activation. However, the increase in Trk activity as a result of the transactivation can be inhibited with the Trk receptor inhibitor K252a. Transactivated Trk receptors leads to the activation of PI3K-Akt pathway which results in increased cell survival after NGF or BDNF withdrawal in PC12 cells and hippocampal neurons respectively [42, 43].

1.1.2 p75NTR receptor signaling

Unlike Trk receptors, p75NTR binds all NTs with approximately the same affinity [44, 45]. p75NTR was the first neurotrophin receptor to be identified and is the founding member of the TNF family of receptors. As such, p75NTR is a single transmembrane protein containing an extracellular cysteine-rich domain and a cytoplasmic death domain, but unlike other TNF receptors, it does not require trimerization for proper signaling. p75NTR participates in diverse signaling pathways including cell survival and apoptosis, neurite outgrowth induction, growth cone collapse, differentiation and proliferation [46]. Such diversity is rooted in the promiscuity of the receptor; p75NTR is capable of interacting with several intracellular adaptor proteins and transmembrane receptors that drive the downstream signaling in the absence of its own catalytic activity. As mentioned above, p75NTR functional interaction with Trk receptors - augmenting Trk-mediated survival by increasing its binding affinity for NTs - is perhaps the quintessential example of its co-participation with other transmembrane receptors [6, 7]. Given that NTs are typically present in limiting amounts, the co-expression of p75NTR becomes essential in the context of developmental neuronal competition proposed by the neurotrophic factor hypothesis (see below). In addition, p75NTR form a high affinity complex with the VPS10-domain protein sortilin to mediate proNTs actions [47-49]. p75NTR also participates as a signal transmitting subunit of the Nogo complex (NogoR, Lingo, p75NTR) to mediate inhibitory effects on axon growth of myelin-associated glycoproteins (MAG; oligodendrocyte myelin glycoprotein, OMgp; and Nogo-66) [50-52].

p75NTR solo-signaling - without co-receptors - is also diverse and antagonistic. Upon NTs binding, p75NTR promotes the activation of the NF- κ B pro-survival pathway [53, 54]. Such action requires several adaptor proteins including TRAF6, p62, interleukin-1 receptor-associated kinase (IRAK) and receptor interacting protein-2 (RIP2) [55-58]. p75NTR activation of the NF- κ B pro-survival pathways could work in synergy with Trk receptor-mediated survival [59]. Notably, only NGF, but not BDNF or NT3, is able to trigger NF- κ B activation through p75NTR in Schwann cells [60]. Nevertheless, no difference between NGF and BDNF has been found in the capacity of p75NTR to activate

the pro-survival pathway Akt in PC12 and cerebellar granule neurons respectively [61]. The phosphorylation of Akt by p75NTR can take place in the presence or absence of Trk receptors activation [62-64] and requires the cleavage of p75NTR and the release of its intracellular domain [61]. Axon growth can also be modulated by the single action of p75NTR. This effect is obtained by the direct regulation of the small GTPase RhoA, a member of the RhoA family of protein that control the organization of the actin cytoskeleton in many cells. p75NTR activates RhoA through a direct interaction, thereby inhibiting neurite outgrowth. NT binding to p75NTR eliminates p75NTR-dependent activation of RhoA, stimulating neurite outgrowth [65].

Perhaps, the most investigated function of p75NTR is its ability to induced cell death in response to ligand binding. This has been observed in a wide variety of neuronal and non-neuronal cells including sympathetic cervical ganglia (SCG) neurons, hippocampal neurons, motoneurons and Schwann cells [56, 66-68]. In the context of neuronal development, the best studied example is sympathetic neurons of the superior cervical ganglia. Sympathetic neurons express TrkA and p75NTR, which together mediates survival in response to NGF. However, the selective activation of p75NTR by BDNF secreted by “winning” neurons - those able to sequester more NGF - induce apoptosis of neighboring neurons receiving insufficient NGF signal [66, 69]. Several studies have shown that the mechanisms behind p75NTR-mediated cell death require the stimulation of the stress kinase c-Jun N-terminal kinase (JNK) [46]. JNK activation causes cell death by inducing phosphorylation of the transcription factor c-Jun and the tumor suppressors p53 and p73 [70], resulting in transcriptional upregulation of an array of pro-apoptotic genes, including BAX, BAK, PUMA and caspase-6, or by the direct phosphorylation and inhibition of several pro-survival members of the Bcl-2 family proteins [71-76]. The activation and inhibition of these players inexorably leads to a mitochondrial-driven cell death [75, 77, 78]. The cleavage of p75NTR intracellular domain [79, 80] and its association with different adaptor proteins contribute to JNK activation. These include the family of TNF receptor-associated factors (TRAFs, 1 to 6) [57, 81], the neurotrophin receptor-interacting factor (NRIF) [82, 83] and the neurotrophin receptor-interacting MAGE homolog, NRAGE [77]. Synergistically, the increase in ceramide levels prompt by p75NTR-dependent activation of acidic sphingomyelinase in response to NTs have

shown to stimulate JNK phosphorylation and activation. However, increasing ceramide levels does not always result in cell death. In fact, p75NTR-mediated ceramide production has also been linked to promotion of cell survival [84, 85], probably because ceramide simultaneously control pro-survival pathways including ERK, NF- κ B as well as the activity of TrkA through phosphorylation of this receptor on serine residues [86]. Conversely, Trk receptors act at several steps to suppress JNK activation by p75NTR but do not suppress NF- κ B-mediated signaling by p75NTR [59]. Thus, ceramide contribution, but overall, p75NTR-signaling outcome is greatly dependent on the expression of Trk receptors in the presence of NTs. In sympathetic neurons, NGF treatment in the presence of both TrkA and p75NTR promotes neuronal survival whereas stimulation of these neurons with BDNF results in cell death, as these neurons do not express TrkB [66]. As outlined here and will be seen later, the action of NTs and that of their receptors is greatly dependent on the cellular type and context.

1.2 Dorsal root ganglia sensory neurons

The somatosensory system processes information that organisms “feel”. Somatosensation uses organs and tissues as the receptive fields of specialized nerve endings arising from primary sensory neurons of the trigeminal ganglia (TG) in the head region and of the dorsal root ganglia (DRG) in the trunk. This system is responsible for the most diverse types of sensory modalities: nociception (pain), pruriception (itch), thermoception (temperature), tactioception (touch) and proprioception (body position and muscle strength). Although the autonomic sensory system - responsible for sensing internal body organs status - is different from the somatosensory nervous system, their primary sensory neurons share similarities and locations, and therefore can be discussed together.

Primary sensory neurons (PSN) have a pseudounipolar design. One process emerges from the soma and bifurcates, projecting either to the periphery, termed the distal process, and to the dorsal horn of the spinal cord - or brain stem - named the proximal branch, where it connects with secondary sensory neurons, interneurons or motoneurons [87]. By leaving the soma out of the way, rapid propagation of action potentials occurs between the periphery and the spinal cord. Only about 0.2% of the cytoplasm of a PSN is located in the soma, whereas 99.8% is found in the axon.

PSN are a highly heterogeneous population with specialized roles. Neuronal subgroups are categorized by their sensory modality (cold, heat, chemical, mechanical), their conduction velocity (slow bare axons and rapid myelinated fibers), sensory intensity (low versus high threshold) and by the neurotransmitter they release (aminoacidic neurotransmitters versus peptidergic). Based only on the conduction velocity of the action potentials, sensory neurons group into four types of fibers: 1) A α fibers or type I afferents, highly myelinated with fast conduction velocity and associated with Pacinian Meissner corpuscles; 2) A β fibers, moderately myelinated and associated with touch receptors like Merkel or Ruffini's corpuscles and Meissner corpuscles; 3) A δ fibers, emanating from intermediated-diameter thinly-myelinated sensory neurons, with intermediate conduction velocity and polymodal; 4) the slow-conducting C fibers, unmyelinated, small-diameter and polymodal associated with nociception [87].

Focusing on the skin - the biggest innervation target of the sensory system - specialized PSN allow the perception of the environment through different modalities including pain, itch, touch and temperature. The epidermal sensory nerves consist of “free” nerve endings or intraepithelial fibers as well as “hederiform” nerve endings in contact with Merkel cells, Langerhans cells or keratinocytes. The dermis contains free nerve endings, the hair nervous network, and the encapsulated endings or sensory corpuscles (Ruffini, Meissner, Krause, Pacini) [88]. Cutaneous nociceptors - mediating pain sensation in their response to noxious stimulus (thermal, chemical or mechanical) - are free nerve endings arriving to both dermis and epidermis layers mainly belonging to A δ and C fibers and less to A β fibers. Cutaneous nociceptors are classified in peptidergic nociceptors expressing peptides such as Substance P and calcitonin gene-related peptide (CGRP), and non-peptidergic nociceptors, which do not express neuropeptides but bind to the histological marker isolectin IB4. It is worth mentioning that some overlap exists between these markers. Neuropeptides are also found in other fibers types [89], while some non-peptidergic C fibers do not express IB4 [90]. Indeed, partially overlapping with nociceptors, cutaneous itch receptors mostly belong to C-type fibers and in less extend to A δ fibers [91]. It was once hypothesized that itch is simply a low-intensity form of pain and is not encoded by distinguishable neuronal populations [92]. Indeed, recent evidence demonstrated that a subpopulation of C-afferents expressing the Mas-related G-protein-coupled receptor A3 (MrgprA3) display intrinsic multimodality for pain and itch [93]. Accordingly, capsaicin, the classical pain stimulus, and histamine, the golden standard itch agent, have shown to elicit very similar sensations at low doses [94]. However, previous genetic and functional studies determined the existence of itch-specific neurons in the DRGs defined by the expression of MrgprA3, an orphan G-protein coupled receptor. Ablation of MrgprA3⁺ neurons showed substantial reductions in scratching evoked by multiples pruritogens and occurring spontaneously under chronic itch conditions, whereas pain sensitivity remained intact [95, 96]. Cutaneous thermal receptors include cold and warm modalities, responding either to temperature in the innocuous range, or to damaging temperatures, in which case are consider to overlap with the nociception modality. Transient receptor potential (TRP) ion channels, such as TRPV1, TRPV2, TRPM8 and TRPA1, are finely tuned to detect temperatures ranging

from extreme cold to noxious heat, and therefore serve as molecular mediators of thermal and pain sensation [97]. Cutaneous low-threshold mechanoreceptors (LTMRs) mediate light or innocuous touch sensations and target the skin as A β , A δ and C fibers. These neurons form two specialized sensory organs in the primate glabrous skin (without hair): the Meissner and Pacinian corpuscles, characterized by rapid adaptation to a sustained stimulus, and the Merkel and Ruffini endings, characterized by a slower adapting response [87].

1.2.1 Development of sensory neurons and the role of neurotrophins

Like other neuronal populations in the nervous system, the emergence, diversity and maturation of sensory neurons involves the synchronous concatenation of complex transcriptional programs during embryonic and post-natal stages. Over the years, the accumulated evidence has shown the importance of NTs and their receptors in the development of sensory neurons, functioning as one of the most important molecular effectors in the specification, growth, survival and death of the sensory lineages.

1.2.1.1 Early origins of sensory neurons

From mouse embryonic day (E) 8.5 to 10, neural crest cells (NCC) delaminate from the neural tube and some migrate ventrally to generate the DRG [98]. During NCC migration, sensory neurogenesis occurs in three successive waves that are controlled by the expression of the pro-neural genes neurogenin-1 (*ngn1*) and neurogenin-2 (*ngn2*). Sensory progenitors expressing *ngn1* give rise to small-size unmyelinated sensory neurons, including peptidergic and non-peptidergic nociceptors, while those expressing the pro-neural gene *ngn2* become the precursors of large-size myelinated sensory neurons, including proprioceptors, mechanoreceptors and A δ nociceptors [99].

The role of NTs in sensory neurons development has been observed as early as during gangliogenesis. Some reports have suggested that NT3 is essential *in vivo* for the survival of precursor cells in developing DRGs [100, 101]. Coincidentally, evidence for actions of NT3, NGF and BDNF on precursor cells have been obtained *in vitro* in different

systems [102-105]. Data on Trk receptor expression, however, have not been as coincident. While some have identified a small subset of TrkC-positive migratory NCC in chicks [106], others reported non-detectable levels of Trk proteins in early sensory precursors in mice [107]. Interestingly, genetic knockdown of TrkB and TrkC reduces proliferation and differentiation of embryonic cortical precursors whereas overexpression of BDNF in cortical precursors promotes proliferation and enhances neurogenesis *in vivo* [108]. p75NTR was also reported to be expressed on the vast majority of migrating NCC including dividing NCC *in vivo* [106], suggesting that it may function to transduce some of the neurotrophin activities previously identified on NCC *in vitro* [102-105], and/or influencing their migration during DRG gangliogenesis.

1.2.1.2 Neurotrophin-mediated sensory neuron specification

The passage from the neurogenic to the post-mitotic phase requires activation of an intrinsic program guided by the transcription factors *Islet1* and *Brn3a* which drives the diversification of sensory lineages through the expression of NT receptors TrkA, TrkB, TrkC and the GDNF receptor *Ret* [99, 109, 110]. The *ngn2* group exit the proliferative phase first, driving the appearance of two major post-mitotic neuronal sub-populations: a first group co-expressing TrkC and TrkB, and a second group co-expressing TrkC and TrkA. The expression of Trk receptor in these populations is highly overlapping and follows a sequential order. TrkC is the first receptor to be expressed in early post-mitotic neurons - from E9 to E10.5 in mice - reaching the majority of immature sensory neurons by E11.5. Its expression is rapidly followed by TrkB and TrkA from E10.5 to E11.5 [99, 111]. Coincidentally, several studies have shown the primordial role of locally-secreted NT3 in the survival and differentiation of post-mitotic sensory neurons at the early stages of mice embryo development [103, 104, 112]. Since the DRG neuronal loss in TrkC-null mice is much less pronounced than in NT3-null animals at early stages [113-115], it is believed that locally-produced NT3 also activates TrkB and TrkA to sustain the survival of these neurons [100, 107, 114, 116-122].

Another important function of the intrinsic transcriptional program guided by *Islet1* and *Brn3a* is the induction of the transcription factors *Runx1*, *Runx3*, *Shox2*, and *MafA*,

among others. These proteins exert repressor functions, extinguishing the expression of Trk and Ret receptors and thereby driving the segregation of mixed lineages into unique sensory neuron types [99]. Thus, the TrkC-TrkB subgroup comprising 75% of all neurons at E11.5, drops to 40% at E12, to 10% at E12.5, and finally to zero at E14 [123]. Other studies have shown a fifth of mature mechanoreceptors still co-expressing TrkC and TrkB in adult mice [124, 125]. Runx3 expression represses TrkB expression, opening up a TrkC exclusive lineage committed to proprioceptive functions and a subclass of LTMR [114, 126]. Meantime, Shox2 expression is maintained in neurons with extinguished Runx3 expression (which occur independently of Shox2); in these neurons, Shox2 represses TrkC and thus promotes a TrkB-exclusive lineage of sensory mechanoreceptors [127, 128]. Coincidentally, mice deficient in TrkB or its ligands BDNF and NT4 show significant deficits in DRG and petrose-nodosal ganglia (PNG) mechanoreceptors [129-133]. These early lineages diversify and become even more complex when the role of the transcription factor MafA is considered. Its action is related to the modulation TrkB and early Ret expression in *ngn2* subgroup of sensory progenitors [134]. The interplay between MafA and Shox2, regulating the levels of Ret and TrkB receptors, determines the ultimate proportion of mechanoreceptors in adult animals [99, 135].

The nearly universal TrkC expression in DRG cells during the early post-mitotic phase at E11.5 is substituted by TrkA, which becomes the most prevalent receptor on sensory neurons at E13 [107]. The onset of TrkA expression starts in a few neurons at E10.5 [136, 137], later than any other Trk receptor [111], and at this point its expression is coincidental with TrkC [99]. Later, the TrkA lineage of sensory neurons increases dramatically to 20% by E11.5 and to 80% from E13 to E15, dropping finally to 30% in adult mice [138]. These two waves of TrkA expression are the product of two different neurogenic origins. The first wave or early TrkA lineage has its origin in the aforementioned TrkC-TrkA co-expressing sub-group of post-mitotic neurons earlier derived from the *ngn2* group of sensory progenitors. Later in adulthood this first wave gives origin to the TrkA lineage of A δ nociceptors. Exactly how TrkC is downregulated in these neurons is not yet fully understood. However, earlier in development this subset of neurons is characterized by the expression of the transcription factor Cux2 [139]. Cux2-deficient mice do not show any particular change in sensory neuronal numbers or their specific markers during

development, however adult *Cux2*-deficient mice are hypersensitive to mechanical stimuli [139], which suspiciously suggests *Cux2* as the player behind the diversification of TrkA-dependent nociceptors and TrkC-dependent mechanoreceptors in the initial *ngn2* group of sensory progenitors

The first contribution to the predominance of TrkA receptors in sensory neurons at E13-E15 has its origin in the specification of the *ngn1* group of sensory progenitors. As previously mentioned, the *ngn1* group exit the neurogenic phase later than the *ngn2* group (origin of the early TrkA lineage), and under the influence of *Islet1* and *Brn3a*, the *ngn1* group slowly but consistently differentiates into TrkA-positive post-mitotic sensory neurons giving rise to the second TrkA expression wave. This increases the number of TrkA-positive neurons to 80% from E13 to E15, overcoming the early predominance of TrkC. The subsequent induction of *Runx1* by *Islet1* and *Brn3a* in these neurons seems to be crucial to repressing TrkA levels [123, 140], dropping to 30% of total sensory neurons in postnatal mice [138]. At the same time, *Runx1* triggers the expression of Ret receptor, also known as the late Ret wave [141, 142]. The late TrkA lineage is composed of two functionally differentiated sensory neurons: TrkA-positive peptidergic nociceptors and Ret-positive non-peptidergic nociceptors. Whether it originates in early or late lineages, TrkA signaling is fundamental for the development of all nociceptors since TrkA-null or NGF-null mice lack all types of nociceptors at birth [143, 144].

1.2.1.3 Neurotrophin-mediated axonal growth and target innervation

As sensory neurons diversify following intrinsic transcriptional programs that modulate the neurotrophin-based specification and survival of the different lineages, a parallel process of axonal growth and pathfinding takes place to innervate peripheral targets. Sensory neurons innervate target tissue starting at E11.5 [145], coincidentally with a switch in their dependency from NT3 to other NTs expressed by the targeted organs [145, 146]. Several *in vitro* and *in vivo* studies have shown that NTs play a fundamental role in fostering the guidance and growth of sensory axons during this process (reviewed in [147]). For example, mice overexpressing NGF in the epidermis showed excessive innervation of both sensory and sympathetic axons [148]. In addition,

BDNF overexpression in mouse epithelial targets has identical effects on BDNF-dependent sensory neurons [149]. However, the clearest demonstration of the ability of NTs to promote sensory axon growth *in vivo* was carried out by Tucker et al. (2001), following GFP-tagged axons in response to ectopically placed beads containing any of the four NTs or blocking antibodies. Whereas beads with blocking antibodies for NGF, BDNF, NT3 or NT4 inhibited the growth of sensory neurons, beads coated with NTs stimulated and directed their growth toward them [150].

Regardless of their demonstrated capacity to stimulate axonal growth, NTs have their own particularities regarding stimulation of axonal growth in sensory neurons. For instance, total neurite length and tortuosity were reported to be influenced differently depending on which neurotrophin is used as trophic support. NGF and BDNF stimulate the tortuous growth of DRG sensory fibers, while NT3 enhances neurite growth in terms of length and linearity allowing for a more organized and directed axonal elongation towards a peripheral target compared to the other NTs [151]. In terms of potency, NT4 is more potent than BDNF at promoting and attracting sensory axon growth from the geniculate ganglia [152]. Despite the fact that both NTs bind and activate TrkB, evidence suggests that they can differently regulate the requirement of downstream adaptor proteins to the receptor [153]. Also, given the mixed expression of Trk receptors in sensory neurons mostly during development, the combinatorial effect of different NTs over axonal growth has been addressed *in vitro* using compartmentalized chambers. NGF and NT3 applied together showed a significant synergism in promoting DRG axonal growth compared to single trophic factors or co-application of NGF and BDNF [154].

In addition to their role in axonal growth, NTs have also been suggested to act as axonal guidance cues in the navigation of growing axons during development (for review [155]). Each member of the neurotrophin family shows a chemoattractive or repellent effect on the growth cones of DRG axons depending on the sensory neuron lineage [156]. NT3 was shown to be chemoattractant for all DRG neurons except for NT4-dependent ones; NGF was attractive in all except for NT3-dependent DRG neurons, whereas BDNF and NT4 only acted as attractive cues for BDNF-dependent neurons. Additionally, BDNF and NT4 caused inhibition of neurite growth and neurite retraction in NGF- and NT3-dependent DRG cultures. As axonal guidance cues acting on the growth cones, NTs can

also interact or interfere with guidance cues of other nature. For example, BDNF-dependent DRG neurons are more sensitive to the repulsive axon guidance cue Semaphorin 3A (Sema3A) than NGF- or NT3-dependent cultures. Indeed, Sema3A stimulation of DRG neurons induces the co-localization of TrkA and Sema3A receptor Plexin A4 [157]. In addition, growth cones chronically cultured with BDNF show a rapid decrease in sensitivity to Sema3A upon acute exposure to NGF, while conversely, a rapid increase in sensitivity was observed in NGF-dependent cultures upon BDNF exposure [158]. Coincidentally, during embryonic development, Sema3A negatively regulates the innervation of the mouse male mammary gland by BDNF-dependent DRG axons [159].

1.2.1.4 Neurotrophin-based competence after target innervation

The observation that about half of peripheral neurons are eliminated around the time they contact their target tissue, and that altering the levels of target-derived NTs caused predictable changes in the final number of neurons, gave rise to the neurotrophic hypothesis [160-162]. This theory has been the prevailing model for the regulation of neuronal cell death during development. It proposes that neurons produced in excess during development compete for limited amounts of trophic support provided by their target tissues. Neurons which receive appropriate levels of trophic factors survive while neurons which do not, degenerate and are eliminated.

Importantly, built into the neurotrophic theory is the assumption that the probability of individual neurons to survive to the competition for NTs cannot be predicted [69, 163] implying that all neurons are endowed with an equal potential to compete. However, the principle of this one-side control of cell death by the environment and a stochastic selection of the surviving neurons has been challenged by recent evidence. Wang et al. (2019) reported that the transcriptional programs activated during early development stages, which determines the specificity of sensory neuron lineages, are also able to predict the final probability of individual neurons to respond to environment-derived survival signals and thus, to survive the cell death period. In particular, this group found that prior to cell death, sensory neurons exhibit distinct functional and survival states that are genetically encoded through Runx3 transcriptional activity. High-Runx3 expressing

sensory neurons showed higher probability of survival than low-Runx3 cells. This effect is probably due to the higher levels of TrkC expression in high-Runx3 neurons. While TrkC levels are independent of the signals derived from the target tissue, including local NT3 signalling, this crucially determines the capacity of cells to translate the survival signal of target-derived NT3, thus promoting survival of sensory neurons with higher TrkC levels [164]. The new model suggests, in opposition to the neurotrophic theory, that the main factor influencing the selection of sensory neurons during the period of developmental cell death is not the level of target-derived NTs but levels of their Trk receptors, which in the end is rooted in intrinsic transcriptional programs. In some aspects, the developmental cell death mechanisms of PSN may resemble that in *Caenorhabditis elegans* where survival of neurons precursors is genetically determined [165].

Ultimately, the neurotrophic theory and the intrinsic paradigm coincide in that the elimination of sensory neurons during development is caused by the lack of a neurotrophin-dependent survival signal. In that regard, several mutant mice for NTs and their receptors have shown unequivocally that neurotrophin-mediated trophic support determines the final number of sensory neurons in the DRG [166]. Inactivation of TrkA or NGF in mice results in similar neuronal deficits, most notably a decrease of the number of small-diameter nociceptive afferents in mice [167]. Similarly, inactivation of either TrkB or BDNF results in an equivalent loss of mechanoreceptive neurons [10]. NT3-null mice present a dramatic phenotype, with sensory neuronal loss reaching 70% at birth [100, 107, 114, 119, 129]. However, TrkC-null animals, exhibit a much less severe phenotype with only 20-35% loss of DRG neurons; an expected result given the capacity of NT3 to activate of TrkA and TrkB [100, 107, 114, 116-122]. In addition, numerous studies have revealed the importance of retrograde transport of the neurotrophin-mediated survival signal, a particular unique challenge for cells whose survival factors are produced at distances far from the cell body and nucleus [168, 169]. Indeed, the alteration of NTs retrograde transport through the axon, which act as a highway to transport neurotrophic factor signaling, generates permanent and detrimental alterations in the survival and function of DRG neurons [170].

The study of the mechanisms through which the lack of trophic support triggers the death of sensory neurons during development progressed substantially when it was discovered that three of the four receptors for NTs are dependence receptors. This category is exclusive for the receptors that are able to activate apoptotic pathways following the withdrawal of trophic factors or other supportive stimuli. More specifically, dependence receptors display the property that they transduce different signals in the presence or absence of ligand: in complex with the ligand, these receptors transduce a positive signal leading to survival, and in absence of ligand they initiate or amplify a signal leading to cell death [171]. This property has been identified in TrkA and TrkC but is lacking in TrkB [12, 172-176]. Tauszig-Delamasure et al. (2007) have shown that TrkC mediates the death of sensory neurons upon NT3 withdrawal, process that is abolished by the expression of a mutant form of TrkC bearing a substitution on the caspase cleavage site D641 in its intracellular domain. This group proposed that the pro-apoptotic pathway triggered by TrkC in the absence of NT3, requires caspase cleavage of the receptor to generate a “killer fragment” (TrkC KF). TrkC KF is subsequently translocated into the nucleus by importins, where it associates with the b-HLH transcription repressor Hey1 and stabilizes p53 [172]. p53 then activates the transcription of Cobra1 which shuttles TrkC KF to the mitochondria, activating the extrinsic-intrinsic apoptotic pathway [174, 176]. Interestingly, mice deficient for Hey1 display an increase number of TrkC positive neurons in the DRG at birth, suggesting that this pro-apoptotic pathway is indeed triggered by TrkC in sensory neurons *in vivo* [177]. In a key study, Nikolettou et al. (2010) demonstrated that mice embryos with an additional copy of *Ntrk1* and *Ntrk3*, meaning an increase in TrkA and TrkC protein levels respectively, display an excess of apoptosis, leading to the complete disappearance of the sensory neurons at E13.5 [12]. These pro-apoptotic actions of TrkA and TrkC in peripheral neurons did not seem to involve the activation of the kinase domain since cell death was unaltered in the presence of the Trk kinase inhibitor K252a or a TrkA (K538A) kinase-inactive mutant. However, others have shown that unliganded kinase-active TrkA induces the death of neural tumor cells, cultures of hippocampal neurons and sympathetic neurons deprived of NGF [173, 175, 178]. This suggests that other phosphorylation sites could mediate TrkA pro-death action. Interestingly, blocking the amyloid-beta peptide was found to decrease TrkA

phosphorylation-mediated death of hippocampal neurons deprived of NGF, while NGF deprivation is able to induce amyloid-beta production [173]. Thus, amyloid-beta has been proposed to induce unliganded TrkA pro-apoptotic activity.

p75NTR itself has also been categorized as a dependence receptor [171]. The finding that p75NTR expression induces apoptosis in the absence of ligand, but inhibits apoptosis following ligand binding suggested that p75NTR expression creates a state of cellular dependence on NGF [179-181]. The evidence that p75NTR-deficient mice have an increased number of cholinergic neurons further supported this notion [182, 183]. However, p75NTR action is complex and dependent on the cellular context [184]. Interestingly, p75NTR works in concert with TrkA to promote survival while antagonizes TrkA to promote death in sympathetic and trigeminal sensory neurons in the absence of trophic support. The pro-death action of p75NTR in those contexts proved to be ligand-dependent, functioning as a death receptor and not as a dependence receptor [185-189]. In DRG sensory neurons, p75NTR is necessary for survival and growth, but not for developmental cell death. Neurons lacking p75NTR require a higher concentration of NTs to promote survival *in vitro* compared to wild-type controls [53, 185, 190-193]. Furthermore, p75NTR is critical for restricting the magnitude of developmental cell death in TrkA, TrkB and TrkC sensory lineages [194]. Mice lacking p75NTR have a reduced number of DRG sensory neuron subtypes, including peptidergic and non-peptidergic nociceptors, TrkB-positive mechanoreceptors and TrkC-positive proprioceptors, resulting in a 50% decrease in lumbar sensory neurons by E14.5 [180, 186, 187, 195-197].

The only neurotrophin receptor whose signaling has not been linked to death mechanisms of any sort has been TrkB; unlike TrkA and TrkC, TrkB overexpression does not induce cell death [12]. How TrkB dependent sensory neurons undergo the cellular mechanisms of programmed cell death during embryonic development has not been investigated. Exploring the death mechanisms of BDNF-dependent sensory neurons in the absence of trophic support is one of the objectives of this work (Chapter 3).

1.3 The diversity of neuronal cell death mechanisms

Developmental neuronal cell death is an open field of study where different neuronal populations are subject to selection by cell death triggered by a complex array of different intrinsic and extrinsic signals. This section summarizes the molecular signaling cascades involved in three neuronal cell death types: apoptotic cell death, necrotic cell death and autophagic cell death. For further details on this vast field refer to the expert and comprehensive reviews of Yamaguchi and Miura (2015) [198], Orrenius et al. (2015) [199], Fricker et al. (2018) [200], Galluzzi et al. (2018) [201] and Hollville et al. (2019) [202].

1.3.1 Classification of neuronal cell death

Cell death is classified based on three parameters: 1) by the type of insult or trigger that leads to cell death, 2) by the morphology observed in the dying cells or 3) by the molecular mechanisms involved. The first classification broadly distinguishes between two groups: accidental cell death - the instantaneous and catastrophic demise of cells due to insults of physical, chemical or mechanical nature - versus regulated cell death (RCD), which relies on a specific molecular machinery, and therefore is susceptible to pharmacological or genetic interventions. RCD occurs either in the absence of an exogenous perturbation, operating as a built-in program known as programmed cell death (PCD) [164, 165, 198] or it can be triggered by intracellular or extracellular perturbations altering the cellular homeostasis state, simply referred as stress-driven RCD. The developmental cell death in the nervous system could be framed within the PCD category. The stress-driven RCD is mostly observed in the pathological context, where “programmed” gene cascades are activated [201, 203, 204]. However, the nature of cell death pathways triggered during development makes the above distinction debatable. Some of the mechanisms proposed to induce cell death during development are: induction by death ligands, and/or pro-apoptotic proteins, loss of survival signals, growth factor signaling, cell-cell interaction, and intrinsic transcription factor expression [198].

From a morphological point of view, cell death can be classified into three forms: 1) apoptosis, displaying cytoplasmic shrinkage, chromatin condensation, nuclear fragmentation and plasma membrane blebbing, ending in the formation of vesicles or apoptosomes that are phagocytosed and degraded by neighbouring cells; 2) autophagy, characterized by cytoplasmic vacuolization, phagocytic uptake and degradation; and 3) necrosis, manifesting no morphological distinctions from apoptotic or autophagic cell-death types except that there is no obvious removal of cell corpses by phagocytic neighbouring cells [201].

As in the morphological classification, mechanistically, neuronal cell death is divided in three main executing pathways: apoptosis, necrosis and autophagy; although a fourth and fifth form of neuronal death, known as paraptosis and phagoptosis have also been distinguished [200]. This classification is far from static, since some overlapping exists due to shared molecular executors.

1.3.2 The apoptotic pathway

Apoptosis is a form of RCD and the most common pathway identified during development. Depending on the inducer, it can involve the intrinsic (mitochondrial) pathway or the extrinsic (death/dependence receptor) pathway [204, 205].

The extrinsic apoptotic pathway can be mediated by death receptors, generally activated by soluble or membrane-anchored ligands at the cell surface. Receptor binding allows the assembly of a dynamic multiprotein complex at its intracellular tail which operates as a molecular platform to regulate the activation and function of caspase-8. The execution of this pathway can follow the caspase-8-dependent proteolytic maturation of executioner caspase-3 and caspase-7, which are sufficient to drive RCD. This pathway cannot be inhibited by the overexpression of anti-apoptotic Bcl-2 family proteins or the deletion of the pro-apoptotic members BAX, BAK and BID. The TNF α /TNFr1-mediated cell death constitutes the canonical example of the extrinsic apoptotic pathway. It has been seen involved in developmental cell death of sensory neurons [206].

Alternatively, dependence receptors also trigger the extrinsic apoptotic pathway [201]. Oncosuppression and developmental neuronal remodelling are among their

multiple realms of action [171]. As discussed previously, TrkA and TrkC, but not TrkB, are dependence receptors with fundamental roles during the period of cell death in sensory neuron development. The downstream mechanisms so far reported for the deadly action of unliganded TrkA and TrkC indicate fairly divergent pathways [12, 172-176]. The mechanisms of unliganded-TrkA-mediated degeneration in sensory neurons will be discussed in detail in section 1.4.

The intrinsic apoptotic pathway is initiated by a variety of perturbations including but not limited to DNA damage, reactive oxygen species (ROS) overload, endoplasmic reticulum (ER) stress and trophic factor withdrawal [207-209]. A critical step on this pathway is centered on the regulation of mitochondria outer membrane permeabilization (MOMP) by the pro-apoptotic and anti-apoptotic members of the Bcl-2 family, a group of proteins sharing one to four Bcl-2 homology (BH) domains. The pro-apoptotic members BAX and BAK are thought to be essential for the execution of apoptosis via the intrinsic pathway [210, 211]. Neurons have the particularity that BAK is transcribed as a translationally repressed product (N-BAK) and does not participate in apoptosis [212]. Thus, the induction of intrinsic apoptosis in neurons is entirely dependent on BAX activation, and its deletion or inhibition completely prevents neuronal death in a variety of *in vivo* and *in vitro* models [167, 213, 214].

In healthy conditions, the majority of BAX exist as a cytoplasmic monomer. Upon induction of apoptosis, BAX translocates to the mitochondria, forming dimers followed by ring-shaped homo-oligomers that result in MOMP. Formation of BAX rings on the mitochondria allows the release of cytochrome *c* [215, 216], which is essential to activate the downstream executioner phase of the apoptotic cascade (see below). For maximum cytochrome *c* release, mitochondrial cristae remodelling is also a crucial step. This is driven by the fusion protein Drp1 [217] and by cleavage of Opa1, the mitochondrial cristae sealing protein, by the mitochondrial protease OMA1 [218]. MOMP is antagonized by the anti-apoptotic members of the Bcl-2 family, including Bcl-2 itself, Bcl-xL, Mcl-1 and Bcl-w. These proteins are usually inserted into the outer mitochondrial membrane (OMM) or the ER membrane and exert anti-apoptotic functions by directly binding the pro-apoptotic members BAX and BAK, preventing their oligomerization. Because of their relevance in cellular homeostasis, pro-survival Bcl-2 members are an important node of regulation in

the apoptotic pathway. PUMA, BIM, BID, BAD, Bmf, Hrk, NOXA and Bik, also part of the Bcl-2 family, are able to bind and block the anti-apoptotic role of the pro-survival Bcl-2 proteins and thus facilitate BAX-mediated MOMP [200, 201].

MOMP promotes the cytosolic release of several apoptogens that normally reside within the mitochondrial intermembrane space [219, 220]. These include cytochrome *c*, SMAC/Diablo, the apoptosis inducing factor (AIF) and endonuclease G (Endo G). The role of cytochrome *c* in induction of neuronal apoptosis is best understood. Conventionally, cytochrome *c* cytosolic pool binds the apoptotic peptidase activating factor 1 (Apaf-1) and pro-caspase-9 in dATP-dependent manner to form the supramolecular complex known as apoptosome. Recruitment of pro-caspase-9 by the apoptosome allows the autocleavage and activation of caspase-9, which in turn cleaves and activates pro-caspase-3 [221]. Interestingly however, while Apaf-1 levels are maintained at high levels in mitotic cells, its levels decrease during neuronal differentiation, transitioning from markedly low level in young post-mitotic neurons, to almost no expression in mature neurons [202, 222, 223]. Whether cytochrome *c* is able to activate caspases independently of Apaf-1 is unknown [224] but low levels of Apaf-1 limits the amount of apoptosome activation that occurs in young neurons, enabling a very effective control of caspase activation by inhibitor of apoptosis protein (IAPs) [222, 225]. The X-linked inhibitor of apoptosis protein (XIAP) has the most potent activity to inhibit apoptosis via its ability to direct bind and inhibit executioner caspases [226, 227]. XIAP levels are regulated during apoptosis by different mechanisms including its specific degradation by the proteasome or its direct targeting and inhibition by the IMM-protein SMAC after MOMP [228, 229]. Released from its brakes, activated caspase-3 and other executioner caspases mediate the systematic disassembly of cells undergoing apoptosis, including DNA fragmentation [230], phosphatidylserine (PS) exposure [231] and the formation of apoptotic bodies [232].

Lastly, the intrinsic apoptotic pathway can be fed by the extrinsic pathway, particularly when caspase-3 is restrained by IAPs. In such contexts, death receptor-mediated activation of caspase-8 induces the proteolytic cleavage of BID, leading to the generation of its truncated form tBID, who translocate to the OMM inducing BAX/BAK activation and MOMP [200].

1.3.3 Necrotic pathways

Necrosis encompasses a set of RCD pathways that, unlike apoptosis, are not characterized by the removal of cell corpses by phagocytic neighbouring cells and therefore usually end with rupture of the plasma membrane. Necrosis can be programmed and genetically controlled - involving active cellular process - or unregulated and resulting from tissue trauma or toxin insult. Various forms of regulated necrosis have been recognized including necroptosis, parthanatos, and mitochondrial permeability transition [200, 201] .

Necroptosis is a form of RCD initiated either through extrinsic stimulus detected by death receptors, such as TNFr1 and its ligand TNF α [233], or by intrinsic perturbations, especially the accumulation of ROS [234]. At a molecular level, necroptosis is critically dependent on the kinase activity of receptor interacting protein kinase 1 (RIPK1), RIPK3 and the subsequent activation of the pseudokinase mixed lineage kinase domain-like (MLKL). Upon receipt of a necroptosis stimulus, RIPK1 phosphorylates and activates RIPK3, which in turn phosphorylates and activates MLKL, forming a complex known as the necrosome [233, 235]. The necrosome results from the oligomerization of phosphorylated MLKL and its translocation to the plasma membrane, where - by the regulation of Na⁺ or Ca²⁺ channels or by a direct pore-forming activity - is able to induce cell membrane permeabilization, rupture and necrosis. A complex interplay between necroptosis and apoptosis exist, particularly through the activation of TNFr1 by TNF α . TNFr1 activation induces both caspase-8-mediated apoptosis or necroptosis through RIPK1 activation. These two pathways are mutually exclusive given that the assembly of the necrosome upon TNF α stimulation requires the pharmacological or genetic inactivation of caspase-8 [236, 237] while catalytically inactive or necrostatin-1-mediated inhibition of RIPK1, reportedly contributes to specific forms of caspase-8-dependent apoptosis [238, 239].

Alternatively, parthanatos is a type of regulated necrotic cell death that is dependent on the activity of polyADP-ribose polymerases (PARP) [240]. PARP-catalytic activity increases the levels of PAR which induces the translocation of the mitochondrial-

intermembrane space protein AIF to the nucleus where it mediates large-scale DNA fragmentation and chromatin condensation. AIF, normally anchored to the inner mitochondrial membrane (IMM), has to be liberated from its membrane anchor to be released into the cytosol. The action of Ca^{2+} -dependent proteases calpains to cleave AIF anchorage is a fundamental step in parthanatos induction [241]. Additionally, excessive PARP activity is able to decrease NAD^+ levels, compromising cellular metabolic processes and favouring cell death [242].

The mitochondrial permeability transition (mPT) constitutes another relevant form of regulated necrosis. Oxidative stress, cytosolic Ca^{2+} overload and decrease ATP are among the most common intracellular perturbations that cause mPT. Mechanistically, mPT implies the loss of IMM impermeability to small solutes followed by the dissipation and loss of the mitochondrial membrane potential ($\Delta\Psi_m$), the loss of osmotic balance and the breakdown of the OMM and the cellular membrane. mPT-driven necrosis implies the formation and opening of the mitochondrial permeability transition pore complex (mPTPc), a supramolecular formation assembled at the junctions between the IMM and OMM [243, 244]. Although the composition of this complex is still debated, cyclophilin D is the only protein whose requirement for mPT induction has been formally validated *in vitro* and *in vivo*. Pharmacological inhibition of cyclophilin D with cyclosporine A (CsA) have shown to limit mPT-driven necrosis in multiple animal and cellular models [245, 246]. Other components proposed to be part of mPTPc are the voltage-dependent anion channel (VDAC) and the adenine nucleotide translocase (ANT) [247]. Several physical or functional mPTPc interactors have been shown to regulate mPT-driven necrosis such as the pro-apoptotic Bcl-2 family members BAX, BAK and BID [248-251] and the anti-apoptotic Bcl-2 and Bcl-xL. Additionally, the mitochondrial fusion protein Drp1 has been shown to promote mPTPc opening [252] while the transcription factor p53 also seems to participate in mPT-driven necrosis upon physical interaction with cyclophilin D [253]. Neurotoxic amyloid oligomers have shown to sensitize mPTPc in isolated brain mitochondria, allowing the pore to open at physiological levels of Ca^{2+} [254]. In some circumstances mPTPc opening may cause degradation of NAD^+ due to PARP activation, resulting in energy depletion and parthanatos-like necrotic cell death [255].

1.3.4 Autophagy-mediated cell death

Autophagy is a regulated process that operates to cope with stress, mediating cytoprotective effects. Autophagy is used by cells undergoing growth factor withdrawal or starvation to provide themselves with anabolic substrates derived from lysosome-mediated digestion and recycling of cellular constituents. The delivery of these cellular components to lysosomes occurs via vesicles known as autophagosomes. The formation of autophagosomes is initiated through a cascade of signals targeted at three distinct multi-protein complexes comprising autophagy-related (ATG) genes. Knockout of key ATG genes, such as *Atg5* or *Atg7*, necessary for the autophagosome formation, showed that basal autophagy plays a central role in preventing neurodegeneration due to build-up of misfolded proteins and proteostasis in mice [256, 257]. However, in a number of developmental and pathophysiological settings, the molecular machinery for autophagy contributes to a distinct type of cell death that is neither apoptotic, nor necrotic, but associated with the presence of many autophagosomes, autolysosomes and lysosomes [258]. This was defined as autophagic cell death (ACD). In its most strict definition, ACD is mediated and executed solely by autophagy without the involvement of any other cell death machinery. For example, it was shown that ACD can be prevented by knockdown of key ATG genes (*Atg13* and *Atg14*, as well as *Atg6* or Beclin-1), but not by inhibition of key apoptotic (BAX/BAK) or necroptotic (RIPK1/3) death commitment genes. However, both apoptosis and necrosis are known to use the autophagy apparatus to favour cell death [259]. For example, Beclin-1, key for the autophagosome formation, is held inactive via its BH3 motif by binding to anti-apoptotic Bcl-2 family members or to Bim when it is tethered on microtubules. Accordingly, mice deficient for apoptosis (BAX and BAK double knockout, DKO) are viable, but when autophagy is also blocked (by *Atg5* KO), mice shows embryonic lethality by day E13.5 with enhanced brain exencephaly [260]. As an example, cell death-dependent loss of interdigital webbing was even more delayed in the BAX::BAK double knockout-ATG5-null mice compared to BAX::BAK double knockout mice. This implies that in the absence of apoptosis, autophagy is activated to facilitate developmental death of the interdigital web [261].

1.3.5 Calcium in neuronal cell death

Calcium (Ca^{2+}) is a ubiquitous intracellular signaling molecule responsible for controlling numerous cellular processes, such as protein synthesis and secretion, gene expression, cell cycle progression, metabolism and cell death [241, 262-264]. The intracellular Ca^{2+} concentration fluctuates in response to several extra and intracellular stimuli and signals. To keep an appropriate homeostasis of Ca^{2+} inside cells, its levels are tightly regulated by the simultaneous interplay of multiple counteracting processes, which can be divided into Ca^{2+} ON and Ca^{2+} OFF mechanisms depending on whether they serve to increase or decrease cytosolic Ca^{2+} concentration respectively. The ON mechanisms depend either on channels located at the plasma membrane that control the entry of external Ca^{2+} from extracellular space or on channels that release Ca^{2+} from the intracellular stores. Channels at the plasma membrane include voltage-operated calcium channels (VOCCs), normally expressed in excitable cells like neurons, receptor-operated calcium channels (ROCCs), typically activated by agonist like glutamate, ATP, or capsaicin, and store-operated calcium channels (SOCCs), which are activated in response to depletion of the intracellular Ca^{2+} stores. On the contrary, the OFF mechanisms rapidly remove Ca^{2+} from the cytoplasm by various pumps and exchangers. The plasma membrane Ca^{2+} -ATPase (PMCA) pump extrudes Ca^{2+} to the outside and sarco-endoplasmic Ca^{2+} -ATPase (SERCA) pump returns Ca^{2+} to the ER. Also, $\text{Na}^+/\text{Ca}^{2+}$ exchangers can extrude Ca^{2+} to the outside from the cytoplasm. The mitochondria is another important component of the OFF mechanisms, sequestering Ca^{2+} under conditions of local elevated cytoplasmic Ca^{2+} to later release it back slowly during the recovery phase [264].

Sustained perturbances of any of the Ca^{2+} ON and OFF mechanisms by different types of insults may alter Ca^{2+} homeostasis, causing depletion or overload, with pernicious consequences for the cell; for this reason, altering Ca^{2+} homeostasis may be defined as an “intrinsic stress”, meaning that it is auto-induced by the cells as a consequence of an extrinsic stress of a different nature.

When stress leads to Ca^{2+} overload, Ca^{2+} -induced damage may reach levels sufficient to cause necrotic cell death [265-267]. Damage and death are due to excess

stimulation of Ca^{2+} -sensitive targets such as the calpain family of Ca^{2+} -activated cysteine proteases. Ca^{2+} overload and acute calpain activation precipitates necrosis, probably via catastrophic cleavage of regulatory and structural proteins [268]. Moreover, calpains can cleave and activate caspases (and *vice versa*), favouring apoptosis instead of necrosis. It is conceivable that the degree of Ca^{2+} elevation - and therefore calpain activation - may determine whether cells die by apoptosis or necrosis. High Ca^{2+} overload could favor necrosis while mild Ca^{2+} elevation may favour apoptosis [269]. In addition, calpains can cleave and deactivate components of the autophagosome, like ATG5, disrupting autophagy in favour of apoptosis [270, 271].

An additional form of Ca^{2+} -overload damage is caused by mitochondria that, taking up the excess of cytosolic Ca^{2+} for scavenging purposes, may be subjected to stress and even collapse through MPTP, if it exceeds a physiological threshold [272]. After mitochondrial rupture, the captured Ca^{2+} can be dissipated, creating a new cytosolic Ca^{2+} increase, which can be in turn taken up by an intact mitochondria [267]. Although MPTP opening is related with necrotic cell death, mild Ca^{2+} overload and cycling may cause the release of cytochrome *c* (even in the absence of BAX translocation) [265], which in turn may activate caspases and promote apoptosis [266]. Another form of damage caused by cytosolic Ca^{2+} overload may come from energy failure, starving Ca^{2+} -ATPases that stop pumping Ca^{2+} against gradient to the ER (SERCA), or to the extracellular environment (PMCA). This enhances cytosolic Ca^{2+} overload, mitochondrial failure and ultimately cell death [266].

When referring to stress caused by intracellular Ca^{2+} depletion, the emphasis is on emptying of the ER, the main Ca^{2+} store within cells [266]. Damage by Ca^{2+} depletion is a non-catastrophic early event within the apoptotic process that is usually followed by a later catastrophic damage by Ca^{2+} overload. Because of its central role in the regulation of Ca^{2+} storage and signaling, as well as protein folding and sorting, the ER is particularly susceptible to fluctuations in Ca^{2+} concentrations inside its lumen. Therefore, compromising Ca^{2+} sequestration by the ER can be sufficient to induce ER stress and trigger the unfolded protein response (UPR), a branch of a major stress-mitigation program known as the intrinsic stress response (ISR) [273]. The ISR/UPR has three major roles: a) adaptive response, reducing ER stress and restoring ER homeostasis; b)

feedback control, in order to block the UPR when ER homeostasis is regained; and c) balancing cellular survival and death through the regulation of apoptosis [274]. In other words, UPR can evolve into repair or apoptosis; typically, the longer it is activated, the more likely it ends up inducing cell death [273, 275, 276]. One way the UPR induces cell death is by the direct activation of caspase-12 (in rodents, caspase-4 in humans), which in turn activates the apoptotic effector caspase-3 via caspase-9, independently of the mitochondrial-cytochrome *c* release and Apaf-1 activation [277]. In parallel, the UPR relies on the activation of three ER-resident transmembrane proteins or stress sensors: activating transcription factor-6 (ATF6), inositol requiring protein-1 (IRE1), and protein kinase RNA-like ER kinase (PERK). In homeostatic conditions the three sensors bind the ER chaperone glucose-regulated protein 78 (GRP78/BiP). Under ER stress, BiP dissociated from these sensors and promotes their activation inducing phosphorylation and oligomerization of PERK and IRE1 and the translocation of ATF6 to the Golgi [278]. Following IRE1 activation, it recruits TNFR-associated factor-2 (TRAF2) and activates apoptosis-signaling-kinase 1 (ASK1) which leads to the activation of JNK and p38 MAPK [279]. Activated JNK can translocate to the mitochondrial membrane and induce activation of BIM and the inhibition of Bcl-2, whereas p38 MAPK phosphorylation leads to the activation of the pro-apoptotic transcriptional factor C/EBP homologous protein (CHOP) [274, 280]. In turn, ATF6 translocation to the Golgi induces its proteolytic cleavage. Subsequently, cleaved ATF6 can translocate to the nucleus where it can induce the transcription of the pro-apoptotic transcription factor CHOP [274, 281]. Lastly, PERK activation triggers the phosphorylation of the eukaryotic initiation factor 2 alpha (eIF2 α), which results in general inhibition of protein translation [282, 283]. Paradoxically, eIF2 α phosphorylation also result in the translation of selective mRNAs that contain the internal ribosomal entry site (IRES), leading to the translation of genes associated with the UPR, namely the activating transcription factor 4 (ATF4) [282, 284]. Sustained activation of PERK can also trigger the ATF4-dependent transcription of the pro-apoptotic factor CHOP [285], which induces the up-regulation of the ER oxidase 1 α (ERO1 α), leading to excessive generation of oxidant species and depletion of the antioxidant glutathione [286], the downregulation of the anti-apoptotic Bcl-2, and the up-regulation of the pro-apoptotic proteins BAX and BAK [280].

A crucial link between Ca^{2+} and apoptosis was established by studying the Bcl-2 family and its mechanisms of action. Beside regulating the MOMP during apoptosis, this family of proteins can regulate the ER Ca^{2+} content and the Ca^{2+} transfer between the ER and the mitochondria in various cells [274, 287]. Several studies have shown that overexpression of Bcl-2 prevents the reduction of Ca^{2+} concentration in the ER, decreases the amount of Ca^{2+} released from the ER and provides resistance to Ca^{2+} -dependent apoptosis [288-291]. Overexpression of BAX/BAK at the ER induces a transient rise in ER Ca^{2+} content followed by store depletion due to induction of apoptosis [292-294], while the loss of BAX/BAK leads to a decrease in ER Ca^{2+} stores and resistance to Ca^{2+} -dependent apoptotic stimuli [292, 295], even following reconstitution with mitochondria-targeted BAX/BAK [296].

The IP_3 receptor (IP_3R) is well-known as a constitutive Ca^{2+} release channel from the ER [297], as are members of the ryanodine receptor (RyR) family [298]. Usually in tight contact, the mitochondria take up Ca^{2+} released from the ER through IP_3R , which is required for optimal respiration and ATP production. During apoptosis, IP_3R conductance is regulated by the Bcl-2 family members by direct interaction and phosphorylation [299, 300]. While Bcl-2 physically interacts with IP_3R at the ER surface, inhibiting IP_3R - Ca^{2+} conductance, this can be overcome by pro-apoptotic members of the Bcl-2 family [299, 301, 302]. Further, IP_3R is targeted by caspase-3 to increase the channel conductance, promoting Ca^{2+} accumulation by the mitochondria, increase in ROS production, and apoptosis [303-305]. Moreover, cytochrome *c* can also bind IP_3R and block the naturally-occurring feedback inhibition induced by the rising cytosolic Ca^{2+} concentration on IP_3R conductance [306].

Autophagy can also be triggered by ER stress, suggesting a potential role for Ca^{2+} in autophagy. Indeed Ca^{2+} mobilization by thapsigargin, an inhibitor of SERCA pump and consequent inducer of the ER stress response, triggers autophagy, while Ca^{2+} chelation with BAPTA-AM inhibits the formation of the autophagosome [307]. Additionally, autophagy was shown to occur by the direct Ca^{2+} -dependent activation of AMP-protein kinase (AMPK), which requires upstream activation of the Ca^{2+} /calmodulin kinase beta. Moreover, it has been demonstrated that IP_3R regulates autophagy through its interaction

with Beclin-1, establishing a functional and physical connection between the ER and mitochondria not only in apoptosis but also in autophagy [308].

1.3.6 Phosphatidylserine engulfment signal

Loss of phospholipid asymmetry in the plasma membrane with externalization of phosphatidylserine (PS) facilitates the recognition of dying cells by phagocytes. The development of fluorescently labelled Annexin-V, which binds specifically to PS residues on the cell surface, enables detection of dying cells with externalized PS both *in vitro* and *in vivo*. In the plasma membrane, the distribution of PS between the two leaflets is regulated by a Ca^{2+} -dependent scramblase that catalyzes the non-specific randomization of phospholipids across the bilayer and an ATP-dependent amino-phospholipid-translocase that mediates movement of amino-phospholipids from the outer to the inner leaflet [241]. Although the exposure of PS on the outer plasma membrane has long been considered a unique feature of apoptotic cells, PS exposure has also been reported in dying cells undergoing non-apoptotic pathways such as necroptosis or parthanatos [240, 309]. It should be noted that under *in vitro* culture conditions, where phagocytic cells are normally absent, apoptotic cells and their fragments lyse in a process similar to necrosis. This is termed “secondary necrosis” or “post-apoptotic necrosis”, and as a consequence of having followed an initial apoptotic pathway these cells also expose PS [241]. Importantly, PS externalization can be decoupled from degeneration; elevation of energetic status in sensory neurons hinders PS exposure, while inhibition of mitochondrial activity causes PS exposure, without degeneration [231].

1.4 Mechanisms of PCD in NGF-dependent embryonic DRG sensory neurons

Our current understanding of the molecular mechanisms underlying the death of sensory neurons during development is derived primarily from studies of neurons withdrawn from NGF *in vitro*. Explants or dissociated DRG neurons are isolated - typically from E12 to E14 mice embryos - and cultured in the presence of NGF, promoting the survival and growth of axons on the culture substrate. Subsequently withdrawing NGF from the culture media leads to asynchronous degeneration over the next 15 to 35 hours [310]. Since its establishment in mid twenty century, this and similar models have offered a powerful approach to dissect the molecular mechanisms underlying the degenerative process by pharmacological and genetic deletion of candidate proteins, using different biochemical markers of degeneration as quantifiable outputs [311]. This section summarizes the main pathways and players discovered using this paradigm.

Two distinctive phases characterize the degeneration of NGF-deprived embryonic DRG neurons: the latent or incubation phase, and the catastrophic phase. During the latent phase, axons are morphologically indistinguishable from those receiving trophic support [312], although - as in any period of adaptation to stress - axonal growth deceleration and arrest occurs over first 12 hours after deprivation. During the catastrophic phase, axonal transport ceases, neurofilaments become fragmented, the cytoskeleton disintegrates, and neurons start showing blebbing and fragmentation typical of degeneration and reminiscent of apoptosis and expose extracellular PS as an “eat me” signal for phagocyte engulfment [313, 314]. The latent phase builds the degenerative program through transcriptional and translational mechanisms, but the re-addition of trophic support or mild depolarization is capable of rescuing degeneration. The catastrophic phase executes the degenerative program, representing a point of no-return, after which reintroduction of neurotrophic support does not rescue degeneration [315].

According to the type of insult that triggers the death of sensory neurons (NGF withdrawal), the degenerative process fits into the extrinsic apoptotic pathway, and - as explained earlier - could be mediated by death receptors or dependence receptors. The accumulated evidence has demonstrated the co-participation of both types of receptors in the degeneration of DRG neurons. As a dependence receptor, TrkA switches from pro-

survival to pro-death in the absence of its ligand [12]. Several studies depict it as the most important player in the initiation of the degenerative cascade [173, 175, 316]. Accordingly, genetic deletion of TrkA protects DRG neurons in the absence of trophic support *in vitro* and *in vivo* during the period of developmental cell death [12]. In addition, inhibition of TrkA signaling with foretinib completely abrogates the degenerative process of DRG neurons during NGF deprivation [175]. How TrkA switches from pro-survival to pro-death is not clear, but several signaling pathways have been proposed.

An important function of TrkA pro-survival signaling is to suppress activation of pro-death pathways. For example, PI3K-mediated Akt activation inhibits the transcription factor FoxO, which normally regulates the expression of pro-apoptotic genes [30, 317] while Akt-mediated phosphorylation and inactivation of GSK-3 β , blocks cell death by inhibiting BAX-mediated MOMP [318]. In DRG sensory neurons deprived of NGF, the induction of the degenerative program critically depends on the release of those brakes. GSK-3 β is at the center of a concerted signaling program required for regulated axonal degeneration of sensory neurons following NGF deprivation and activates a transcriptional cascade through the transcription factor TBX6 [319]. Several studies have shown the importance of the MLK dual leucine zipper kinase (DLK) in the regulation of JNK-mediated axonal degeneration in NGF-deprived sensory neurons [320-322]. Furthermore, it has been shown that lack of TrkA/Akt survival signaling activates DLK-mediated JNK/c-Jun signaling, inducing the activation of FoxO3a-mediated transcriptional program for the upregulation of pro-death genes during the degeneration of embryonic DRG neurons upon NGF deprivation [316]. In addition, NGF deprivation in sensory neurons induces the expression of the pseudo-kinase Trib3, which binds and blocks Akt signaling, thus amplifying the loop involving Akt inhibition, FoxO activation, and transcriptional induction of pro-apoptotic genes [323].

Evidence also points to PLC γ as an alternative effector of unliganded-TrkA death signaling. In the presence of NGF, TrkA phosphorylates and activates PLC γ promoting ERK pro-survival signaling [37]. However, after NGF deprivation of hippocampal neurons, the initial loss of phosphorylated PLC γ is rescued by anomalous TrkA phosphorylation [173]. PLC γ re-activation is dependent on unliganded TrkA and on the action of CDK5 and Src kinases, whose mediate TrkA phosphorylation independently of NGF [324].

Abnormal TrkA and PLC γ phosphorylation have also been observed in sympathetic and DRG neurons deprived of NGF [175]. Interestingly, the pan-kinase inhibitor foretinib selectively inhibits unliganded TrkA and PLC γ phosphorylation and rescues DRG neurons from degeneration induced by NGF deprivation [175]. Phosphorylation of PLC γ induces PKC activation through DAG and IP $_3$ -IP $_3$ R-induced ER-Ca $^{2+}$ release [325-328]. Although no direct link between PLC γ and PKC has been established in a degenerative context in sensory neurons, recent evidence shows that PKC activation promotes DRG degeneration in response to NGF deprivation through the stimulation NOX-mediated ROS production and the induction a catastrophic TRPV1-mediated Ca $^{2+}$ influx [329].

PLC γ is also able to induce Ca $^{2+}$ mobilization from intracellular stores, particularly from the ER [327, 330]. Sustained decrease in ER-Ca $^{2+}$ concentration triggers the ER-stress UPR response, a PERK-mediated aspect of the integrated stress response (ISR) induced to cope with the accumulation of unfolded proteins [273]. Sympathetic and DRG sensory neurons deprived of NGF induce the ER-stress response with the concomitant increase in active PERK and ATF4 early during the latent phase [314, 322]. Interestingly, the inhibition of unliganded TrkA/PLC γ phosphorylation with foretinib downregulate the gene expression downstream of ATF4 in sympathetic neurons deprived of NGF [175]. Other studies have shown that NGF withdrawal drives a DLK-dependent induction of the integrated stress response [322].

Death receptors also participate in the degenerative process of DRG sensory neurons. Interestingly, the obvious candidate, the p75NTR receptor, that actively drives the degeneration of sympathetic neurons upon NGF deprivation during development [66, 69, 189] only contributes with the survival but not the death of deprived DRG sensory neurons [12, 194]. However, the death receptor TNFr1 and its ligand TNF α participate in the developmental cell death of primary peptidergic and non-peptidergic nociceptors. TNFr1- or TNF α -deficient E14.5 mice embryos displayed nociceptive fiber hyperinnervation at the skin and a hypersensitive response to thermal and mechanical stimuli in adult animals. *In vitro*, TNFr1-deficient DRG neurons have a hypertrophic growth in response to NGF but are able to maintain further activated the pro-survival pathway ERK1/2 in the absence of trophic support [206].

Other studies have proven the participation of the death receptor 6 (DR6) in the developmental degeneration of DRG neurons. Its genetic deletion, or the use of blocking antibodies against DR6, delayed sensory axons degeneration after NGF withdrawal *in vitro* [331, 332]. The amyloid-precursor protein (APP) was shown to bind and induce DR6-mediated axonal degeneration in DRG neurons [331, 332], although its role during NGF deprivation was previously reported as pro-survival instead of pro-degenerative [333]. Different studies have reported a tight inter-regulation between TrkA and APP, with APP showing a similar pro-survival to pro-death switch in the absence of NGF [173, 334, 335]. These observations suggest a TrkA-mediated modulation of APP-DR6 interaction in deprived sensory neurons, although more research is needed to determine if this is the case. Section 1.5.5.4 will discuss this and other aspects of APP during developmental cell death in DRG neurons.

DR6 downstream signaling has not been characterized in sensory neurons, but the pathway of apoptotic cell death induced by its overexpression in non-neuronal cell types differs from the canonical death receptor pathway involving caspase-8 activation [336]. In these settings, DR6 has been reported to induce apoptosis via a mitochondria-dependent pathway by interacting with BAX [336]. Whether this pathway occurs in sensory neurons deprived of NGF is unknown, but studies of DR6 in such context suggests that BAX is required for DR6-dependent death [331].

Developmental degeneration of DRG and sympathetic neurons requires *de novo* mRNA and protein synthesis [337-339]. One of the main targets of this coordinated intrinsic program is the modulation of the mitochondria permeability through the balance of pro-survival and pro-death Bcl-2 family proteins, which promotes apoptotic pathways observed in degenerating sensory neurons deprived of NGF.

Bcl-2 family members are critical determinants of neurotrophin survival responses. In sensory neurons, Bcl-w (Bcl2l2), an antiapoptotic member of this family, is selectively regulated by target-derived neurotrophins [340-342]. A continuous neurotrophin supply is required to coordinate the transcription, mRNA transport, and translation of Bcl-w in space and time to promote sensory neuron survival of cell bodies and axons. Bcl-xL is abundantly expressed in axons, and double-deficient Bcl-w/Bcl-xL degenerate spontaneously, even in the presence of NGF [316]. Lack of neurotrophin supplementation

diminishes the capacity of sensory neurons to inhibit the pro-apoptotic activity of BAX [338, 343]. In parallel, multiple transcriptional pathways induced by NGF deprivation in sympathetic and DRG neurons (via c-Jun, FoxO1, FoxO3a, TBX6, p53, ATF4 and CHOP) target the induction of the pro-apoptotic members of the Bcl-2 family PUMA and BIM [316, 322, 339]. Accordingly, PUMA-deficient embryos show denser skin innervation and PUMA-null DRG explants do not experience degeneration upon NGF deprivation *in vitro* [316, 339]. PUMA and BIM proteins are able to de-repress the pro-apoptotic activity of BAX by inhibiting Bcl-w and Bcl-xL [339]. Several studies have reported the importance of BAX activation in the degenerative process of NGF-deprived DRG sensory neurons *in vitro* and *in vivo* [167, 213, 214]. The most significant consequence of BAX activation is the induction of MOMP and the release of cytochrome *c* into the cytosol.

The release of cytochrome *c* coincides with the point-of-no-return, operationally defined as the last time at which NGF re-addition can rescue an NGF-deprived neuron. However, whether cytochrome *c* is indispensable for the degeneration of DRG neurons upon NGF deprivation is debatable. Due to its essential function in mitochondrial respiration, experiments that knockout or silence cytochrome *c* are problematic. Instead the use of Apaf-1-deficient models have been considered a valid alternative. Honarpour et al. (2001) analyzed the effect that Apaf-1 deficiency has on the number of DRG neurons during the period of developmental cell death. The authors found that absence of Apaf-1 during development increases the number of neurons, but its deficiency is unable to rescue neurons from cell death in Apaf-1::TrkA compound double null animals [344]. Earlier, Patel et al. (2000) reported that DRG neurons that normally die in the absence of TrkA survive in a BAX-null background [167] implying that while BAX deficiency compensates for the survival function of TrkA, Apaf-1 deficiency cannot. These observations suggest that Apaf-1 drives cell death in neural progenitor stages but perhaps not at later stages; this correlates with a more restricted expression of Apaf-1 in post-mitotic neurons compared to neuronal progenitors [202]. The observation that cell death proceeds in Apaf-1::TrkA compound null mice suggests that DRG neurons can use alternative paths to achieve developmental cell death. Indeed, it has been shown that Apaf-1-deficient post-mitotic DRG neurons undergo developmental programmed cell death by a caspase-independent, non-apoptotic pathway involving autophagy [345].

These observations however, did not rule out an active role of Apaf-1 and the apoptosome formation during developmental cell death of DRG neurons and the fact that cytochrome *c* microinjection in embryonic NGF-dependent DRG neurons induces extensive cell death [346] suggests that the apoptosome is an active player during developmental cell death. Therefore, although it may not be essential, DRG neurons deprived of NGF may normally employ the apoptosome to accelerate and execute cell death.

Caspase activation is an important component of apoptotic cell death and apoptosome formation contributes to the acceleration of executioner caspase activation. However, additional routes may induce caspase activation, including pathways involving downstream death receptors [332]. In fact, sub-lethal levels of caspase activation can take place during the latent phase even before MOMP [213, 347]. Several groups have determined the importance of caspase-9, caspase-7, caspase-6 and caspase-3 in the execution of degeneration upon NGF deprivation in DRG neurons [213, 214, 225, 230, 331, 348]. Caspase substrates are numerous, ranging from themselves, cytoskeleton proteins, ER/mitochondrial components and targets that through gain-of-function or loss-of-function are able to foster the progression of the degenerative process [349]. For example, Hertz et al. (2019) recently reported the neuronally enriched protein RUFY3 as a caspase-3 target during the degeneration of DRG sensory neurons upon NGF deprivation. The authors showed that *Rufy3* loss of function dramatically delays axonal degeneration without blocking caspase-3 activation, positioning it as an effector of degeneration downstream of or in parallel to, caspase activation in DRG neurons [350].

Caspase activation is also necessary to induce Ca^{2+} -dependent proteases calpains upon NGF deprivation in DRG neurons. In substantial agreement with studies in non-neuronal cell types [269, 351-353], Yang et al. (2013) found that caspase-3 targets and cleaves the endogenous calpain inhibitor calpastatin in sensory neurons [354]. Their genetic and biochemical data support a model in which active caspase-3 in NGF-deprived DRG axons directly cleaves calpastatin, which in turn releases the suppression of calpains, leading to cytoskeleton degradation and axon degeneration. It worth mentioning that the activity of calpains requires high concentrations of Ca^{2+} , and depletion of endogenous calpastatin alone is not sufficient to cause axon degeneration *in vitro* and *in vivo* [354, 355]. Therefore, besides proteolyzing calpastatin, caspases need to activate

additional downstream pathway(s) to increase cytosolic Ca^{2+} . Different mechanisms for catastrophic Ca^{2+} overload have been proposed to underlie DRG neuronal degeneration. Those mechanisms include direct Ca^{2+} influx through a damaged plasma membrane [232, 356], ROS-dependent activation of TRPV1 channels [329], activation of VGCC [354, 357], reverse operation of $\text{Na}^+/\text{Ca}^{2+}$ exchangers [358], and opening of the MPTP [359]. Ca^{2+} chelation completely blocks DRG neurons degeneration upon NGF deprivation [329, 360].

Due to the restricted expression of Apaf-1 in post-mitotic neurons, the activation of executioner caspases is tightly coordinated by mechanisms that allow strengthening their activation either directly or indirectly. The redox state of cytochrome *c* is a good example. It is a more potent activator of caspases in its oxidized form than in its reduced form [361]. The balance between antioxidant defenses and ROS production becomes a key point of regulation. During apoptosis, an increase in ROS creates a more oxidized cellular environment, making neurons more permissive to cytochrome *c*-mediate activation of caspases [361-365]. NGF deprivation in DRG neurons upregulates ROS levels via PKC-mediated NOX activation [329], while sympathetic neurons deprived of NGF trigger IRS/CHOP-mediated increase in Txnip, a protein who binds and inhibits thioredoxin, a major antioxidant protein [366]. The potent anti-oxidant N-acetylcysteine (NAC) completely rescues DRG cultures from NGF deprivation [329].

The release of SMAC after MOMP constitutes another mechanism to potentiates caspase activation during neuronal apoptosis by inhibiting IAPs. Importantly, XIAP plays a pivotal role in the regulation of caspase activity during developmental degeneration of sympathetic and DRG neurons. Its level is actively downregulated in sympathetic and DRG neurons deprived of NGF such that apoptosis can proceed [225, 367]. The observation that SMAC release after MOMP is not sufficient to downregulate XIAP activity in sympathetic neurons indicates that additional mechanisms must be involved [367]. The activation of the ISR observed in sympathetic and DRG neurons deprived of NGF could be one of these mechanisms. Evidence from different cell lines has shown that the ISR-components PERK downregulates XIAP translation through the phosphorylation of $\text{eIF}2\alpha$, while ATF4 promotes XIAP protein degradation through the ubiquitin-proteasome system [368]. Whether this is the case in DRG neurons remains to be seen but it is clear that the

reduction in XIAP levels is key to remove the brake on caspases, permitting the execution of the apoptotic pathway.

The transition from the latent to the catastrophic phase marks a coordinated effort to increase the activity of caspases and other proteases like calpains. As was previously mentioned, the catastrophic phase is a point-of-no-return after which reintroduction of neurotrophic factors does not rescue degeneration, meaning that neurons are destined to die [315]. However, the observation the inhibition of caspase activity extends the point-of-no-return in NGF-deprived sympathetic neurons suggested that caspases are not the ultimate catastrophic event. Instead, the point-of-no-return in neurons seems to be the loss of the mitochondrial membrane potential ($\Delta\Psi_m$), which is ultimately dependent on the cellular ATP content, but only when caspase activation is inhibited [202]. It has been suggested that in the presence of caspase blockade, NGF-deprived neurons rely on glycolysis to produce ATP and sustain the proton gradient that maintains $\Delta\Psi_m$. When ATP ultimately drops, neurons enter into a second point-of-no-return, losing $\Delta\Psi_m$ and die by a mechanism known as secondary necrosis or mPT-dependent necrosis [202, 369, 370].

Interestingly, the transition from the latent to the catastrophic phase in DRG neurons seems to involve the participation of molecular players thought to have a much earlier role in the degeneration process. Phenomenologically, the transition period has been described as a time span where the axonal membrane acquires the typical blebbing pattern of degenerating DRG neurons deprived of NGF [232]. According to Yong et al. (2019), these blebs - or "spheroids" - eventually rupture in a form of necrotic cell death, leading to the expulsion of axoplasmic material containing "pro-degenerative molecules" to the extracellular environment. Thus, Yong et al. proposed that the material expelled from ruptured spheroids triggers catastrophic degeneration. The death receptor DR6 is required to hasten the entry into this phase of degeneration in response to pro-degenerative signals of unknown nature derived from degenerated axons. Interestingly, previous studies have shown that APP or secreted APP-derived proteolytic products act as DR6 ligands in the degeneration of deprived DRG neurons [331, 332]. In an interesting twist, p75NTR-Rho-actin signaling was shown to be necessary for cytoskeleton remodelling and spheroid formation - in parallel to caspase-mediated cytoskeleton

disintegration - during the transition period but prior to the catastrophic phase [232]. Thus, this new evidence contradicts previous studies showing no role for p75NTR during the developmental cell death of DRG neurons [12, 194].

1.5 The amyloid-precursor protein

The identification of the amyloid-beta peptides (A β) in senile plaques of patients with Alzheimer's disease (AD) prompted intense scrutiny of its origin and led to the discovery of the amyloid-precursor protein (APP) more than 30 years ago [371-373]. More than 200 dominantly inherited missense mutations in either APP gene or Presenilin-1 or 2 genes (subunits of the γ -secretase complex that cleaves APP to generate A β) have now been linked to early-onset familial AD. Mutations within APP are known to increase A β production, A β aggregation or changes in the ratio of A β species. Typical features of AD, such as tau aggregation, inflammation, reduced metabolism, degeneration of neural networks and cognitive impairments, are proposed to follow casual events associated with A β increase [374]. Given its well-established role on AD pathogenesis, intensive research has been done to understand the biological functions of APP. As a result, important physiological functions including neuronal plasticity, memory, and neuroprotection has been related to APP action. However, despite substantial progress, the full array of APP functions is uncertain, and efforts continue to focus on understanding its roles. With the need to delve into these issues, the last decade has produced interesting but contradictory results about the role of APP in peripheral neuronal degeneration during development. This section summarizes the most relevant aspects of APP biology, including a closing section on its role in developmental neuronal apoptosis in DRG neurons.

1.5.1 The APP family

Mammalian APP belongs to the APP family of proteins, which also includes the orthologs APP-like protein 1 and 2 (APLP1 and APLP2). The APP family is evolutionary conserved across a variety of species, with members found in invertebrates that include *C. elegans* (APP-like 1, APL-1) and *D. melanogaster* (APP-like, APPL) [375, 376]. Prokaryotes, plants and yeast do not express members of the APP family suggesting that evolutionary appearance of these proteins coincide with the evolution of the earliest nervous system with functioning synapse [377].

The human APP gene is localized on chromosome 21 (21q21.2-3), contains 18 exons that span approximately 270 kilobases, and undergoes several alternative-splicing events. APP is expressed ubiquitously, with the highest levels in the brain (including glia and neurons). The most abundant isoforms are APP695 (exons 1-6 and 9-18, predominantly isoform in neuronal tissues), APP751 (exons 1-7 and 9-18) and APP770 (exons 1-18) [378]. Expression levels of each isoform have been reported to increase progressively from early stages of embryogenesis (starting at E9 for rats and at the gastrulation stage for mice), suggesting important roles in development and beyond [379-382].

The APLP1 and APLP2 genes are located in chromosomes 19 and 11, respectively [383, 384]. Similar to the APP protein, the alternative splicing of APLP2 can produce a number of isoforms [385], while the APLP1 gene produces only a single transcript [386]. APLP1 and APLP2 share 40 to 50% amino acid identity with APP [387] and both undergo a similar proteolytic processing but without the production of A β peptide [388]. While APLP2 is ubiquitously expressed throughout the body, APLP1 expression is restricted to the nervous system [379, 389].

1.5.2 APP structure

Members of the APP family are type I single-pass transmembrane glycoproteins with a large extracellular N-terminal domain, a transmembrane domain and a short cytoplasmic C-terminal domain [371]. Although the complete X-ray structure of APP has not been resolved, individual domains within the ectodomain of the protein have been structurally characterized [382], with regions of high flexibility that likely enable multiple conformational changes and have interesting implication for APP functions and proteolytic processing [382, 390, 391].

The N-terminus region is the most divergent between APP family members and splice variants. It is composed of four main domains: the E1, the acidic, the E2 and the juxta-membrane domain. The E1 domain has three subdomains: a heparin-binding domain (HBD)/growth factor like (GFLD) domain, a copper binding domain (CuBD) and a zinc binding domain (ZnBD) [382]. Likewise, the E2 domain can be subdivided into a

second heparin binding domain and a random coil sequence. Together the E1 and E2 domains share a relative high sequence homology [387]. The acidic domain contains aspartic and glutamic acids residues linked to the E1 and E2 domains. This linking region could also contain the Kunitz-type protease inhibitor (KPI) domain and OX-2 domain (present only in APP770, 751 and APLP2). The KPI domain affects APP trafficking and processing *in vivo* [392], and inhibits multiple serine proteases *in vitro* [393]. The A β peptide resides partly within the extracellular linker sequence and within the transmembrane domain (TMD). The juxta-membrane region, including the A β peptide, is highly divergent and only APP gives rise to the A β peptide [388]. The TMD is followed by the short unstructured C-terminal domain with no obvious homology with other types of proteins but it is highly conserved among the APP family members. The APP intracellular domain (AICD) contains several phosphorylation sites and YENPTY, a conserved sequence that serves as a site for numerous functional protein interactions [394].

The APP family members can associate through the E1 and E2 domains to form homotypic or heterotypic *cis* dimers. Dimer formation can be modulated by heparin binding. Trans dimers are also possible between APP and APLPs, enabling them to function as synaptic adhesion molecules *in vitro* [395-397], and at the neuromuscular junction *in vivo* [396].

1.5.3 Proteolytic processing of APP

APP cleavage is a constitutive process generating different soluble variants that may have specific and even opposing roles. APP can undergo amyloidogenic and non-amyloidogenic processing depending on the proteases involved and on its cellular location [398]. In the amyloidogenic pathway APP is initially cleaved by β -secretase to produce a soluble secreted form of APP (sAPP β) and a C-terminal fragment (β APP-CTF). The subsequent cleavage of β APP-CTF by γ -secretase produces the A β peptide and the AICD. In the non-amyloidogenic pathway, APP is first cleaved by α -secretase within the A β sequence to generate the soluble secreted sAPP α fragment and the membrane-tethered α APP-CTF. This is followed by γ -secretase cleavage of α APP-CTF, resulting in release of the P3 peptide and AICD. The cleavage sites for α -secretase and β -secretase

are found in the flexible juxta-membrane region that links E2 with TMD, whereas the γ -secretase cuts within the TMD [399].

The α -secretase belongs to the A Disintegrin and Metalloproteinase (ADAM) family and three enzymes have been identified to have α -secretase activity against APP: ADAM9, ADAM10 and ADAM17 [400]. Of these, ADAM10 is thought to be a central player in the processing of APP [401]. APP undergoes constitutive cleavage by ADAM10, which is reported to release approximately 30 % of cell surface APP as sAPP α [402]. Rates of APP cleavage increase above constitutive levels through 'regulated' cleavage particularly in neurons, mostly guided by ADAM17/TACE [403, 404]. The regulated pathway involves the activation of PKC [405], with PKC-regulated α -secretase activity largely localized to intracellular trans- or post-Golgi compartments [406], and constitutive α -secretase activity predominantly at the cell surface [407].

The β -secretase (also known as β -site APP cleaving enzyme, or BACE) activity initiates the amyloidogenic pathway. BACE is a type I single-transmembrane aspartyl protease highly expressed in the brain. BACE1 is most active in acidic environments, which suggest that APP cleavage by the β -secretase occurs within the Golgi apparatus and endosomes [408]. However, secreted sAPP β is found in cerebrospinal fluid [409], and can be secreted by neurons indicating that sAPP β might be additionally generated at the plasma membrane or sorted to the secretory trans-Golgi network. Due to its promiscuous proteolytic activity in the juxta-membrane domain, several species of A β peptide (ranging from 37 to 49 residues long) can result from the cleavage of the β APP-CTF by γ -secretase [410]. Of these species the most abundant are A β 40 (80 to 90%) and A β 42 (5 to 10%) [411].

The γ -secretase is an intramembrane cleaving aspartyl protease made up of a multi-subunit complex consisting of four proteins: anterior pharynx-defective-1 (APH-1), nicastrin, presenilin-1 (PS1) or presenilin-2 (PS2) and presenilin enhancer-2 (PEN-2) [412]. Presenilin is the catalytic component of the complex, structured as a multipass, nine-membrane domain protein [413]. Presenilin is activated after cleavage [414]. PEN-2 facilitates the cleavage of presenilin allowing for its trafficking from the ER to the Golgi apparatus [415]. Presenilin cleaves APP at several sites within the TMD and contributes to the production of A β peptides of different lengths [416]. In addition, the γ -secretase

releases the AICD from the membrane; the AICD has been suggested to translocate to the nucleus where it may act as a transcription factor [417, 418].

Additional APP cleavage pathways yielding N-terminal APP fragments have been discovered. These include the δ -pathway, η -pathway and meprin pathway [419]. Some of the fragments derived from these pathways have been implicated in AD pathogenesis. With the exception of the A η fragment, which reportedly attenuates neuronal activity [420], very little is known about their physiological relevance. Furthermore, caspase cleavage of APP-CTF may contribute to accumulation of various APP fragments [421-424]. This multiplicity of cleavage pathways and the production of several soluble fragments increases the complexity of APP functions in the nervous system.

1.5.4 APP trafficking and transportation

Full-length APP is synthesized at the ER, subject to N-glycosylation and then transported through the Golgi/trans-Golgi network (TGN) where it undergoes O-glycosylation to form mature APP. Subsequently, secretory vesicles shuttle APP from the TGN to plasma membrane [425]. APP localization at the cell surface is regulated by a balance between the efficiency of APP secretory trafficking and internalization, and the efficiency of secretase processing. Residency of APP at plasma membrane correlates with higher stability of the protein and its potential to dimerize, which favours the non-amyloidogenic processing leading to a reduction of A β production while diminution of APP at the cell surface increases BACE1-dependent amyloidogenic processing and secretion of A β [426]. Interestingly, only about 10% of total cellular APP localizes at the plasma membrane [399], and it is estimated that it remains there as a full-length protein for only 10 minutes or less before being recycled or cleaved. The presence of the YENPTY endocytic sorting motif on the C-terminus domain of APP (residues 682-687 of the APP695 isoform) allows APP re-internalization via clathrin-coated pits [427, 428]. The endocytic re-entry can carry APP to sorting/recycling endosomes and then back to the plasma membrane, to the TGN/Golgi, late endosome/lysosome or to the ER/nuclear envelope. Another interesting destination is the ER-mitochondria contact site where APP

and/or APP fragments have been shown to accumulate [429, 430]. Notably, mitochondria have been shown to contain full-length APP and its fragments [431].

Within neurons, APP has been detected in almost every compartment, from the presynaptic growth cones and axons to postsynaptic compartments, where APP processing can be regulated by synaptic activity [432-434]. In axons, APP undergoes fast anterograde and retrograde transport in non-clathrin coated vesicles complex through the YKFFE sequence of the C-terminal domain to the μ 4 subunit of the heterotetrametric adaptor protein (AP) complex AP4 [435]. The scaffolding protein JNK-interacting protein (JIP1), originally identified to recruit multiple kinases to the JNK pathways [436], regulates the directionality of APP axonal transport in a phosphorylation-dependent manner by coordinating kinesin and dynein motors [437]. Anterograde fast transport of APP-containing vesicles depends on the activity of Rab3A, promoting the disassembly of vesicles coats and the recruitment of microtubule-based molecular motors [438]. Interestingly, cumulative evidence indicates that APP, presenilin-1 and BACE1 are transported in different membrane components along axons [439]. Some reports have failed to detect A β within the axonal compartment [439, 440], whereas others have indicated that impaired axonal transport of APP correlates with an increase production of A β [441].

1.5.5 Biological functions of the APP family during neuronal development

APP has been called the “All Purpose Protein” in response to the widely-ranging proposed functions, many of which remain controversial [397, 442]. APP has been predicted to be a cell surface receptor since its initial discovery [372], although accumulated evidence suggests a more diverse and multimodal repertoire of actions, including co-receptor and ligand roles [331, 332]. Because the APP family proteins have no intrinsic enzymatic activities, APP-mediated signal transduction relies on interactions with other membrane and/or adaptor proteins. More than 200 extracellular and intracellular binding partners have been so far identified, including diverse extracellular matrix proteins, transmembrane receptors and intracellular signaling adaptors [443-445]. As the vast signaling of APP and its soluble variants have already been expertly reviewed

[444-446], this section will address the signaling and biological functions of APP in relation to the processes of neuronal development.

1.5.5.1 Lessons from knockouts

Genetic deletion of APP and its homologues in animal models have offered important insights on their biological significance. Mice lacking every possible combination of APP family protein have been generated [447, 448]. Individual deletions of APP or APLPs produce mild phenotypes, likely due to overlap in functions between family members. Nevertheless, single APP-null mice display altered circadian activity, and defects in spatial learning and long-term potentiation (LTP). Attempts to examine dendritic spine density in APP-null mice have revealed mixed results. Apical dendrites of layers III and V neurons of the somatosensory cortex at 4-6 month of age have a two-fold higher density of spines than wild-types [449], and the number of functional synapses in cultured hippocampal neurons increases in APP-null mice [450]. However, a significant decrease in spine density has been found in cortical layers II/III and hippocampal CA1 pyramidal neurons in 1-year old APP-null mice compared to wild-type controls [451] while cultured hippocampal neurons of APP-deficient mice show reduced spine density and synapse formation [452].

APP-null mice have also shown decreased locomotor activity and grip strength [453-455], implying a defect in neuromuscular transmission or muscle contraction. APP-null mice have reduced body and brain weight [454, 456], reactive gliosis [454], axonal growth/white matter defects [456], axonal transport defects [457-459], increased levels of copper [460], sphingomyelin and cholesterol in the brain [461], as well as decreased plasma glucose levels and hyperinsulinemia [462].

The function of APP in the PNS has not been extensively explored but it is established that APP is expressed in sensory neurons [331, 333], and is targeted to presynaptic terminals [438, 463, 464]. APP695 has been reported as the predominant isoform synthesized in sensory neurons [464] and sciatic nerves of adult APP-null mice present higher G-ratios, meaning thinner myelin sheaths and increased distances between nodes of Ranvier, a region where APP seems to be particularly clustered [465].

Myelination of sciatic nerves of postnatal day 14 was not altered by APP deletion but the optic nerve of APP-null mice shows a reduction of myelinated segments. Truong et al (2019) reported that overall axonal density in both nerves is slightly increased in APP-null mice but the difference from wild-type littermates did not achieve statistical significance [466]. Interestingly, mice overexpressing APP have reduced sensitivity to pain [467] but pain sensation in APP-null mice is normal [468].

Single APLP1-null and APLP2-null mice exhibit subtle phenotypes; APLP1-null mice have decreased in weight [469] and APLP2-null mice exhibit elevated copper levels in the cerebral cortex [460]. In contrast to these minor phenotypes, some double knockouts have more remarkable outcomes. Perinatal lethality was observed in APP::APLP2 and in APLP1::APLP2 compound null mice whereas APP::APLP1 compound null mice only display a modest decrease in body weight [469, 470]. These data suggest that APLP2 may be indispensable for life and that it can compensate the loss of APP or APLP1 [448]. Accordingly, triple deficient mice (APP::APLP1::APLP2) exhibit cranial abnormalities, focal dysplasia, partial loss of cortical Cajal-Retzius cells and die shortly after birth [471]. Together, these findings support the idea that the APP family of proteins play an essential role in normal brain development.

1.5.5.2 APP in neurogenesis, differentiation and migration

APP has been shown to regulate various aspects of neurogenesis. As noted above, APP mRNA is expressed as early as E9.5 in the mouse neural tube, which coincides with the peak of neural differentiation and neurite outgrowth (Salbaum and Ruddle, 1994) [472]. Ablation of APP in mice enhances neural progenitor cell (NPC) differentiation during embryonic development *in vivo*, while increases neurogenesis up to 40-50% during *in vitro* differentiation [473]. Zhang et al. (2014) have shown that APP represses miR-574-5p in NPCs in the subventricular zone (SVZ) and cortical plate (CP). The reduction of miR-574-5p expression enhances the proliferation of neural progenitor pool, which is primarily composed of radial glial cells (RGCs). Reduction of miR-574-5p also impedes the differentiation of RGCs into neurons and inhibits the migration of immature neurons from the SVZ to the CP in the developing cortex. Coincidentally, the

overexpression of APP in NPCs accelerates their migration into the cortex [474]. Rice et al. (2012) have shown that pancortins, which are glycoproteins highly expressed in the developing cortex, functionally interact with APP to regulate NPC migration in the mammalian cortex [475].

Several studies have also shown that sAPP α increases the proliferation of embryonic neural stem cells (NSC) *in vitro* [476, 477]. The reduction of NPC proliferation in the subventricular zone of adult mice that occurs on APP knockdown can be rescued by sAPP α infusion *in vivo* [478]. Moreover, the reduced proliferation of NPC upon inhibition of α -secretase activity can be overcome by adding recombinant sAPP α to the cultured media [479].

In contrast, AICD negatively regulates the transcription of the gene encoding the endothelial growth factor receptor (EGFR), which is known to drive the proliferation of NPC [480, 481]. Furthermore, the expression of AICD in APP-null mice reduces NPC proliferation and neurogenesis in the hippocampus [482]. TAG1, a member of the F3 family, binds APP and induces generation of AICD to negatively regulate neurogenesis [483]. Recent evidence suggests that AICD negative regulation of neurogenesis stimulates gliogenesis [484].

The role of A β during neurogenesis have been contradictory [485]. A β peptides decrease the proliferation of NSC and induce gliogenesis [486] but a careful dissociation between species showed that A β 40 preferentially enhances neurogenesis in NSCs and primary NPCs, while A β 42 appear to favour gliogenesis in the same cells [487, 488]. However, it has been also reported that A β 42 and not A β 40 favours neurogenesis of hippocampal-isolated NSCs, and that this activity is a property of A β oligomers and not A β fibrils [489].

1.5.5.3 APP in neurite outgrowth and guidance

Numerous *in vitro* studies have established that APP plays a role in neurite outgrowth, either independently or through its interaction with other proteins such as integrins [490] or Disabled-1 [491, 492]. APP is found in the lamellipodia of murine growth cones [438, 493], where it colocalizes with Fe65 [493], thus modulating actin dynamics

through Rac1 [494]. Furthermore, sAPP α interact with Sema3A, a secreted axonal outgrowth inhibitor, and inhibits Sema3A-induced growth cone collapse [495, 496]. In addition, the neurotrophin receptor p75NTR has been reported to bind sAPP α and promote neurite outgrowth in cortical neurons [497]. Accordingly, distal axonal outgrowth and total neurite branching are reduced in APP-null hippocampal neurons *in vitro*, although cellular and local neurite adhesion is increased [452].

The chemotropic factor netrin-1 has been proposed to act as a functional ligand for APP, while negatively regulating A β production [498]. In addition, it has been shown that the netrin receptor DCC forms a complex with APP and that this complex is required for the proper guidance of commissural axons [499]. Consistent with this, APP-null mice display smaller ventral projections than wild-type counterparts [456]. More recently, APP has been identified as a novel receptor for Slit, another axon guidance ligand. Slit binding to APP through the E1 triggers APP ectodomain shedding, recruitment of the intracellular Fe65 and Pak1 complex, and associated Rac1-GTPase activation [500].

1.5.5.4 The role of APP in developmental neuronal cell death of DRG neurons

Several studies over the last decade have investigated the role of APP in developmental apoptosis of DRG neurons [331-333, 348]. The overlap between the molecular mechanisms driving developmental cell death and those mediating axonal degeneration in pathological conditions have driven interest in understanding APP function in the context of sensory axon degeneration [441]. Axonal degeneration is one of the primary pathological hallmarks preceding neuronal death in AD and Cuello and colleagues have proposed that a lack of trophic support is a critical contributing factor to the brain pathology associated with AD [501-503]. Thus, the study of APP functions in developmental neuronal pruning and death may provide insights that are relevant to APP-related neurodegenerative disease.

1.5.5.4.1 APP in DRG development: pro-survival versus pro-degenerative

As with many other aspects of APP biology, studies of its role during naturally occurring cell death of peripheral neurons have produced contradictory results. In an early

study, Nishimura et al. (2003) proposed that APP is an intrinsic trophic factor required for NGF-induced DRG maturation, axonal growth and survival [333]. The authors reported that APP accumulates in axons of primary DRG neurons *in vitro* during the course of NGF-induced development and that the blocking its extracellular domain impaired neuronal maturation [333, 454]. In line with APP trophic action, reduction of APP levels by antisense oligonucleotides during trophic deprivation significantly increased neuronal degeneration [504]. Additionally, several other studies have shown that cell-associated APP enhances neuronal viability in normal and noxious conditions in various neuronal cell types [447].

Another set of studies suggested that APP has a dark side in developmental contexts, facilitating the degeneration of axons *in vitro* and *in vivo* [331, 332]. APP genetic deletion was reported to impair the developmental degeneration of RGC axons *in vivo* while protecting DRG axons from degeneration in NGF-deprivation conditions *in vitro* [332, 348]. Initially, it was proposed that BACE1-mediated cleavage of APP generates a ligand for the death receptor DR6 that exerts pro-degenerative effects [331]. In these experiments, BACE1 inhibitors or antibodies against APP N-terminal domain effectively rescued DRG neuronal degeneration [331, 348]. However, this model was revised in light of results showing that the genetic deletion of BACE1 did not rescue the degeneration of DRG neurons after NGF deprivation [332]. This suggested that BACE1-mediated APP cleavage is not required and that DR6-mediated neuronal cell death in the absence of trophic support requires association with full-length APP. Some structural analyzes have supported the hypothesis that DR6 and full-length APP can directly interact [505, 506].

Separate studies have shown the capacity of A β to mediate neuronal death through DR6 and/or p75NTR [507-513]. However, degeneration induced by synthetic A β is not blocked by the genetic deletion of DR6 and degeneration of DRG neurons upon NGF deprivation is not rescued by blocking antibodies against A β peptide [331]. Thus, APP may have a double role that is dependent on the trophic factor context: pro-survival in the presence of trophic support and pro-death in absence of trophic support. With some caveats, particularly in its controversial pro-death role during NGF derivation in DRG neurons [331, 333] APP actions resemble those associated with dependence receptors.

1.5.5.4.2 The interplay between APP and the neurotrophin receptor TrkA

TrkA has been described as a dependence receptor, exerting pro-survival or pro-death functions depending on the presence or absence of NGF respectively [12]. Interestingly, some studies have demonstrated an intricate bidirectional interplay between TrkA and APP in CNS and PNS neurons, including DRG neurons, on the basis of a complex regulation of APP phosphorylation state in its C-terminal domain.

The crosstalk between TrkA and APP was initially observed two decades ago in studies showing that APP potentiates NGF/TrkA survival signaling [514], and that a NGF/TrkA signaling pathway promotes APP phosphorylation [515, 516]. Based on this evidence Matrone et al. (2011) hypothesized that APP and NGF/TrkA crosstalk may take place through the phosphorylation of tyrosine residues on the APP C-terminal domain [334]. This region contains an evolutionary conserved Y⁶⁸²ENPTY⁶⁸⁷ motif that often represents a crucial docking site for intracellular adaptors. Several studies have shown that YENPTY motif of APP can bind different proteins, some when Y682 is phosphorylated, such as Grb2, Shc, Grb7 and Crk [515, 517, 518], and others, such as Fe65, that bind when Y682 is not phosphorylated [518]. Matrone et al. (2011) demonstrated that NGF-dependent TrkA activity leads to APP tyrosine phosphorylation at Y682 that in turn enhances a direct interaction of TrkA with APP. In APP-Y682G knock-in mice, NGF fails to induce the phosphorylation of APP and TrkA does not bind APP [334, 519]. Other studies have also reported that TrkA and APP interact in response to NGF [520, 521] and that the capacity of TrkA to impede APP homodimerization influences A β production [522-525]. The Y682G mutation alters TrkA cellular distribution and induces the accumulation of APP in intracellular compartments [334, 526, 527]. Additionally, Y682G seems to disrupt the interaction between APP and the sortilin-related receptor SorLA, resulting in endo-lysosomal dysfunctions and neuronal degeneration [528]. Y682G knock-in mice display a premature, age-dependent decline in cognition, learning and locomotor performance [529], coincident with the phenotypic defects observed in APP-null mice described previously. Notably, DRG neurons from Y682G knock-in animals, which require NGF to grow and differentiate *in vitro*, die a few days after culturing [334], suggesting an interplay between TrkA and APP in NGF signaling.

Threonine 668, located just upstream the YENPTY motif (T668, referring to APP695 numbering), is another important phosphorylation site within the APP C-terminal domain that dramatically regulates the APP interactome. The phosphorylation of APP at T668 affects the YENPTY motif, in this case through remote conformational changes, therefore altering the binding specificity and affinity of APP intracellular domain for other cytosolic partners [518, 530, 531]. A recent study has demonstrated that NGF/TrkA signaling modulates APP phosphorylation at T668 as it does with Y682, but in an opposite manner. Triaca et al. (2016) showed that adding NGF to hippocampal slices decreases T688 phosphorylation, while the opposite occurs when PC12 cells are deprived of NGF [335]. In addition, APP-T688 phosphorylation depends on JNK and CDK5 activation, while NGF/TrkA-mediated inactivation of JNK/CDK5 decreases phospho-APP-T668 levels. These authors also reported that TrkA does not colocalize or co-precipitate with APP when T688 is phosphorylated, while NGF supplementation increases TrkA-APP complex formation at the expense of BACE1 interaction, thus favoring its non-amyloidogenic processing [335]. Importantly, T668 phosphorylation has been previously related to APP pro-death roles, with AICD-induced cell death was shown to be abrogated in T668A mutants [532]. Several other studies have demonstrated that T668 is directly phosphorylated by JNK1/2/3, CDK1/5 and GSK3 β , all of which are activated in different cell death contexts, including the degeneration of DRG neurons induced by NGF deprivation [533-537].

The following model can be extracted from the study of Matrone et al. (2011) [334] and Triaca et al. (2016) [335]: 1) In the presence of NGF, TrkA binds APP, constituting a hetero-complex that depends on the TrkA-mediated phosphorylation of APP at Y682. In this configuration, APP fosters TrkA-dependent survival and TrkA blocks APP from entering the amyloidogenic route. 2) In the absence of NGF, TrkA switches to its pro-death mode, typical of dependence receptors, the APP-TrkA complex dismantles and Y682 phosphorylation does not occur. JNK mediates APP phosphorylation at T668, and APP enters a pro-degenerative mode, favouring homodimerization and accessibility to BACE1, prompting the amyloidogenic pathway and the generation of the toxic A β peptide. In addition, phosphorylated T668 can recruit the intracellular adaptor Fe65, thereby stabilizing the AICD which translocates to the nucleus to induce FoxO-mediated cell death

[518, 530, 532, 538]. The commonalities of this model with the reported roles of TrkA and APP in DRG neurons grown with and then deprived of NGF is striking. However, the extent to which they coincide is unclear, and several unanswered questions have accumulated, for example: Do TrkA and APP interact during DRG growth in the presence of NGF? Does NGF deprivation or unliganded-TrkA increase T668 phosphorylation in APP? What protein kinases would be involved in APP-T668 phosphorylation? Does T668 phosphorylation facilitates the interaction between APP and DR6? Are there additional pro-degenerative routes taken or controlled by APP in its phosphorylated state at T668? Clearly, the interplay between TrkA and APP in DRG neurons deprived of NGF requires further investigation.

1.5.5.4.3 APP and the regulation of intracellular Ca²⁺: fostering ER stress?

Ca²⁺ is a major player in the regulation of cell death, both at the early and late stages of apoptosis. Early Ca²⁺ dysregulation can induce the ER-stress response and the induction of the intrinsic apoptotic pathway [241, 539], while late increases in cytoplasmic Ca²⁺ are necessary to initiate the catastrophic phase [232, 540]. The degeneration of DRG neurons deprived of NGF have shown evidence in both directions. Several molecular markers of the ER-stress response increase in DRG neurons upon NGF deprivation [322]. During later phases of degeneration, right before axonal blebbing and the formation of spheroids, axoplasmic Ca²⁺ rises [232, 329, 360], and EGTA is able to rescue degeneration of DRG axons deprived of NGF [329, 360].

The role of APP in the modulation of Ca²⁺ and the ER stress response in DRG neurons deprived of NGF is unknown. However, several studies have demonstrated a relationship between APP and ER stress-induced cell death in different cell types. For example, APP overexpression in PC12 cells induces the ER-stress marker CHOP and potentiates the increase in cytoplasmic Ca²⁺ during apoptosis induced by the depletion of ER Ca²⁺ content with thapsigargin, an inhibitor of the ER Ca²⁺ pump SERCA [541]. In addition, tunicamycin or dithiothreitol-induced ER stress increases both APP mRNA expression and the levels of the AICD. Accumulated AICD associates with the promoter region of the *CHOP* gene and facilitates CHOP expression. Notably, cell death and CHOP up-regulation induced by ER stress are attenuated by APP knockdown [542].

Interestingly, the activation of the major regulator of the ER stress response, the translation factor eIF2 α , promotes BACE1-mediated accumulation of the A β peptide [543]. In addition, blockage of ER Ca²⁺ release using inhibitors of IP₃R or ryanodine receptors (RyR) prevents cortical neuronal death in response to A β [544].

ER Ca²⁺ release must be followed by rapid Ca²⁺ replenishment to avoid ER stress. Ca²⁺ reuptake from the cytosol occurs via SERCA pumps and cytosolic Ca²⁺ levels reach homeostasis by Ca²⁺ entering the cell from the extracellular milieu. In neurons, the entry of extracellular Ca²⁺ occurs via channels at the plasma membrane operated by voltage (VOCCs), ligands (ROCCs) or - induced by depletion of intracellular Ca²⁺ stores - via SOCCs. Typically, Ca²⁺ flux through SOCCs is referred as capacitive Ca²⁺ entry (CCE) or store-operated Ca²⁺ entry (SOCE). Stromal interaction molecule 1-2 (STIM1 or 2) are the ER Ca²⁺ sensors activating SOCCs at the plasma membrane, whereas Orai1 is the pore forming component of SOCCs. Other less selective Ca²⁺ channels are also activated upon depletion of ER Ca²⁺ stores, particularly TRPC channels [545, 546]. SOCE was originally thought to be absent or negligible in neurons [547], given VOCCs and ROCCs, however, several studies have shown a functional SOCE in different types of neurons including DRG neurons [548-551].

Although somewhat controversial, APP may play a role in SOCE regulation, altering the basal ER Ca²⁺ levels in different cell types. In astrocytes, ER Ca²⁺ store content is significantly reduced by the genetic deletion of APP, while the expression of Orai1 and TRPC1 proteins, essential components of SOCE, are downregulated in APP-null astrocytes [552]. No alterations of ER Ca²⁺ levels, SOCE and expression of TRPC1/4/5 were observed in cultured astrocytes from Tg5469 mice overexpressing APP [552], yet previous studies have shown that APP knockdown in a neuronal cell line derived from cerebral cortex of a trisomy 16 mouse (Ts16) - which normally overexpress APP five to six times - decreases intracellular basal Ca²⁺ levels [553]. Interestingly, it was previously reported that Ts16 neurons die faster than diploid neurons under identical culture conditions, while age-dependent Ca²⁺ levels are elevated in Ts16 neurons [554]. In addition, overexpression of the A β peptide was shown to potentiate SOCE in neuronal 2a cells [555] while HEK293 cells lacking APP or AICD showed lower levels of ER Ca²⁺ [556].

Other studies have shown the involvement of APP in the maintenance of physiological ER Ca²⁺ levels, but with opposite results. Recently, knockdown of APP expression was shown to elevate resting ER Ca²⁺ levels in T84 epithelial cell line, to prolong emptying of ER Ca²⁺ stores upon SERCA inhibition, and to delay STIM1 translocation to Orai1 [557]. In addition, SOCE is dramatically attenuated in mouse neural N2a cells stably expressing APP [555, 558]. An attenuation of SOCE has also been reported in hippocampal neurons isolated from FAD-APP knock-in mice. These mice show high levels of A β , overfilled ER Ca²⁺ stores, and a compensatory downregulation of STIM2 expression [559].

Based on the above evidence, would be worth exploring whether APP modulates SOCE and ER Ca²⁺ levels in embryonic DRG neurons during developmental degeneration. Interestingly, SOCE attenuation and reduced ER Ca²⁺ levels have been reported in fibroblasts deficient of the pro-apoptotic proteins BAX and BAK [296, 560]. Thus, exploring how APP modulates SOCE and ER Ca²⁺ levels in DRG neurons may help to determine the still controverted role of APP in the degeneration of NGF-deprived DRG neurons. These questions are addressed in chapter 2 of this thesis.

1.5.5.4.4 APP and mitochondria

Mitochondria act as decision nodes in multiple physiological and pathological processes. Some of these functions include the regulation of the energy metabolism, the modulation of intracellular Ca²⁺ stores, in close contact with the ER, and - in intimate relation with it - the control of cell death decisions [561]. The degeneration of DRG neurons deprived of NGF take place through the mitochondrial/intrinsic apoptotic pathway, with the decisive participation of BAX, the induction of MOMP and the downstream activation of executioner caspases [167, 213, 214, 316]. Although APP is involved in the degeneration of sensory neurons deprived of NGF [331] nothing is known about its interaction with the mitochondria.

The close interplay between the ER and mitochondria suggest that the deficiencies in SOCE and ER Ca²⁺ observed in cell deficient or overexpressing APP may cause, or be the consequence of, mitochondrial defects. Indeed, decreased SOCE and/or ER Ca²⁺ levels resulting from reduced AICD levels correlates with reduced ATP content and

mitochondria hyperpolarization [556]. Interestingly, APP-null astrocytes not only show decreased active Ca^{2+} microdomains, reduced frequency of spontaneous Ca^{2+} transients and slower Ca^{2+} kinetics but also display fragmented mitochondria [562]. Microdomains of intracellular Ca^{2+} are often shaped by the mitochondrial Ca^{2+} buffering capacity [563-565]. Using the mitochondrial Ca^{2+} sensor mito-GcAMP, Montagna et al. (2019) showed that the capacity of the mitochondria to buffer Ca^{2+} is impaired in APP-null astrocytes [562].

Other studies have shown alterations of mitochondria-dependent biochemical parameters in the absence of APP. For example, Pera et al. (2017) showed that the oxygen consumption rate of APP-null MEFs is significantly increased compared to wild-type MEF cells [430], while others showed reduced mitochondrial membrane potential and ROS production in APP-null MEFs [566]. Also, Pan et al. (2018) recently reported that APP-null osteoblasts show a reduction in ATP production by oxidative phosphorylation, together with a deficiency in spare respiratory capacity [567].

APP has been reported to localize to mitochondria and form a complex with the translocase of the outer mitochondrial membrane (TOMM40) and the translocase of the inner mitochondrial membrane 23 (TIM23). Studies suggest that this complex arrests the import of nuclear-encoded mitochondrial proteins, causing disruption of mitochondrial ATP synthesis, reduction of mitochondrial membrane potential and cytochrome oxidase activity [568, 569]. Three positively charged residues of the APP N-terminal domain seem to guide APP localization to mitochondria [568]. More recent evidence suggests a 12 amino acid stretch located in the juxtamembrane region of the C-terminal domain of APP acts as an important mitochondrial localization signal. Deletion of this sequence decreases APP mitochondrial localization while increasing ROS, decreasing ATP levels and depolarizing the mitochondrial membrane potential. Mitochondrial morphology was also altered, resulting in an increase of spherical mitochondria in cells expressing the mutant APP variant [570]. Interestingly, this sequence contains several phosphorylated sites including Y728, T729 and S739 (APP-KPI splice variants numbering), suggesting that the loss of phosphorylated residues might disrupt transport to the mitochondria [570]. It would be interesting to determine whether APP-phosphorylation regulators such as TrkA influence localization of APP to the mitochondria.

Mitochondria contain functional γ -secretase that can cleave the 83 aa C-terminal fragment (CTF83) of APP. Such cleavage is the last step required to generate AICD and A β [571]. A β has been found within the mitochondria and reportedly alters mitochondrial functionality [572, 573]. As noted above ER-mitochondrial contact sites are domains where APP is processed and A β produced [574, 575]. Interestingly, in young hippocampal neurons, A β oligomers increase the number of ER-mitochondria contact sites and enhance Ca²⁺ transfer from the ER to mitochondria. However, in aged hippocampal neurons, A β oligomers exacerbate the loss of SOCE, increase the resting cytosolic Ca²⁺ concentration and the Ca²⁺ store content, suppress Ca²⁺ transfer from ER to mitochondria, decrease mitochondrial potential and enhance ROS generation [576, 577]. A β toxicity appears to be mediated mainly through its effects on the mitochondrial respiratory chain, given that Rho-0 cells (ρ 0), which lack a functional respiratory chain due to an absence of mitochondrial DNA, do not experience the increase in ROS production, cytochrome *c* release and caspase activation induced by A β in wild-type cells [578]. Notably, the AICD can enter the mitochondria, particularly in complex with the intracellular adaptor Fe65, decreasing mitochondrial membrane potential, ATP levels and superoxide production [579].

1.6 Developmental cell death of BDNF-dependent DRG neurons

Beyond the concept “selection of the fittest”, rooted in the neurotrophic theory and implemented through competition for limited amount of trophic support, little is known about the mechanisms of developmental cell death of BDNF-dependent DRG neurons. This section brings together the studies that directly or indirectly shed light onto this still obscure episode of DRG neuron development. Chapter 3 addresses the developmental cell death of BDNF-dependent DRG neurons from an experimental point of view.

1.6.1 Supporting developmental survival of DRG neurons by BDNF

Implicit in the neurotrophic theory is the fact that the trophic factors for which neurons compete to avoid developmental death, like NGF or BDNF, must support neuronal survival. As obvious as it sounds, the capacity of BDNF to support the survival of DRG sensory neurons during development has been controversial. Initial studies addressing the spectrum of activity of BDNF [580], among nine distinct populations of sensory neurons from embryonic chicks of 3 to 14 days incubation (E3-E14) showed that explants maintained *in vitro* responded to BDNF with sustained survival and profuse outgrowth [581-584]. In all explants, including DRG, trigeminal, geniculate and petrosednodosal ganglia, the response was maximal between E10 and E12, and there was a decline in the magnitude of the response from E12 to E14 [582]. Soon after, the concept that BDNF regulates neuronal survival during normal development was reinforced *in vivo*. Just as with the prototypical neurotrophic factor NGF [585, 586], Hofer and Barde (1988) demonstrated that repeated administration of exogenous BDNF into quail embryos daily from E3 to E7 significantly rescued and increased the number of DRG neurons at E8 compared with non-treated embryos [586]. Similarly, BDNF absorbed on laminin-coated silastic membranes and grafted in chick embryos at the 30-32 somite stage rescued a population of developing DRG neurons [587].

The generation of BDNF-deficient animals helped strengthen the hypothesis that BDNF was required for the survival of neuronal populations during development. Several studies have shown that BDNF-null mice display a significant decrease (~30%) in DRG

sensory neurons at P0 [129, 130, 588]. Similar DRG neuron losses were observed earlier in E13 BDNF-deficient embryos [588]. Survival of sympathetic, midbrain dopaminergic and motor neurons was not affected in BDNF-null animals and no gross anatomical structural abnormalities were observed in the CNS [129, 130]. Interestingly, although most BDNF-null mice die within 2 days after birth, a fraction survives for 2-4 weeks. These animals develop symptoms of nervous system dysfunction, including severe deficiencies in coordination and balance, associated with excessive degeneration of various sensory ganglia (vestibular, trigeminal, petrose-nodosal and dorsal root ganglia).

Animals lacking the neurotrophin receptor TrkB develop to birth but most die by P1. These animals display a more severe phenotype than mice lacking BDNF, with neuronal deficiencies in the central (facial and spinal cord motor neurons) and peripheral (trigeminal and DRG neurons) nervous system [589]. However, the scale of DRG neuronal loss is the same in BDNF- and TrkB-deficient mice [115, 129, 130, 589].

Several studies of transgenic mice that overexpressed either NGF or NT3 showed that these NTs caused a significant increase in the survival of trigeminal and DRG neurons and increased sensory innervation at the skin [148, 590]. To determine whether over-expressed BDNF could also have an impact on neuronal survival *in vivo*, LeMaster et al. (1999) produced transgenic mice that overexpressed BDNF in the skin. In contrast to NGF and NT3, overexpression of BDNF did not increase the number of trigeminal or DRG neurons present at P7 but did induce a 38% increase in number of neurons in the petrose-nodosal ganglia [149]. Similar results were reported in studies of LoPresti and Scott (1994) where BDNF had only a slight effect on survival of DRG neurons supplying chicken skin [591]. Thus, sensory neurons of different origins showed inherent difference in their response to skin-derived BDNF; petrose-nodosal ganglia neurons showed increased survival whereas survival of trigeminal and DRG neurons were unaffected. Cutaneous BDNF overexpression did result, however, in enhanced innervation to hair follicles, Meissner corpuscles and Merkel cells [149], suggesting that BDNF produced by the skin does not function as a target derived survival factor for developing DRG sensory neurons that innervate the skin but rather as a regulator of neuronal differentiation once their axons reach their target. Perhaps, other BDNF-sensitive sensory neurons than those innervating the skin are lost in DRG and trigeminal ganglia.

Interestingly, overexpression of NT4 in the skin, another known ligand for TrkB, enhances myelinated sensory endings but, similar to BDNF overexpression, does not influence sensory neuron number in either the DRG or trigeminal ganglia [592]. This is consistent with results of Liebl et al. (2000), who had previously demonstrated that NT4 is a required for differentiation but not survival of BDNF-dependent mechanoreceptors and others who showed that sensory neuron populations in the DRG and trigeminal ganglion are not altered in NT4 knockout mice [120, 130, 131, 588, 593]. Interestingly, although BDNF-null mice display loss of DRG sensory neurons whereas NT4-nulls do not, expression of NT4 from the BDNF locus rescues neurons that would otherwise be lost in the BDNF-null [594]. However, mutant mice with a point mutation in the cytoplasmic domain of TrkB that alters the binding site for the intracellular adaptor protein Shc, show the loss of NT4-dependent sensory neurons (50% of petrose-nodosal ganglia and D-hair mechanoreceptors) while BDNF-dependent sensory neurons (50% of petrose-nodosal ganglia, vestibular ganglia neurons) were only modestly affected [153]. Taken together, these data indicate that BDNF and NT4 signaling pathways are partially, but not entirely, overlapping.

Instead of being target-derived, the effect of BDNF on DRG survival was suggested to be autocrine and important for adult neurons, but not required during embryonic development. Early, Acheson et al. (1995) showed that reducing endogenous BDNF in cultured adult DRG cells using antisense oligonucleotides substantially reduced neuronal survival. Exogenously added BDNF rescued virtually all of the antisense susceptible DRG neurons, suggesting an autocrine role for BDNF in mediating the survival of adult DRG neurons. Similar effects were found with NT4, however neither NGF, bFGF, EGF and CNTF were effective in rescuing adult DRG neurons [595]. Interestingly, NT3 also rescued neurons from BDNF antisense oligonucleotide-mediated cell death in a dose-dependent fashion with similar potency and efficacy as BDNF. The rescue with NT3 agrees with data showing that the majority of TrkB expressing neurons in adult DRG also express TrkC [124]. Meanwhile, Huber et al. (2000) established dissociated E12 mouse cultures of DRG neurons from wild-type and BDNF-null embryos that were grown in defined medium without added NTs. Interestingly, both wild-type and BDNF-deficient DRG neurons survived equally well under these conditions, indicating that

a BDNF autocrine loop does not play a role in sustaining the survival of embryonic sensory neurons during early development [596]. An exhaustive and comparative *in vitro* survival analysis performed by Baudet et al (2000) in which responses of E12, E16, P0 and P7 mouse DRG neurons to NGF, BDNF, NT3 and NT4 were characterized, pointed in the same direction. They showed that survival requirements of DRG neurons for NGF decreased with time: from 100% at E12, to ~80% at E16, to ~60% at P0 and lastly to ~50% at P7. NT3 and NT4 followed a partially similar pattern: starting with a survival rate of ~20% at E12, then decreasing to 5% at E16 to finally rise to back to ~10% and ~20% at P0 and P7 respectively. However, DRG survival response to BDNF went from low to high over time: ~5% of survival at embryonic stages E12 and E16, to 10% at P0 and finally to more than 30% of DRG survival at P7 [597]. Accordingly, studies from Silos-Santiago et al. (1997) reported no significant loss of DRG neurons of newborn TrkB-null mice, but they did observe a 30% loss of their lumbar DRG neurons by the second postnatal week [598], suggesting that the survival effect of BDNF in DRG neurons is most relevant postnatally.

Supporting the trophic role of BDNF in postnatal DRG neurons, Valdes-Sanchez et al. (2010) demonstrated that immediately after birth, a fraction of nociceptors requires BDNF for survival [599]. These authors observed that DRG neuron loss in BDNF-deficient mice occurs significantly at postnatal stages between P0 and P15. Despite the expression of TrkB receptors in DRG neurons during development [107, 146, 600, 601], deficits in DRG numbers during embryogenesis at E12 and E15 were not observed [599]. However, the lack of BDNF resulted in the postnatal loss of adult C-fibres sensory afferents, an overall decrease in the density of free nerve endings in the hairy/glabrous skin (as well as in the dorsal horn of the spinal cord), and a reduction in the number of IB4+ and CGRP+ neurons in lumbar DRGs. Moreover, the *in vitro* survival of neonatal DRG neurons in the presence of NGF showed a significant reduction either in the presence of anti-BDNF antibodies or in a BDNF-null background. Therefore, the authors suggested that this early postnatal survival is elicited by BDNF released by DRG neurons themselves in an auto/paracrine manner, probably in response to NGF, and that the time-window for BDNF actions on DRG neuronal survival is likely restricted to postnatal development.

[599]. These results are consistent with a model in which NGF regulates BDNF and TrkB expression and ganglion-derived BDNF ensures the survival of nociceptive neurons.

In summary, the role of BDNF as a trophic factor sustaining the survival of different neuronal populations in the PNS depends on the type of neuron, the cellular source of neurotrophin and the developmental stage. Sensory neurons from petrose-nodosa, vestibular and geniculate ganglia, are almost completely lost in TrkB-null deficient animals [598], indicating that their survival is highly dependent on BDNF and NT4. In contrast, the expression of TrkB in DRG neurons is restricted to a small population of cells during development, with TrkB-immunoreactive cells accounting for only 40% of thoracolumbar DRG neurons in E11 mice. The coincidence of TrkB and TrkC positive neurons in lumbar DRG is ~75% at E11.5; given this co-expression, it is possible that most TrkB+ DRG neurons rely on NT3 for their survival during early developmental stages [124]. Consistent with this, double TrkB::TrkC compound null animals display a 40% decrease in the number of DRG neurons versus 20% in TrkC-null mice and no decrease in TrkB-nulls [598]. Therefore, the capacity of BDNF to support the survival of DRG neurons during development seems at best restricted to a small portion of neurons. How these observations can be reconciled with studies showing a ~30% decrease of DRG neurons in BDNF-null mice E13 embryos [588] remains an outstanding question in the field.

1.6.2 Dying in the absence of BDNF: from DRG neurons and beyond

The mechanisms of developmental cell death in sensory neurons have been preferentially explored in DRG neurons dependent on NGF. This neuronal population constitutes a fundamental reference for any research intending to deepen our understanding of the developmental selection of neurons dependent on other trophic factors. Section 1.4 has reviewed these mechanisms. Special attention was paid to TrkA, the neurotrophin receptor through which NGF-dependent sensory neurons sense the lack of trophic support. Nikolettou et al. (2010) were the first to evidence TrkA as a dependence receptor, supporting neuronal survival in the presence of NGF and triggering cell death in its absence [12]. Different studies have confirmed over the years the active role of TrkA in inducing neuronal death upon NGF deprivation in different neuronal

populations, including DRG neurons [175, 316]. However, Nikolettou et al. (2010) also provided evidence suggesting that not all DRG neuronal populations during development may sense and react to the lack of trophic support in the same way. These authors demonstrated that while TrkA and TrkC are dependence receptors, triggering cell death in the absence of their ligands, TrkB is not. Neurons derived from embryonic stem cells engineered to express TrkA or TrkC die between 4 and 6 days *in vitro*, and their death could be prevented by the addition of NGF or NT3 respectively. By contrast, TrkB expressing derived neurons did not die [12]. Conversely, a similar logic can be observed *in vivo* where the supplying or overexpression of NGF or NT3 in the skin of mice rescues or increases the number of DRG and trigeminal neurons [148, 590, 602, 603], while the overexpression of BDNF or NT4 increases skin innervation without altering the total number of DRG neurons [149, 592]. These results suggest that BDNF-dependent DRG neurons may undergo mechanisms of developmental cell death different from the prototypical population of NGF-dependent sensory neurons. How TrkB⁺ sensory neurons initiate the degenerative cascade upon BDNF deprivation without the dependence properties of their main trophic-sensing receptor is unknown. It is worth mentioning, however, that TrkB activation in absence of its ligand, called TrkB transactivation, is an important mechanism through which TrkB exerts specific signaling functions [604-606]. Activation of TrkB receptors in the absence of neurotrophins can be mediated by ligand activation of the G-protein-coupled adenosine 2A receptor (A2A-R) or the dopamine D1 receptor [42, 604, 607, 608]. During development of the cortex, intracellular TrkB and TrkC can be activated by a Src kinase-dependent pathway induced by EGF binding to EGF receptor [605]. No pro-degenerative role has been attributed to TrkB transactivation [606, 609], however, TrkB overactivation has been linked to hyperactivity-mediated cell death in pathological contexts such as epilepsy and amyotrophic lateral sclerosis [609].

Developmental degeneration of BDNF-dependent DRG axons take place during the innervation of the embryonic mammary gland (MMG). In mice, the initial stages of MMG development are virtually identical in males and females until E13 where, in response to androgens, the male MMG begin to regress. The innervation of the MMG in males and females follows the same pattern. Early by E12, male and female mammary rudiments are innervated by comparable number of fibers but in females, the number of

fibers surrounding the MMG increase dramatically during the subsequent 24 hours while in males, innervation increases until E13 then drops during the subsequent 8 hours. As a result, by late E13 female MMGs are richly innervated whereas few fibers are associated with male MMGs. Liu et al. (2012) reported that BDNF produced in MMG mesenchyme promotes the initial ingrowth and maintenance of TrkB⁺ sensory fibres. Accordingly, BDNF-null, TrkB-null or conditional embryos in which TrkB is ablated exclusively in DRG neurons, dramatically attenuates the innervation of female MMG by E13. The rapid loss of male MMG innervation from early to late E13 is the consequence of androgen-mediated expression of the truncated form of TrkB (TrkB.T1) in the surrounding mesenchyme of the MMG. Increase TrkB.T1 levels in males neutralizes the BDNF-TrkB mediated trophic function in the sensory fibers, leading to their withdrawal from the MMG [610]. Recently, Shalom et al. (2019) demonstrated that the genetic ablation of Plexin A4 delayed axonal degeneration in the MMG of male mouse embryos, while exogenous Sema3A application to BDNF-dependent DRG neurons *in vitro* induced growth cone collapse in a Plexin A4-dependent manner [159]. Interestingly, it has been reported that Plexins can interact with Trk receptors [157], and more importantly, that Plexins could function in a ligand-independent manner to drive apoptosis [611]. Thus, plexins may be an alternative pathway driving axon loss in the male MMG.

Axonal remodeling of TrkB⁺ sensory fibers in male MMG is independent of the pro-apoptotic protein BAX, suggesting that BDNF deprivation-induced axonal degeneration may not follow the intrinsic apoptotic pathway. BAX-deficient embryos in which apoptotic cell death in DRG sensory neurons is completely eliminated [167] exhibit a sexual dimorphic pattern no distinct from wild-types embryos [610]. Curiously, similar results have been reported in dopaminergic neurons deprived of BDNF. Yu et al. (2008) showed that deprivation of BDNF triggers a novel mitochondria-independent death pathway in cultured embryonic dopaminergic neurons: cytochrome *c* was not released from the mitochondria to cytosol, BAX was not activated, and overexpressed Bcl-xL did not block cell death induced by BDNF deprivation. Caspases, however, were critical; death of dopaminergic neurons deprived of BDNF was completely blocked by caspase inhibitors or by overexpression of dominant-negative mutants of caspase-9, -3, and -7. The death receptor pathway may also be involved given that blockage of caspase-8 or FADD (Fas-

associated protein with death domain), an adapter required for caspase-8 activation, inhibited death induced by BDNF deprivation [612]. Although the degeneration observed in DRG sensory neurons innervating the MMG is BAX-independent, the massive loss of cranial sensory neurons in BDNF-null mice, including petrose-nodosal and vestibular ganglion cells [130-132, 593], is rescued in BDNF::BAX compound null mice [613]. This demonstrated that BAX is essential for the developmental degeneration of this particular sub-population of BDNF-dependent cranial sensory neurons.

Lastly, autophagic cell death can lead to developmental programmed cell death of DRG neurons in the absence of Apaf-1 [345]. Interestingly, several studies have shown that BDNF-dependent survival of hippocampal neurons [614], BDNF-dependent long-term potentiation and the increase in synaptic spine numbers [615], requires suppression of autophagy. Particularly, Nikolettou et al., (2017) demonstrated that BDNF signaling via TrkB and the PI3K pathway regulates autophagy by transcriptionally suppressing key components of the autophagic machinery required for early steps of autophagosome nucleation and elongation [615]. Alternatively, Smith et al. (2014) previously reported that BDNF-dependent survival of hippocampal neurons under withdrawal of serum from the culture media depends on the mammalian target of rapamycin (mTOR). Surprisingly, BDNF does not promote neuronal survival by upregulation of mTOR-dependent protein synthesis or through mTOR-dependent suppression of caspase-3 activation but through suppression of autophagic flux [614]. Whether autophagy - or other cell death mechanisms - is behind the developmental degeneration of BDNF-dependent DRG neurons will be addressed experimentally in chapter 3 of this thesis.

1.7 Developmental axonal pruning and its modelling *in vitro*

Along with programmed cell death, neurite pruning constitutes a major physiological event that shapes and refines the nervous system. Neurite pruning refers to the active process of elimination of unnecessary, misguided or excessive dendritic or axonal segments without compromising overall neuronal survival. A number of regions of the central and peripheral nervous system including the visual and motor cortices [616, 617], the cerebellum [618], the hippocampus [619, 620], the neuromuscular system [621], and the mammary gland [610], show dendritic and axonal pruning events in embryos and adults. Dysregulation of neurite pruning during development has been associated with neurological disorders such as schizophrenia [622], and autism [623]. This section describes the different types of neurite pruning, the models used to mimic neurite pruning *in vitro*, and the molecular mechanisms that differentiates neurite pruning from apoptosis in DRG and sympathetic neurons.

1.7.1 Types of neurite pruning

Neurite pruning largely occurs through three distinct mechanisms: 1) retraction, 2) severing and fragmentation and 3) degeneration. Neurite pruning could be stereotyped, meaning that one can predict the identity of the axonal or dendritic branches destined for elimination as well as the developmental stage in which this elimination will occur, or non-stereotyped, usually entailing the adaptation of the circuit based on limiting trophic factors or neuronal activity.

Neurite pruning by retraction comprises the complete reabsorption of neurite materials which are shuttled to other parts of the cell without the generation of fragments. Remodelling of axonal projections by retraction can be observed in the immature hippocampus. Granule cells of the dentate gyrus extend two bundles of mossy fibre axons, a main bundle that courses adjacent to the apical dendrites of CA3 pyramidal cells and a transient infrapyramidal bundle (IPB) of axon collaterals that course adjacent to the basal dendrites a few days later [624]. The IPB projection elimination occurs stereotypically by retraction [619, 625]. Repulsive guidance cues of the Semaphorin family are responsible for the retraction of the IPB projection. During the pruning process,

granule cells express Plexin A3, a receptor for secreted Sema3F [626]. Sema3F is expressed in a spatially restricted manner along the areas coursed by the IPB projections, and - along with Plexin A3 - is crucial for regulating IPB stereotyped axonal pruning [619]. Knockouts for either Sema3F or Plexin A3 results in profound pruning defects in the IPB [619, 627, 628]. Similarly, Sema3A and Plexin A4 have been recently reported to be crucial for the pruning of BDNF-dependent sensory axons in the mammary gland (MMG) of male mice embryos [159], suggesting that axonal pruning in the MMG may happen through retraction. However, the axonal pruning type in the MMG has not been specified [159, 610] and not all repulsive guidance cues can be associated uniquely to retraction mechanisms during axonal pruning (see below).

A variant of the classical axonal pruning by retraction is axosome shedding. In this mechanism, axons retract but leave behind membrane-bound remnants which contain organelles that are engulfed by neighboring glial cells. The neuromuscular junction (NMJ), which is one of the best studied models of developmental axonal pruning and refinement [628] is the classic example of this type of mechanism. Time-lapse imaging analysis during synapse disassembly show that the retreating axons leaves behind distal portions of the axons, later known as “axosomes”. This process is aided by Schwann cells, engulfing axosomes from terminal arbors that have disassembled from the NMJ [621]. Some have suggested that axosome shedding is an intermediate mechanism between retraction and degeneration [628].

Severing and fragmentation is a type of neurite pruning observed particularly during the stereotyped developmental remodelling of ddaC sensory neurons in *Drosophila* [629-631]. A combination of descriptive and molecular studies has shown that during morphogenesis, the dendrites of ddaC sensory neurons, but not the axon, are first severed from the cell body and subsequently fragmented [629]. Proximal dendritic severing involves transient elevation of endocytic activity at the severing site [632], microtubule severing by protein Katanin p60-like 1 [633], and the assistance of peripheral glial cells that wrap the proximal dendrites, probably regulating the location of the severing point [634]. Fragmentation of the dendritic arbor depends on the ubiquitin-proteasomal system (UPS) [635], and activation of the apoptotic machinery, particularly the executioner caspases [636, 637]. The course of dendritic pruning in these neurons

resembles Wallerian degeneration (WD), a particular type of degeneration induced by injury-mediated axotomy, with fragmentation of the distal axonal segment distal to the severing point [638, 639].

The *Wld^S* mutation encodes a fusion protein between the ubiquitination factor E4b and the NAD⁺ biosynthetic enzyme nicotinamide mononucleotide adenylyl transferase 1 (*Nmnat1*) that fully protects from WD in vertebrates [638]. The mechanisms underlying WD are conserved in flies, as transgenic expression of *Wld^S* protect neurons against injury-induced axonal degeneration in *Drosophila* [640, 641]. However, *Wld^S* only partially protects the stereotypical dendritic pruning of *ddaC* sensory neurons, suggesting that mechanisms of WD may function in parallel to apoptosis-like degenerative mechanisms in that context [213, 642].

Axonal pruning by degeneration, involves blebbing and fragmentation of an entire axon into short segments, which are then removed by phagocytic cells such as locally activated glia or macrophages. Axonal pruning by degeneration differs from retraction in several ways: 1) retraction is the preferential pruning process for the elimination of shorter branches, whereas degeneration tends to affect longer axonal segments [643, 644], 2) retraction does not requires microtubule disruption while axonal degeneration involves disassembly of microtubule filaments as an early and possible critical process [644], 3) pruning by axonal degeneration requires transcriptional processes in neurons that confer intrinsic competence for degeneration, while retraction may predominantly involve local regulation events [645].

The demonstration that axonal degeneration is a major mechanism for pruning during early postnatal life in mammals came from studies pioneered by O'Leary and colleagues in the cortex, where a subset of axons from neurons in layer V undergo fragmentation without affecting neuronal survival that leaves to specific connectivity [646, 647]. This pruning process exhibits typical features of axon degeneration including blebbing and rapid removal of axonal remnants [640, 644]. The selectivity in the process of axon elimination showed to be dependent on the patterns of neuronal activity [644].

Another example for temporally and spatially regulated developmental axon pruning by local degeneration is the formation of the retinotopic map of retinal ganglion cells (RGC) at the superior colliculus (SC). Work also pioneered by O'Leary's group has

shown that RGCs initially send long axonal processes that extend throughout the length of the SC and sprout axon collaterals in an area that will become the “target zone” [648]. Later during visual system development, an ephrinA-EphA counter-gradient in the SC acts instructively in the fragmentation-mediated degeneration-like pruning of overshooting RGC axons, setting up a template for topographic map formation. Ephrin-mediated elimination of overshooting primary axons is independent of neuronal activity [644] but the retinotopic map refinement requires spontaneous retinal activity waves during a brief critical period of development [649]. Thus, the combination of retinal waves and ephrin A signaling facilitates the establishment of topographic maps, highlighting the importance of the coordinated actions of neural activity and guidance cue signaling during circuit refinement by axon pruning.

Axonal pruning by degeneration has also been reported in *Drosophila*. The γ neurons of the mushroom body (MB), which are essential for olfactory learning and memory, undergo axon degeneration to prune their dorsal and medial axon branches [650]. The process of MB remodeling is dependent on ecdysone, a hormone secreted by surrounding glia (related to retinoic acid signaling in vertebrates) [651, 652], and on the cell autonomous expression and function of corresponding nuclear hormone receptors in MB neurons [651, 653]. The degeneration process proceeds in a temporally well-defined manner, and its stages have been characterized in great detail [644, 650, 654]. This analysis revealed that axonal degeneration first involves microtubule depolymerization, followed by axonal blebbing, axon fragmentation, neurofilament degradation, and removal of the axonal swellings [650].

From the examples described above, there are clearly diverse means of triggering and executing pruning in specific contexts (e.g. activity patterns, “punishment” hormones and axon guidance molecules). Morphologically, however, these pruning events recapitulate the same fragmentation patterns that are also present during injury-induced WD, as well as in the regressive processes observed in “dying back” neurodegenerative diseases in which the breakdown of the axons occurs before and even in the absence of cell death. Convergence to similar executioner mechanisms of axonal fragmentation have been proposed to explain the morphological resemblance of events with different origins

[628, 655]. However, the diversity of mechanisms can also be observed at the executioner level.

Caspases, the key mediators of apoptosis-induced cell death, are needed for efficient developmental pruning of RGCs axons in the SC [214, 331, 656]. Similarly, studies on fly *ddaC* neurons provided clear evidence that the initiator caspase, DRONC (the Casapses-9 homolog), and the executor caspases, DRICE and DCP-1 (homologs of Casapse-3), are essential for developmental *ddaC* dendrite pruning [213, 636, 637]. However, caspases are not required for axon or dendrite pruning of fly MB neurons [630], and activated caspases are not present during MB remodeling [657]. Therefore, caspases do not seem to play a role in all developmental pruning processes, even within the same organism.

The morphological resemblance of injury-induced WD with degenerative axonal pruning encouraged the cross-study of both processes to determine similarities at the molecular level. As described above, the WD-resistant *Wld^S* partially protects the dendritic pruning of *ddaC* sensory neurons in *Drosophila*, suggesting certain levels of conservation in their executioner molecular mechanisms [213, 642]. The requirement of UPS activity either for WD or axonal degeneration in different pruning contexts further reinforced the idea of conserved execution mechanisms between both processes [635, 640, 650, 658]. Moreover, elevated levels of intra-axonal Ca^{2+} or the active role of Ca^{2+} -dependent proteases are required events for axonal fragmentation in WD and for neurite pruning [354, 638, 659]. However, despite these commonalities and the fact that *Wld^S* protects lesion-induced axonal degeneration in *Drosophila* or in RGC axons at the SC in the age of naturally occurring degenerative pruning, *Wld^S* expression is not able to suppress developmental degeneration in MB neurons in *Drosophila* or RGC axons in vertebrates [640, 644]. Thus, compelling experimental evidence shows that *Wld^S* specifically inhibits WD but not developmental axonal degeneration. In conclusion, the executioner mechanisms of axonal degeneration induced during developmental pruning in different context, and upon lesions, is more diverse and complex than the common morphological patterns of axonal fragmentation might have initially suggested.

1.7.2 *In vitro* models to mimic axonal pruning

The last decade has seen a proliferation of *in vitro* models of axonal pruning. Because of their morphological simplicity, the long extension of their projections and their dependency on NGF, embryonic DRG and postnatal SGC neurons have been preferred neuronal subtypes to study axonal pruning *in vitro* [660]. Contrary to the globally-deprived DRG or SCG explants, mostly used to investigate developmental cell death, the *in vitro* models that mimic axonal pruning require constraining NGF deprivation to distal axons without disrupting the trophic support of the cell body. Technically, this has been resolved by two different *in vitro* culture devices that allow physical and fluid isolation of cell bodies from axons.

Robert Campenot developed the first culture device capable of differentially treating cell bodies and axons [661, 662]. Campenot chambers consist of a single reusable Teflon piece composed of three compartments. On the perimeter of each compartment, at the base of the device, a silicone vacuum grease layer is applied. Subsequently, the Campenot chamber is placed on a plastic petri dish such that the grease layer forms a hydrophobic barrier between the device and the dish. This way the inner chamber is isolated from the outer chamber and the compartments from each other, thus preventing the exchange of soluble factors. Dissociated DRG or SCG neurons are seeded in one compartment, usually the middle and narrowest one (the soma compartment), and growing axons fueled by NGF in all compartments can cross the grease barrier to the two adjacent compartments (the axonal compartments). Thus, cell bodies and proximal axons can be physically and fluidically isolated from distal axonal segments. The selective deprivation of NGF on the axonal compartments has been used to induce axon-specific degeneration of distal axons, mimicking pruning, without affecting the trophic support of proximal axons and cell bodies in the soma compartment [214, 316, 331, 661, 663].

The second technique to mimic axon pruning *in vitro* uses microfluidic devices. First designed by Taylor et al. (2005), microfluidics employs tiny reservoir and microchannels to manipulate very small amounts of fluid [664, 665]. The most basic design to model axonal pruning *in vitro* is composed of two compartments connected by

microgrooves [664, 666]. Similar to Campenot chambers, dissociated neurons seeded in one compartment (proximal/soma compartment) grow their axons through the microgrooves into the second compartment (distal/axonal compartment). The size of the microgrooves (3 x 10 μm) allows axon growth but is small enough to avoid soma migration between compartments. Axonal pruning can be induced by exposing the distal compartment to media lacking NGF and containing blocking antibodies against NGF (αNGF). To avoid exposing the cell bodies to the αNGF media, risking global deprivation and apoptosis, the volume in the distal compartment is reduced compared to the proximal compartment, creating a hydrostatic pressure inside the device that fluidically isolates the cell bodies from the lack of trophic support.

Microfluidic devices offer some advantages over the Campenot chambers: 1) the in-house ability of fabricate custom-designed devices using photolithography and biocompatible polymers such as poly(dimethylsiloxane) (PDMS), 2) the easier establishment and manipulation of the devices in opposition to Campenot chambers, which require a higher level of expertise to achieve compartment isolation, and 3) its compatibility with high-resolution and live microscopic techniques, which are fundamental to visually trace different aspects of the axonal pruning process [667]. The only caveat compared to Campenot chambers is that microfluidic devices are not suitable for recovering large amounts of axonal lysates for proteomic purposes. However, this problem can be partially solved using custom designs [668]. Thus, since their invention, we and several other groups have preferred the use of microfluidic devices to mimic axonal pruning *in vitro* [224, 338, 339].

1.7.3 Mechanisms of axonal pruning in DRG - and SCG - neurons

Over the last decade, the use of compartmentalized culture techniques has contributed to clarify the axonal pruning process at multiple levels: 1) the cross-talk between the axon and the cell body during the pruning process, 2) the execution of degeneration in axonal pruning versus cell death, and 3) the strategies used by neurons to compartmentalize or stop the degenerative machinery.

1.7.3.1 Soma-axon communication during axonal pruning

Axonal pruning is not a compartment-autonomous process. Several studies have demonstrated that although the apoptotic machinery is present and functional in axons, it is not activated directly by distal trophic deprivation. Instead, for the axon to degenerate, the segment under trophic deprivation needs to maintain a communication with the cell body. The dynamic of the cross-talk between both cellular compartments implies a retrograde signal to the cell body, the activation of a transcriptional pro-apoptotic program in the soma, and an anterograde pro-degenerative signal back to the axon [316, 322, 339, 663].

The chain of events described above were not self-evident. Initially, it was assumed that the communication between the axon and the cell body exists primarily to maintain the healthy conditions of the axon rather than to actively regulate degeneration. It has been known for decades that NGF applied to axon terminals is internalized in complex with TrkA, and subsequently transported in signaling endosomes along the axons to the cell bodies to support neuronal survival [669, 670]. Alternatively, NGF stimulation in distal axons is able to induce the axonal translation of *Creb*, a transcription factor who is retrogradely transported to the soma, also promoting neuronal survival [671]. The end result of any of these mechanisms is the transcription of a battery of genes whose mRNA are anterogradely transported to into distal axons [338, 671-674]. Among these transcripts is mRNA encoding for *Bcl-w*, a pro-survival member of the Bcl-2 family, who accumulates and translates in embryonic DRG and SCG axons in response to continuous NGF exposure, suppressing axonal degeneration mediated by BAX and caspase-6 [338].

The lack of NGF support in distal axons may well induce local axonal degeneration by interrupting the supply of pro-survival transcripts from the cell body. However, axonal pruning is guided by a pro-active signaling mechanism. Mok et al. (2009) were the first to propose a fundamental survival mechanism in which NGF at distal axons suppresses an apoptotic signaling mechanism. This axon apoptotic signal, when unrepressed in response to NGF withdrawal, results in a retrograde signal to the cell body that drives activation of the pro-degenerative transcription factor c-Jun in the nucleus [663]. More recent studies have demonstrated that the loss of Akt signaling in distal axons upon NGF

deprivation activates the DLK/JNK pro-degenerative pathway [175, 316, 320, 322], which activates the transcription factors FoxO3a and c-Jun [316, 322, 663]. Interestingly, almost identical mechanisms can be induced by global deprivation [322, 339]. DLK activation and retrograde signaling by distal NGF deprivation also promotes PERK activation and the translation of the transcription factor ATF4 in the cell body to drive UPR [322]. Like JNK, p38MAPK/GSK3 β signaling acts largely in the cell body to regulate distal axon degeneration in DRG neurons and axonal pruning of RGCs in the SC, likely via a transcriptional cascade that include the *dleu2/miR15a/16-1* cluster, and the transcription factor *tbx6* [319]. Transcription factors like c-Jun, FoxO3a and ATF4 converge into the induction of the pro-apoptotic member of the Bcl-2 family PUMA [175, 316, 339, 675], which is classically described as a transcriptionally regulated gene induced by cellular stress [676]. The rise in PUMA expression levels seems induce both cell death and axon pruning, given that its genetic deletion protects DRG axons from global and local NGF deprivation [316, 339]. Moreover, PUMA-deficient mice show increase skin innervation without alteration in the number of DRG neurons, suggesting that PUMA controls axonal pruning *in vivo* [339]. Surprisingly however, PUMA expression showed to be confined to the cell body of DRG neurons, even in conditions of distal axonal NGF deprivation [316]. Thus, the mechanism through which PUMA controls axonal pruning from the cell body, and the identity of its anterograde signal, need to be further investigated.

1.7.3.2 Execution of degeneration in axonal pruning versus cell death

At the executioner phase, axonal degeneration induced by either global (cell death) or local (axonal pruning) NGF deprivation activates the intrinsic apoptotic pathway. Two key pillars of this pathway, BAX and caspases, are essential in both degenerative processes [214]. However, some differences between the local and global pathways can be discerned.

BAX genetic deletion completely inhibits axon pruning [213, 224, 331], suggesting that BAX induction of MOMP is required. Consistent with this, cytochrome *c* release from mitochondria is observed in axons undergoing local NGF deprivation [224]. However, the role of cytochrome *c* during axonal pruning is uncertain. As previously mentioned, due to

its essential function in mitochondrial respiration, experiments that silence or knockout cytochrome *c* are problematic, and the use of Apaf-1-deficient models have been considered a valid alternative. Interestingly, it is at this point where cell death and axonal pruning seems to use different pathways. While Apaf-1-deficiency protects DRG embryonic neurons from cell death induced by global NGF deprivation [222, 316], Apaf-1-null DRG axons locally deprived of NGF have normal capacity to undergo axonal pruning *in vitro* [224]. Despite the apparent lack of a requirement for Apaf-1 in axonal pruning [224], caspase-9, caspase-3 [214, 224], and caspase-6 [214, 224, 331], are activated and required during axonal pruning. Globally deprived SCG neurons require caspase-9 and caspase-3 but not caspase-6 to execute the apoptotic program [224]. Thus, the requirement for caspase-6 in pruning but not apoptosis is the second main difference between NGF deprivation-induced cell death and axonal pruning. How BAX-induced MOMP and cytochrome *c* release activates caspases without Apaf-1 during axonal pruning remains to be determined.

Despite sharing a common intrinsic-apoptotic route, cell death and axonal pruning presumably rely on different molecular players to execute degeneration. The preferential use of Apaf-1 in apoptosis but not in pruning helps distinguish these pathways and protect neurons that are undergoing axonal pruning from “falling into the trap” of switching from pruning to cell death. However, the question that naturally arises is whether these differences are enough to explain the restriction of degeneration during the pruning process. It is worth recalling that Apaf-1 is not essential to drive developmental programmed cell death in NGF-dependent neurons, as derived from the comparison between Apaf-1::TrkA (which do undergo cell death) and BAX::TrkA (which do not undergo cell death) compound double null mice [167, 344]. These observations suggested that DRG neurons can take alternative pathways to execute the cell death program [167, 344, 345]. Thus, although the “no need” for Apaf-1 in axonal pruning represents a physiological reality [224] it may not be enough to protect neurons from taking the step towards cell death. Are there additional molecular mechanisms that prevents neurons undergoing axonal pruning from switching into apoptosis? The compartmentalization and restriction of the apoptotic machinery seems to be the key to separate pruning from cell death.

1.7.3.3 Compartmentalization of the apoptotic machinery: a matter of age?

Protecting the cell body, at least from the degeneration that occurs in distal axon terminals, constitutes the essence of axonal pruning: “neurite elimination without causing cell death”. Compartmentalization of the apoptotic machinery is therefore an essential aspect of the axonal pruning process. However, despite classifications that distinguish between morphological and functional cellular compartments within neurons (soma versus axon), the cytoplasm is a continuum. Thus, mechanisms that differentially control the expression, localization and activation of the apoptotic machinery between the cell body and axons, or between deprived and non-deprived axons, are essential tools for neurons to appropriately manage axonal pruning.

The strategies used by neurons to control the expression, location and activation of the apoptotic machinery can be divided depending on whether they lay upstream or downstream of the mitochondria [677]. On the post-mitochondrial side, these strategies are oriented to modulate caspase activity. The first is based on the already mentioned role of Apaf-1, which accelerates the rate of caspase activation in an ATP-dependent manner. Axonal pruning does not require Apaf-1 [224], and this may help avoid uncontrollable bursts of caspase activation. The second post-mitochondrial protectant strategy is based on the inhibitor of apoptotic proteins, IAPs, a group of endogenous inhibitors of activated caspases. XIAP in particular is known to strictly regulate caspase activity during apoptosis in NGF-dependent SCG neurons [367]. Indeed, XIAP-deficient neurons not only exhibit enhanced axonal degeneration but also display aberrant caspase activation in the cell bodies during axonal pruning [224, 225]. This suggests that XIAP normally plays a key role restricting caspase activity to the axon. Interestingly XIAP-null adult mice show decreased skin innervation without changes in the number of DRG neurons, suggesting a role for XIAP in axonal pruning *in vivo* [225]. In *Drosophila*, the homologous Death-associated Inhibitor of Apoptosis-1, DIAP1, is known to inhibit local caspase activation and degeneration during dendritic pruning of ddaC sensory neurons [636]. Moreover, the *Drosophila* IKappa-related kinase (Ik2), known to phosphorylate and induce the degradation of DIAP1 through the proteasome [678], is essential for pruning ddaC sensory dendrites but not for axonal pruning in MB neurons [633]. Thus, differential

regulation of IAPs may enable either a permissive or a repressive environment to spatially restrict caspase activity during axonal pruning [660].

Upstream of the mitochondria, a strategy that neurons may use to control the spatial activation of the intrinsic apoptotic pathway, and therefore axonal pruning, could be based on microRNAs (miR). MiRs are small, approximately 20-22 nucleotide RNAs that are generated by the processing of longer RNA precursor and inhibit protein translation by binding to specific mRNAs [679]. The Deshmukh group found that miR29 is expressed in SCG neurons and controls the expression of multiple members of the BH3-only family, including PUMA, which are key proteins necessary for BAX activation during apoptosis and axonal pruning [224, 680]. With opposing roles, miR15a and miR16-1 target and repress the expression of the anti-apoptotic protein Bcl-2 [681, 682] and showed to be part of the transcriptional cascade induced by GSK3 β in DRG axons distally deprived of NGF [319]. Interestingly, ROS-mediated oxidation of miR184 represses Bcl-xL and Bcl-w translation and thereby induces apoptosis, suggesting that ROS could locally regulate the apoptotic machinery through miRs [683]. However, how the action of these miRs is translated into spatial activation of the apoptotic machinery is still elusive.

A similar question can be raised regarding the mRNAs products of the transcriptional programs triggered by the retrograde pro-apoptotic signal originated in distal deprived axons [316, 322, 339, 663]. One mechanism that may be important is the regulation of local translation of anti- and pro-apoptotic proteins in the cell body and axons. It is now well established that a rich repertoire of miRs precursors and mRNAs are transported into axons and dendrites and processed or translated in response to various stimulus in different neuronal types including DRG and SCG neurons [684-687]. Could the regulation of local translation play a role during axonal pruning? It is already known that supplying transcription inhibitors to the cell body prevents axonal pruning but as expected, they have no effect when applied locally on distal axons deprived of NGF [319]. However, when the translation inhibitor cycloheximide is applied on distal deprived axons, local axonal degeneration is completely prevented. Importantly, no rescue of distal axons is observed when translation is inhibited in the soma compartment, suggesting that protein translation is needed in axons but not in the cell body for axonal pruning [688]. Although there is currently no direct evidence that axonal pruning factors are locally

translated, there is evidence that protective proteins like Bcl-w and the myo-inositol monophosphatase-1 (Impa1), a key enzyme in the inositol cycle, are translated in axons in response to NGF exposure [338, 689]. The role that protein synthesis may have in neurite pruning is well exemplified by the fragile-X mental retardation protein (FMRP). FMRP is an RNA-binding protein capable of regulating miR and mRNA transport, stability and mRNA translation in different cellular compartments including axons of DRG neurons [690-692]. The loss of dFMRP in *Drosophila* causes severe axon pruning defects in MB neurons during development, with overgrowth and excessive branching [693]. FMRP is able to modulate the translation of APP [694], who plays a pro-degenerative role during axonal pruning in DRG and RGC neurons [331, 332]. Moreover, FMRP-deficiency inhibits programmed cell death in the developing brain through the increase of the expression levels of the pro-survival protein Bcl-xL, impairing adequate neuronal elimination [695, 696]. Importantly, loss of function of FMRP is associated with the neurodevelopmental Fragile-X syndrome, part of the complex and heterologous autism spectrum disorders (ASD) and known for showing developmental pruning defects [697]. Thus, translation regulation could potentially confer a powerful tool to regulate the apoptotic machinery during axonal pruning.

Interestingly, some of the strategies just discussed, oriented to modulate the grade of activation and location of the apoptotic machinery within neurons, are differentially expressed with age. Several studies have shown that the expression of caspase-3, caspase-9, and Apaf-1 is strongly reduced after neuronal maturation [200, 677, 698-701]. These changes suggest that immature neurons have a higher susceptibility to apoptotic stimulus. Consistent with this, immature SCG neurons from mice lacking XIAP die within 24 hours after microinjection of cytochrome *c*, while mature neurons from XIAP-null mice are almost completely resistant to cell death induced with cytochrome *c* [222]. This capacity could be attributed to the almost complete loss of Apaf-1 expression in mature neurons [702]. Similarly, total BAX levels decrease with neuronal maturation in DRG neurons and in the rat forebrain [703, 704]. Meanwhile, BAX translocation to mitochondria seems to be impaired in mature SGC neurons and BAX remains completely cytosolic after NGF deprivation [705]. Consistent with these findings, exogenous activation of JNK induces apoptosis less effectively in mature as compared with neonatal DRG neurons

[706]. The inability of mature neurons to activate BAX is extremely effective as a survival mechanism, as BAX deletion has been shown to confer complete resistance of neurons to many intrinsic apoptotic stimuli including NGF deprivation [707]. In the same line, miR29 is specially upregulated in mature SGC neurons both *in vitro* and *in vivo* compared with immature neurons [677, 680]. Ectopic expression of miR29 alone in young SCG neurons confers marked resistance to multiple apoptotic stimuli including NGF deprivation. Moreover, mature neurons with high levels of miR29 do not show induction of BH3-family proteins in response to apoptotic stimuli [680].

The resistance to death acquired by mature neurons is not only related with the regulation of direct components of the apoptotic machinery. The dephosphorylation of TrkA following NGF withdrawal is one of the first events that initiates apoptosis and studies using compartmentalized cultures chambers have shown that phospho-TrkA is significantly more stable in mature neurons following NGF deprivation than the immature counterparts. Indeed, TrkA dephosphorylation upon NGF deprivation in distal axons occurs in 6 hours in immature neurons versus 2 days in mature SCG neurons [677, 708]. As signaling downstream of TrkA is key to promoting survival and cell death [12, 175] the capacity of mature neurons to maintain TrkA phosphorylation for longer periods of time in the absence of NGF could also contribute to their ability to resist apoptosis.

In light of the accumulated evidence, does neuronal maturation reduce axonal pruning capacity? Cusack et al. (2013) showed that despite the resistance of mature SCG neurons to apoptosis and axon degeneration induced by global NGF deprivation, aged SCG neurons still degenerate their axons after local NGF withdrawal in compartmentalized chamber [224]. Thus, the ability to restrict cell death does not correlate with reduced capacity for axonal degeneration. This is not surprising - more control over the apoptotic pathway means a better capacity to decide how and where to employ it. However, in view of the increased susceptibility of developing neurons to apoptotic stimulus, their capacity to safely modulate degenerative axonal pruning without causing cell death is surprising. How is this possible? It could be argued that pruning and cell death may rely on completely different signaling pathways. That is true to some extent. So far, only Apaf-1 and caspase-6 were shown to participate differently in these degenerative events. However, caspase-6 have shown to lie downstream of caspase-3

and caspase-9, which are both necessary for pruning and cell death [214]. Meanwhile, Apaf-1, which is not needed for axonal pruning [224], is present in young neurons more abundantly than in mature ones, constituting a risk factor that needs to be controlled [677]. Again, in view of these observations, how can axonal pruning proceed in developing neurons without causing apoptosis? Mok et al. (2009) has suggested that the amount of degenerative retrograde signaling converging on the cell body can determine whether a neuron executes the cell death program [663]. It is possible therefore that the number of axonal branches facing deprivation may be decisive in determining whether a neuron undergoes apoptosis or pruning. This may not be a decisive factor in mature neurons, given their capacity to resist cell death, but it may be an important factor in the fate of developing neurons. Chapter 4 on this thesis test these ideas using compartmentalized cultures of DRG neurons in microfluidic devices.

1.8 Aim of this thesis

The remodelling of neuronal populations during development is a fundamental process required to generate a mature and functional nervous system. Alteration of this process could have serious pathological consequences. Despite the great progress in the field, our understanding of this complex process is still far from complete. This thesis aims to shed light into three different but connected aspects of developmental neuronal remodelling:

Study I (Chapter 2): The role of the amyloid-precursor protein in the developmental remodelling of NGF-dependent DRG sensory neurons.

Study II (Chapter 3): The mechanisms of developmental cell death in BDNF-dependent DRG sensory neurons.

Study III (Chapter 4): Modelling developmental axonal pruning *in vitro* using compartmentalized microfluidic chambers.

Chapter 2

The role of the amyloid-precursor protein in the developmental remodeling of NGF-dependent DRG sensory neurons

de León A.¹, Gibon J.², Johnstone A.¹, Barker P.²

1- Montreal Neurological Institute, McGill University, Montreal, QC, Canada. 2- Irving K. Barber School of Arts and Science, University of British Columbia – Okanagan Campus, Kelowna, BC, Canada.

2.1 Abstract

The activation of self-destructive cellular programs helps to sculpt the nervous system during development, but the molecular mechanisms employed are still not fully understood. Prior studies have investigated the role of the amyloid-precursor protein (APP) in the developmental degeneration of sensory neurons with contradictory results. In this work we seek to re-examine the role of APP using the well-established *in vitro* culture model of developmental degeneration in dorsal root ganglia (DRG) sensory neurons. Our results show that genetic deletion of APP delays axonal degeneration triggered by NGF deprivation, indicating that APP plays a pro-degenerative role in this setting. *In vivo*, we observed an increase in the number of sciatic nerve axons present in adult APP-null mice, consistent with the hypothesis that APP normally plays a pro-degenerative role in peripheral axons. The pro-degenerative role of APP may be determined by the regulation of its phosphorylation state at threonine 668 (T668). We observe a transient increase of the phosphorylated APP at T668 after 3 hours of NGF deprivation. We show - using K252a - that phosphorylation of APP at T668 depends on Trk receptor signaling. Our results indicate that phospholipase C gamma (PLC γ) and protein kinase C (PKC) may also be crucial for APP phosphorylation, given that their pharmacological inhibition not only rescue axonal degeneration but attenuates the rise of

phosphorylated APP at T668 upon NGF withdrawal. We found that that the rise of axoplasmic Ca^{2+} that normally occurs in DRG neurons upon NGF deprivation is reduced in APP null neurons and detailed examinations revealed that a lack of APP significantly reduces endoplasmic reticulum (ER) Ca^{2+} levels, decreases store-operated Ca^{2+} entry (SOCE), and diminishes mitochondrial membrane potential in DRG neurons. Taken together, these results support the hypothesis that APP play a pro-degenerative role in developmental degeneration of DRG sensory neurons.

2.2 Introduction

The maturation of the nervous system requires the elimination of neuronal cells and connections generated in excess during early stages of embryonic development [709]. This physiological process implies the activation of intrinsic self-destruction programs in response to embryonic stage-dependent inducers such as guidance cues, neuronal activity patterns or by competition for limited target-derived trophic factors [644]. The dysregulation or aberrant activation of mechanisms that resemble developmental neuronal cell death is observed in several neurodevelopmental and neurodegenerative disorders [623, 710]. However, despite its biological importance and clinical relevance, the exact molecular mechanisms driving the process of neuronal elimination during development are still not fully understood.

The amyloid-precursor protein (APP), intimately related to the pathogenesis of Alzheimer's disease (AD), was reported to be actively involved in the elimination of neuronal connections during the development of the central nervous system [331, 332]. APP has been proposed to bind to the death receptor 6 (DR6) and to induce a degenerative cascade that ends with the activation of the apoptotic machinery and the elimination of neuronal connections during development [331, 332]. However, as in other aspects of APP biology, the evidence supporting its participation in the peripheral nervous system remains controversial, ranging from pro-survival [333] to pro-degenerative [331, 332, 348], suggesting a more complex pattern of actions.

In the present study, we test the hypothesis that APP mediates degeneration of dorsal root ganglia (DRG) sensory axons during developmental conditions. With that goal, we used a well-known model of axonal degeneration *in vitro* and showed that APP deletion protects sensory neurons from NGF deprivation-induced degeneration. We also explored the peripheral nervous system (PNS) of adult APP-null mice, finding a striking increase of sciatic nerve axon number compared with wild-type mice. Interestingly, no corresponding increases in the DRG or motoneuron number or in number of neuronal fibers at the skin were observed.

At a molecular and cellular level, we report several interesting findings: 1) APP protein levels increase in the first hours of NGF deprivation, together with the levels of

phosphorylated APP at threonine 668 (T668), a phosphorylation site previously associated with APP pro-degenerative roles [335, 536]. 2) the inhibition of the signaling axis TrkA>PLC γ >PKC reduces APP phosphorylation at T668 and protects DRG neurons from degeneration induced by NGF deprivation. 3) no differences are detected in the levels of cleaved caspase-3 between wild-type and APP-null DRG neurons deprived of NGF, however, APP deficiency significantly reduces the rise of axoplasmic Ca²⁺ that normally occurs upon NGF deprivation. 4) lack of APP reduces the capacity of DRG neurons to refill the cytoplasm with Ca²⁺ from the extracellular space in response to ER Ca²⁺ stores depletion, and 5) APP-null DRG neurons have an increase in total mitochondrial mass but a decrease in functionally active mitochondria.

Thus, this study presents evidence *in vitro* and *in vivo* that supports a pro-degenerative role of APP during the development of the PNS. Moreover, this work provides alternative mechanisms through which APP may influence the process of developmental death of sensory neurons related with the modulation of Ca²⁺ homeostasis.

2.3 Materials and methods

2.3.1 Mouse strains

CD1 mice were purchased from Charles River Laboratories (Montreal, Canada). The previously described APP knockout mice [454] and DR6 knockout mice [711] were maintained in a C57Bl6 strain background. Animal procedures and experiments were approved by the University of British Columbia animal care committee and the Canadian Council of Animal Care. Efforts were made to reduce animal handling and use.

2.3.2 Culture and NGF deprivation of DRG explants

Dorsal root ganglia (DRG) were dissected from E13.5 mouse embryos and seeded in 12-well plastic (Grenier) or 4-well glass-bottom dishes (CellVis) sequentially coated with 1 mg/ml poly-D-lysine (Sigma-Aldrich), 10 µg/ml laminin-entactin complex (Corning) and 0.1 mg/ml PurCol bovine collagen (Advanced Biomatrix). Explants were grown in phenol-red Neurobasal media (Invitrogen) supplemented with 2% B27 serum-free supplement (Invitrogen), 1% L-glutamine (Wisent), 1% penicillin/streptomycin (Wisent), 10 µM 5-fluoro-2'-deoxyuridine (FDU, Sigma-Aldrich) and 12.5 ng/ml NGF (CedarLane) at 37°C, 5% CO₂. Deprivation of neurotrophic support was accomplished using 2.0 µg/ml of function blocking antibodies against NGF (rabbit polyclonal antibody raised against NGF (rabbit polyclonal antibody raised against 2.5s NGF; [712]) in complete fresh media without neurotrophic supplementation.

2.3.3 β III-tubulin immunocytochemistry, imaging and quantification of axon degeneration

DRG explants were fixed in 4% paraformaldehyde solution in phosphate saline buffer (PBS) for 15 minutes, washed once in PBS and blocked in 5% milk in Tris-Borate buffer and 0.3% Triton-X100 for one hour at room temperature (RT). Explants were incubated overnight at 4°C with mouse monoclonal antibody against β III-tubulin (Millipore, MAB5564) diluted 1:10000 in blocking solution. DRGs were washed twice in PBS and then incubated with goat anti-mouse conjugated to Alexa Fluor 488 (Jackson ImmunoResearch, 115-545-003) diluted 1:5000 in blocking solution for a minimum of 3 hours at RT. Explants were imaged using a Zeiss ObserverZ.1 inverted epifluorescence

microscope with an automated motorized stage (5x magnification with tilling). From a stitched master image of the plate generated by Zen 2 software (Zeiss, Canada), quarter DRG fields were cropped to generate a set of images for analysis using the R script program Axoquant 2.0 [360]. Final measurements were plotted as the mean axonal area of DRGs from three embryos. Increments of 500 μm were used for statistical analysis (normalized to same increments in control condition).

2.3.4 APP immunocytochemistry, imaging and quantification

DRG explants were fixed in 4% paraformaldehyde solution in phosphate saline buffer (PBS) for 15 minutes, washed once in PBS and blocked in 5% milk in Tris-Borate buffer and 0.3% Triton-X100 for one hour at room temperature (RT). Explants were incubated overnight at 4°C with mouse monoclonal antibody against β III-tubulin (Millipore, MAB5564) diluted 1:10000 and rabbit anti-APP-Y188 (Abcam ab32136) diluted 1:1000 in blocking solution. DRGs were washed twice in PBS and then incubated with goat anti-mouse conjugated to Alexa Fluor 488 (Jackson ImmunoResearch, 115-545-003) diluted 1:5000 and goat anti-rabbit conjugated to Alexa Fluor 546 (Invitrogen, A-11035) diluted 1:5000 in blocking solution for a minimum of 3 hours at RT. Explants were imaged using a Zeiss Observer Z.1 inverted epifluorescence microscope with an automated motorized stage (40x magnification). Final measurements were plotted as the mean intensity per axonal area from three embryos relative to control condition with NGF.

2.3.5 Tissue processing and histological assessment of DRG, sciatic nerve, hind-paw skin innervation and spinal cord motoneurons

Wild-type and APP-null adult mice were anesthetized and perfused transcardially with 4% paraformaldehyde in PBS. Dissected tissues were post-fixed by immersion in 4% paraformaldehyde in PBS ON at 4°C, profusely washed with PBS and stored either in phosphate buffer 20 mM pH 7.4 with 0.1% sodium azide at 4°C or cryoprotected with 20% sucrose, blocked in OCT medium embedding compound (Sakura Finetek) on dry ice and stored at -80°C.

Sciatic nerve processing, staining and counting - OCT embedded sciatic nerves were transverse sectioned (15 μm), mounted in gelatin-coated slides, air-dried,

rehydrated in PBS, permeabilized, blocked and immunostained with mouse anti- β III-tubulin (Millipore, MAB5564) diluted 1:10000 in blocking solution (0.3% TritonX-100, 5% Normal Goat Serum in PBS) ON at 4°C. Slides were washed in PBS and incubated with goat anti-mouse conjugated to Alexa Fluor 488 (Jackson ImmunoResearch, 115-545-003) diluted 1:5000 in blocking solution at RT for 3 hours. Slides were mounted with Fluoroshield mounting media (Sigma, F6182) and stored at 4°C. Sciatic nerve sections were tiled-imaged in Leica DMI8 confocal microscope and LAS X software with 488 nm laser in 1 μ m z-increments with 40x oil immersed objective. Using NIH Image J software Z-stacks were converted into a maximum intensity projection image. Mean axonal number per animal was obtained from averaging the blind counting of 3 sections using a manual particle trace and count in NIH Image J software.

DRG processing, staining and counting - OCT embedded L4 DRG were completely serially sectioned (30 μ m) and every fifth section was collected onto separate gelatine-coated slides. Sections were air-dried ON, rehydrated in PBS, permeabilized, blocked and immunostained with mouse anti- β III-tubulin (Millipore, MAB5564) diluted 1:10000 in blocking solution (0.3% TritonX-100, 5% Normal Goat Serum in PBS) ON at 4°C. Slides were washed in PBS and incubated with goat anti-mouse conjugated to Alexa Fluor 488 (Jackson ImmunoResearch, 115-545-003) diluted 1:5000 in blocking solution ON at 4°C. Sections were counterstained with 1 μ g/ml of DAPI and mounted with Fluoroshield mounting media (Sigma, F6182). DRG sections were tiled-imaged in Leica DMI8 confocal microscope and LAS X software with 488 nm laser in 1 μ m z-increments with 10x objective. The number of immunopositive DRG neurons was determined by counting neurons with nucleus every fifth section as described previously [713].

Hind-paw skin processing, staining and free nerve ending (FNE) counting - OCT embedded hind-paw skin was transverse sectioned (20 μ m) and every third section was collected onto separate gelatin-coated slides (0.5 mm total skin area sectioned per animal). Sections were air-dried ON, rehydrated in PBS, permeabilized, blocked and immunostained with rabbit anti-CGRP (Sigma, C8198) diluted 1:3000 in blocking solution (0.3% TritonX-100, 5% Normal Goat Serum in PBS) ON at 4°C. Slides were washed in PBS and incubated with goat anti-rabbit conjugated to Alexa Fluor 546 (Invitrogen, A-11035) diluted 1:5000 in blocking solution ON at 4°C. Sections were counterstained with

1µg/ml of DAPI and mounted with Fluoroshield mounting media (Sigma, F6182). Skin sections were imaged in Leica DMI8 confocal microscope and LAS X software with 546 nm laser in 1 µm z-increments with 40x oil immersed objective. Using NIH Image J software, z-stacks were converted into a maximum intensity projection image. The dermis-epidermis borderline within the image area was traced and its length measured. Immunolabeled intraepidermal CGRP-positive fibers at the glabrous skin were manually and blinded counted. At least 3 images per section and 5 sections per animals were analyzed. Counts were normalized to the measured epidermal length and displayed as number of FNE per 500 µm [714, 715].

Lumbar spinal cord processing, motoneuron staining and counting - OCT embedded L3-L5 lumbar spinal cords were trans-sectioned (20 µm) and every fifth section was collected onto separate gelatin-coated slides. Sections were air-dried ON, rehydrated in PBS and subject to heat-induced epitope retrieval by heating to 95°C for 5 minutes in retrieval solution (10 mM Tris base, 1 mM EDTA solution, 0.05% Tween 20, pH 9.0). Slides were washed in PBS, permeabilized, blocked and immunostained with goat anti-CHAT (Millipore, AB144P) diluted 1:300 in blocking solution (0.3% TritonX-100, 5% Normal Goat Serum in PBS) ON at 4°C. Slides were washed in PBS and incubated with donkey anti-goat conjugated to Cy3 (Jackson ImmunoResearch, 705-165-147) diluted 1:1000 in blocking solution ON at 4°C. Sections were counterstained with 1µg/ml of DAPI and mounted with Fluoroshield mounting media (Sigma, F6182). Spinal cord sections were imaged in Leica DMI8 confocal microscope and LAS X software with 546 nm laser in 1 µm z-increments with 40x oil immersed objective. CHAT-positive motoneurons in the spinal cord displaying a prominent nucleolus were counted in every fifth section, a minimum 5 sections per animal. Counts were displayed as number of motoneurons per 500 µm of lumbar spinal cord [716].

2.3.6 Whole-mount immunofluorescence

iDISCO-based tissue clearing for whole-mount forepaw and mammary gland immunostaining was performed as previously described [717]. Briefly E13.5 mice embryos were fixed in 4% paraformaldehyde in PBS, then dehydrated by methanol series (20-100%). Samples were then bleached with 5% H₂O₂ in methanol at 4°C ON, then re-

hydrated and permeabilized first with 0.2% TritonX-100 followed by ON permeabilization with 0.16% TritonX-100, 20%DMSO, 0.3M glycine in PBS. Samples were incubated in blocking solution (0.3% TritonX-100, 10% DMSO, 6% Normal Goat Serum in PBS) for 8 hours, and then incubated with mouse anti- β III-tubulin (Millipore, MAB5564) diluted 1:1000 and guinea pig anti-substance P (Abcam, ab106291) diluted 1:500 in 0.2% Tween-20, 0.001% heparin, 5% DMSO, 3% Normal Goat Serum in PBS at 37°C for 48 hours. Samples were then washed with 0.2% Tween-20, 0.001% heparin in PBS and incubated with goat anti-guinea pig conjugated to Alexa Fluor 488 (Invitrogen, A-11073) diluted 1:500 and goat anti-mouse conjugated to Alexa Fluor 546 (Invitrogen, A-11030) diluted 1:500 in 0.2% Tween-20, 0.001% heparin, 3% Normal Goat Serum in PBS. After 48 hours, samples were extensively washed with 0.2% Tween-20, 0.001% heparin in PBS and dehydrated in methanol. Samples were cleared by successive washes in 66% DCM/33% methanol, 100% DCM and 100% dibenzyl ether. Forepaws were imaged on a Leica DMI8 confocal microscope and LAS X software with 488 nm and 546 nm lasers in 3 μ m z-increments with 5x objective. Similarly, mammary glands were imaged in a Leica DMI8 confocal microscope and LAS X software with 546 nm laser in 0.5 μ m z-increments with 40x oil immersed objective.

2.3.7 Ca^{2+} imaging with Fluo-4 and quantification

DRG explants were seeded on glass bottom dishes (CellVis) and treated with 5 μ M Fluo-4 AM (Invitrogen) in neurobasal media for 15 min at 37°C, washed with HBSS and switched to clear HBSS-based complete media supplemented with HEPES (final concentration 20 mM) to maintain its physiological pH. Explants were tiled-imaged using a Zeiss Observer Z.1 inverted epifluorescence microscope with an automated motorized stage at 40x magnification. Employing NIH Image J software, stitched master images of each explant were cropped to eliminated soma and Schwann-cell area. From there, a binary mask image of remaining axons was created to measure area and mean pixel intensity corrected by background signal. After calculating the intensity per unit of axonal area, DRG explants from the same embryo were pooled and averaged to generate the mean value per embryo. Measurements were normalized and expressed as fold-change from NGF wild-type control.

2.3.8 Live endoplasmic reticulum (ER)-Ca²⁺ content and store-operated Ca²⁺ entry (SOCE) quantification

Dissociated DRG neurons were seeded on glass bottom dishes (CellVis), growth for 24 hours and treated with 5 μ M Fluo-4 AM (Invitrogen) in neurobasal media for 15 min at 37°C, washed with HBSS and then allowed to equilibrate in fresh media for 15 min. Plates were then switched to clear HBSS-based media without Ca²⁺ supplemented with HEPES (final concentration 20 mM) to maintain its physiological pH. Fluo-4 fluorescence was recorded for around a minute to establish baseline intensity. For measurements of ER-Ca²⁺ content, cells were treated while recording with the sarcoplasmic and endoplasmic reticulum Ca²⁺ ATPase (SERCA) pump blocker thapsigargin (1 μ M final, Sigma-Aldrich, T9033). Fluo-4 fluorescence rise corresponds to of ER Ca²⁺ content release to the cytoplasm. Once fluorescence returns to baseline, Ca²⁺ influx through SOCE is measured by adding back HBSS media with Ca²⁺ (2 mM final of CaCl₂) [718]. Fields with at least three DRG neuronal somas were chosen for recording. Fluo-4 intensity were normalized by neuronal soma area and plotted relative to wild-type DRG group at initial fluorescence baseline without Ca²⁺ and thapsigargin.

2.3.9 Immunoblotting

For SDS-PAGE and western blot analysis, a total of 25 DRG explants per well were seeded in 12-well plastic plates (Grenier). For protein harvesting, cultures were washed with PBS, and DRGs were scraped into 90 μ l of sample buffer (4% SDS, 20% glycerol, 10% 2-mercaptoethanol, 0.004% bromophenol blue and 0.125 M Tris-HCl, pH approx. 6.8). Samples were boiled for five minutes, centrifuged and stored at -80°C for later analysis. Antibodies used for immunoblotting were: anti- β III-tubulin (Millipore MAB5564, 1:10000), anti-APP-Y188 (Abcam ab32136, 1:1000), anti-caspase-3 (NEB 9662, 1:1000), anti-APP phosphoT668 (Cell Signaling #3823, 1:1000), anti-TOMM20 (Abcam ab56783, 1:1000). Densitometric analysis was performed using Bio-Rad ImageLab™ software.

2.3.10 Mitochondria and axonal live staining with TMRE and Calcein-AM

DRG explants were treated with 1 µg/ml Calcein-AM (AAT Bioquest) in neurobasal media for 1 hour at 37°C. Twenty minutes before the end of the initial Calcein-AM incubation hour, explants were co-treated with 0.25 µM tetramethylrhodamine, ethyl ester (TMRE) at 37°C. At the end of the incubation hour, DRG were switched to clear HBSS-based complete media supplemented with HEPES to maintain physiological pH. Imaging was performed with a Leica DMI8 confocal microscope and LAS X software with 488 nm and 546 nm lasers in 0.5 µm z-increments with 63x oil-immersed objective. The number of mitochondria and the pixel intensity of TMRE signal in the axons were measured using NIH Image J software, while the density of mitochondria was calculated per square micron of axon quantified by the area of Calcein-AM-stained axons over a specified threshold. Axons from the same DRG were pooled and averaged to generate the mean value for each DRG. Measurements of TMRE intensity were normalized relative to wild-type conditions.

2.3.11 Pharmacological Trk, PLC γ , PKC, and caspase inhibitors.

Stocks of Trk receptor inhibitor K252a (200 µM, Calbiochem #420298, Israel), PLC γ inhibitor U73122 (10 mM, Sigma U6756, USA), PKC inhibitor Gö6976 (10 mM, Tocris 2253, UK), pan-caspase inhibitors Boc-D-fmk (10 mM, Abcam ab142036, USA), zVAD-fmk (20 mM, R&D systems FMK001, USA) were prepared in dimethylsulphoxide (DMSO) and used at 1:1000 dilution (final concentration of DMSO below 0.1%). Unless otherwise noted, drugs were applied at the same time that the trophic factor withdrawal was initiated.

2.3.12 Experimental design and statistical analysis

Data were plotted and analyzed using Prism 6 (Graph-Pad). All data were presented as mean \pm SEM. The number of embryos n in each experiment or condition is described in each figure legend. Unpaired t-test test (unpaired, two-tailed) or Mann-Whitney (unpaired, two-tailed) was used for two-group experiments comparisons. Two-way ANOVA with Dunnets's *post hoc* test, Tukey's or Bonferroni's *post hoc* test was used to analyze differences in multiple groups. In all graphs, non-significant ($p > 0.05$): ns, * $p < 0.05$, ** $p < 0.01$, *** $p < 0.001$ and **** $p < 0.0001$.

2.4 Results

Conflicting results have been reported on the role played by APP during developmental remodelling in DRG sensory neurons. While Nishimura et al. (2003) showed the neuroprotective effect of APP on DRG neurons deprived of NGF [333], Marc Tessier-Lavigne's group claimed it was important in mediating developmental axonal degeneration *in vitro* and *in vivo* [331, 332]. To determine whether APP exerts neuroprotective or neurodegenerative effects in DRG neurons during the period of developmental programmed cell death, we mimicked this process *in vitro*. DRGs from mixed litters of wild-type and APP-knockout E13 mouse embryos were cultured for 60 hours in the presence of NGF (to support survival and neurite outgrowth), and then deprived of NGF for 21 and 24 hours (Figure 2.1 A). The pool of three independent experiments showed a significantly higher axonal density in APP-null DRG explants following 21 and 24 hours of NGF deprivation than in their wild-type counterparts. No significant difference in axon density was found between wild-type and APP-null DRG explants in the presence of NGF (Figure 2.1 B).

The death receptor DR6 was reported to mediate APP pro-degenerative action during axonal pruning and DR6 knockout rescues DRG neurons from degeneration in response to NGF deprivation [331, 332]. Here we also tested the effect of DR6 deficiency in DRG neurons deprived of trophic support (Figure 2.1 C). Our results indicate that, similar to APP-null, DR6-null DRG neurons report a significantly higher axonal area 21 hours after NGF deprivation compared to wild-type explants; with DR6-null DRG neurons, the rescue effect is lost at 24 hours while the rescue effect is still present after 24 hours of deprivation in APP-null neurons (Figure 2.1 D).

The protection observed in APP-null DRG explants under NGF deprivation conditions *in vitro* prompted us to look for consequential effects *in vivo*. Stereometry of sciatic nerve sections revealed that adult APP-deficient mice (7583 ± 157 , SEM) have a significant increase in the number of axons compared with their wild-type counterparts (5359 ± 196 SEM), $t(10) = -8.86$, $p < .01$, (two-tailed); a novel finding not previously reported in literature (Figure 2.2 B). However, no significant differences were observed in the number of L4 DRG neurons, nor in the number of free nerve endings (FNE) at the

hind paw skin between wild-type and APP-null adult animals (Figure 2.2 A and C). The number of lumbar motoneurons, whose axons also constitutes part of the sciatic nerve, was not significantly different between genotypes (Figure 2.2 D). To explore whether adult changes in the sciatic nerve could be the consequence of early alteration during development, whole-mount immunostaining of wild-type and APP-null E13 mouse embryos were performed. Qualitative assessment of the innervation at the fore paw and the mammary gland did not indicate any gross difference between wild-type and APP-deficient embryos at those locations (Figure 2.2 E and F).

To begin to determine how APP promotes degeneration of DRG neurons *in vitro*, APP protein levels were determined by immunocytochemistry (ICC) and western blot (WB) in DRG explants at different time points after NGF withdrawal. Figure 2.3 A shows that the levels of APP measured by ICC increased shortly (3 hrs) after NGF deprivation. We confirmed this result in Figure 2.3 B using WB, where full-length APP protein levels peaked at 3 hours after NGF deprivation then decreased after 9 hours (Figure 2.3 B).

Phosphorylation of APP at threonine 668 (T668) has been associated with the APP pro-degenerative roles in other neuronal types [335, 532, 536]. We thought to measure the level of phosT668-APP during early stages of NGF deprivation. Figure 2.3 C shows a significant increase of phosT668-APP, one hour after NGF deprivation. Triaca et al. (2016) previously reported that APP phosphorylation at T668 is dependent on the pro-death signaling triggered by TrkA in the absence of NGF [335]. We therefore explored whether the early increase in APP phosphorylation at T668 in DRG neurons deprived of NGF was linked with TrkA signaling. Figure 2.4 A shows that the Trk receptor inhibitor K252a not only rescues DRG neurons from degeneration induced by NGF deprivation (Figure 2.4 A) but also significantly blocks the rise of T688-phosphorylated full-length APP in DRG under NGF deprivation (Figure 2.4 B).

PLC γ is well established as an effector of TrkA signaling [10]. Phosphorylation of PLC γ induces PKC activation through DAG and IP $_3$ -IP $_3$ R-induced ER-Ca $^{2+}$ release [325-328]. To address the role of PLC γ and PKC in the DRG degenerative cascade, U73122 and Gö6976, inhibitors of PLC γ and PKC respectively, were used. Figure 2.5 A and B shows that each compound reduced the levels of T688-phosphorylated full-length APP in DRGs deprived of NGF (Figure 2.5 C) and protects axons during NGF-deprivation.

The PLC γ -PKC axis plays an important role in the fine-tuning of Ca $^{2+}$ responses, including the regulation of ER-Ca $^{2+}$ stores [327, 330], the modulation of TRP channels [329], and the facilitation of Ca $^{2+}$ pumps [719]. The rise in axoplasmic Ca $^{2+}$ is a hallmark of degeneration during NGF deprivation [329, 360]. In addition to their apparent effect on APP phosphorylation, the inhibition of PLC γ or PKC with U73122 and Gö6976, significantly reduced the axoplasmic Ca $^{2+}$ levels in DRG explants upon 15 hours of NGF deprivation (Figure 2.5 D). Therefore, we asked whether the rise of intracellular Ca $^{2+}$ is connected with the PLC γ -PKC axis through APP phosphorylation. We could not modulate APP phosphorylation directly so asked how the genetic deletion of APP affects the rise in axoplasmic Ca $^{2+}$ in DRG explants deprived of NGF. Interestingly, the lack of APP significantly reduces the increase of cellular Ca $^{2+}$ during NGF deprivation (Figure 2.6 A). We then addressed whether the lack of APP dysregulates the ER Ca $^{2+}$ store-operated Ca $^{2+}$ entry (SOCE). Dissociated DRG neurons from wild-type and APP-null E13 embryos were treated with the inhibitor of the SERCA pump thapsigargin in media without Ca $^{2+}$. Using the Ca $^{2+}$ dye Fluo-4 we followed the intracellular rise of Ca $^{2+}$ that occurs in response to thapsigargin, which reflects ER Ca $^{2+}$ content without interference of SOCE due to the absence of extracellular Ca $^{2+}$ (Figure 2.6 B and C). Significant differences were found between wild-type and APP-null DRG neurons in terms of their ER Ca $^{2+}$ content (Figure 2.6 D, *Thp*). Re-addition of Ca $^{2+}$ to the extracellular media revealed significantly reduced influx of Ca $^{2+}$ through the SOCE system in APP-null DRGs compared with their wild-type counterparts (Figure 2.6 D, *Thp* + Ca $^{2+}$). These results suggest that DRG sensory neurons lacking APP have decreased ER Ca $^{2+}$ content and attenuated SOCE.

Mitochondria constitute an important decision node, especially during degeneration driven through the intrinsic apoptotic pathway. Using the live dye TMRE, which identifies functional mitochondria based on intact mitochondria membrane potential, we observed a significant reduction in the number of mitochondria and a reduced intensity of TMRE per axon area in APP-null DRG axons compared with wild-types neurons (Figure 2.7 A, B and C). Interestingly total levels of TOM20, a subunit of the mitochondrial protein import complex TOM (often used as a surrogate measure of total mitochondrial mass), are significantly increased in APP-null DRG lysates compared with lysates from wild-types DRG neurons with or without NGF (Figure 2.7 D and E).

Lastly, caspases are key executor proteases during degeneration induced by NGF deprivation in DRG neurons [214, 225]. Although our previous experiments attribute a pro-degenerative role for APP in this context, immunoblots analyzing the content of cleaved caspase-3 in lysates from wild-type and APP-null DRG explants withdrawn from NGF for 15 hours did not yield significant differences between both genotypes (Figure 2.7 D and F).

2.5 Discussion

Developmental neuronal cell death is essential for normal, high fidelity patterning of the nervous system but its molecular mechanisms are still not fully understood. Several research avenues have opened during the last decade, one being the role played by APP, a protein intimately linked with AD pathology. The available data supports an important role for APP in developmental neuronal remodeling, although its nature has been contradictory, ranging from protective to pro-degenerative [331-333]. By demonstrating a pro-degenerative role for APP in DRG sensory neurons, our work helps clarify the physiological role of APP during peripheral neuron development and provides new insights into the mechanisms by which APP contributes to developmental neuronal elimination.

2.5.1 Evidence *in vitro* and *in vivo* supports a pro-degenerative role for APP during PNS development

A role of APP in neuronal remodelling during development has been observed *in vivo* during the pruning process of RGC axons in the superior colliculus at the CNS. Similarly, experience dependent-plasticity and axonal pruning in the adult brain has been shown to be actively dependent on APP [332, 720]. In the sensory PNS, the evidence supporting APP role in developmental neuronal remodelling is contradictory and restricted to *in vitro* models. In an early study, Nishimura et al. (2003) reported that degeneration of DRG neurons deprived of NGF is significantly more severe when APP expression is knock-down [333]. Olsen et al. (2014) later demonstrated that APP deficiency slightly but significantly reduces axonal loss in the same *in vitro* model. Here we report that APP has a pro-degenerative role in DRG neurons deprived from NGF [332]. Its deficiency significantly rescues the loss of axons normally observed in wild-type DRG explants. We also addressed the role of DR6 in this model, previously reported to mediate APP pro-degenerative actions [331]. Our results show that DR6 deficiency is less effective than APP in delaying the degenerative process of DRG neurons deprived of trophic support, given that the protection observed at 21 hours of deprivation is lost at 24 hours. This

suggests that roles of APP and DR6 in the degenerative process may not be as tightly linked as previously indicated [331].

To determine the physiological implications of our *in vitro* results, we performed a broad exploration of the PNS in adult mice deficient from APP *in vivo*. Our results show a significant increase in the number of axons in the sciatic nerve of APP-null adult mice compared with wild-type mice. A recent work similarly observed a tendency towards an increase in total sciatic nerve axons, especially in the smaller non-myelinated axons, in both single APP-null and APLP2-null adult mice, but contrary to our study, this was not statistically significant [466]. The increase in sciatic nerve axons in APP-null mice depicted in our analysis is not the result of an increase in the number of L4 DRG neurons nor due to an increase in the number of motoneurons at the lumbar spinal cord. We observed a trend towards increased CGRP-positive fine nerve endings in footpad skin of APP-deficient animals, but the lack of statistical significance left the sciatic nerve phenotype without a straightforward explanation. Future efforts will be required to determine the nature of this phenotype, specifying what type of axons are indeed increased, before exploring the effect that it might have at the corresponding nerve terminals. Notably, analysis of APP and APLP2 double knockout mice has revealed an axon terminal sprouting phenotype at the neuromuscular junction [721], and APP was recently identified as a novel receptor for the repulsive guidance cue Slit [500], which also plays a role in developmental axonal pruning [722].

2.5.2 TrkA and APP phosphorylation at T668: partners in crime?

APP and the neurotrophin receptor TrkA are engaged in intricate crosstalk, fundamentally determined by the phosphorylation state of APP at the intracellular domain [334, 335]. In the absence of trophic support, TrkA switches to a pro-death mode and induces the phosphorylation of APP at T668 [335], a modification associated with APP pro-degenerative role in several different cellular contexts [532-537]. Our findings that NGF withdrawal increases APP phosphorylation at T668, and that TrkA inhibition by K252a simultaneously block DRG axonal degeneration and the rise of phospho-APP-T668 during NGF deprivation, indicate a close interplay between TrkA and APP in DRG

neurons. Moreover, we demonstrated that the increase in APP phosphorylation at T668 elicited by NGF withdrawal coincides with increased full-length APP levels, consistent with previous findings that suggested that T668 phosphorylation promotes APP stability and evasion of proteasomal degradation [536]. Our results are also consistent with the hypothesis that TrkA-mediated APP phosphorylation requires the PLC γ >PKC signaling axis, given that their pharmacological inhibition not only rescues axonal degeneration but abolishes the increase of APP-T668 phosphorylation normally induced by NGF deprivation. Mutagenesis studies will be important to determine the actual importance of T668 phosphorylation in the overall pro-degenerative action of APP during the developmental degeneration of DRG neurons.

2.5.3 APP deficiency reduces axoplasmic Ca²⁺ rise but does not attenuate caspase activation during DRG degeneration

Axoplasmic Ca²⁺ rise and caspase activation are both fundamental events during the degeneration of NGF-deprived DRG neurons. Either Ca²⁺ chelation with EGTA or the inhibition of caspases through pharmacological or genetic means, rescue axonal degeneration induced by NGF withdrawal [214, 225, 360]. We quantified the levels of cleaved caspase-3 and axoplasmic Ca²⁺ in wild-type and APP-null DRG neurons at the same progression time, 15 hours after NGF deprivation. In accordance with the reduced axonal area loss previously observed, NGF-deprived APP-null explants showed a significant decrease in axoplasmic Ca²⁺ levels compared with wild-type DRGs. However, the quantity of cleaved caspase-3 increases similarly in deprived explants from both genotypes. Assuming that APP deficiency delays but does not completely block axonal degeneration, it is reasonable to expect that increases in caspase activation and axoplasmic Ca²⁺ in APP-null explants will match those of wild-type explants but later in the degenerative process. A recent study suggested that caspase activation lies upstream axoplasmic Ca²⁺ rise in the degenerative cascade [232]. Thus, differences in caspase activation between deprived wild-type and APP-null DRGs may occur well before changes in axoplasmic Ca²⁺ observed 15 hours after NGF withdrawal.

2.5.4 Modulation of intracellular Ca²⁺ by APP: from the ER to the mitochondria

ER Ca²⁺ dysregulation and the consequent induction of the ER stress response facilitates the intrinsic apoptotic pathway [241, 539]. Although it is not certain that early ER Ca²⁺ dysregulation is a component of the degenerative process in NGF-deprived DRG neurons, several molecular markers of the ER-stress response increase in DRG neurons upon NGF deprivation [322]. Importantly, the PLC γ >PKC signaling axis plays a role in the fine-tuning of Ca²⁺ responses, including the regulation of ER-Ca²⁺ stores [327, 330]. PLC γ activation is able to trigger the release of ER Ca²⁺ to the cytosol through the activation of IP₃ receptors by IP₃ [325-328]. Here, we showed that inhibition of PLC γ and PKC significantly reduces the axoplasmic Ca²⁺ rise observed in DRG neurons deprived of NGF, consistent with the importance of the PLC γ >PKC signaling axis in the regulation of intracellular Ca²⁺.

ER Ca²⁺ release is followed by rapid Ca²⁺ replenishment to avoid ER stress. Ca²⁺ reuptake from the cytosol occurs via SERCA pumps and this allows cytosolic Ca²⁺ levels reach homeostasis, with Ca²⁺ entering the cell from the extracellular milieu via SOCE [539]. Several studies have demonstrated that APP participates in ER stress-induced cell death in different cell types [541-543], and others have highlighted the capacity of APP to alter the basal ER Ca²⁺ levels and regulate SOCE [552, 555-558]. Our work demonstrates that in the absence of APP, the ER Ca²⁺ content and SOCE are significantly attenuated in DRG neurons. Interestingly, APP is not the only protein with pro-degenerative functions whose deficiency decreases ER Ca²⁺ levels and downregulates SOCE. Embryonic fibroblasts lacking the pro-apoptotic protein BAX, also have reduced ER Ca²⁺ content and SOCE responses [296]. Interestingly, the resistance of BAX-null cells to cell death in part reflects the reduced capacity of the ER to transfer Ca²⁺ to the mitochondria and thereby trigger the mitochondrial apoptotic pathway [299, 723]. Although SOCE replenishes ER Ca²⁺ stores and decrease ER stress, it could also be contributing in the opposite direction, fostering the accumulation of cytosolic and ER Ca²⁺ and increasing Ca²⁺ transferred from the ER to the mitochondria or to the later axoplasmic Ca²⁺ rise observed in DRG upon NGF withdrawal. Precisely how APP regulates ER Ca²⁺ content and SOCE is unknown. However, the fact that the signaling axis TrkA>PLC γ >PKC emerges as a common

denominator for APP phosphorylation, the ER Ca^{2+} content and SOCE activation, raises the possibility that the phosphorylation state of APP modulates - through SOCE - the levels of intracellular Ca^{2+} at early stages of degeneration.

Mitochondria act as decision hubs in multiple physiological and pathological processes, including the modulation of intracellular Ca^{2+} stores and the control of cell death [561]. We found that APP-null DRG neurons have an increase in TOM20 levels, yet the axonal density of TMRE-stained active mitochondria is reduced in APP-null DRG neurons. How this mitochondria phenotype contributes to delay the axonal degeneration in APP-null DRG deprived of NGF is uncertain and requires further investigation. TMRE staining is dependent on the mitochondrial membrane potential, which is necessary, among other functions, for the capacity of mitochondria to buffer cytoplasmic Ca^{2+} [724]. A recent study performed on primary astrocytes demonstrated that mitochondrial Ca^{2+} sequestration is delayed in APP nulls versus their wild-type counterparts, suggesting that the ability of the mitochondria to buffer Ca^{2+} in the absence of APP is impaired [562]. If a similar mitochondrial defect exists in APP-null DRG neurons, it could imply a reduced capacity to cope with cytosolic Ca^{2+} increases. On the other hand, impaired mitochondrial Ca^{2+} buffering ability could work as a defense mechanism against mitochondrial Ca^{2+} overload, a well-known step of the apoptotic pathways that facilitates ROS production, cytochrome *c* oxidation and release, and caspase activation [299, 725]. It will be important to resolve how APP deficiency alters mitochondrial function in DRG neurons deprived of NGF.

In conclusion, this work provides evidence in favour of the pro-degenerative role of APP in a model of developmental degeneration of DRG sensory neurons *in vitro* and suggest a similar function in the PNS *in vivo*. Our study also proposes a new realm of action for APP during developmental neuronal cell death related to the regulation of intracellular Ca^{2+} homeostasis. Further studies are needed to determine the full implication of these mechanisms during development and in adult physiology.

2.6 Figures and figure legends

Figure 2.1. APP and DR6 genetic deficiency protects DRG sensory neurons from degeneration induced by NGF deprivation. A) Wild-type and APP-null DRG explants cultured in the presence of NGF for 48 hours and then either maintained with trophic support or deprived with a function blocking anti-NGF antibody (2 $\mu\text{g/ml}$) for the following 21 or 24 hours, before fixation and immunostaining with $\beta\text{III-tubulin}$ (Scale bar = 250 μm). **B)** Quantification of axonal area as a function of the distance from the soma using Axoquant 2.0 [360], and plotted in 500- μm bins. The difference between the relative axonal area between wild-type and APP-null DRG at different time points were analyzed by two-factor ANOVA and Tukey's *post hoc* comparison and plotted with mean and SEM (n = 7 wild-type embryos, n = 8 APP-null embryos); (*) wild-type vs. APP-null; ***p < 0.001, ****p < 0.0001. **C)** Wild-type and DR6-null DRG explants cultured in the presence of NGF for 48 hours and then either maintained with trophic support or deprived with a function blocking anti-NGF (2 $\mu\text{g/ml}$) for the following 21 or 24 hours, before fixation and immunostaining with $\beta\text{III-tubulin}$ (Scale bar = 250 μm). **D)** Quantification of axonal area as a function of the distance from the soma using Axoquant 2.0 [360], and plotted in 500- μm bins. Differences between the relative axonal area of wild-type and DR6-null DRG at different time points were analyzed by two-factor ANOVA and Tukey's *post hoc* comparison and plotted with mean and SEM (n = 9 wild-type embryos, n = 7 DR6-null embryos); (*) wild-type vs. DR6-null; ***p < 0.001, ****p < 0.0001.

Figure 2.1

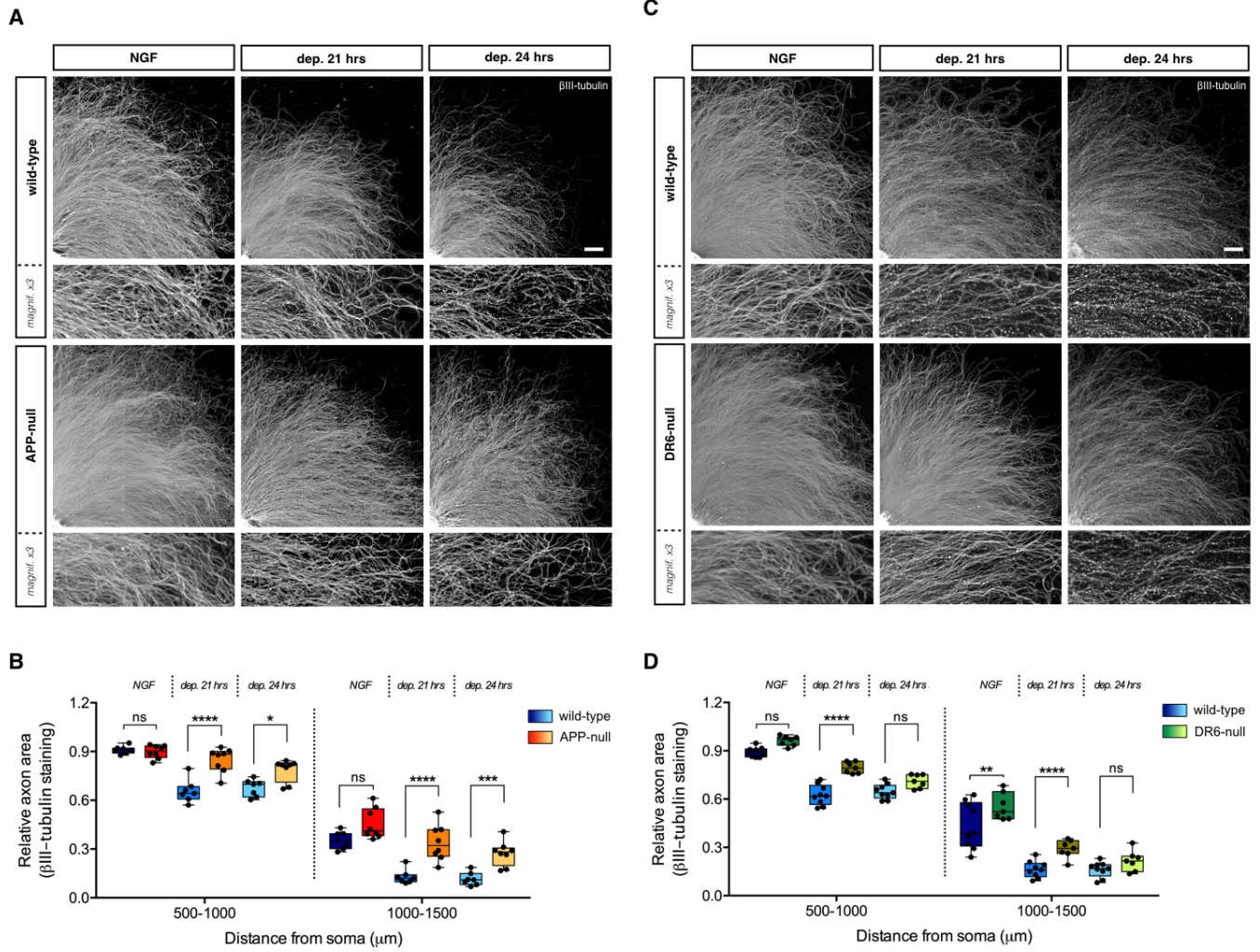


Figure 2.2. Hypertrophy phenotype in adult APP-null mice PNS. A) Representative cross-sections of L4 DRG from adult wild-type and APP-null mice stained with β III-tubulin (Scale bar = 250 μ m). Quantification analysis shows no significant differences in the number of DRG neurons in APP-null adult animals compared with their wild-type counterparts. Results show a mean of 12830 ± 682 neurons in wild-type ($n = 3$) against 13035 ± 876 in APP-null DRG ($n = 3$), analyzed by unpaired t-test $t(4) = 0.184$, $p = .862$, two-tailed. Values are expressed as the mean \pm SEM. **B)** Representative transverse sections of adult wild-type and APP-null mice sciatic nerves stained with β III-tubulin (Scale bar = 100 μ m). Quantification shows a significant increase in the number of sciatic nerve axons in APP-null adult animals compared to their wild-type counterparts. Results show a mean of 5284 ± 292 axons in wild-type ($n = 3$) against 7482 ± 187 in APP-null sciatic nerves ($n = 3$), analyzed by unpaired t-test $t(4) = 6.23$, $p < .01$, two-tailed. Values are expressed as the mean \pm SEM. **C)** Representative sections of adult wild-type and APP-null mice hind-paw skin with CGRP (Scale bar = 10 μ m). There is not a significant difference in the number of FNE in the hind-paw skin of adult APP-null mice compared with their wild-type counterparts. Results show a mean of 32 ± 1.5 FNE per 500 μ m of glabrous skin in wild-type ($n = 3$) against 37 ± 1.2 in APP-null hind-paw skin ($n = 3$), analyzed by unpaired t-test $t(4) = 2.39$, $p = .07$, two-tailed. Values are expressed as the mean \pm SEM. **D)** Representative sections of L3-L5 spinal cord from adult wild-type and APP-null mice stained with CHAT (Scale bar = 250 μ m). There is not a significant difference in the number of CHAT-positive motoneurons in APP-null adult animals compared with their wild-type counterparts. Results show a mean of 240 ± 10 motoneurons per 0.5 mm of lumbar spinal cord in wild-type ($n = 3$) against 266 ± 12 in APP-null adult mice ($n = 3$), analyzed by unpaired t-test $t(4) = 1.70$, $p = .164$, two-tailed. Values are expressed as the mean \pm SEM. **E)** Representative whole-mount co-immunostaining of wild-type and APP-null E13.5 forepaws for the peptidergic nociceptor marker substance P and the neuronal cytoskeleton marker β III-tubulin (Scale bar = 500 μ m). **F)** Representative whole-mount immunostaining of wild-type and APP-null E13.5 female mammary glands for the neuronal cytoskeleton marker β III-tubulin (Scale bar = 5 μ m).

Figure 2.2

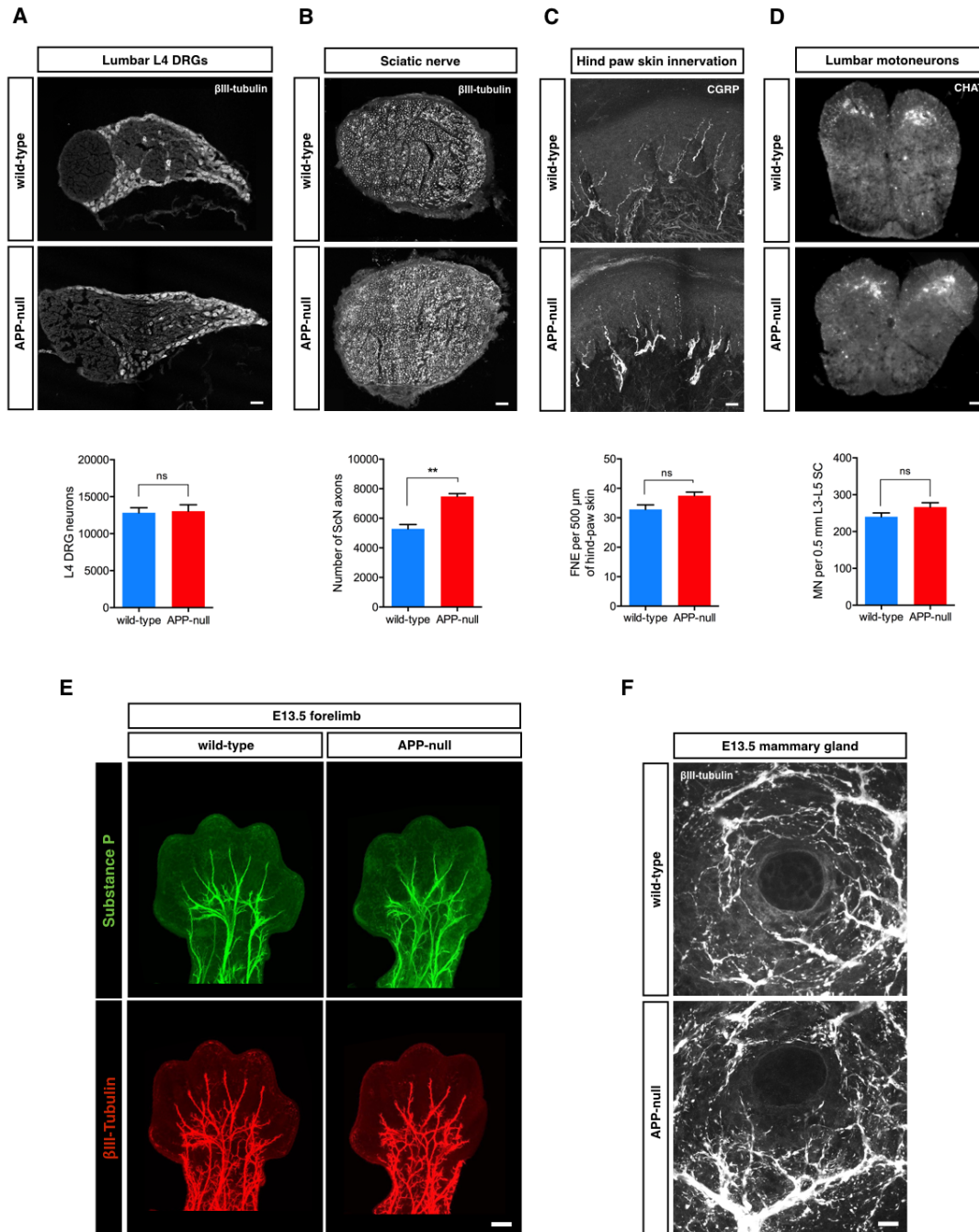


Figure 2.3. NGF-deprivation induces an early increase in full-length APP protein levels and of its phosphorylation state at threonine 668. **A)** Immunocytochemistry of E13.5 DRG explants cultured for 48 hours in the presence of NGF (12.5 ng/ml) and then either maintained with trophic support or deprived with a function blocking anti-NGF antibody (2 µg/ml) for 1, 3 or 6 hours, before fixation and co-immunostaining with APP-Y188 and βIII-tubulin (Scale bar = 20 µm). The right panel shows the quantification of APP intensity normalized by axonal area and relative to non-deprived DRG axons. Results show a significant increase of APP immunofluorescence at 3 hours after NGF deprivation relative to NGF control analyzed by two-factor ANOVA and Dunnett's *post hoc* comparison and plotted with mean ± SEM (representative of 3 independent experiments). **B)** Protein lysates from E13.5 DRG explants cultured for 48 hours in the presence of NGF (12.5 ng/ml) and then either maintained with trophic support or deprived with a function blocking anti-NGF (2 µg/ml) for 1, 3, 6, 9 or 12 hours were western blotted against APP-Y188 and βIII-tubulin. The right panel represents the densitometric analysis of the corresponding bands of full-length APP normalized by βIII-tubulin levels and relative to NGF control. Results show a significant increase of full-length APP levels 3 hours after deprivation and a significant decrease at 9 and 12 hours after NGF withdrawal relative to non-deprived condition, analyzed by two-factor ANOVA and Dunnett's *post hoc* comparison, and plotted with mean ± SEM (representative of 3 independent experiments). **C)** Same as in B) but with equal quantity of full-length APP among all conditions and Western blotting using a monoclonal antibody against phosphorylated APP at threonine 668. The right panel represents the ratio between the densitometry of the corresponding bands for phosphoThr668-flAPP and full-length APP relative to NGF control. Results show a significant increase of phosphorylated APP levels at 3 and 6 hours after NGF deprivation relative to non-deprived condition, analyzed by two-factor ANOVA and Dunnett's *post hoc* comparison, and plotted with mean ± SEM (representative of 3 independent experiments).

Figure 2.3

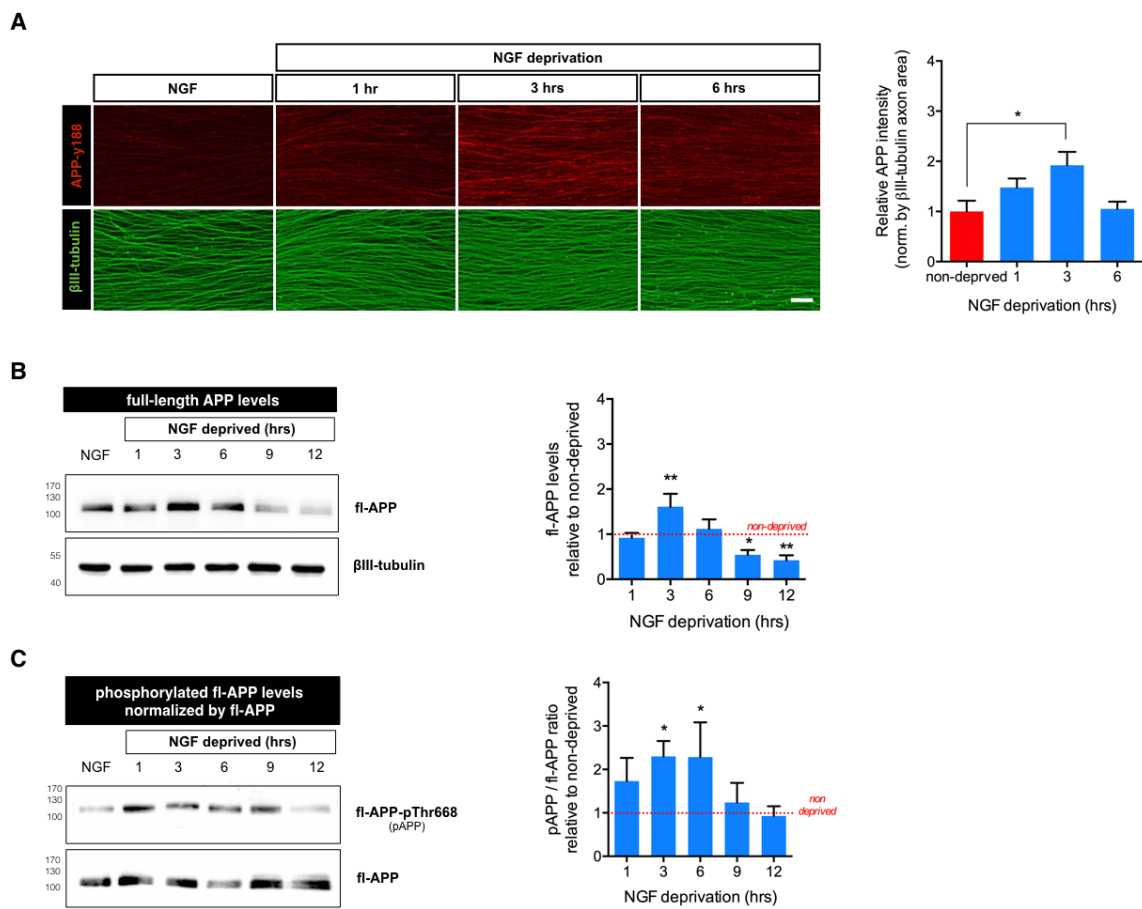


Figure 2.4. Trk receptor inhibition protects axons from NGF deprivation and reduces levels of phosphorylated APP at threonine 668. A) DRG explants cultured in NGF were either maintained in trophic media or withdrawn from trophic support with or without Trk receptor inhibitor K252a (200 nM) for 24 hours before fixing, immunostaining for β III-tubulin and imaged by epifluorescence microscopy (Scale bar = 1000 μ m). K252a rescued degeneration induced by NGF deprivation. Quantification of axonal area as a function of the distance from the soma using Axoquant 2.0 [360], and plotted in 500- μ m binned segments relative to 0-500 μ m NGF control. The relative axonal area was analyzed by two-factor ANOVA followed by Tukey's *post hoc* comparison and plotted with mean and SEM (n = 3 embryos per condition); (*) ctr. versus dep. 24h; (#) dep. 24h versus dep. 24h + K252a; ns: non-significant, **p < 0.01, ***p < 0.001, ****p < 0.0001. **B)** Protein lysates from E13.5 DRG explants cultured for 48 hours in the presence of NGF (12.5 ng/ml) and then either maintained with trophic support or deprived with a function blocking anti-NGF antibody (2 μ g/ml) for 3 hours with or without K252a (200 nM) were analyzed against APP-Y188, phosphoAPP-T668 and β III-tubulin. The bar graph represents level of full-length phosphoAPP-T668 compared to full-length APP. Results show that K252a significantly inhibits the increase of phosphorylated full-length APP levels at 3 hours after NGF deprivation. These results were analyzed by two-factor ANOVA and Tukey's *post hoc* comparison and plotted with mean \pm SEM (representative of 3 independent experiments).

Figure 2.4

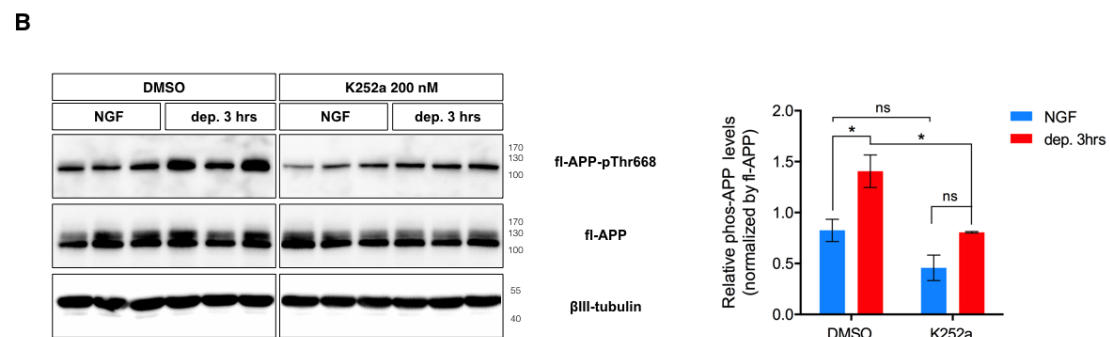
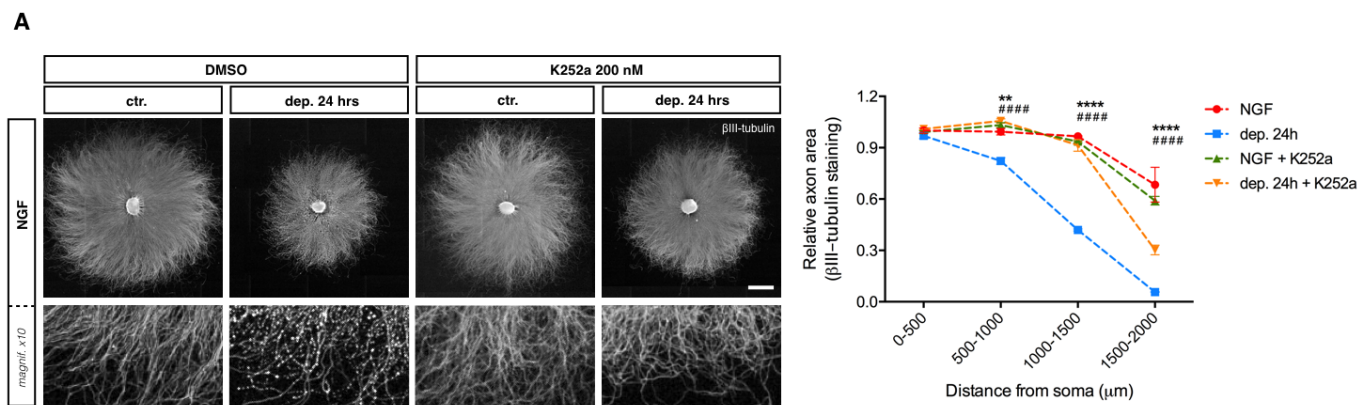


Figure 2.5. PLC γ and PKC inhibitors protect axons from NGF deprivation, reduce the rise of axoplasmic Ca $^{2+}$ during degeneration and abolish the rise of APP phosphorylation at threonine 668 upon NGF withdrawal. **A)** DRG explants cultured in NGF were maintained in trophic media or withdrawn from trophic support, with or without PLC γ inhibitor U73122 (10 μ M) for 24 hours before fixing, immunostaining for β III-tubulin and imaged by epifluorescence microscopy (Scale bar = 1000 μ m). Plot represents the quantification of axonal area as a function of the distance from the soma using Axoquant 2.0 [360], and plotted in 500- μ m bins segments relative to 0-500 μ m 48-hour time point. The relative axonal area was analyzed by two-factor ANOVA followed by Tukey's *post hoc* comparison and plotted with mean and SEM (n = 3 embryos per condition); (*) control versus deprived 24h; (#) deprived 24h versus deprived 24h + Gö6976; ns: non-significant, *p < 0.05, ****p < 0.0001. **B)** DRG explants cultured in NGF were maintained in trophic media or withdrawn from trophic support, with or without PKC inhibitor Gö6976 (10 μ M) for 24 hours before fixing, immunostaining for β III-tubulin and imaged by epifluorescence microscopy (Scale bar = 1000 μ m). Plot represents the quantification of axonal area as a function of the distance from the soma using Axoquant 2.0 [360], and plotted in 500- μ m bins segments relative to 0-500 μ m 48-hour time point. The relative axonal area was analyzed by two-factor ANOVA followed by Tukey's *post hoc* comparison and plotted with mean and SEM (n = 3 embryos per condition); (*) control versus deprived 24h; (#) deprived 24h versus deprived 24h + Gö6976; ns: non-significant, ****p < 0.0001. **C)** Protein lysates from E13.5 DRG explants cultured for 48 hours in the presence of NGF (12.5 ng/ml) and then either maintained with trophic support or deprived with a function blocking anti-NGF (2 μ g/ml) for 3 hours with or without U73122 or Gö6976 were analyzed against APP-Y188, phosphoAPP-T668 and β III-tubulin. Although preliminarily, these results suggest that PLC γ inhibitor and PKC inhibitor may attenuate the increase of phosphorylated APP levels upon NGF withdrawal (blots are representatives of a single experiment per drug; within the experiment, each treatment was performed in triplicates such that each lane represents the DRG lysate of a different embryo). **D)** DRG explants cultured in NGF were maintained in trophic media or withdrawn from trophic support for 15 hours with or without U73122 or Gö6976 before staining with Fluo-4 and imaged by epifluorescence microscopy (NGF scale bar = 1000

μm). NGF deprivation induced a significant increase in axonal Fluo-4 intensity ($n = 4$ embryos in NGF) that is significantly attenuated by PLC γ inhibitor and PKC inhibitor. The box plots show mean, min/max and 25/75% for each panel, analyzed by one-factor ANOVA followed by Bonferroni's *post hoc* comparison ($n = 4$ embryos per condition); *** $p < 0.001$, **** $p < 0.0001$.

Figure 2.5

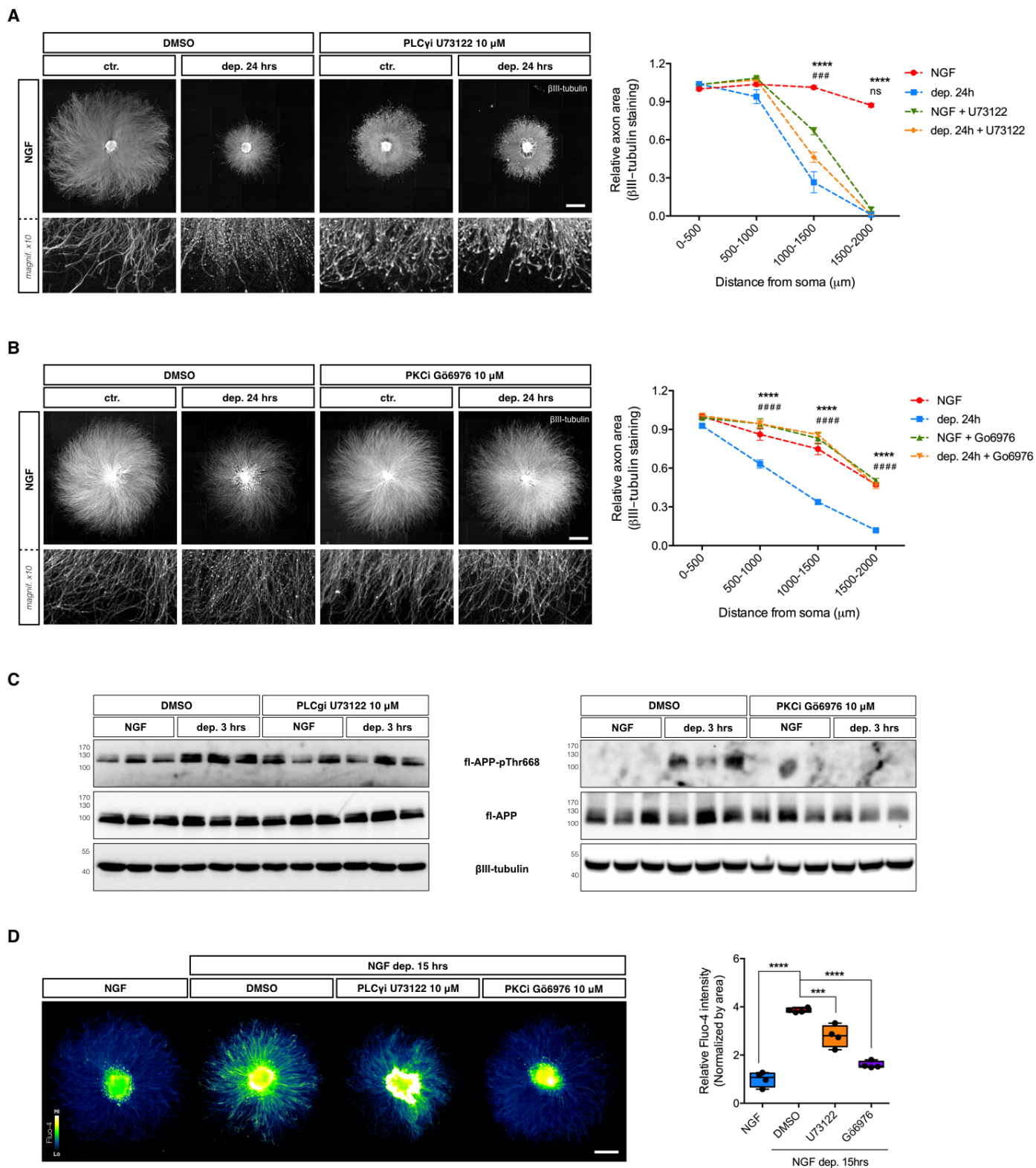
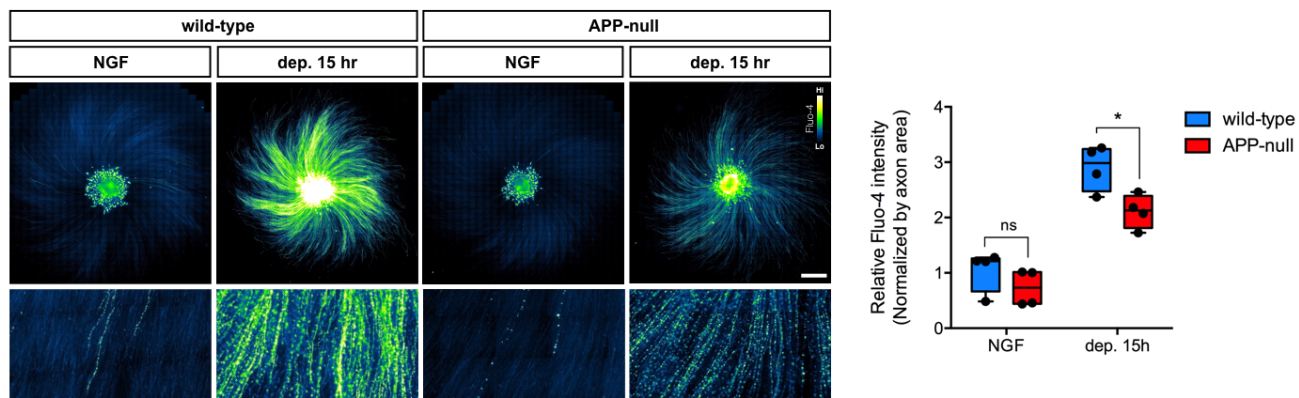


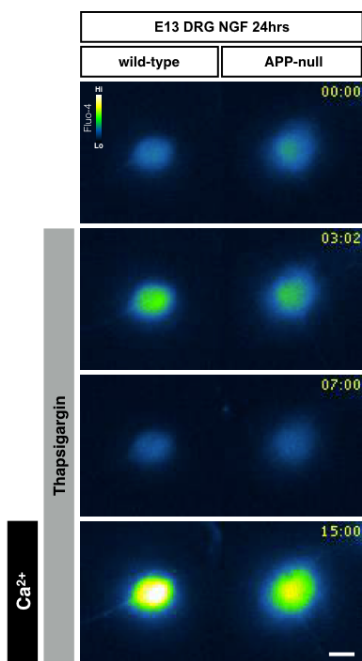
Figure 2.6. APP genetic deficiency reduce axoplasmic Ca^{2+} rise upon NGF deprivation and attenuates ER Ca^{2+} content and SOCE in DRG neurons. **A)** Wild-type and APP-null DRG explants cultured in NGF were maintained in trophic media or withdrawn from trophic support for 15 hours before staining with Fluo-4 and imaged by epifluorescence microscopy (Scale bar = 1000 μ m). The rise in axonal Fluo-4 intensity observed in wild-type DRG explants upon 15 hours of NGF deprivation is significantly attenuated in deprived APP-null DRG axons. The box plots show mean, min/max and 25/75% for each panel, analyzed by two-factor ANOVA followed by Bonferroni's *post hoc* comparison (n = 4 embryos per condition); ns: non-significant, * $p < 0.05$. **B)** Dissociated wild-type and APP-null embryonic DRG were cultured for 24 hours in the presence of NGF (12.5 ng/ml), stained with Fluo-4 and live imaged. The recording was initiated in Ca^{2+} -free media to establish the baseline, followed by the treatment with the SERCA pump inhibitor thapsigargin (1 μ M final) and ending in media with Ca^{2+} (2 mM $CaCl_2$ final). Panel B shows representative dissociated DRG soma stained with Fluo-4 at indicated stages during live recording (Scale bar = 20 μ m). **C)** Plot shows the Fluo-4 intensity across time of wild-type and APP-null DRG somas relative to the wild-type baseline (first minute) and normalized by soma area. **D)** Bar graph showing the mean Fluo-4 intensity between wild-type and APP-null DRG somas at thapsigargin peak (*Thp*) and thapsigargin + Ca^{2+} peak (*Thp* + Ca^{2+}). Significantly reduced Fluo-4 intensity was detected in APP-null DRG somas at *Thp*, and *Thp* + Ca^{2+} conditions compared with wild-type DRGs. Analyzed by two-factor ANOVA followed by Bonferroni's *post hoc* comparison and plotted with mean and SEM (n = 5 embryos per genotype); * $p < 0.05$, ** $p < 0.01$.

Figure 2.6

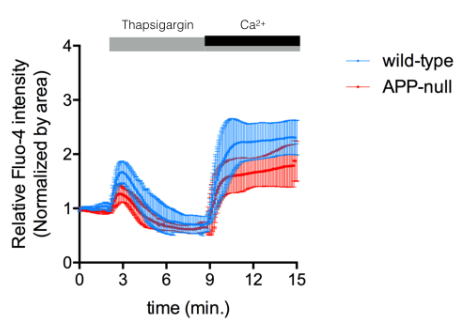
A



B



C



D

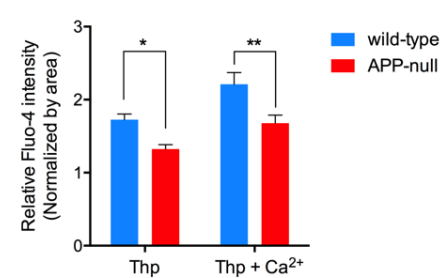
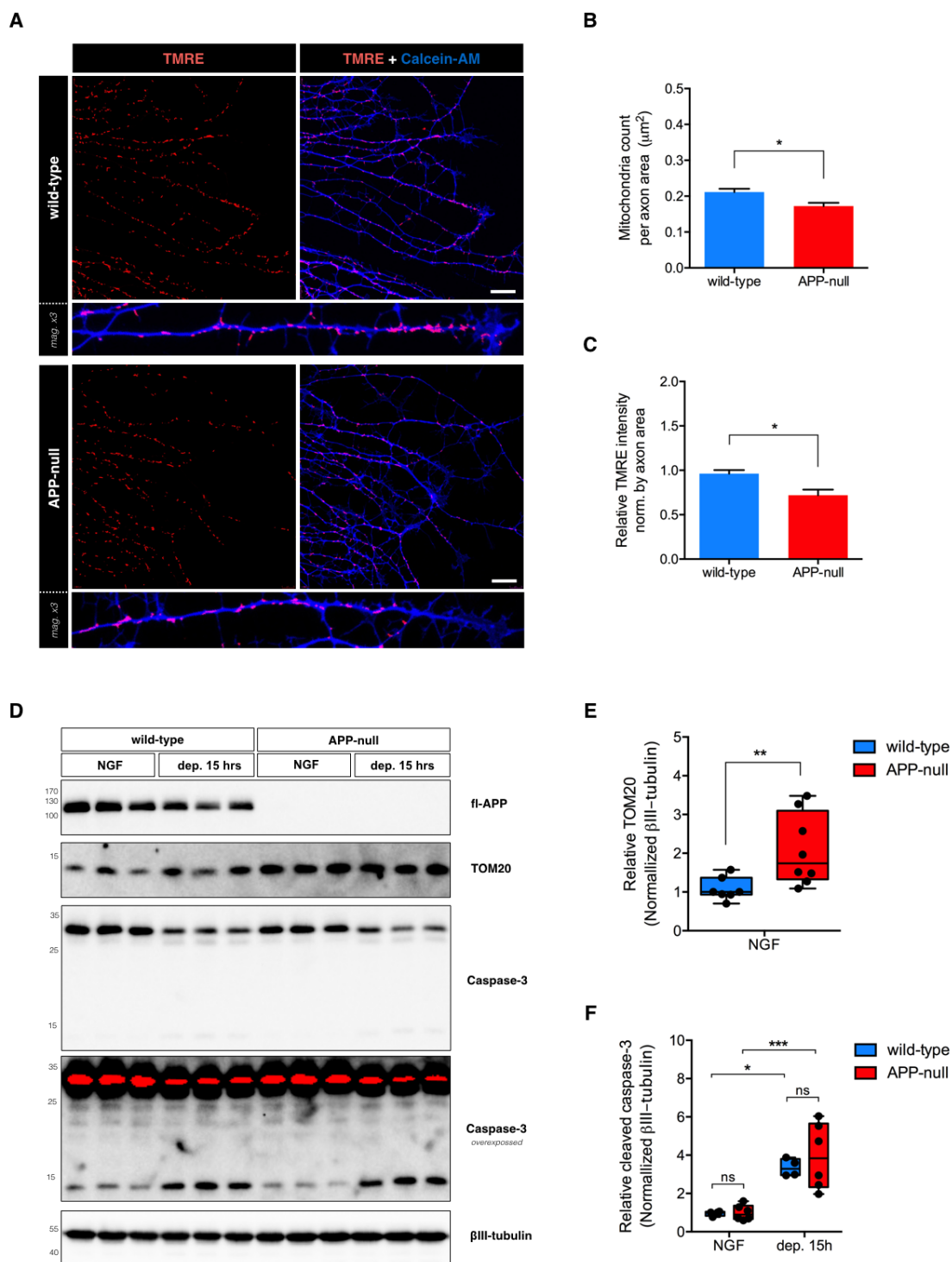


Figure 2.7. DRG sensory neurons lacking APP have reduced functional mitochondria and increased TOM20 levels but do not have defects in caspase-3 activation upon NGF deprivation. **A)** Representative images of wild-type and APP-null DRG explants cultured for 24 hours in the presence of NGF (12.5 ng/ml) and lived-stained with Calcein-AM and TMRE to identify axons and functional mitochondria respectively (Scale bar = 20 μ m). **B)** Number of TMRE-positive mitochondria normalized by axonal area. Quantification shows a significant decrease in the number of TMRE-positive mitochondria in APP-null DRG axons compared with their wild-type counterparts, analyzed by unpaired t-test $t(8) = 3.01$, $p = .016$, two-tailed. Values are expressed as the mean \pm SEM ($n = 5$ DRGs per genotype); * $p < 0.05$. **C)** TMRE intensity normalized by axonal area and relative to wild-type. Quantification shows a significant decrease in relative TMRE intensity in APP-null DRG axons compared with their wild-type counterparts, analyzed by unpaired t-test $t(8) = 3.23$, $p = .012$, two-tailed. Values are expressed as the mean \pm SEM ($n = 5$ DRGs per genotype); * $p < 0.05$. **D)** Protein lysates from wild-type and APP-null E13.5 DRG explants cultured for 48 hours in the presence of NGF (12.5 ng/ml) and then either maintained with trophic support or deprived of NGF and supplied with a function blocking anti-NGF (2 μ g/ml) for 15 hours were analyzed by western-blot against APP-Y188, TOM20, caspase-3 and β III-tubulin. **E)** Quantification by densitometry of the corresponding bands for TOM20 normalized by β III-tubulin levels and relative to wild-type NGF control. Results show a significantly increase of TOM20 levels in lysates from APP-null DRG in the presence of NGF compared to their wild-type counterparts. Analyzed using a two-tailed Mann-Whitney U test yielding the following results $U(7,8) = 6$, $p = .0085$. Values are expressed as the mean, min/max and 25/75% for each panel ($n = 7$ wild-type embryos; $n = 8$ APP-null embryos); ** $p < 0.01$. **F)** Quantification by densitometry of the corresponding bands for cleaved caspase-3 normalized by β III-tubulin levels and relative to wild-type NGF control. Cleaved caspase-3 levels significantly spike upon NGF deprivation in wild-type and in APP-null DRG lysates; no significant difference was noted between the genotypes. Analyzed by two-factor ANOVA followed by Bonferroni's *post hoc* comparison and plotted with mean, min/max and 25/75% for each panel ($n = 4$ wild-type embryos; $n = 6$ APP-null embryos); ns: non-significant, * $p < 0.05$, *** $p < 0.001$.

Figure 2.7



Connecting text: Chapter 2 to 3

In the previous chapter we sought to understand the contribution of APP to the process of developmental neuronal remodeling in the sensory nervous system. For its study *in vitro*, we used the classical model of developmental programmed cell death in embryonic dorsal root ganglia neurons dependent on NGF. This model has provided many key insights about the cell autonomous mechanisms that drive developmental neuronal cell death. However, the mechanisms that drive the elimination of sensory neurons that are dependent on other neurotrophins are mostly unknown. In the next chapter we focus on the DRG subpopulation that is dependent on BDNF for survival. Establishing a new *in vitro* culture model, we explored whether the mechanisms of degeneration observed in embryonic NGF-dependent DRG neurons can be extrapolated to BDNF-dependent sensory neurons.

Chapter 3

NGF- and BDNF-dependent DRG sensory neurons deploy distinct degenerative signaling mechanisms *

de León A.¹, Gibon J.², Barker P.²

1- Montreal Neurological Institute, McGill University, Montreal, QC, Canada. 2- Irving K. Barber School of Arts and Science, University of British Columbia – Okanagan Campus, Kelowna, BC, Canada. * Submitted to *eNeuro*, 24th Jun 2020.

3.1 Abstract

The nerve growth factor (NGF) and brain-derived neurotrophic factor (BDNF) are trophic factors required by distinct population of sensory neurons during development of the nervous system. Neurons that fail to receive appropriate trophic support are lost during this period of naturally occurring cell death. In the last decade, our understanding of the signalling pathways regulating neuronal death following NGF deprivation has advanced substantially. However, the signaling mechanisms promoting BDNF-deprivation induced sensory neuron degeneration are largely unknown. Using a well-established *in vitro* culture model of dorsal root ganglion (DRG), we have examined degeneration mechanisms triggered upon BDNF withdrawal in sensory neurons. Our results indicate differences and similarities between the molecular signalling pathways behind NGF and BDNF deprivation-induced death. For instance, we observed that the inhibition of Trk receptors (K252a), PKC (Gö6976), protein translation (cycloheximide) or caspases (zVAD-fmk) provides protection from NGF deprivation-induced death but not from degeneration evoked by BDNF-withdrawal. Interestingly, degeneration of BDNF-dependent sensory neurons requires BAX and appears to rely on reactive oxygen species generation rather than caspases to induce degeneration. These results highlight the

complexity and divergence of mechanisms regulating developmental sensory neuron death.

3.2 Introduction

The developing nervous system undergoes a period of neuronal cell death during embryogenesis [167, 631, 726]. In this period, neurons that fail to receive trophic support die by apoptosis [727], a type of cell death also commonly observed in neurodegenerative diseases [219, 645, 728-731]. The mammalian peripheral nervous system (PNS) offers a well-characterized context to study developmental neuronal apoptosis. Diverse sub-types of sympathetic and sensory neurons develop, compete, survive or die based on their capacity to bind enough trophic support from their target tissue [645, 732].

Neurotrophins are crucial regulators of survival during the development of the nervous system. Alterations of their levels induce dramatic changes of innervation in the adult PNS [121, 129, 310, 733]. In mammals, the neurotrophin family is composed of the nerve growth factor (NGF), brain-derived neurotrophic factor (BDNF), neurotrophin-3 (NT3) and neurotrophin-4/5 (NT4/5). With equal low affinity and no selectivity, each neurotrophins can bind to the pan-neurotrophin receptor p75 (p75NTR), and with high affinity to the tropomyosin-related kinase (Trk) receptor family: with NGF binding to TrkA, BDNF and NT4/5 to TrkB and NT3 to TrkC. Sympathetic and sensory neurons can be classified based on their expression profile of Trk receptors and their requirement for neurotrophins. Most sympathetic and sensory neurons depend on the NGF-TrkA signaling pathway during development [99, 734, 735]. *In vitro* models using cultured sympathetic and dorsal root ganglia (DRG) neurons that are maintained and then withdrawn from NGF have provided many key insights into the cell autonomous mechanisms that drive developmental neuronal cell death [225, 660, 736]. Recent work has shown that embryonic sensory neurons deprived of NGF results in PKC activation, ROS production, and TRPV1 activation which in turn induces a large increase in axoplasmic Ca^{2+} required for degeneration [329, 360]. To date, almost all studies have focused on NGF sensitive peripheral neurons and mechanisms driving developmental neuronal death in other peripheral neuronal populations remains essentially unknown. In the present study, we asked whether the degenerative cascade initiated by NGF withdrawal could be extrapolated to population of neurons dependent on other

neurotrophins, with a particular focus on the degenerative processes affecting BDNF-sensitive neurons.

Here, we show that NGF- and BDNF-dependent DRG neurons undergo axonal blebbing, reduced axonal area, increased extracellular phosphatidylserine, and rise in intracellular Ca^{2+} when withdrawn from trophic support. Further, degeneration of both classes of neurons require the pro-apoptotic protein BAX. However, unlike NGF-sensitive neurons, degeneration of BDNF-dependent deprivation does not require Trk activity, PKC activity or caspase activity and instead requires reactive oxygen species (ROS). Together, these results highlight the complexity and divergence of the mechanisms underlying trophic factor deprivation-induced neuronal cell death during development in the PNS.

3.3 Materials and Methods

3.3.1 *Mouse strains*

CD1 mice were purchased from Charles River Laboratories (Montreal, Canada). The previously described p75NTR knockout mice [185] and BAX knockout mice [737], were maintained in a C57Bl6 strain background. Animal procedures and experiments were approved by the University of British Columbia animal care committee and the Canadian Council of Animal Care. Efforts were made to reduce animal handling and use.

3.3.2 *Culturing and trophic factor deprivation of DRG explants*

Dorsal root ganglia (DRG) were dissected from E13.5 mouse embryos and seeded in 12-well plastic (Grenier) or 4-well glass-bottom dishes (CellVis) sequentially coated with 1 mg/ml poly-D-lysine (Sigma-Aldrich), 10 µg/ml laminin-entactin complex (Corning) and 0.1 mg/ml PurCol bovine collagen (Advanced Biomatrix). Explants were grown in phenol-red Neurobasal media (Invitrogen) supplemented with 2% B27 serum-free supplement (Invitrogen), 1% L-glutamine (Wisent), 1% penicillin/streptomycin (Wisent), 10 µM 5-fluoro-2'-deoxyuridine (FDU, Sigma-Aldrich) and 12.5 ng/ml NGF (CedarLane) or 37.5 ng/ml BDNF (CedarLane) at 37°C, 5% CO₂. Deprivation of neurotrophic support was accomplished using 2.0 µg/ml of function blocking antibodies against NGF (homemade rabbit polyclonal antibody raised against 2.5s NGF; [712]) or BDNF (mouse monoclonal, DSHB #9-b) in complete fresh media without neurotrophic supplementation.

3.3.3 *βIII-tubulin immunocytochemistry, imaging and quantification of axon degeneration*

DRG explants were fixed in 4% paraformaldehyde solution in phosphate saline buffer (PBS) for 15 minutes, washed once in PBS and blocked in 5% milk in Tris-Borate buffer and 0.3% Triton-X100 for one hour at room temperature (RT). Explants were incubated overnight at 4°C with mouse monoclonal antibody against βIII-tubulin (Millipore, MAB5564) diluted 1:10000 in blocking solution. DRGs were washed twice in PBS and then incubated with goat anti-mouse conjugated to Alexa Fluor 488 (Jackson ImmunoResearch, 115-545-003) diluted 1:5000 in blocking solution for a minimum of 3 hours at RT. Explants were imaged using a Zeiss ObserverZ.1 inverted epifluorescence

microscope with an automated motorized stage (5x magnification with tiling). From a stitched master image of the plate generated by Zen 2 software (Zeiss, Canada), quarter DRG fields were cropped to generate a set of images for analysis using the R script program Axoquant 2.0 [360]. Final measurements were plotted as the mean axonal area of DRGs from three embryos. Increments of 500 μm were used for statistical analysis (normalized to same increments in control condition).

3.3.4 Assessment of DRG explant survival with live Calcein-AM staining

DRG explants were treated with 1 $\mu\text{g}/\text{ml}$ Calcein-AM (AAT Bioquest) in neurobasal media for 1 hour at 37°C then switched to clear HBSS-based complete media supplemented with HEPES to maintain physiological pH. Explants were tiled-imaged using a Zeiss ObserverZ.1 inverted epifluorescence microscope with an automated motorized stage. From a stitched master image of the plate generated by the Zen 2 software, cell bodies and Schwann cells were cropped out and a binary mask image of each explants was created using NIH Image J software. Explant area and mean pixel intensity value corrected by the background signal were quantified to provide either the area of Calcein-AM-stained axons over a specified threshold or Calcein-AM fluorescence intensity per unit of area. DRG explants from the same embryo were pooled and averaged to generate the mean value for each embryo. Measurements were normalized relative to NGF or BDNF wild-type conditions.

3.3.5 Annexin-V staining, imaging and quantification

DRG explants seeded on glass bottom dishes (CellVis) were incubated with 1 $\mu\text{g}/\text{ml}$ Annexin-V (AAT Bioquest) in annexin-V buffer (10 mM HEPES/NaOH, pH7.4, 140 mM NaCl, 2.5 mM CaCl_2) for 15 min at room temperature. DRGs were washed and tiled-imaged in the annexin-V buffer using a Zeiss Observer Z.1 inverted epifluorescence microscope (40x magnification). Stitched master images of each explant generated by Zen 2 software were cropped to eliminate soma and Schwann-cell area and axonal annexin-V area was measured using a binary mask over an established threshold for all explants. DRG explants from the same embryo were pooled and averaged to generate

the mean value for each embryo. Measurements were normalized relative to NGF or BDNF controls.

3.3.6 Ca^{2+} imaging with Fluo-4 and quantification

DRG explants were seeded on glass bottom dishes (CellVis) and treated with 5 μ M Fluo-4 AM (Invitrogen) in neurobasal media for 15 min at 37°C, washed with HBSS and switched to clear HBSS-based complete media supplemented with HEPES (final concentration 20 mM) to maintain its physiological pH. Explants were tiled-imaged using a Zeiss ObserverZ.1 inverted epifluorescence microscope with an automated motorized stage at 40x magnification. Employing NIH Image J software, stitched master images of each explant were cropped to eliminated soma and Schwann-cell area. From there, a binary mask image of remaining axons was created to measure area and mean pixel intensity corrected by background signal. After calculating the intensity per unit of axonal area, DRG explants from the same embryo were pooled and averaged to generate the mean value per embryo. Measurements were normalized and expressed as fold-change from NGF or BDNF controls.

3.3.7 Immunoblotting

For SDS-PAGE and western-blot analysis, a total of 25 DRG explants per well were seeded in 12-well plastic plates (Grenier). For protein harvesting, cultures were washed with PBS, and DRGs were scraped into 90 μ l of sample buffer (4% SDS, 20% glycerol, 10% 2-mercaptoethanol, 0.004% bromophenol blue and 0.125 M Tris-HCl, pH approx. 6.8). Samples were boiled for five minutes, centrifuged and stored at -80°C for later analysis. Antibodies used for immunoblotting were: anti- β III-tubulin (Millipore MAB5564, 1:10000), anti-neurofilament M (Millipore AB1987, 1:1000), anti-caspase-3 (NEB 9662, 1:1000), anti-TrkA (Millipore 06-574, 1:1000), anti-TrkB (Millipore 07-225, 1:1000), anti-TrkC (Millipore 07-226, 1:1000) and the previously described anti-p75NTR (Barker and Shooter, 1994).

3.3.8 Pharmacological PKC, Trk, caspase, autophagy, translation and necroptosis inhibitors

Stocks of PKC inhibitor Gö6976 (10 mM, Tocris 2253, UK), Trk receptor inhibitor K252a (200 μ M, Calbiochem #420298, Israel), pan-caspase inhibitors Boc-D-fmk (10 mM, Abcam ab142036, USA), zVAD-fmk (20 mM, R&D systems FMK001, USA), and necroptosis inhibitor necrostatin-1 (NEC-1, 100 mM, Sigma-Aldrich N9037, USA) were prepared in dimethylsulphoxide (DMSO) and used at 1:1000 dilution (final concentration of DMSO below 0.1%). The translation inhibitor cycloheximide (CHX, R&D systems 0970/100, USA) was dissolved at 1.0 g/L in water and used at 1:1000. Autophagy inhibitor 3-methyladenine (3MA, Sigma-Aldrich M9281, Israel) was dissolved at 10 mM in phenol-red neurobasal media. Drugs were applied at the same time that the trophic factor withdrawal was initiated.

3.3.9 EGTA, NAC and NAD⁺ preparation

Ethylene glycol-bis (β -aminoethyl ether)-N,N,N',N'-tetraacetic acid (EGTA, AlfaAesar A16086, UK, final concentration 5 mM), N-acetylcysteine (NAC, Sigma, A9165, China, final concentration 20 mM) or nicotinamide adenine dinucleotide (NAD⁺, Sigma-Aldrich, N7004, USA, final concentration 5 mM) were dissolved in Neurobasal media, pH adjusted to 7.4 and filtered by 0.22 μ m for final treatment of DRG explants. After 48 hours of growth in NGF or BDNF, cultures were either maintained with trophic support or deprived of it, in the absence or presence of each specific compound for the entire deprivation period.

3.3.10 Experimental design and statistical analysis

Data were plotted and analyzed using Prism 6 (Graph-Pad). All data were presented as mean \pm SEM. The number of embryos n in each experiment or condition is described in each figure legend. Mann-Whitney test (unpaired, two-tailed) was used for two-group experiments comparisons. Two-way ANOVA with Bonferroni's *post hoc* test or Tukey's *post hoc* test was used to analyze differences in multiple groups. In all graphs, non-significant ($p > 0.05$): ns, * (or other symbols) $p < 0.05$, ** $p < 0.01$, *** $p < 0.001$ and **** $p < 0.0001$.

3.4 Results

The apoptotic machinery involved in NGF deprivation-induced axonal degeneration in DRG neurons is well-characterized [660]. However, our knowledge of axonal degeneration induced by BDNF deprivation is rudimentary. To begin to address this, we characterized BDNF withdrawal-induced axon degeneration in DRG neurons generated from E13.5 mice embryos. Figure 3.1 A shows that E13.5 DRGs cultured in the presence of BDNF survived and developed neurites (quantified in 3.1 B). The extent and density of neurites was maximal at a BDNF concentration of 125 ng/ml (Figure 3.2 A) but even at this concentration, processes were significantly less dense and shorter than within parallel DRGs cultured in NGF (data not shown). It was also noted that DRGs derived from the lumbar and cervical parts of the spinal cord extended more exuberant processes in response to BDNF than DRGs derived from the thoracic region (Figure 3.2 B). For subsequent experiments, cervical DRG neurons were routinely cultured using 37.5 ng/ml of BDNF or 12.5 ng/ml of NGF. For BDNF-deprivation studies, cells were grown in BDNF for 48 hours and then switched to BDNF-free media supplemented with an anti-BDNF monoclonal antibody for 24 hours. Axons maintained and then deprived of BDNF in this manner showed morphological signs of degeneration and blebbing (Figure 3.1 C higher magnification, quantified in 3.1 D).

Cell biological and biochemical indications of BDNF-withdrawal induced axonal degeneration were also established. DRG axons that were maintained and then deprived of either NGF or BDNF show a significant increase of extracellular phosphatidylserine, determined using Annexin-V staining, and a drastic decrease of viable axons, determined using Calcein-AM (Figure 3.3 A, quantified in 3.3 B). It has been previously shown that NGF deprivation induces a large increase in axoplasmic Ca^{2+} ~15 hours after deprivation [329, 360], and here show that BDNF-withdrawal induces a similar elevation in axonal Ca^{2+} 15 hours after trophic deprivation (Figure 3.3 C, quantified in 3.3 D).

To characterize the neurotrophin receptor complement in DRG explants, protein lysates from E13.5 DRGs maintained in NGF or BDNF for 72 hours were analyzed by immunoblot. DRGs cultured in NGF expressed abundant TrkA, TrkB, and p75NTR but

low amounts of TrkC. In contrast, DRG neurons cultured in BDNF expressed abundant TrkB, TrkC and p75NTR (Figure 3.4 A) but essentially no TrkA.

Previous studies have indicated that p75NTR is required for cell death of sympathetic neurons during development [69] but not for apoptosis of DRG sensory neurons. p75NTR has also been shown to be required for sympathetic neuron axon degeneration [66, 189]. To determine if p75NTR is required for axonal loss after NGF or BDNF deprivation in DRG axons, we assessed axonal loss in DRGs from p75NTR-null embryos (Figure 3.4 B). When maintained and then withdrawn from NGF or BDNF, the degree of axonal degeneration was the same in wild-type and p75NTR-null DRGs (Figure 3.4 C), ruling out a direct role for p75NTR in axon loss induced by neurotrophin withdrawal.

TrkA and TrkC have been implicated as dependence receptors [12] and recent studies have suggested that NGF deprivation activates a TrkA-dependent apoptotic signalling pathway [175]. Consistent with this, Figure 3.4 D and E show that a low concentration of the pan-Trk inhibitor K252a (200 nM) rescues NGF-deprivation induced axon degeneration of DRG sensory neurons but has no effect on BDNF deprivation-induced DRG axon degeneration (Figure 3.4 D, quantified in 3.4 E). These results are consistent with previous findings showing that TrkB does not have dependence receptor activity [12].

To begin to discern signaling mechanisms driving BDNF deprivation-induced axon loss, we tested several compounds known to inhibit NGF withdrawal-induced axon degeneration or to inhibit neuronal cell death. PKC inhibitor Gö6976 rescues NGF deprivation-induced apoptosis [329] but had no effect on BDNF deprivation (Figure 3.5 A, quantified in 3.5 B). Likewise, the Ca²⁺ chelator EGTA is a potent inhibitor of axon loss induced by NGF withdrawal in DRG neurons [360] but did not protect against BDNF deprivation (Figure 3.5 C, quantified in 3.5 D). The translation inhibitor cycloheximide (CHX) significantly protects axons from degeneration induced by NGF-deprivation (Figure 3.6 A) but has no effect on axon degeneration induced by BDNF withdrawal. Finally, neither the autophagy inhibitor 3-methyladenine (3-MA), the necroptosis inhibitor necrostatin-1 (NEC-1) nor nicotinamide adenine dinucleotide (NAD⁺) blocked BDNF

withdrawal-induced axonal degeneration of DRG sensory neurons (Figure 3.6 B, C and D).

BAX is a central player in neuronal apoptosis and crucial for NGF-deprivation induced axonal degeneration [167, 213, 214]. To address the role of BAX in BDNF-deprived DRG sensory neurons, BAX-null DRG neurons were maintained in NGF or BDNF and then deprived of trophic support. Figure 3.7 shows that axons lacking BAX were significantly protected from degeneration induced by NGF- and BDNF-deprivation (Figure 3.7 A, quantified in 3.7 B).

Caspase-3 is crucial for NGF deprivation-induced axonal degeneration [214, 225] and the requirement for BAX in BDNF withdrawal-induced axonal loss suggests that caspases may also play a role in axonal degeneration induced by BDNF deprivation. However, Figure 3.8 A shows that while caspase inhibition efficiently rescued axons from NGF deprivation, two distinct pan-caspase inhibitors (Boc-D-fmk and zVAD-fmk) did not reduce axonal degeneration in neurons that were maintained and then withdrawn from BDNF (Figure 3.8 A, quantified in 3.8 B and Figure 3.9 A, quantified in 3.9 B). Correspondingly, NGF deprivation decreased levels of pro-caspase-3 and increased cleaved caspase-3 whereas levels of pro- and cleaved caspase-3 did not change in neurons maintained and then withdrawn from BDNF for 15, 24 and 30 hours (Figure 3.9 C and data not shown). Taken together, these results indicate that BAX activity mediates BDNF deprivation-induced axonal degeneration through a caspase-independent pathway.

Several reports have shown that BAX can facilitate production of mitochondrial reactive oxygen species [362, 364, 738, 739]. To explore whether ROS play a role in neurotrophin deprivation-induced axonal degeneration, axons maintained in NGF or BDNF were exposed to N-acetylcysteine (NAC), a ROS scavenger, and then withdrawn from trophic support. Figure 3.10 shows that axonal degeneration induced by either NGF or BDNF deprivation was blocked in the presence of NAC, indicating that ROS are required for axonal degeneration induced by neurotrophin deprivation.

3.5 Discussion

The mammalian peripheral nervous system has proven a useful system for identifying specific mechanisms that are required for developmental neuronal degeneration. Substantial understanding of processes that mediate neuronal cell death and axonal destruction has been obtained from analyses of NGF-dependent DRG neurons maintained *in vitro*. However, less is known about signaling pathways that lead to the developmental loss of other sensory neuron populations. In this study, we have examined mechanisms that promote the developmental degeneration of BDNF-dependent sensory neurons. Our observations show that BDNF-dependent DRG sensory neurons employ destructive mechanisms distinct from those employed by NGF-dependent sensory neurons.

3.5.1 Growth differences in NGF- and BDNF-dependent DRG populations

Several studies point to BDNF as a key trophic factor required to sustain the survival of different neuronal populations, including DRG sensory neurons *in vivo* and *in vitro* [120, 587, 740]. Cranial sensory neurons are highly dependent on BDNF for survival and growth [613] whereas only a subpopulation of DRG sensory neurons requires BDNF for survival during development [596, 599]. Here we showed that BDNF supports the survival and growth of neurons within E13.5 DRG explants, with neurite length steadily increasing with the time of trophic factor exposure. However, BDNF-dependent outgrowth was considerably less than that supported by NGF, consistent with the observation that only 8% of DRG neurons are TrkB⁺ while 80% are TrkA⁺ [107, 111]. Thus, in the absence of NGF, the vast majority of DRG sensory neurons degenerate, leaving behind a small number of TrkB⁺ neurons. The reduced capacity of BDNF to promote neurite extension in culture may also reflect the fact that TrkB, but not TrkA, is down-regulated after exposure and binding to its ligand [18, 19] and that BDNF activates Ras considerably less effectively than NGF [17, 741].

3.5.2 Trophic deprivation-induced degeneration of BDNF-dependent DRG sensory neurons

To mimic BDNF deprivation that occurs during embryonic development, E13.5 DRGs were maintained in BDNF and then withdrawn from the factor. A function blocking monoclonal antibody directed against BDNF was deployed to inactivate any residual BDNF remaining. BDNF deprivation resulted in neurite blebbing, a hallmark morphology of degenerating neurites, and caused a significant reduction of area occupied by neurites. Axonal degeneration provoked by BDNF deprivation was confirmed using the live dye Calcein-AM and by staining with Annexin-V, which detects phosphatidylserine on the outer leaflet of the plasma membrane, a prototypical signal driving phagocytosis of cells undergoing cell death [231, 742]. Calcein-AM is a sensitive staining technique to quantify axonal integrity. However, Calcein-AM binds calcium after being hydrolyzed by intracellular esterase and its use was not compatible with some of our treatments (e.g. EGTA). Therefore, Calcein-AM staining was used to follow the effect of p75NTR or BAX deficiency on axonal integrity during trophic deprivation conditions and the effects of drugs on axonal degeneration was studied based on β III-tubulin staining and quantified with Axoquant 2.0 (as described in [360]).

3.5.3 How does BDNF deprivation trigger degeneration in BDNF-dependent sensory neurons?

Several studies have indicated that unliganded TrkA promotes pro-apoptotic signaling in sympathetic and sensory neurons withdrawn from NGF [12, 172, 175]. In this sense, TrkA can be considered a 'dependence receptor' that promotes survival signaling when bound by ligand but drives death signaling upon ligand withdrawal [12]. Here we showed that the pan-Trk kinase inhibitor K252a prevented degeneration normally induced by NGF deprivation but had no effect on degeneration induced by BDNF deprivation, indicating that TrkA, but not TrkB, behaves as a dependence receptor. This finding agrees with those of Barde's group who found that TrkA and TrkC behave as dependence receptors but the BDNF receptor TrkB is incapable of doing so [12].

We also questioned the role of p75NTR in BDNF-deprivation. Depending on the cellular and molecular context, the low-affinity neurotrophin receptor can drive pro-survival or pro-death signaling [171, 743]. Although p75NTR is crucial for sympathetic neuronal remodeling during embryonic development [66, 189], here we found that p75NTR had no effect on degeneration of sensory neurons maintained and then withdrawn from either NGF or BDNF.

PKC plays an indispensable role in DRG degeneration induced by NGF withdrawal [329] but PKC inhibitors had no effect on BDNF-withdrawal induced degeneration. Likewise, cycloheximide, a potent blocker of NGF-withdrawal induced degeneration had no effect on BDNF-withdrawal induced degeneration. Therefore, degeneration mechanisms of sensory neurons maintained and then withdrawn from BDNF are fundamentally distinct from those in NGF-dependent sensory neurons.

3.5.4 Role of Ca^{2+} in BDNF deprivation induced degeneration of BDNF-dependent DRG sensory neurons

In NGF-dependent DRG neurons, extracellular Ca^{2+} chelation blocks both the axoplasmic Ca^{2+} rise and the subsequent degenerative process that normally occur upon NGF withdrawal [329, 360]. Here we showed that BDNF deprivation induces Ca^{2+} rise in neurites of BDNF-dependent DRG explants yet Ca^{2+} chelation with EGTA did not rescue BDNF-deprivation induced degeneration. We observed that Ca^{2+} chelation in non-deprived DRG explants induced growth arrest and previous work has established that the ability of BDNF to sustain neuronal survival is reduced in comparison to NGF [17, 741]. These results suggest a more delicate homeostasis within BDNF-dependent DRG neurons. The lack of Ca^{2+} paired up with the trophic support deprivation could - in these sensitive cells - favor degeneration instead of protection. Therefore, our results do not completely rule out an active role of Ca^{2+} in the degenerative mechanism of BDNF-deprived DRG neurons.

3.5.5 ROS play a central role in the degeneration induced by BDNF deprivation

ROS were initially described solely as toxic cellular by-products, but a growing body of evidence has established ROS as endogenous modulators of numerous physiological functions [744]. A recent study showed that NGF deprivation in sensory neurons induces ROS production through a PKC/NOX pathway and that ROS scavengers rescue degeneration of NGF-dependent sensory neurons after trophic deprivation [329]. In the present work we showed that the antioxidant NAC partially protects DRG neurons from BDNF-deprivation, suggesting that ROS are crucial for the degeneration of BDNF-dependent sensory neurons. However, blocking PKC during BDNF deprivation had no effect on degeneration, indicating that the contribution of NOX-derived ROS to BDNF degeneration pathway is minor. Consistent with this, we found that NOX inhibitors that block NGF-withdrawal induced degeneration had no effect on BDNF-withdrawal-induced degeneration (data not shown).

Aside from NOX complexes, the other major source of ROS in the cell is mitochondria. Our results show that BAX is required for BDNF-deprivation induced degeneration of DRG neurons *in vitro*, consistent with *in vivo* data showing the importance of BAX during developmental cell death of BDNF-dependent cranial sensory neurons, particularly from nodose, petrosal and vestibular ganglia [613]. BAX translocates to the mitochondria and induces mitochondria outer membrane permeabilization (MOMP) [745]; in many circumstances MOMP provokes the release of the pro-apoptotic proteins SMAC and cytochrome *c*, engaging in the recruitment and activation of executioner caspases. However, since cleaved caspase-3 levels did not rise - and caspase blockers did not slow neuronal loss - in DRG sensory neurons deprived of BDNF, BAX must facilitate cell loss through a caspase-independent mechanism in this setting. BAX-dependent and caspase-independent cell death typically involves mitochondrial potential loss and failure [369, 370, 746, 747], with BAX-mediated MOMP inducing an increase of mitochondrial ROS production [748, 749]. In some circumstances, BAX-mediated MOMP and ROS production can trigger the formation of the mitochondria permeability transition pore which has been implicated in several forms of neuronal death [750].

A recent review by Fricker et al. (2018) proposed the existence of at least twelve different cell death pathways, highlighting the diversity and complexity of cellular death mechanisms [200]. Here, we examined pro-degenerative pathways such as necroptosis

and autophagy and mechanisms such as protein translation and NAD⁺ metabolism. Our results showed that several of these pathways impinge on the degenerative process induced by NGF deprivation but blockade of necroptosis, autophagy or translation nor NAD⁺ supplementation rescued degeneration evoked by BDNF withdrawal.

In conclusion, we have provided the first in depth characterization of the mechanisms that mediate degeneration of BDNF-dependent DRG sensory neurons upon trophic factor withdrawal. We show that the pathways regulating the degeneration of BDNF-dependent DRG sensory neurons requires BAX and ROS but are Trk- and caspase-independent and distinct from those invoked upon NGF-withdrawal.

3.6 Figures and figure legends

Figure 3.1. Comparative growth of NGF- and BDNF-dependent DRG sensory neurons and their degeneration induced by trophic factor withdrawal. A) β III-tubulin staining of embryonic mice DRG explants cultured in the presence of NGF (12.5 ng/ml) or BDNF (37.5 ng/ml) for 48, 72 or 120 hours (Scale bar = 1000 μ m). **B)** Quantification of axonal area as a function of the distance from the soma using Axoquant 2.0 [360] and plotted in 500- μ m bins. The difference between the relative axonal area between NGF-dependent and BDNF-dependent DRG growth at different time points were analyzed by two-factor ANOVA and Bonferroni's *post hoc* comparison and plotted with mean and SEM (n = 3 embryos for each condition; data shown is representative of 3 independent experiments); (*) NGF vs. BDNF; ***p < 0.001, ****p < 0.0001. **C)** DRG explants cultured in the presence of NGF or BDNF for 48 hours and then either maintained with trophic support or deprived with a function blocking anti-NGF (2 μ g/ml) or anti-BDNF (2 μ g/ml) for the following 24 hours, before fixation and immunostaining with β III-tubulin (Scale bar = 1000 μ m). **D)** NGF and BDNF deprivation for 24 hours results in a significant loss of β III-tubulin-stained axons expressed as axonal area relative to 0-500 μ m NGF or BDNF controls; analyzed by two-factor ANOVA and Bonferroni's *post hoc* comparison and plotted with mean and SEM. **p < 0.01, ***p < 0.001, ****p < 0.0001.

Figure 3.1

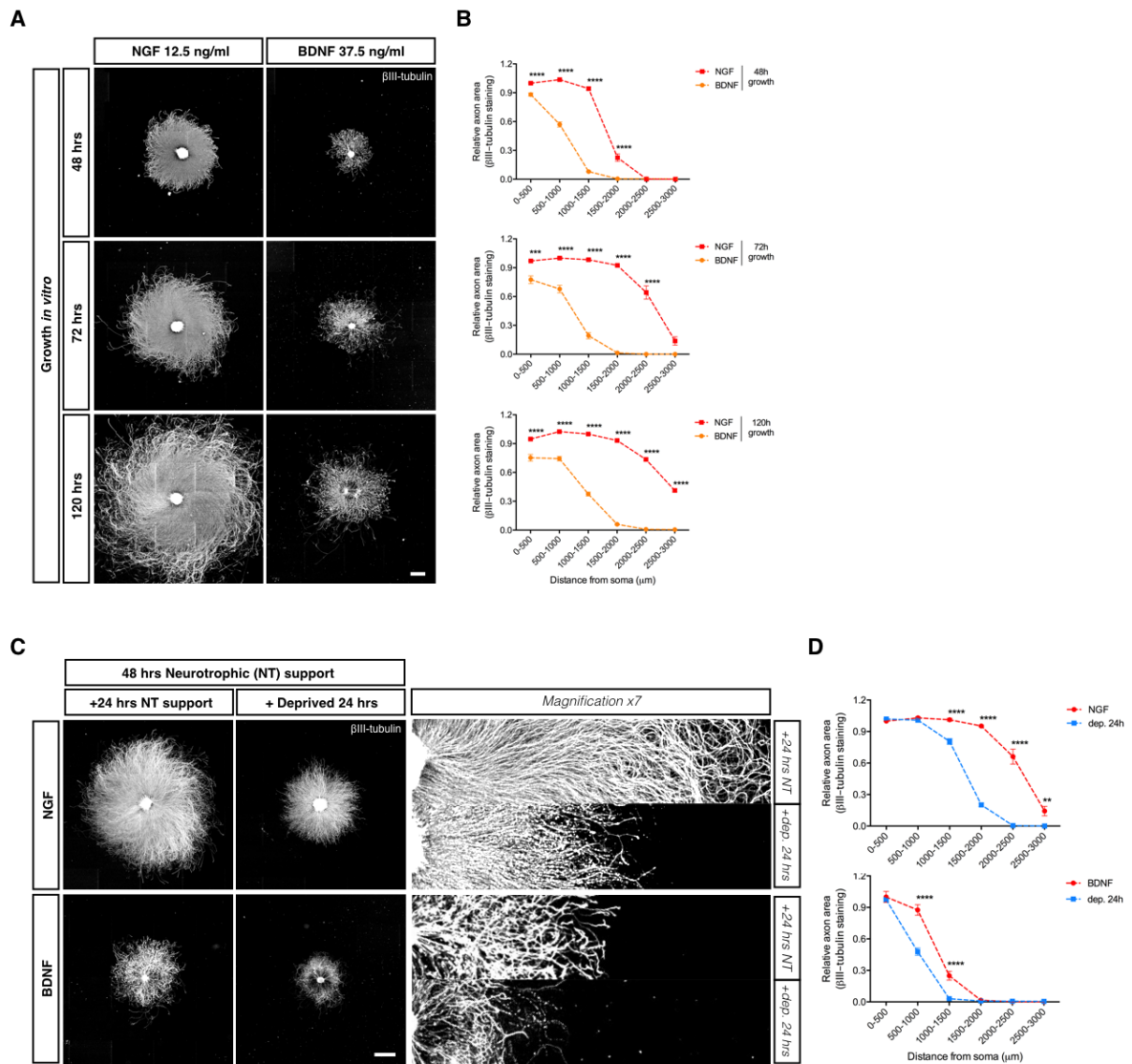


Figure 3.2. Axon growth of BDNF-dependent DRGs from the cervical, the thoracic or the lumbar region of the spinal cord with several concentration of BDNF. A) Calcein-AM stained DRGs from cervical, thoracic or lumbar spinal cord segments of E13.5 mice embryos were grown for 48 hours in 0, 12.5 or 125 ng/ml of BDNF (Scale bar = 500 μ m). **B)** Quantification of Calcein-AM stained axonal area relative to Calcein-AM stained axonal area of lumbar DRGs at 125 ng/ml analyzed by one-factor ANOVA and Tukey's *post hoc* comparison and plotted with mean and SEM (n = 3 embryos for each condition; data shown is representative of 3 independent experiments). ns: non-significant, *p < 0.05.

Figure 3.2

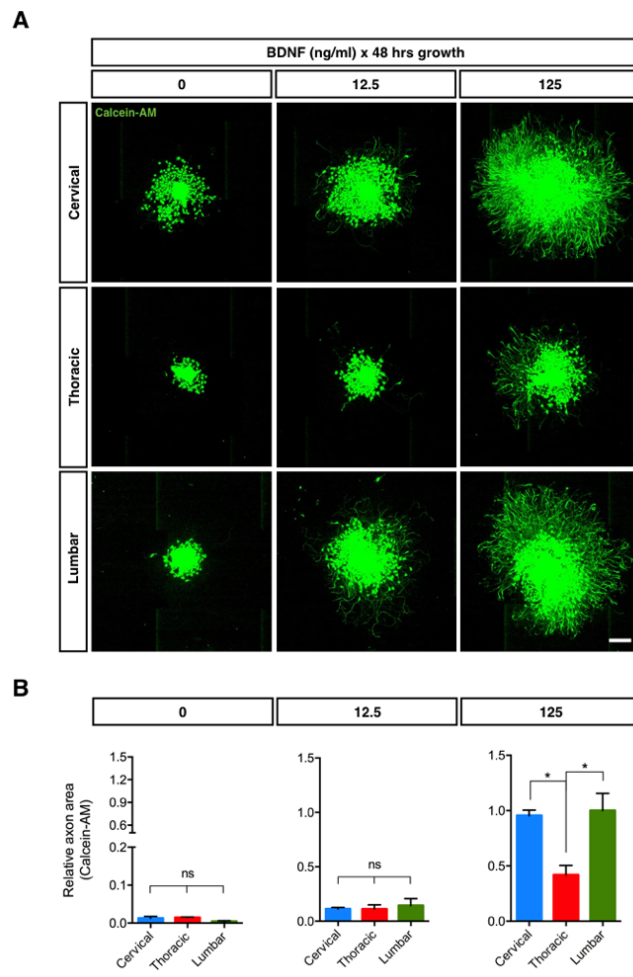


Figure 3.3. DRG sensory neurons undergoing BDNF deprivation display increased extracellular phosphatidylserine and increased axoplasmic Ca²⁺. **A)** DRG explants cultured in the presence of NGF or BDNF for 48 hours and then either maintained with trophic support or deprived with an antibody against NGF or BDNF for the following 24 hours were co-stained with Calcein-AM (green) and Annexin-V (red) to measure the area of healthy axons versus axons displaying phosphatidylserine, an apoptotic marker, respectively (NGF scale bar = 1000 μm , merge scale bar = 50 μm ; BDNF scale bar = 500 μm , merge scale bar = 50 μm). **B)** Both NGF and BDNF-deprivation induced a significant decrease in Calcein-AM positive axonal area (n = 5 embryos in NGF and n = 8 embryos in BDNF from pooled litters) and a significant increase in Annexin-V area (n = 5 embryos in NGF dep. 24h and n = 10 embryos in BDNF dep. 24h from pooled litters). The bar plots show mean, min/max and 25/75% for each panel, analyzed by two-tailed Mann-Whitney tests with *p < 0.05, **p < 0.01, ***p < 0.001. **C)** DRG explants cultured in NGF or BDNF were maintained in trophic media or withdrawn from trophic support for 15 hours before staining with Fluo-4 and imaged by epifluorescence microscopy (NGF scale bar = 1000 μm ; BDNF scale bar = 200 μm). **D)** Both NGF and BDNF deprivation induced a significant increase in axonal Fluo-4 intensity (n = 4 embryos in NGF and n = 6 embryos in BDNF from pooled litters). The bar plots show mean, min/max and 25/75% for each panel, analyzed by two-tailed Mann-Whitney tests with *p < 0.05.

Figure 3.3

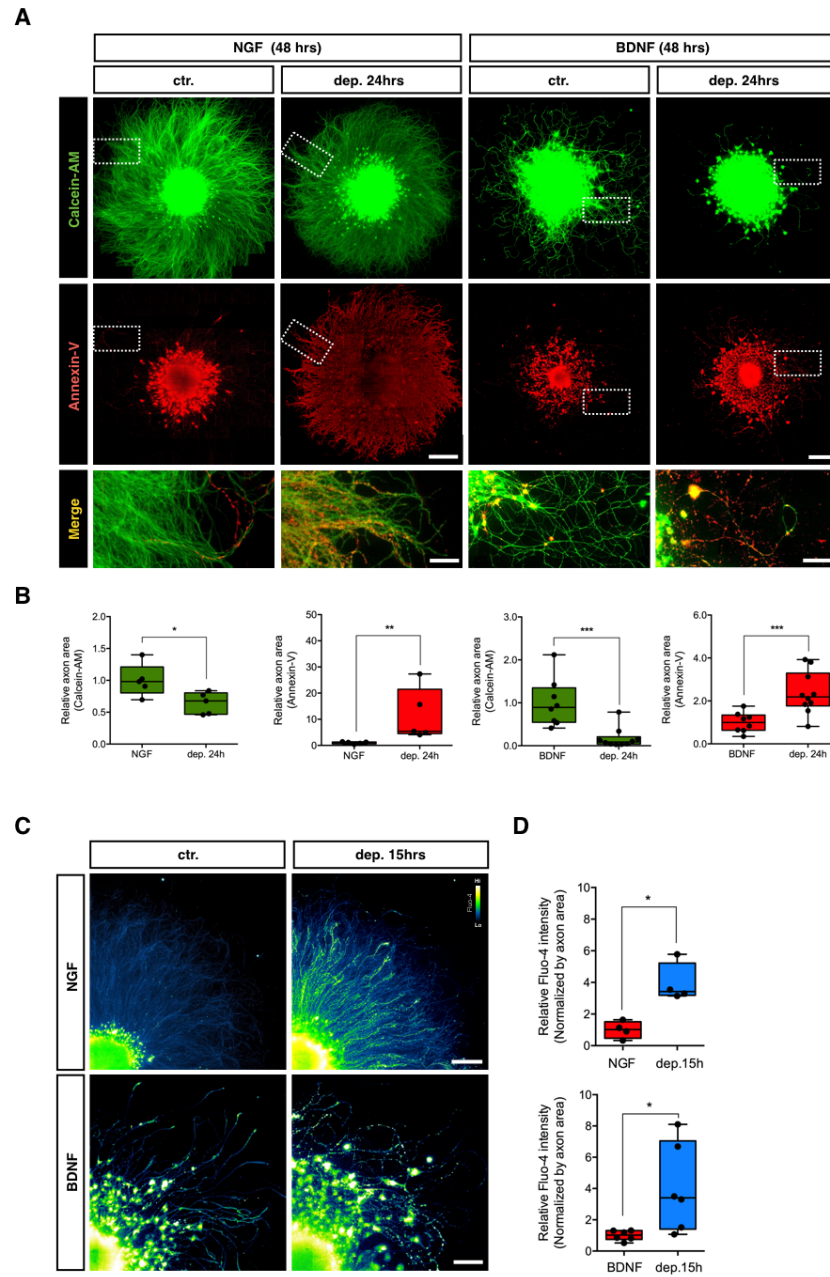


Figure 3.4. Trk receptor inhibition protects axons from NGF deprivation but not from BDNF-deprivation whereas p75NTR deficiency confers no protection to axons established in NGF or BDNF. **A)** Protein lysates collected from E13.5 DRG explants cultured in the presence of NGF (12.5 ng/ml) or BDNF (37.5 ng/ml) for 48 hours were analyzed by immunoblot against TrkA, TrkB, TrkC, p75NTR and, β III-tubulin. **B)** p75NTR knock-out does not rescue axons from degeneration after NGF or BDNF withdrawal. DRG explants from mixed-genotyped E13.5 litters were cultured in the presence of NGF or BDNF for 48 hours and then either maintained or withdrawal from trophic support for 24 hours before being live stained with Calcein-AM (NGF scale bar = 1000 μ m; BDNF scale bar = 500 μ m). **C)** Quantification of Calcein-AM intensity normalized by axonal area and relative to wild-type control. Non-significant difference was observed between wild-type and p75NTR-null DRG explants deprived of NGF or BDNF (n = 4 embryos in NGF and n = 4 embryos in BDNF from pooled litters). Analyzed by two-way ANOVA and Tukey's *post hoc* comparison and plotted with median and SEM. *p < 0.05, **p < 0.01, ***p < 0.001, ****p < 0.0001. **D)** DRG explants cultured in NGF or BDNF were either maintained in trophic media or withdrawn from trophic support with or without the Trk inhibitor K252a (200 nM) for 24 hours before fixing, immunostaining for β III-tubulin and imaged by epifluorescence microscopy (NGF scale bar = 1000 μ m; BDNF scale bar = 500 μ m). **E)** K252a rescued degeneration induced by NGF deprivation but not by BDNF deprivation. Quantification of axonal area as a function of the distance from the soma using Axoquant 2.0 [360] and plotted in 500- μ m binned segments relative to 0-500 μ m NGF control (upper panel) or BDNF control (lower panel). The relative axonal area was analyzed by two-factor ANOVA followed by Tukey's *post hoc* comparison and plotted with mean and SEM (n = 3 embryos for each condition; data shown is representative of 3 independent experiments); (*) ctr. versus dep. 24h; (#) dep. 24h versus dep. 24h + K252a; ns: non-significant, **p < 0.01, ***p < 0.001, ****p < 0.0001.

Figure 3.4

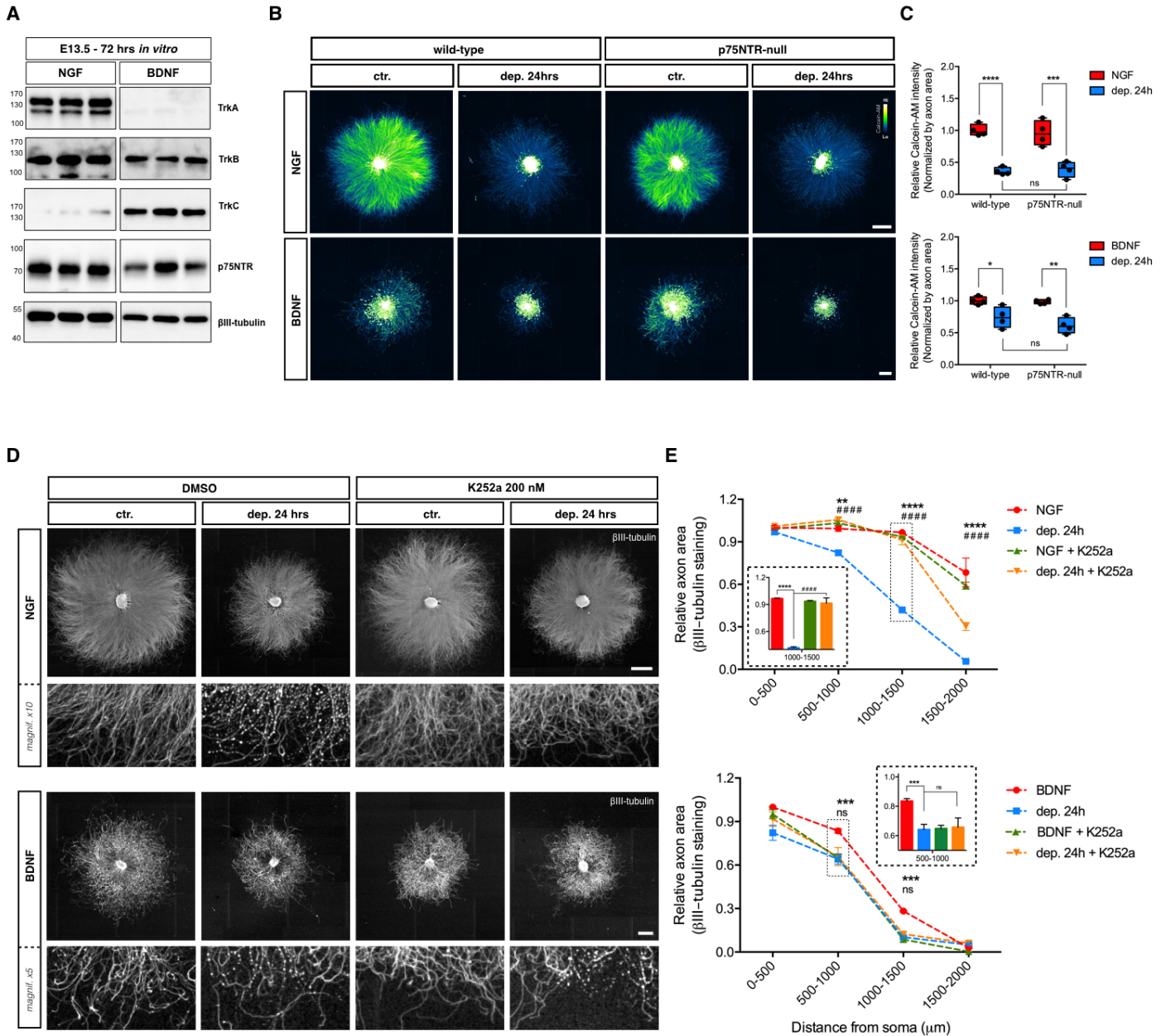


Figure 3.5. PKC inhibitor Gö6976 and EGTA rescue degeneration induced by NGF deprivation but not BDNF deprivation. **A)** DRG explants cultured in NGF or BDNF were either maintained in trophic media or withdrawn from trophic support with or without PKC inhibitor Gö6976 (10 μ M) for 24 hours before fixing, immunostaining for β III-tubulin and imaged by epifluorescence microscopy (NGF scale bar = 1000 μ m; BDNF scale bar = 500 μ m). **B)** Quantification of axonal area as a function of the distance from the soma using Axoquant 2.0 [360] and plotted in 500- μ m bins segments relative to 0-500 μ m 48-hour time point. The relative axonal area was analyzed by two-factor ANOVA followed by Tukey's *post hoc* comparison and plotted with mean and SEM (n = 3 embryos for each condition; data shown is representative of 3 independent experiments); (*) control versus deprived 24h; (#) deprived 24h versus deprived 24h + Gö6976; ns: non-significant, *p < 0.05, ****p < 0.0001. **C)** DRG explants cultured in NGF or BDNF were either maintained in trophic media or withdrawn from trophic support with or without Ca²⁺ chelator EGTA (5 mM) for 24 hours before fixing, immunostained for β III-tubulin and imaged by epifluorescence microscopy (NGF scale bar = 1000 μ m; BDNF scale bar = 500 μ m). **D)** Quantification of axonal area as a function of the distance from the soma using Axoquant 2.0 and plotted in 500- μ m binned segments. Ca²⁺ chelation rescued degeneration induced by NGF deprivation but not by BDNF deprivation. The relative axonal area was analyzed by two-factor ANOVA followed by Tukey's *post hoc* comparison and plotted with mean and SEM (n = 3 embryos for each condition; data shown is representative of 3 independent experiments); (*) ctr. versus dep. 24h; (#) dep. 24h versus dep. 24h + EGTA; ns: non-significant, ****p < 0.0001.

Figure 3.5

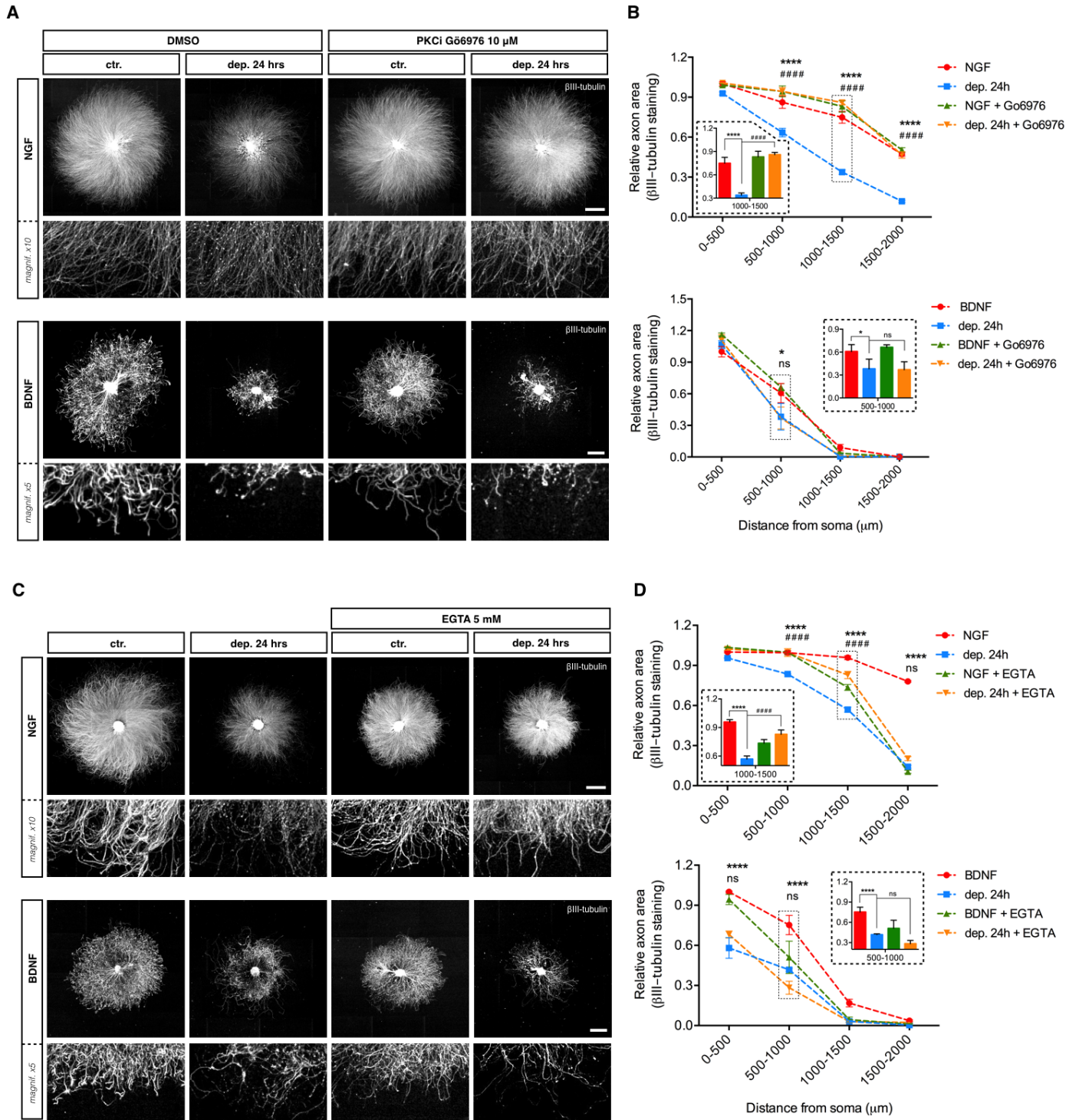


Figure 3.6. Translation, autophagy, necroptosis or Wallerian-like degeneration are not involved in BDNF deprivation-induced degeneration. **A)** DRG explants cultured in NGF or BDNF were maintained in trophic media or withdrawn from trophic support with or without translation inhibitor cycloheximide (CHX, 1 $\mu\text{g/ml}$) for 24 hours before fixing, immunostaining for β III-tubulin and imaging by epifluorescence microscopy (NGF scale bar = 1000 μm ; BDNF scale bar = 500 μm). Quantification of axonal area as a function of the distance from the soma plotted in 500- μm bins segments relative to 0-500 μm BDNF control. CHX rescued degeneration induced by NGF deprivation but not by BDNF deprivation. The relative axonal area was analyzed by two-factor ANOVA followed by Tukey's *post hoc* comparison and plotted with mean and SEM (n = 3 embryos for each condition; data shown is representative of 3 independent experiments); (*) ctr. versus dep. 24h; (#) dep. 24h versus dep. 24h + CHX; ns: non-significant, ****p < 0.0001. **B)** DRG explants were withdrawn from trophic support with or without the autophagy inhibitor 3-methyladenine (3-MA, 10 mM) for 24 hours before being immunostained for β III-tubulin (NGF scale bar = 1000 μm ; BDNF scale bar = 500 μm). Quantification of axonal area as a function of the distance from the soma plotted in 500- μm bins segments relative to 0-500 μm BDNF control. 3-MA rescued degeneration induced by NGF deprivation but not by BDNF deprivation. The relative axonal area was analyzed by two-factor ANOVA followed by Tukey's *post hoc* comparison and plotted with mean and SEM (n = 3 embryos for each condition; data shown is representative of 3 independent experiments); (*) ctr. versus dep. 24h; (#) dep. 24h versus dep. 24h + 3-MA; ns: non-significant, *p < 0.05, **p < 0.01, ***p < 0.001, ****p < 0.0001. **C)** DRG explants were withdrawn from trophic support with or without the necroptosis inhibitor necrostatin-1 (NEC-1, 100 μM) for 24 hours before being immunostained for β III-tubulin (NGF scale bar = 1000 μm ; BDNF scale bar = 500 μm). Quantification of axonal area as a function of the distance from the soma plotted in 500- μm binned segments relative to 0-500 μm BDNF control. NEC-1 slightly rescued degeneration induced by NGF deprivation but not by BDNF deprivation. The relative axonal area was analyzed by two-factor ANOVA followed by Tukey's *post hoc* comparison and plotted with mean and SEM (n = 3 embryos for each condition; data shown is representative of 3 independent experiments); (*) ctr. versus dep. 24h; (#) dep. 24h versus dep. 24h + NEC-1; ns: non-significant, *p < 0.05, ***p < 0.001, ****p < 0.0001.

D) DRG explants were withdrawn from trophic support with or without NAD⁺ (5 mM) for 24 hours before being immunostained for β III-tubulin (NGF scale bar = 1000 μ m; BDNF scale bar = 500 μ m). Quantification of axonal area as a function of the distance from the soma plotted in 500- μ m bins segments relative to 0-500 μ m BDNF control. NAD⁺ rescued degeneration induced by NGF deprivation but not by BDNF deprivation. The relative axonal area was analyzed by two-factor ANOVA followed by Tukey's *post hoc* comparison and plotted with mean and SEM (n = 3 embryos for each condition; data shown is representative of 3 independent experiments); (*) ctr. versus dep. 24h; (#) dep. 24h versus dep. 24h + NAD⁺; ns: non-significant, *p < 0.05, **p < 0.01, ****p < 0.0001.

Figure 3.6

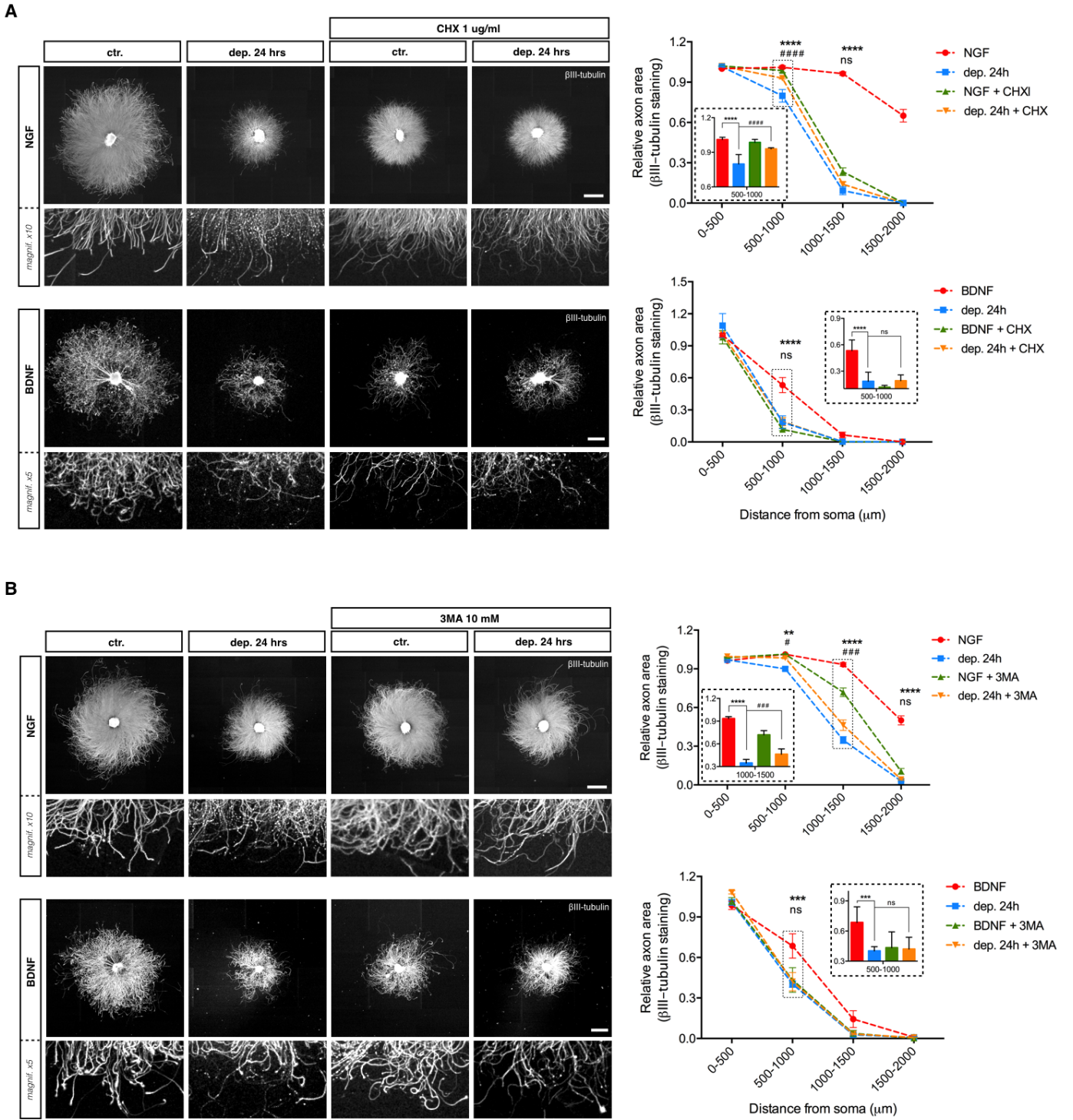


Figure 3.6 cont.

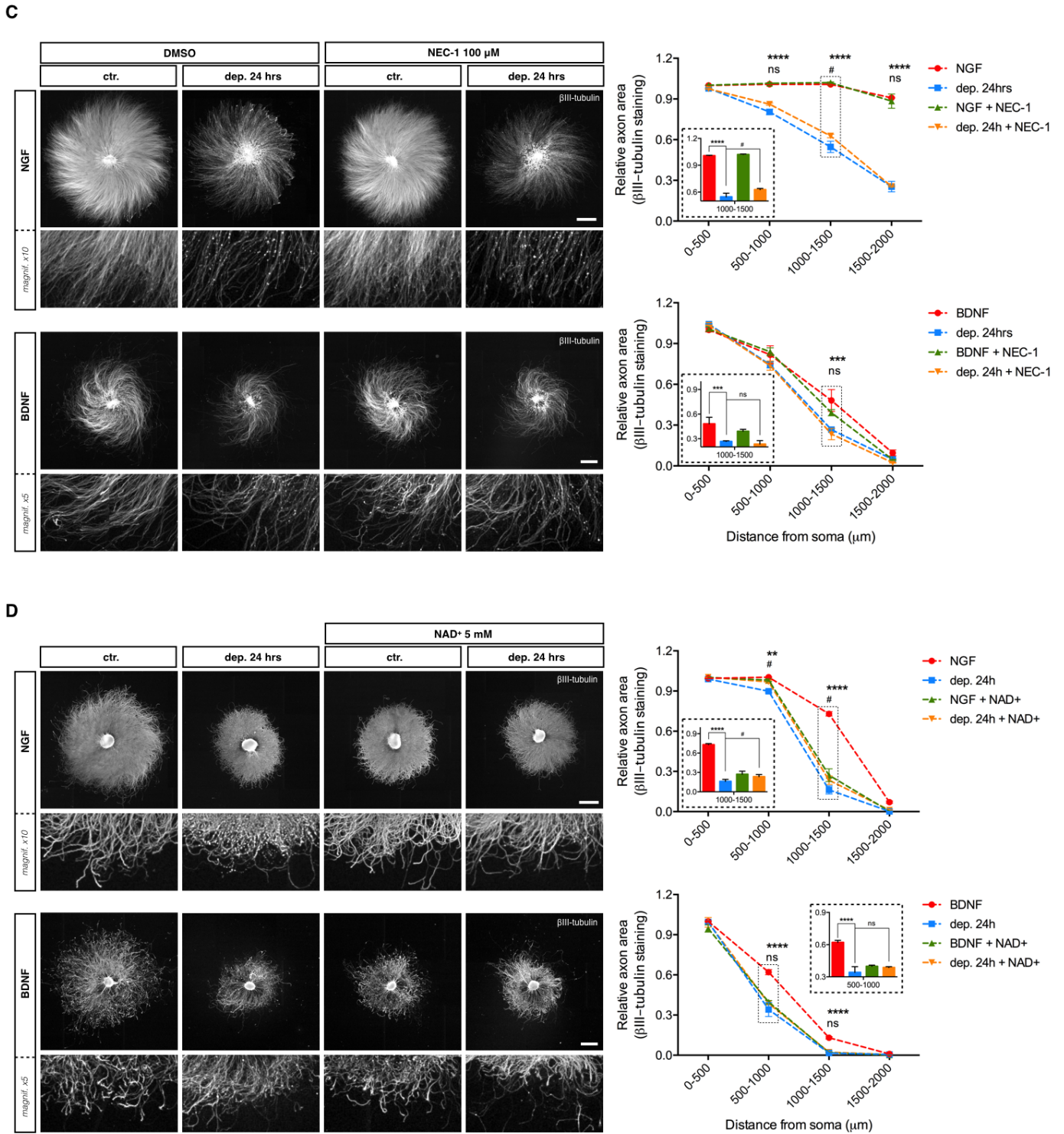


Figure 3.7. NGF and BDNF deprivation-induced degeneration require BAX. **A)** DRG explants from mixed-genotyped E13.5 litters were cultured in the presence of NGF or BDNF for 48 hours and then either maintained or withdrawn from trophic support for 24 hours before being live stained with Calcein-AM (NGF scale bar = 1000 μm ; BDNF scale bar = 500 μm). **B)** Quantification of Calcein-AM intensity normalized by axonal area and relative to wild-type control. A significant increase in Calcein-AM intensity was observed in both NGF or BDNF deprived BAX-null DRG explants compared with their deprived wild-type counterparts (n = 7 embryos in NGF/BDNF ctr., n = 5 embryos in NGF/BDNF dep. 24h, from pooled litters). Data was analyzed by two-way ANOVA and Tukey's *post hoc* comparison and plotted with median and SEM. ns: non-significant, *p < 0.05, **p < 0.01, ****p < 0.0001.

Figure 3.7

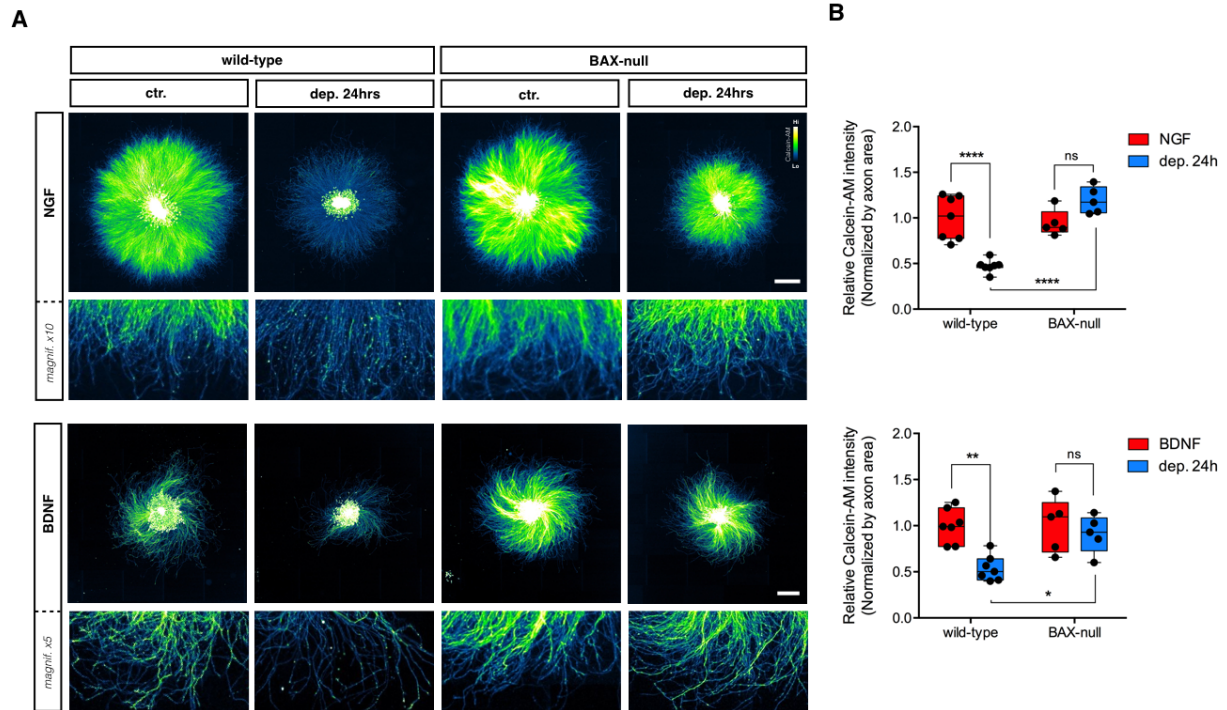


Figure 3.8. pan-Caspase inhibition does not block degeneration induced by BDNF deprivation. **A)** DRG explants cultured in NGF or BDNF were maintained in trophic media or were withdrawn from trophic support with or without pan-caspase inhibitor Boc-D-fmk (10 μ M) for 24 hours before fixing, immunostaining for β III-tubulin and imaging by epifluorescence microscopy (NGF scale bar = 1000 μ m; BDNF scale bar = 500 μ m). **B)** Quantification of axonal area as a function of the distance from the soma was performed using Axoquant 2.0 [360] and plotted in 500- μ m binned segments relative to 0-500 μ m NGF/BDNF controls. Pan-caspase inhibitor Boc-D-fmk rescued degeneration induced by NGF deprivation but not by BDNF deprivation. The relative axonal area was analyzed by two-factor ANOVA followed by Tukey's *post hoc* comparison and plotted with mean and SEM (n = 3 embryos for each condition; data shown is representative of 3 independent experiments); (*) ctr. versus dep. 24h; (#) dep. 24h versus dep. 24h + Boc-D-fmk; ns: non-significant, ****p < 0.0001.

Figure 3.8

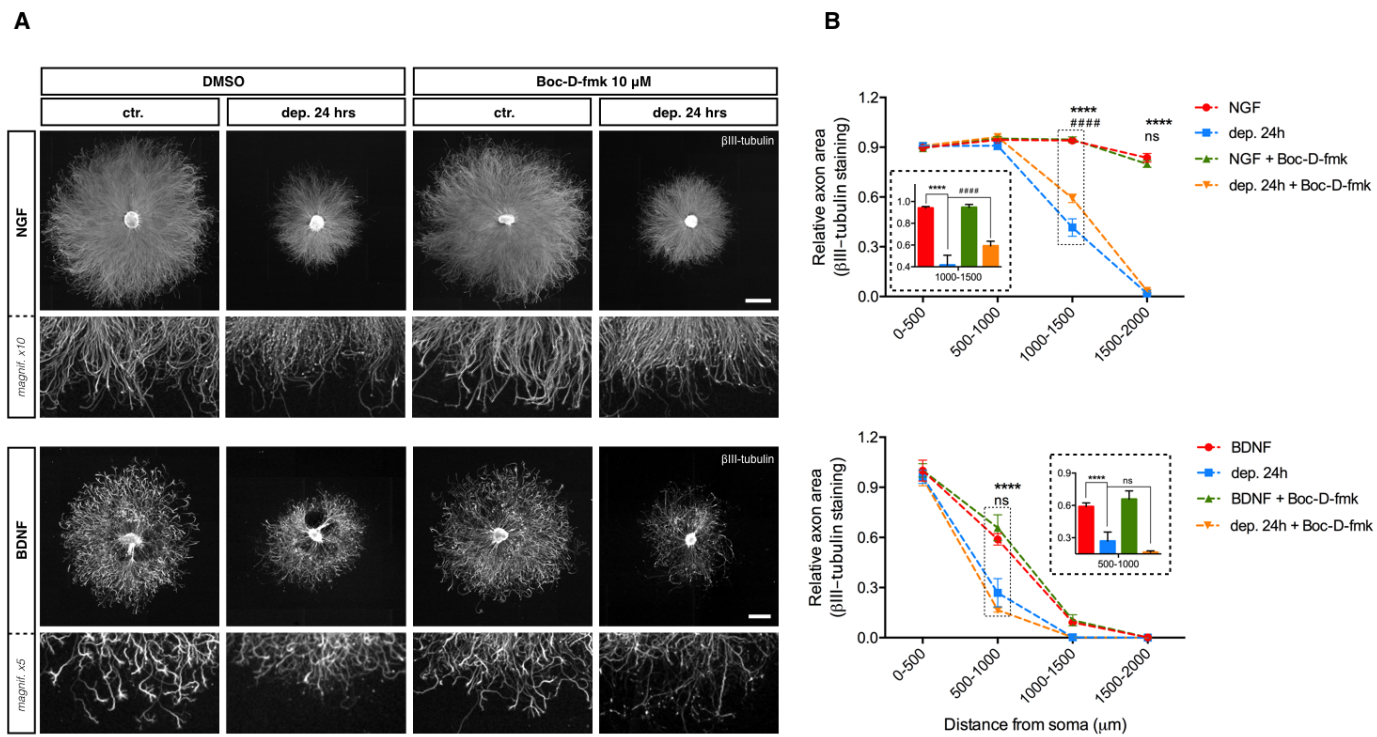


Figure 3.9. Cleaved form of executioner caspase-3 does not increase during BDNF deprivation. **A)** DRG explants cultured in NGF or BDNF were either maintained in trophic media or withdrawn from trophic support with or without pan-caspase inhibitor zVAD-fmk (20 μ M) for 24 hours before fixing, immunostaining for β III-tubulin and imaged by epifluorescence microscopy (BDNF scale bar = 1000 μ m). **B)** Quantification of axonal area as a function of the distance from the soma plotted in 500- μ m bins segments relative to 0-500 μ m BDNF control. Pan-caspase inhibitor zVAD-fmk does not rescue degeneration induced by BDNF deprivation. The relative axonal area was analyzed by two-factor ANOVA followed by Tukey's *post hoc* comparison and plotted with mean and SEM (n = 3 embryos for each condition; data shown is representative of 3 independent experiments); (*) ctr. versus dep. 24h; (#) dep. 24h versus dep. 24h + zVAD-fmk; ns: non-significant, *p < 0.05, ***p < 0.001, ****p < 0.0001. **C)** Protein lysates collected from E13.5 DRG explants cultured in the presence of NGF (12.5 ng/ml) or BDNF (37.5 ng/ml) for 48 hours were maintained or withdrawn from trophic support for 24 hours and then analyzed by immunoblot against Neurofilament-M (Nf-M) and caspase-3. Levels of Nf-M significantly decreased after either NGF and BDNF deprivation but only NGF deprived DRG lysates show a significant change in pro- and cleaved caspase-3 levels. Data were analyzed by two-tailed Mann-Whitney plotted with mean and SEM (n = 3 embryos for each condition; data shown is representative of 3 independent experiments); ns: non-significant, *p < 0.05, **p < 0.01.

Figure 3.9

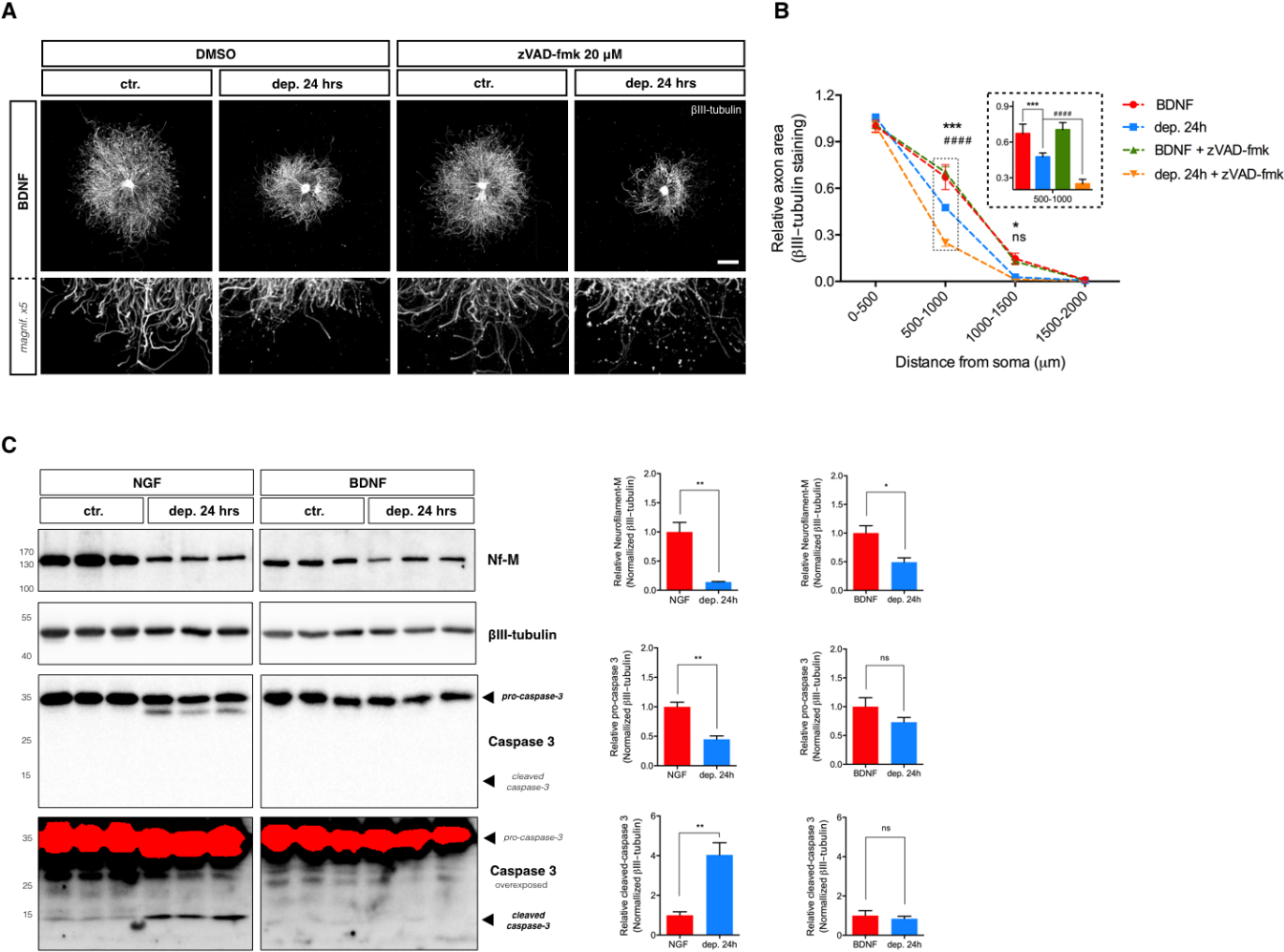
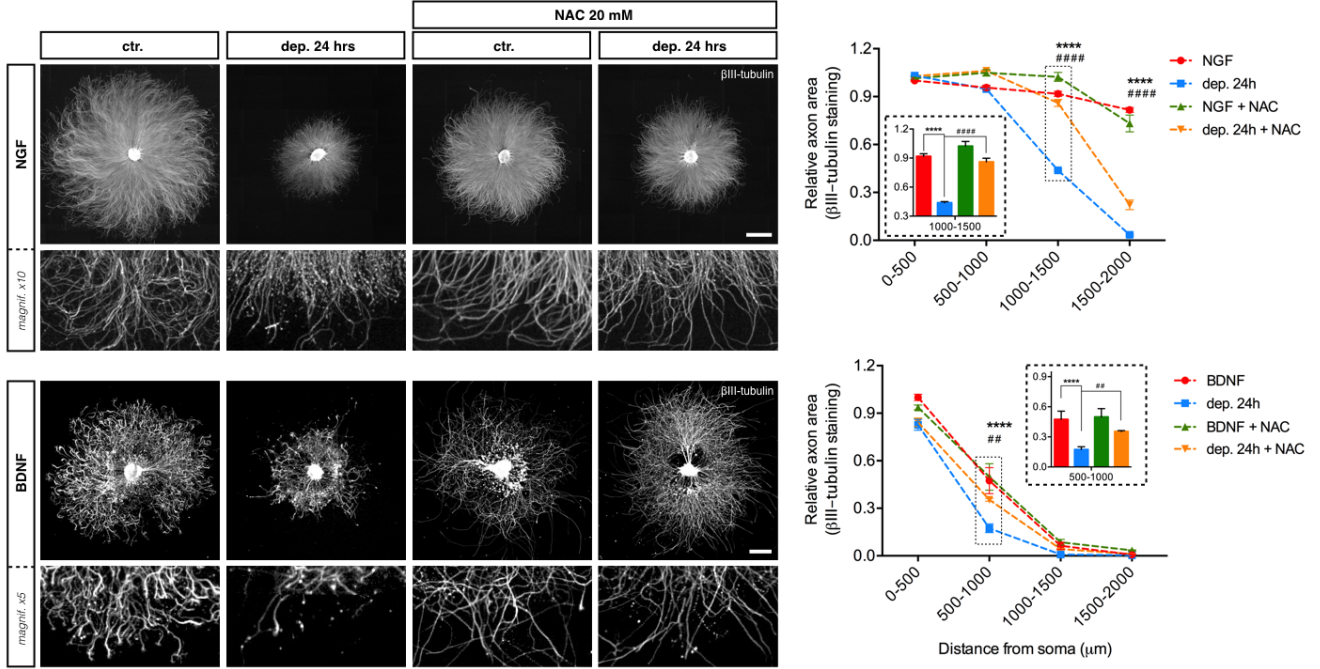


Figure 3.10. Reactive oxygen species are required for axon degeneration induced by BDNF deprivation. **A)** DRG explants cultured in NGF or BDNF were either maintained in trophic media or withdrawn from trophic support with or without ROS scavenger N-acetyl-cysteine (NAC, 20 mM) for 24 hours before fixing, immunostaining for β III-tubulin and imaged by epifluorescence microscopy (NGF scale bar = 1000 μ m; BDNF scale bar = 500 μ m). **B)** Quantification of axonal area as a function of the distance from the soma and plotted in 500- μ m bins segments relative to 0-500 μ m 48-hour time point. NAC rescued degeneration induced by NGF deprivation and BDNF deprivation. The relative axonal area was analyzed by two-factor ANOVA followed by Tukey's *post hoc* comparison and plotted with mean and SEM (n = 3 embryos for each condition; data shown is representative of 3 independent experiments); (*) ctr. versus dep. 24h; (#) dep. 24h versus dep. 24h + NAC; **p < 0.01, ****p < 0.0001.

Figure 3.10



Connecting text: Chapter 3 to 4

In the previous chapters we studied the process of developmental neuronal cell death in two subpopulations of DRG sensory neurons. Along with programmed neuronal death, pruning of axons is another major remodelling process during the maturation of the nervous system. Although axonal pruning utilizes apoptotic signaling cascades, the elimination of axon branches does not compromise neuronal survival. The ability of neurons to restrict and compartmentalize the mechanisms of degeneration is crucial to differentiate pruning from cell death. However, the study of axonal pruning *in vitro* is normally performed using compartmentalized cultures of embryonic neurons, whose capacity to restrict the cell death machinery in comparison with mature adult neurons is significantly limited. In the next chapter, we question the reliability of using compartmentalized cultures of embryonic DRG neurons to mimic the process of axonal pruning.

Chapter 4

Modelling developmental axonal pruning *in vitro* using compartmentalized microfluidic chambers

de León A.¹, Gibon J.², Barker P.²

1- Montreal Neurological Institute, McGill University, Montreal, QC, Canada. 2- Irving K. Barber School of Arts and Science, University of British Columbia – Okanagan Campus, Kelowna, BC, Canada.

4.1 Abstract

Neurons use the apoptotic machinery to prune misguided or excessive axonal segments during the maturation of the nervous system and to sustain synaptic plasticity throughout adulthood. Mechanisms that compartmentalize or restrict the apoptotic machinery are therefore crucial to allow axon pruning that does not affect neuronal survival. Mature neurons are more resistant to cell death than their younger counterpart; how embryonic neurons that are poised to undergo apoptosis remain alive during axon pruning remain unknown. NGF-dependent embryonic dorsal root ganglia (DRG) neurons maintained in compartmentalized devices are used as a model of developmental axonal pruning *in vitro*. It is widely assumed that local NGF deprivation in distal axons induces axonal degeneration without causing cell death, but this assumption has not been profusely tested. Here, we used compartmentalized cultures of embryonic DRG neurons subjected to different trophic support scenarios: global NGF supply, global NGF deprivation or local NGF deprivation in distal axons. We then assessed survival of DRG soma over the course of their maturation *in vitro*. We found that, as expected, global NGF deprivation produces massive loss of young DRG cell bodies but surprisingly, we also found that NGF deprivation in distal axons induces a sharp drop in embryonic DRG cell bodies that is not observed in mature neurons or in young neurons maintained in NGF.

Thus, the compartmentalized deprivation of NGF in axons from young neurons is not simply mimicking pruning but causes a mix of cell death and axonal pruning. These results indicate that embryonic DRG neurons may not be a perfect model for axonal pruning *in vitro* but also raise the possibility of using compartmentalized embryonic DRG neurons to identify retrograde death signals initiated by NGF withdrawal.

4.2 Introduction

Neurite pruning - together with naturally-occurring neuronal death - is a critical regressive event necessary for the maturation and fine-tuning of connections in the developing nervous system. Naturally-occurring neuronal death eliminates neurons unable to appropriately connect with their targets; neurite pruning removes dendritic or axonal segments that are unnecessary, misguided or excessive for the efficient functioning of active neuronal circuits without affecting neuronal survival. The apoptotic pathway becomes highly restricted once neurons are integrated in the nervous system, enabling neurons to survive for the lifetime of the organism [677, 702, 751, 752]. The selective pruning of neurites in mature neurons is critical for permitting plasticity in the adult nervous system [628, 644] and the dysregulation of neurite pruning has been implicated in serious neurological disorders such as schizophrenia and autism [622, 623].

Mammalian axonal pruning occurs via retraction, axosome shedding, or degeneration mechanisms [631]. The study of axonal pruning by degeneration has been of particular interest because of its morphological and molecular resemblance to axonal degeneration that precedes apoptotic cell death [660] an event also observed in several neurodegenerative diseases [655]. In fact, key players of the apoptotic machinery such as the pro-apoptotic protein BAX or caspases are employed in mechanisms of axonal pruning [213, 214, 224, 331, 348]. How neurons undergoing axonal pruning restrict or compartmentalize the apoptotic machinery while avoiding damaging the rest of the cell body, especially the soma, is a hot topic in the axonal pruning field. The discovery that the apoptotic protease activator factor 1 (Apaf-1), which accelerates the activation of caspases, is dispensable for the axonal pruning process provided the first clue on how neurons may contain the apoptotic machinery during axonal pruning [224]. In addition, the differential expression of anti- and pro-apoptotic members of the Bcl-2 family through mechanisms involving, for example, the control of local translation by micro RNAs (miRs), has been suggested as a way to restrict or locally trigger the apoptotic machinery during axonal pruning [319, 338, 688, 753]. Despite this progress, the processes that control axonal pruning during development are still largely unknown. Mechanisms that restrict or compartmentalize apoptosis increase with neuronal maturation, meaning that developing

neurons are more susceptible to death stimulus [660, 702]. If axonal pruning by degeneration relies in part on strategies that locally restrict the apoptotic machinery, then the borders between cell death and axonal pruning in developing neurons could be more diffuse than originally thought.

Over the last decade, the culture of embryonic sensory and early-postnatal sympathetic neurons in compartmentalized culture devices has emerged as the main model to mimic axonal pruning *in vitro*. These immature neurons depend on nerve growth factor (NGF) for survival and growth. Compartmentalized NGF deprivation of distal axons has been shown to induce local axonal pruning by degeneration and it has been assumed that this local degeneration is not accompanied by cell death. Taking into consideration the susceptibility of young neurons to cell death, the extent to which young neurons resist cell death by a distal apoptotic (pruning) stimulus has not been investigated in detail. The present study uses NGF-dependent embryonic dorsal root ganglia (DRG) neurons cultured in microfluidic devices to address this point. In a series of proof-of-concept experiments, we observed that local NGF deprivation in axons of young DRG neurons causes a sharp decrease in the number of surviving cell bodies. In contrast, cell bodies of mature DRG neurons subjected to local NGF deprivation in axons remain viable, as do young neurons maintained in NGF. These results suggest local deprivation of axons not only initiates axon pruning but also initiates a retrograde death signal in a subpopulation of DRG sensory neurons.

4.3 Materials and methods

4.3.1 Mouse strains

CD1 mice were purchased from Charles River Laboratories (Montreal, Canada). Animal procedures and experiments were approved by the University of British Columbia animal care committee and the Canadian Council of Animal Care. Efforts were made to reduce animal handling and use.

4.3.2 Microfluidic cultures and trophic factor deprivation

Dorsal root ganglia (DRG) from E13.5 mice were aseptically removed and pelleted in Hank's balanced salt solution (HBSS, Gibco), dissociated with 0.25% trypsin (Gibco) at 37°C for 10 minutes, plus 10 minutes with 1 µg/ml of DNase (Sigma-Aldrich) at 37°C. Trypsin was neutralized with 5% fetal bovine serum in Neurobasal media (Invitrogen). DRGs were centrifuge at 1000 rpm at 21°C for 5 minutes and resuspended in phenol-red free Neurobasal media (Invitrogen) supplemented with 2% B27 serum-free supplement (Invitrogen), 1% L-glutamine (Wisent), 1% penicillin/streptomycin (Wisent) 10 µM 5-fluoro-2'-deoxyuridine (FDU, Sigma-Aldrich) and 12.5 ng/ml NGF (CedarLane). DRGs were mechanically dissociated with fire-polished Pasteur pipets and neurons were seeded and grown at 37°C, 5% CO₂ in microfluidic devices (XONA microfluidics, RD450 and TCND500) previously assembled in glass coverslips coated with 1 mg/ml poly-D-lysine (Sigma-Aldrich), 10 µg/ml laminin-entactin complex (Corning) and 0.1 mg/ml PurCol bovine collagen (Advanced Biomatrix). To achieve global deprivation of NGF, the media in all compartments was switched to deprivation media containing 2.0 µg/ml of function blocking antibodies against NGF (rabbit polyclonal antibody raised against 2.5s NGF [712]) without neurotrophic supplementation. For local deprivation, only the axonal compartment was filled with deprivation media. A 50 µl volume differential was established between the deprived compartment and the adjacent - non-deprived - compartment such that the flow runs to the former. This volume gradient was re-established every 24 hours to maintain fluidic isolation [664].

4.3.3 Assessment of DRG neuronal survival with live Calcein-AM staining

The progression in the number of healthy DRG cell bodies and axonal area in microfluidic devices was followed at different days *in vitro* (DIV) using differential interference contrast (DIC) and immunofluorescent microscopy of live-stained neurons with Calcein-AM (AAT Bioquest). Briefly, compartmentalized cultures were treated with 1 µg/ml of Calcein-AM in phenol-red free Neurobasal media for 1 hour at 37°C (Calcein-AM was diluted in the media present in each compartment at each staining occasion). Back to complete Neurobasal media without Calcein-AM, DRG cultures were tiled-imaged using a Zeiss ObserverZ.1 inverted epifluorescence microscope with an automated motorized stage and an atmosphere-controlled incubation chamber (Pecon) controlled by ZEN2 software at 40x magnification (oil-immersed). After the scanning, cultures were placed back to the incubators for future re-staining and re-scanning. DIC and 488 nm (Calcein-AM) stitched master images were generated using ZEN2 software. Healthy DRG cell bodies were quantified manually using NIH Image J software. DRG cell bodies were counted as healthy when they showed non-apoptotic morphology by DIC and Calcein-AM positive staining. Axon area in distal (and medial) compartment was quantified from stitched images of Calcein-AM-stained axons over an established threshold for all axonal compartments across time. The number of healthy DRG cell bodies and the axonal area were expressed as the percentage relative to their respective quantities at the first staining record (normally between 3 to 5 DIV).

4.3.4 Mitochondria live staining with TMRE

Compartmentalized cultures of DRG neurons in microfluidic devices were treated with 0.25 µM tetramethylrhodamine, ethyl ester (TMRE) at 37°C for 20 minutes (usually in co-incubation with Calcein-AM). At the end of the incubation time, cultures were switched to back to clear complete Neurobasal media (with or without trophic support depending on the compartment and the experimental stage). Imaging at 555 nm was performed using a Zeiss ObserverZ.1 inverted epifluorescence microscope with an automated motorized stage and an atmosphere-controlled incubation chamber (Pecon) controlled by ZEN2 software with 40x magnification (oil-immersed).

4.4 Results

The study of the axonal pruning process *in vitro* relies on compartmentalized culture devices [661, 664]. Embryonic DRG and postnatal SGC neurons have been the preferred neuronal subtypes to study axonal pruning *in vitro* because of their morphological simplicity, the long extension of their projections and their dependency on NGF [660]. Figure 4.1 A shows a classic microfluidic chamber, one of the two compartmentalized culture techniques mostly used, originally designed by Taylor et al. (2005) [664]. Its most basic design is composed of two compartments connected by microgrooves large enough to allow axon growth but small enough ($3 \times 10 \mu\text{m}$) to prevent soma migration between compartments and achieve the physical separation between cell bodies and axons (Figure 4.1 B). Dissociated DRG neurons are seeded in one compartment (proximal/soma compartment, red); with NGF supplied in both compartments, neurons extend their axons through the microgrooves into the second compartment (distal/axonal compartment, blue). Figure 4.1 C shows a representative tiled-image of the classic microfluidic device with dissociated DRG neurons lived-stained with Calcein-AM. Axonal pruning is induced by exposing the distal compartment to media without trophic support plus blocking antibodies against NGF (αNGF). To avoid exposing the cell bodies to the αNGF media, risking global deprivation and apoptosis, the volume in the distal compartment is reduced compared to the proximal compartment, creating a hydrostatic pressure inside the device that fluidically isolates the cell bodies from the lack of trophic support (Figure 4.1 D).

After having successfully established the culture of embryonic DRG neurons in microfluidic devices, we performed a series of proof-of-concept experiments to test whether this technique mediates local degeneration without causing cell death. Two microfluidic devices were seeded with dissociated DRG neurons from E13.5 mouse embryos and grown for 48 hours in the presence of NGF. Next, one device was deprived of NGF locally at the axonal compartment while the other was kept with NGF in all compartments (Figure 4.2 A, indicated as Day 0). 72 hours later, both cultures were lived-stained with Calcein-AM, imaged and placed back into the incubator. On the next day (96 hours since Day 0) both devices were re-stained with Calcein-AM and re-scanned (Figure

4.2 A). Figure 4.2 B shows the control device with global NGF support, and Figure 4.2 C represents the device deprived of NGF at the axonal compartment. As expected we observed a massive decrease in axons upon distal NGF deprivation from 72 to 96 hours (Figure 4.2 C), while no change in axon density was observed in the same period of time in the control device (Figure 4.2 B).

The second test sought to compare the progression of pruning versus cell-death in microfluidic devices (Figure 4.3; see panel E for experimental timeline). Again, two 2-compartment devices were seeded with embryonic DRG neurons and grown for 3 days in the presence of NGF (Figure 4.3 A). Next, one device was deprived of NGF at the distal/axonal compartment, mimicking axonal pruning (Figure 4.3 B), while the other was globally deprived to induce cell death (Figure 4.3 C). Changes in axonal area were followed with Calcein-AM over the following days. As expected, a dramatic loss of axons and cell bodies in both distal and proximal compartments was observed after 2 days of global NGF withdrawal (Figure 4.3 C). In comparison, it required 6 days of distal NGF deprivation to observe the almost complete disappearance of live axons from the distal compartment (Figure 4.3 B). Interestingly, the massive death of cell bodies induced by global NGF deprivation is not observed in the device mimicking axonal pruning. In fact, the re-addition of NGF back to the distal compartment prompted the re-growth of axons, confirming that cell soma that remained after distal NGF deprivation viable. However, we observed a significant loss of cell bodies between the first and the sixth day of distal NGF deprivation (Figures 4.2 C and 4.3 B). This observation suggested that cell death is taking place in a subpopulation of DRG neurons subjected to distal NGF withdrawal.

Previous studies have shown that early postnatal sympathetic neurons aged *in vitro* (28 days *in vitro* or 28 DIV) become resistant to cell death induced by global NGF deprivation but are still able to prune their axons when these are locally deprived of NGF [224]. Similar resistance to global NGF deprivation has been reported for DRG neurons after 21 DIV [754]. To examine whether the deprivation of distal axons from NGF is responsible for the decrease of DRG cell bodies in the proximal compartmented, presumably through cell death, we compared the response of young and aged DRG neurons to pruning in microfluidic devices. For this, we used a single 3-compartment microfluidic device, in which a middle compartment (axons) acts as a buffer between the

proximal (cell bodies) and the distal (axons) compartments. This protects the cell soma compartment from any leakage from the distal compartment containing α NGF antibody. Figure 4.4 A shows the starting point of the culture at 4 DIV, after which NGF deprivation was applied at the distal compartment. The device was re-stained with Calcein-AM and imaged ten days later at 14 DIV (Figure 4.4 B). We noted an almost complete loss of distal axons, an increase of live-axon area at the middle compartment and an approximately 30% decrease of DRG cell bodies at the proximal compartment (quantified in Figure 4.4 F). Then, the distal compartment was filled back with NGF for 6 days to support axonal re-growth. Figure 4.4 C shows a representative image of the culture at 20 DIV. We observed re-growth of distal axons, the continued growth of middle axons and almost no cell body loss (Figure 4.4 F). At this point (20 DIV) the remaining DRG neurons were considered mature and based on previous studies they should be able to prune their axons following local NGF deprivation but resist cell death under global NGF withdrawal [224, 754]. NGF deprivation was applied in the distal and middle axonal compartments for 6 days until 26 DIV, time at which the compartmentalized culture was re-stained with Calcein-AM and imaged (Figure 4.4 D). A reduction in live-axonal area was observed in distal and middle compartments, correlating with the lack of trophic support, but no significant loss of cell bodies was observed in the proximal compartment (Figure 4.4 F). These observations confirm that young neurons subjected to distal NGF deprivation undergo cell death whereas mature DRG neurons locally prune their axons while maintaining cell body viability. To corroborate the resistance of aged DRG neurons to cell death, the compartmentalized culture was then globally deprived of NGF for 2 days. Although a clear loss of middle axonal area was observed by 28 DIV, no drastic loss of cell bodies occurred (Figure 4.4 F), contrasting with a previous global-deprivation experiment done in young DRG neurons (5 DIV) at Figure 4.3 C.

Lastly, we explored the possibility that the drop in the number of cell bodies in young DRG neurons distally deprived of NGF was caused by our *in vitro* culture conditions and not by our trophic factor deprivation protocol. To test this idea, we cultured embryonic DRG neurons in a 3-compartment microfluidic device maintained with trophic support in all three compartments during the course of its *in vitro* maturation. The number of DRG cell bodies and axonal area was recorded at 4, 14 and 20 DIV (Figure 4.5 A). In addition

to the sustained increase in live-axonal area, no sharp drop in the number of DRG cell bodies was observed in any of these young stages (Figure 4.5 C). Beyond 20 DIV the culture was subjected to trophic deprivation at the distal axonal compartment for six days. By 26 DIV we noted a clear decrease in distal axonal area but no drastic drop of the number of cell bodies in the proximal compartment (Figure 4.5 B and C). These results confirm that mature DRG neurons can prune their axons without dying. Although a difference in the number of cell bodies is observed between the top panel of Figure 4.5 A and 4.5 B, this decrease was mostly driven by a sharp drop in glial cells rather than DRG cell bodies. Culture media contains FDU, a cytostatic drug that stops the growth and induces cell death in mitotic cells like glia. Over time, FDU reduced the number of glial cells in culture. Figure 4.5 D exemplifies the quantification of DRG versus glial cells in a region of the proximal compartment using a combination of DIC and Calcein-AM staining. Future DRG soma quantification may take advantage of additional live-dyes, for example TMRE, which labels active mitochondria. TMRE staining readily differentiates healthy from dying DRG cell bodies, and glial cells from DRGs (Figure 4.5 E).

4.5 Discussion

The compartmentalization of the death stimulus - such as the deprivation of trophic support - is the main reason for using microfluidic devices to mimic axonal pruning *in vitro*. In other words, localizing the death stimulus at the axon is enough to meet the fundamentals of the axonal pruning process: axonal degeneration without causing cell death. In the present study we have followed the response of DRG sensory neurons cultured in microdevices to different trophic-deprivation scenarios including the localized deprivation of NGF in axons. Our observations suggest that the compartmentalization of the death stimulus does not mimic developmental axonal pruning but instead results in a mix of cell death and pruning.

The results that motivate such assertion are resumed in Figure 4.6. The schema shows the combination of two distinct culture parameters: the localization of the death stimulus (global *versus* distal/axonal NGF deprivation) and the age of cultures (young *versus* mature). It is well known that young DRG cultures are highly susceptible to cell death in a global NGF-deprivation scenario. This was manifested by a complete loss of cell bodies in the proximal compartment (Figure 4.6, top left panel). In contrast, mature cultures are resistant to cell death induced by global NGF deprivation, but they prune their axons in response to global or distal NGF withdrawal (Figure 4.6, bottom left and right panels) [224, 702, 754]. The devastating effect of a global NGF withdrawal in young DRG cultures is lost in a distal deprivation scenario during which distal axons still degenerate but without massive death of cell bodies in the proximal compartment. This comparison has settled the idea that the stimulating death at the axon is sufficient to mimic axonal pruning in developing neurons (Figure 4.6, top left and right panels). However, the novel aspect of our study was to follow the number of cell bodies in the same culture over time, before and after the distal deprivation of NGF. Using that internal comparison, the drop in the number of young DRG cell bodies after distal NGF deprivation was evident (Figure 4.6, top right panel). Because mature neurons are resistant to cell death and no evident drop in the number of mature cell bodies was observed before and after distal NGF deprivation (Figure 4.6 bottom right panel), we conclude that the drop of DRG somas in young cultures is due to cell death induced by distal deprivation. No cell body loss is

observed in young cultures globally supplied of NGF, ruling out interference of the *in vitro* culture system or imaging conditions. Thus, the results presented in this study suggest that the localization of the death signal is not sufficient to purely mimic axonal pruning in young DRG neurons, but rather a mixture of cell death and pruning. Instead, the age of the culture seems to be at least as relevant as the localization of the death signal to properly model axonal pruning in NGF-dependent DRG neurons *in vitro*.

The fact that the age of *in vitro* cultures is a determining factor in modeling axonal pruning, emphasizes the importance of mechanisms that restrict apoptotic machinery. Compared to developing neurons, mature neurons have a better capacity to restrict the activation of the apoptotic pathway [702]. For example, neuronal maturation increases the expression of miR29, especially in the cell body, which is able to inhibit the translation of multiple members of the BH3-only family, including PUMA, necessary for BAX activation during apoptosis and axonal pruning [224, 316, 677, 680]. In addition, several studies have shown an almost complete reduction in Apaf-1 protein levels in mature neurons, reducing their capacity to accelerate caspase activation [702]. Interestingly, unlike BAX, Apaf-1 deficiency does not block axonal degeneration triggered by local NGF deprivation in young SCG neurons, suggesting that Apaf-1 is dispensable for the axonal pruning pathway [224]. However, Apaf-1 is not essential either to drive developmental programmed cell death in NGF-dependent neurons, as derived from the comparison between Apaf-1::TrkA (which do undergo cell death) and BAX::TrkA (which do not undergo cell death) compound double null mice [167, 344]. Although Apaf-1 may not be essential for axonal pruning, its higher expression in developing neurons could constitute a threat in the control of caspase activation, thus risking an easier switch between axonal pruning and cell death. In the future, it will be interesting to investigate whether Apaf-1 gets activated during axonal pruning and if Apaf-1 deficiency or miR29 expression rescue the loss of cell bodies in young axonal-deprived DRG neurons.

The capacity to restrict the apoptotic machinery may be decisive in determining whether a developing neuron undergoes axonal pruning or apoptosis. Given that immature neurons possess a poorer battery of tools to fight the activation of the apoptotic machinery, the decisive factor in their case could be determined by the amount of death stimulus to which they are exposed. It is well established that axonal pruning depends on

an intimate communication between the axon and the cell body. In such cross-talk, the deprived axonal segment sends a retrograde deadly signal back to the soma, activating a transcription pro-apoptotic program that is meant to destroy of the original deprived segment [316, 322, 339, 663]. The amount of retrograde signal integrated in the cell body could be directly proportional to the amount of death stimulus to which a neuron is exposed. The only way this could be translated *in vitro* is through the expanse of axonal segment that is under to trophic deprivation conditions (*in vivo*, it may additionally be the actual amount of trophic support that the neuron is receiving at the innervation target). Thus, it will be interesting to explore the effect that the size of the deprived axonal segment has on the number of cell bodies surviving during distal NGF deprivation of embryonic DRG neurons cultured in microfluidic devices.

In conclusion, an *in vitro* model is never a complete expression of an *in vivo* biological process. Understanding the backstage of the model itself constitutes an important aspect towards the comprehension of what the model is expected to mimic. The present study shows that a system used extensively to mimic developmental axonal pruning *in vitro*, may be in fact modelling an intermingle of axonal pruning with the closely related process of cell death. Further investigation is necessary to clearly establish the boundaries of this *in vitro* approximation to the study of developmental axonal pruning.

4.6 Figures and figure legends

Figure 4.1. Establishment of dissociated DRG cultures in microfluidic devices. A) Two-compartment microfluidic device made of polydimethylsiloxane (PDMS). **B)** Schematic representation of the internal structure of a microfluidic device composed of a cell body compartment (red) and an axonal compartment (blue) connected by microchannels. **C)** Stitched tile-image of dissociated E13.5 mice DRG neurons grown in a microfluidic device for 72 hours in the presence of NGF in both compartments. DRG neurons were stained with live-dye Calcein-AM for 1 hour and then tiled-imaged exciting at 488 nm using an epifluorescence microscope equipped with an automated motorized stage at 40x magnification. The proximal compartment contains a mix of cell bodies and axons while the distal compartment contains pure axons. Axons cross to the axonal compartment through 450 μm long microgrooves of 3 x 10 μm , separated 50 μm from each other. The small size of the channels avoids soma migration between compartments (Scale bar = 200 μm). **D)** Schematic cross-section representation of a microfluidic device showing the procedure to achieve fluidical isolation of the proximal (cell body) compartment during the process of mimicking axonal pruning (distal/axonal NGF deprivation). Briefly, once axons reach the distal compartment, axonal pruning is induced by exposing them to media lacking NGF and containing blocking antibodies against NGF (αNGF). To avoid exposing the cell bodies to the αNGF media, risking global deprivation and apoptosis, the volume in the distal compartment is reduced compared to the proximal compartment, creating a hydrostatic pressure inside the device that fluidically isolates the cell bodies from the lack of trophic support.

Figure 4.1

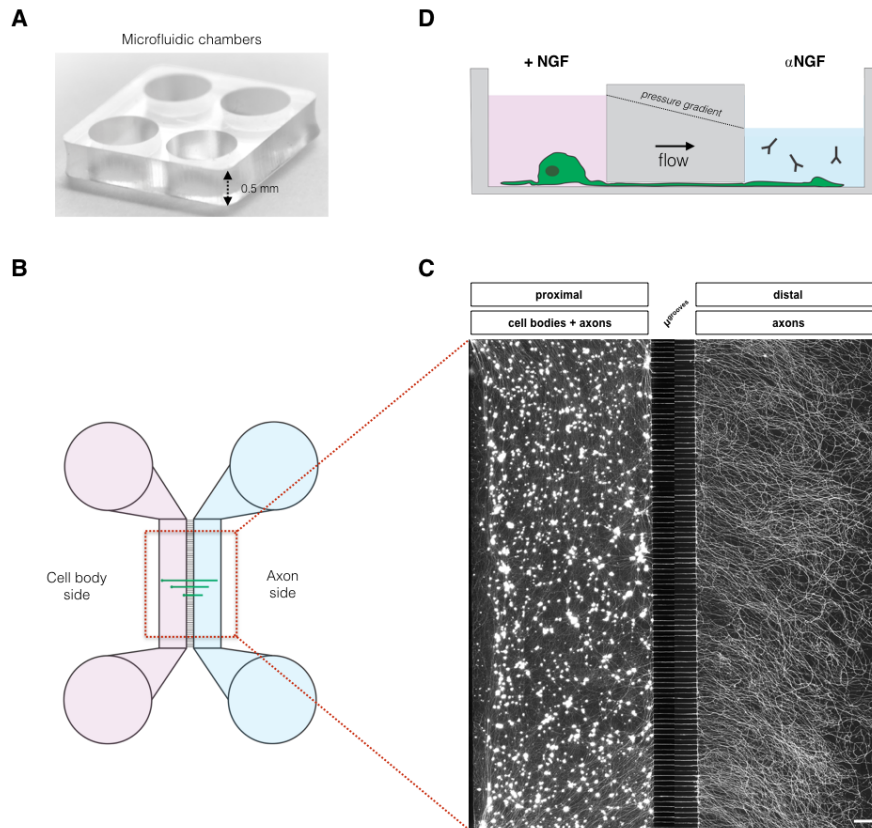


Figure 4.2. Serial Calcein-AM staining and imaging enable tracking of cellular changes induced by an axonal pruning protocol without altering the integrity of the cell culture. A) Experimental time-line of two embryonic DRG compartmentalized cultures in microfluidic devices subjected to constant NGF supply (B) or distal NGF deprivation (C). Green arrows indicate Calcein-AM staining and imaging. **B)** Representative stitched images of a microfluidic device DRG culture undergoing Global NGF support protocol, imaged at 72 and 96 hours passed Day 0. **C)** Representative stitched images of a microfluidic device DRG culture undergoing Distal NGF deprivation or axonal pruning protocol, imaged at 72 and 96 hours passed Day 0 (Scale bar = 200 μm).

Figure 4.2

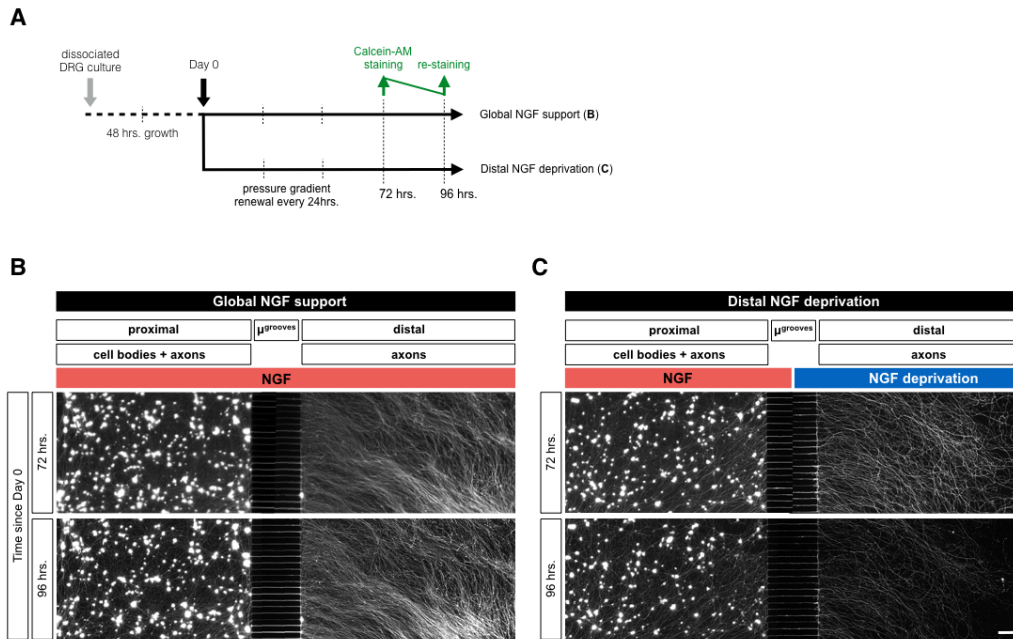


Figure 4.3. Progression of axonal pruning versus cell death in young DRG neurons maintained in microfluidic devices. **A)** Representative image of compartmentalized DRG cultures live-stained with Calcein-AM before inducing the axonal pruning protocol, 72 hours after seeding. **B)** Representative images of DRG neurons undergoing axonal pruning at 1, 3 and 6 days after NGF deprivation at the distal compartment. **C)** Representative images of DRG neurons undergoing cell death at 1 and 2 days after starting global NGF deprivation. **D)** Representative of the same microdevice previously experiencing distal NGF deprivation (B), now at 3 days after re-addition of NGF to the distal compartment (Scale bar = 200 μm). **E)** Experimental time-line. Green arrows indicate Calcein-AM staining and imaging.

Figure 4.3

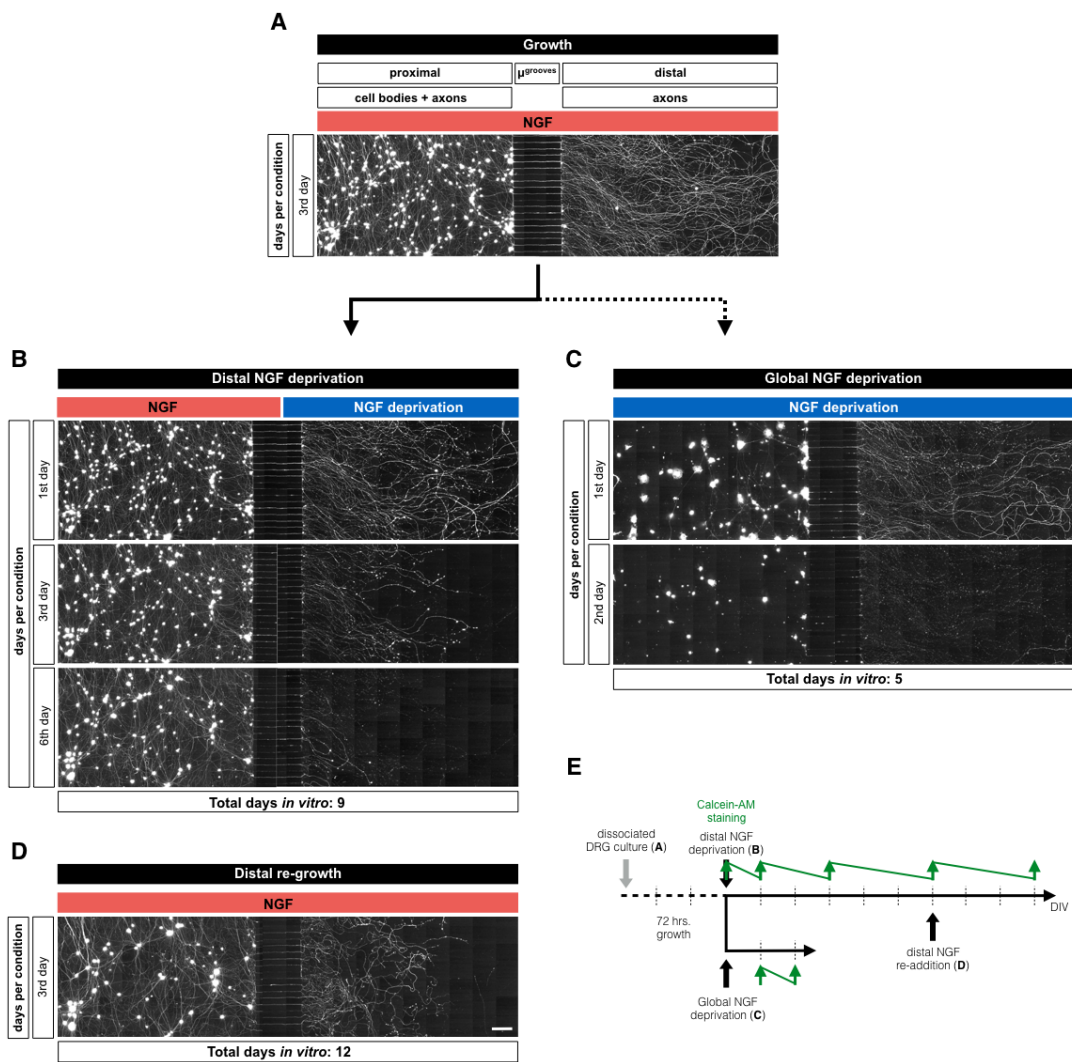


Figure 4.4. Distal NGF deprivation in young DRG neurons induces a significant drop in the number of DRG cell bodies that is not observed in mature DRG neurons undergoing axonal pruning. **A)** Representative image of DRG neurons cultured in three-compartment microfluidic device and live-stained with Calcein-AM, 4 days after seeding. **B)** Axonal pruning protocol in young DRG neurons: representative image at 10 days after initiating the deprivation of NGF at the distal compartment. **C)** Re-growth stage: representative image at 6 days after the re-addition of NGF to the distal compartment. **D)** Axonal pruning protocol in mature DRG neurons: representative image at 6 days after initiated deprivation of NGF at the medial and distal compartment. After 20 days *in vitro* (DIV) DRG neurons are considered mature [754]. **E)** Cell death-inducing protocol in mature neurons: representative image at 2 days after initiating NGF deprivation in all compartments (Scale bar = 200 μm). **F)** Quantification of Calcein-AM stained axonal area in medial and distal compartments, and the number of DRG cell bodies in the proximal compartment expressed as the percentage of remaining DRG soma at each time point (A).

Figure 4.4

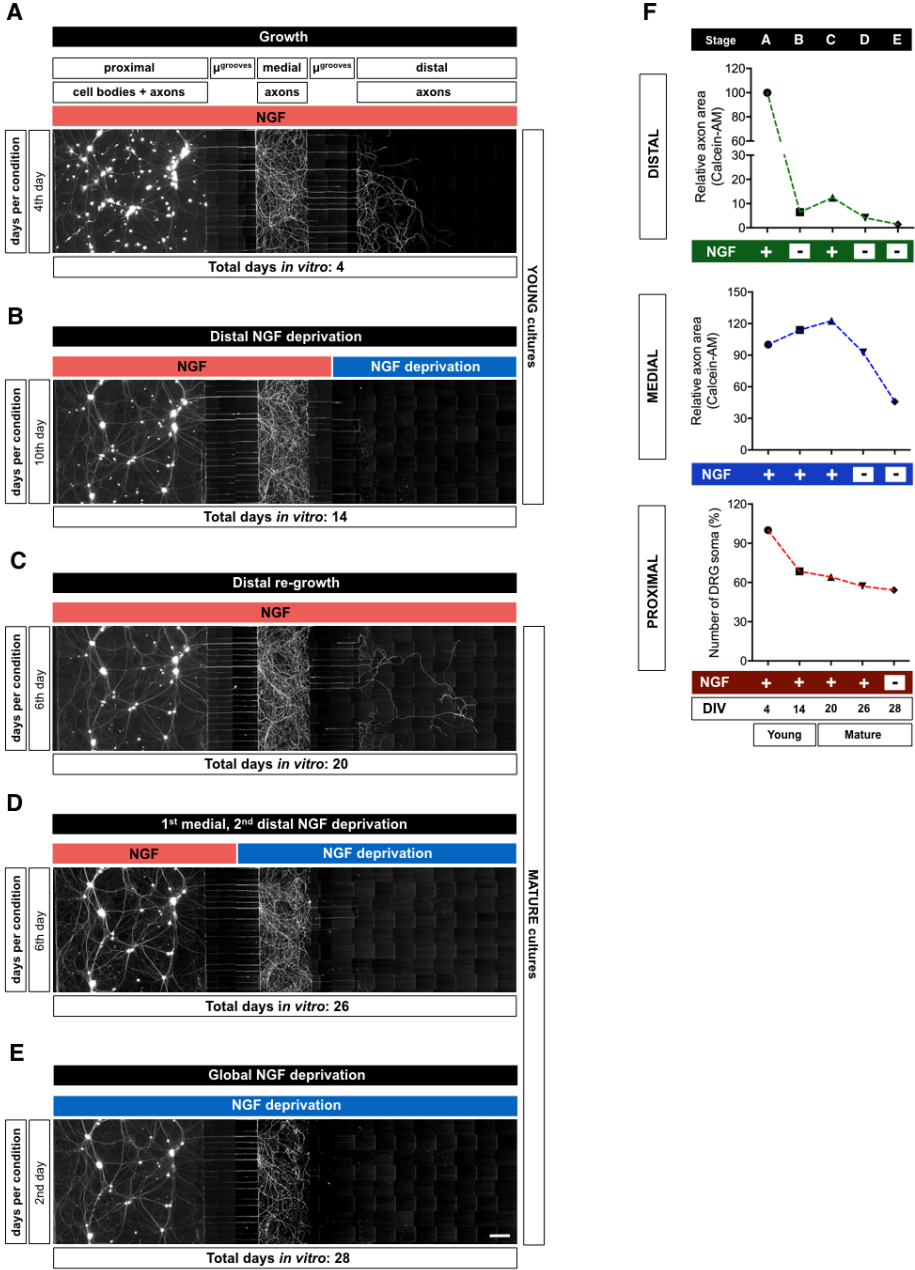


Figure 4.5. Young DRG neurons only experience a minor loss of cell bodies if no distal NGF deprivation is applied during their culture in microfluidic devices. A) Representative image of mouse E13.5 DRG neurons cultured in three-compartment microfluidic device and live-stained with Calcein-AM at 4, 10 and 20 days after seeding. **B)** Axonal pruning protocol in mature DRG neurons: representative image at 6 days (26 DIV) after initiated deprivation of NGF at the distal compartment (20 DIV). After 20 days *in vitro* (DIV) DRG neurons are considered mature [754]. Yellow dashed area related to panel D) (Scale bar = 200 μ m). **C)** Quantification of Calcein-AM stained axonal area in medial and distal compartments, and the number DRG cell bodies in the proximal compartment expressed as the percentage relative to the corresponding amount at the initial growth stage (A, '4th day' panel). **D)** DRG cell body manual counting using DIC and Calcein-AM staining at the proximal compartment over the experimental course. Blue dots: healthy DRG cell bodies; red dots: glial cells; yellow dots: DRG or glia entering the region of interest after 4 DIV. Plot represents the number of DRG, glial and total cells expressed as the percentage relative to their respective category at 4 DIV. **E)** Live imaging of DRG cell bodies at the proximal compartment co-stained with Calcein-AM (green) and the active mitochondrial dye TMRE (red). Arrowhead indicates a healthy DRG cell body (co-localization of Calcein-AM + TMRE). Arrow represents a glial or DRG cell in a quiescent state or heading to its death.

Figure 4.5

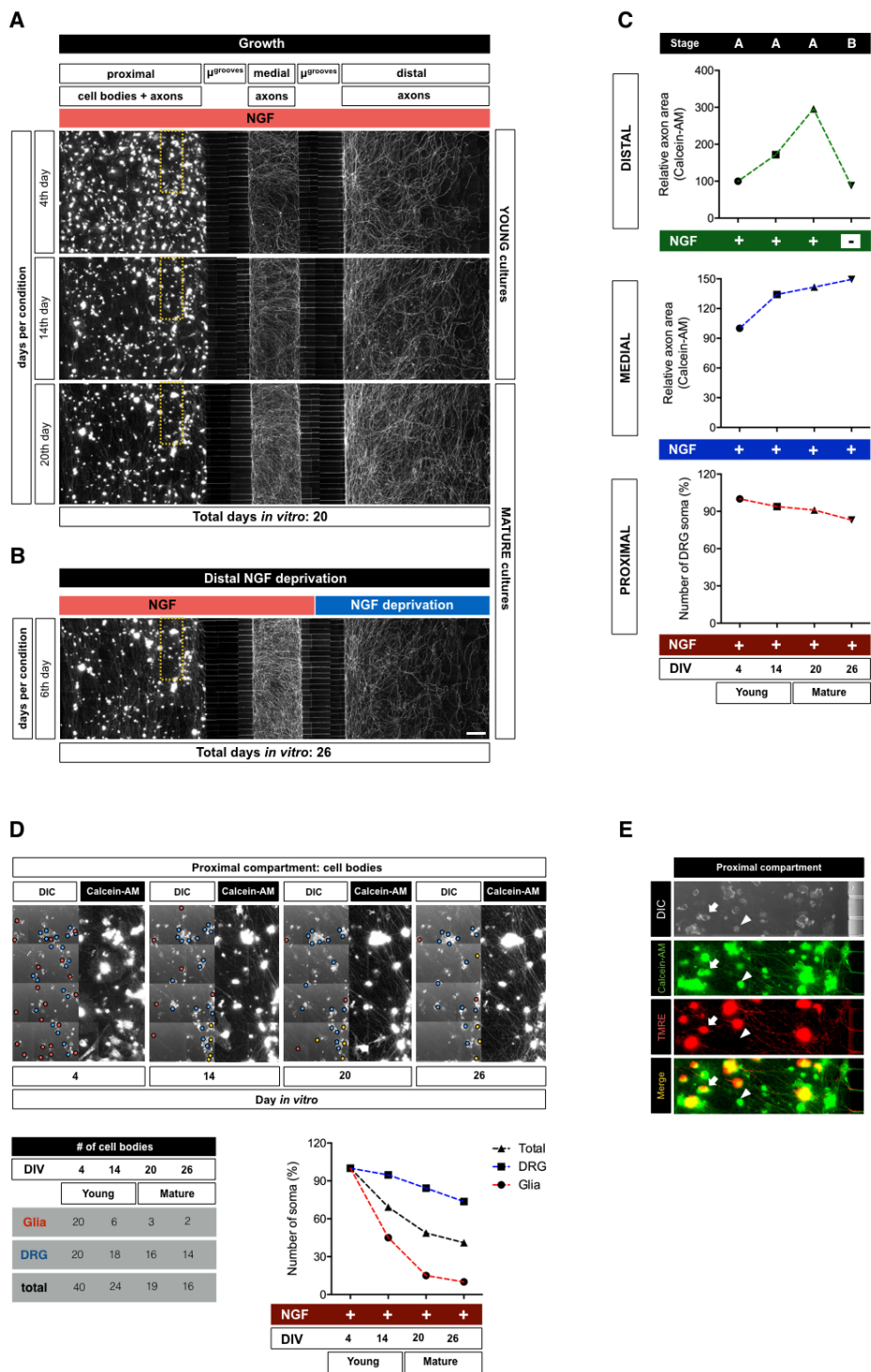
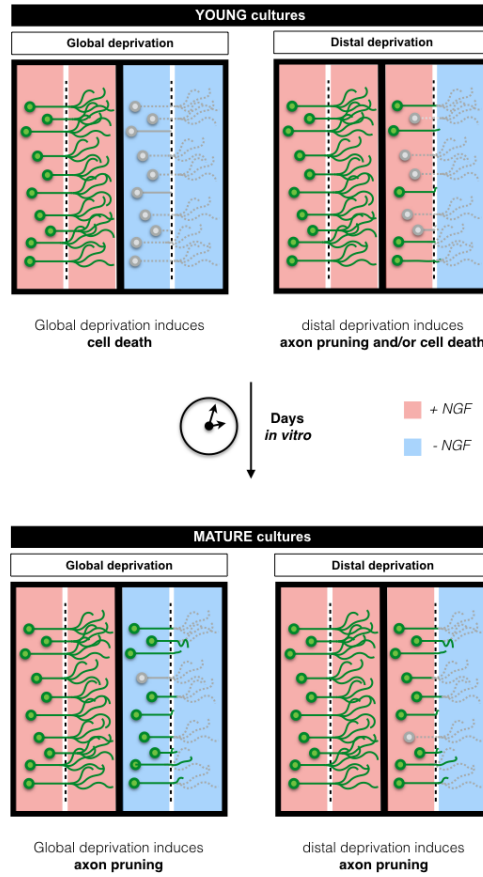


Figure 4.6. Graphic summary: the compartmentalization of NGF deprivation in axons of immature DRG neurons mimics a combination of developmental axonal pruning and cell death. Global NGF deprivation in young embryonic DRG neurons induces massive cell death (*top left panel*). Distal NGF deprivation in young DRG neurons induces a significant drop in the number of DRG cell bodies as well (*top right panel*). In contrast, embryonic DRG neurons aged *in vitro* acquire properties of mature neurons [702, 754]. They are resistant to global NGF deprivation (*bottom left panel*) and mature DRG neurons distally deprived of NGF degenerate their axons without dying, thus modelling axonal pruning process *in vitro* (*bottom right panel*).

Figure 4.6



Chapter 5

General Discussion

Neuronal remodeling involves a group of progressive and regressive cellular processes essential for the proper maturation and function of the nervous system. Embryonic development constitutes the largest wave of neuronal remodeling events occurring throughout life, implying a massive elimination of neurons and/or their connections through mechanisms of programmed cell death and axonal pruning. The sensory nervous system offers a suitable model to study neuronal remodeling across developmental stages. The survival of sensory neurons, based on their competence for limited amounts of target-derived trophic factors is easily reproducible *in vitro*, allowing the study of the molecular mechanisms underlying developmental neuronal remodeling. In the previous chapters, we presented original data regarding the developmental degeneration of DRG sensory neurons. This section describes and discusses the major contributions of these studies to our field.

5.1 Study I: The role of APP in developmental remodelling of DRG sensory neurons

The role of the amyloid-precursor protein (APP) in the developmental remodelling of sensory neurons has been contradictory and controversial [331-333]. The data presented in Study I provided four pieces of evidence that support the pro-degenerative role of APP during the developmental remodelling of DRG sensory neurons: **1) APP genetic deletion significantly rescues the loss of DRG axons upon NGF withdrawal.** Developmental axonal degeneration can be modeled *in vitro* by NGF withdrawal in DRG sensory neurons. This model has been used previously to address the role of APP in developmental neuronal remodeling with opposing results. The controversy about the role of APP during the degeneration of DRG neurons made imperative the use of reliable quantification methods to determine unambiguously the effect of NGF deprivation on DRGs knock-out for APP. Johnstone et al. (2018) developed a novel method for the objective quantification of developmental axon degeneration in DRG sensory neurons

deprived of NGF. Axoquant 2.0 - available for free download [360] - assesses the entire area of axonal growth to avoid variability that can be introduced by sampling only small regions within the axonal fields. Its utilization has improved the sensitivity and reliability of cytoskeletal degeneration assays using DRG systems. Taking advantage of such methodology, we showed that the lack of APP significantly reduced the loss of axonal area in DRG explants deprived of NGF. Although still significant, the difference between wild-types and APP-nulls gets smaller with increasing NGF deprivation time spans, suggesting that APP accelerates but does not drive the degenerative process. **2) APP genetic deletion reduces the increase in axoplasmic Ca²⁺ in DRG neurons deprived of NGF.** Johnstone et al. (2018, 2019) demonstrated that the degeneration of DRG neurons deprived of NGF requires Ca²⁺ influx. Consequently, an increase of axoplasmic Ca²⁺ is observed before axonal destruction [329, 360]. We took advantage of this degenerative hallmark to test the effect of APP deletion in DRG deprived of NGF. Our result show unambiguously that the lack of APP reduces the axoplasmic Ca²⁺ levels during NGF deprivation, thus becoming a second piece of evidence for a pro-degenerative role of APP in this model. It will be interesting to confirm these results by following in real time the progression of axoplasmic Ca²⁺ in wild-type versus APP-null DRGs upon NGF deprivation. Currently, crossings of APP-null mice with a line constitutively expressing the cytoplasmic Ca²⁺ reporter GCaMP3 are underway. This new breeding will allow to follow the dynamic of axoplasmic Ca²⁺ in the absence of APP in real time. **3) NGF withdrawal increases the levels of phosphorylated APP at threonine 668.** The phosphorylation of APP at threonine 668 in the intracellular domain has become a hallmark of APP pro-degenerative action in different cell types [335, 532, 536]. APP phosphorylation at T668 has been linked with the pro-death action of TrkA in the absence of NGF [334, 335]. The third piece of evidence provided in our work that argues in favour of the pro-degenerative role of APP, is the finding that NGF withdrawal increases APP phosphorylation at T668, and that TrkA inhibition by K252a simultaneously block DRG axonal degeneration and the rise of phospho-APP-T668 during NGF deprivation. In the future it will be interesting to address how much of APP pro-degenerative role is in fact related with T668 phosphorylation. A mice knock-in line expressing a constitutive non-phosphorylated version of APP at T668 (T668A) is available [526] and would fulfill this

purpose. **4) APP-null adult animals present a significant increase in the number of sciatic nerve axons.** This finding is an important and disconcerting piece of evidence supporting APP pro-degenerative role in developmental remodelling. A similar outcome was recently reported in sciatic nerves of APP-null adult mice, but contrary to our study, this was not statistically significant [466]. The disconcerting aspect of this result is that it is not joined by an increase in the number of DRG, motoneurons or skin innervation. However, a trend towards an increase in CGRP+ axon terminals was observed in the hind-paw skin of adult APP-null mice versus wild-types. Contrary to the analysis in the sciatic nerves, the quantification of the skin innervation was performed with an n of 3 animals per genotype, which may not be enough to draw reliable conclusions. Undoubtedly, a more in-depth characterization of APP-null mice hind-paw skin has to be done. Importantly, APP-null adult animals are characterized by subtle phenotypes when compared with wild-type animals. These phenotypes are substantially enhanced when one of APP homologous proteins, APLP2, is also genetically deleted. In fact, perinatal lethality was observed in APP::APLP2 and in APLP1::APLP2 compound null mice whereas APP::APLP1 compound null mice only display a modest decrease in body weight [469, 470]. These data suggest that APLP2 may be indispensable for life and that it can compensate the loss of APP or APLP1 [448]. It would be certainly interesting to focus on the role of APLP2, not only *in vivo* but in relation to the points previously discussed.

The first study of this thesis has helped untangle the role of APP during developmental remodelling of sensory neurons. APP action in this context has been mechanistically linked with the death receptor DR6. Previous reports have shown that DR6-mediated neuronal cell death in the absence of trophic support requires association with full-length APP [332]. Our results agree with the idea that DR6 may play a role in the degeneration of DRG neurons under trophic deprivation conditions. However, we observed that DR6 deficiency is less effective than APP in delaying the degenerative process of DRG neurons deprived of trophic support, suggesting that APP and DR6 actions on the degenerative process may not be as tightly linked as previously indicated [331]. Rather, this thesis suggests that the pro-degenerative role of APP may be related with the regulation of intracellular Ca^{2+} . The fact that APP deficiency significantly blunts the normal

rise in axoplasmic Ca^{2+} that occurs upon NGF withdrawal prompted us to investigate into the relationship between APP and Ca^{2+} in DRG neurons. Although, several studies have discussed a relationship between APP, ER Ca^{2+} storage, and SOCE in other cell types, their outcomes have been contradictory [552, 555-558]. Our novel results show a clear decrease in the ER Ca^{2+} content and Ca^{2+} influx through SOCE in APP-null DRGs. How APP regulates intracellular Ca^{2+} homeostasis in DRG neurons is uncertain. However, we suggest that it might be due to the intricate cross-talk between TrkA and APP through its phosphorylation at T668. The PLC γ >PKC signaling axis, downstream TrkA, modulates the levels of intracellular Ca^{2+} , including the regulation of ER- Ca^{2+} stores [325-328, 330]. In this thesis we provided evidence showing that the inhibition of PLC γ >PKC signaling cascade not only eases the increase in axoplasmic Ca^{2+} in deprived DRG neurons but attenuates the early rise of APP phosphorylation at T668. A similar effect on APP phosphorylation was observed when TrkA receptor was inhibited. These results suggest that the TrkA>PLC γ >PKC signaling axis could modulate the levels of intracellular Ca^{2+} via the phosphorylation state of APP. How APP alters the homeostasis of intracellular Ca^{2+} once phosphorylated? Different mechanisms could be working in concert: **1) intracellular leakage from the ER:** although it is still controversial, APP phosphorylation at T668 may favour the proteolytic processing by the amyloidogenic pathways and the generation of A β [536, 755-758]. This APP-proteolytic by-product was shown to either foster the release of Ca^{2+} through RyR and IP $_3$ R receptors at the ER [759, 760] or form Ca^{2+} permeable channels at neuronal membranes [761-764]. **2) potentiation of Ca^{2+} channels:** A β enhances Ca^{2+} influx and voltage-dependent channel activity [765]. Alternatively, phosphorylation of APP at T668 increases the association of APP with Na $_v$ 1.6, and the membrane localization of the channel generating greater depolarizing Na $^+$ currents [766] which could lead to the activation of L-type Ca^{2+} channels (LTCC). APP also interacts with LTCC, and loss of APP provokes an inappropriate accumulation and aberrant activity of Ca $_v$ 1.2 [767]. It is unknown whether phosphorylation at T668 modulates such interaction, but it has been shown that inhibition of APP phosphorylation at T668 decreases APP axonal transport and its localization at the plasma membrane, while restores spontaneous Ca^{2+} oscillations in cortical neurons expressing human APP [768]. **3) induction of Ca^{2+} channel expression:** ER Ca^{2+} store

content is significantly reduced by genetic deletion of APP, while the expression of Orai1 and TRPC1 proteins, essential components of SOCE, are downregulated in APP-null astrocytes [552]. The capacity of APP to modulate protein expression is essentially determined by its intracellular domain AICD. AICD is a transcription factor able to modulate transcription of numerous genes [417, 418, 769]. Such function is often supported by AICD ability to interact with cofactors/nuclear modulators [418, 769]. Phosphorylation at T668 may be necessary to trigger the nuclear translocation of AICD [532, 758]. Interestingly, recent studies have shown that AICD affects Ca^{2+} homeostasis in hippocampal neurons through alteration of the plasma membrane Ca^{2+} permeability by the transcriptional-dependent up-regulation of NMDARs and LTCC [770, 771].

4) modulation of mitochondrial dynamics: the mitochondria act as decision nodes in multiple physiological and pathological processes, including the modulation of intracellular Ca^{2+} homeostasis [724, 772-776]. If APP is able to modulate mitochondrial physiology, then these alterations may influence intracellular Ca^{2+} homeostasis. In this thesis we have found that APP genetic deletion in DRG neurons increases the levels of TOM20 (a marker of mitochondrial mass), yet the mitochondria potential (TMRE intensity) and the axonal density of TMRE-stained active mitochondria is reduced. These results suggest that APP modulates mitochondrial physiology. It is possible that APP exerts this modulation via AICD transcriptional activity. Goiran et al. (2017) showed that AICD, generated by the cleavage of APP by the γ -secretase, binds the transcription factor FoxO3a, translocates to the nucleus and induces the expression of the phosphatase and tensin homolog (PTEN)-induced kinase 1 (Pink-1) [777]. Pink-1 controls both mitochondrial dynamics and mitophagy by selectively enhancing mitochondrial fission [778] and by recruiting Parkin to mitochondria [779]. In line with our results, these authors found that when AICD is not expressed or when γ -secretase is inhibited in the presence of Pink-1, TOM20 levels increase and TMRM fluorescence (mitochondrial membrane potential live dye) decreases, respectively [777]. Unfortunately, these authors do not report whether APP phosphorylation at T668 is necessary for its transcriptional function through AICD, as was shown in the context of neurodegeneration [532]. However, it would be certainly interesting to explore whether T668 phosphorylation dictates APP capacity to modulate the intracellular Ca^{2+} homeostasis either through the permeabilization of

cellular membranes, its direct interaction with ion channels or through AICD-dependent transactional activity.

In addition to investigating which mechanisms APP used to alter the homeostasis of intracellular Ca^{2+} , it would be necessary to address to what extent the alteration of early Ca^{2+} homeostasis contributes to the degeneration of DRG neurons deprived of NGF. It is well-known that dysregulation of intracellular Ca^{2+} homeostasis induces ER stress [241, 539] and that several ER stress markers are up-regulated in DRG neurons upon NGF withdrawal [322]. Interestingly, several studies have demonstrated a relationship between APP and ER stress-induced cell death in a variety of cell types. For example, APP overexpression in PC12 cells induces the ER-stress marker CHOP and potentiates the increase in cytoplasmic Ca^{2+} during apoptosis induced by the depletion of ER Ca^{2+} content with thapsigargin [541]. Notably, cell death and the up-regulation of the transcription factor CHOP following ER stress are attenuated by APP knockdown, while AICD associates with the promoter region of the *CHOP* gene facilitating its expression [542]. Currently, no reports have been published relating APP and ER stress in DRG neurons deprived of NGF. Determining the functional relationship between APP, intracellular Ca^{2+} homeostasis, and reticulum stress in the degeneration of NGF-deprived DRG neurons, constitutes an interesting future research prospect.

In summary, Chapter 2 of this thesis has provided the field with evidence that support - unambiguously - the pro-degenerative role of APP in the developmental remodelling of DRG neurons. Moreover, our work has contributed to the first steps into the regulation of intracellular Ca^{2+} by APP in DRG neurons; a potential new mechanism of action for APP in developmental neuronal remodelling that expands its already known role as a DR6 ligand. Understanding to what extent the dysregulation of Ca^{2+} homeostasis is important for the degeneration of DRG neurons upon NGF deprivation will be not only interesting for the field of developmental remodelling, but for what it could imply for fields addressing the mechanisms of pathological neurodegeneration. In addition to the role of APP, failed Ca^{2+} homeostasis is a well-recognized pathological feature of AD [780-784]. On top of that, the progressive cognitive decline in AD pathology has been associated with the selective degeneration of basal forebrain cholinergic neurons (BFCN), to which the dysregulation of the NGF metabolism - generating a *de facto* trophic deprivation -

strongly contributes [785]. The study of developmental neuronal remodelling in DRG neurons dependent on NGF offers a unique opportunity to better understand the interaction of these factors in a simple model.

5.2 Study II: NGF- and BDNF-dependent DRG sensory neurons deploy distinct degenerative signaling mechanisms

For decades, the mechanisms of developmental cell death in sensory neurons have been preferentially explored in DRG neurons dependent on NGF. Study II of this thesis provides the first in-depth characterization of the mechanisms that mediate degeneration of BDNF-dependent DRG sensory neurons upon trophic factor withdrawal. Using cultured DRG neurons deprived of NGF as model for the signaling pathways involved in developmental neuronal remodeling, our study screened the incidence of these mechanisms in BDNF-dependent DRG neurons. Figure 5.1 summarize the results of this investigation (see end of current section).

Divergence in the degenerative pathways of NGF- and BDNF-dependent DRG populations was expected based on the mechanisms of action of their respective neurotrophin receptors TrkA and TrkB. Nikolettou et al. (2010) showed that while TrkA acts as a dependence receptor, supporting neuronal survival in the presence of NGF and triggering cell death in its absence, TrkB lacks the capacity to induce cell death in the absence of BDNF [12]. In line with that, our results showed that the Trk receptor inhibitor K252a rescued axonal degeneration in DRG neurons deprived of NGF but not during BDNF deprivation. Consequently, the signaling cascade downstream TrkA, involving the axis PLC γ >PKC, which is also part of TrkB signalling cascade [786], was not expected to be involved in the degeneration of BDNF-dependent DRG neurons, and our results confirm that.

Other differences emerged when we addressed the role of Ca²⁺ and caspases, both considered critical for the terminal phase of a degenerative cascade. Despite expressing almost identical levels of pro-caspase-3 and showing a similar increase of axoplasmic Ca²⁺ during trophic factor deprivation, the degeneration induced in BDNF-dependent DRG neurons is not rescued either by pan-caspase inhibitors nor by the

chelation of Ca^{2+} with EGTA. However, the contribution of Ca^{2+} to the degeneration of BDNF-dependent neurons cannot be completely excluded without exploring the role of calpains. These executioner proteases depend on Ca^{2+} and their activation play also a role in the degeneration of NGF-dependent DRG neurons [354].

Despite the independence from caspases, BDNF-dependent DRGs do depend on the pro-apoptotic protein BAX for degeneration, similarly to NGF-deprived neurons. How to reconcile the need of BAX without the activation of caspases is a question that we did not address. However, the activation of BAX in the mitochondria could have caspase-independent outcomes that contribute to cell death. For example, the release of the IMM-protein AIF and the induction of parthanatos (a type of necrotic cell death) instead of apoptosis have been shown to depend on BAX and Ca^{2+} [787, 788]. The possibility that BDNF-dependent DRG neurons could be degenerating through alternative pathways to the classic death by apoptosis, promoted the testing of inhibitors that tackle other cell death mechanisms like autophagy (3MA), necroptosis (NEC-1), or Wallerian-like degeneration (NAD⁺). Surprisingly, neither of these inhibitors nor a broad translation inhibitor (CHX) stopped the degeneration of BDNF deprived DRG neurons, contrary to what we observed in NGF-dependent DRGs (excepting for NEC-1). How divergent - or specific - the degenerative mechanisms of BDNF-dependent DRG neurons must be to only be rescued by BAX genetic deficiency and ROS scavenging? Although degeneration triggered by NGF deprivation is catalogued as intrinsic apoptosis, the cell death of NGF-dependent DRG neurons is sensitive to inhibitors that tackle alternative cell-death pathways, suggesting that a mix of cell death mechanisms is acting in concert even in that model.

It will be important to explore more in detail the actual course of degeneration triggered by BDNF deprivation in DRG neurons. The fact that only 2 of 12 pharmacological or genetic interventions rescued DRG neurons deprived of BDNF (Figure 5.1), may be the result of limitations in our study. The most obvious is a slower degenerative progression time in BDNF-dependent DRG neurons. BDNF stimulates a lower axonal growth in DRG compared with NGF, its withdrawal could have a similar level of incidence, especially considering that TrkB does not induce cell death as TrkA does in the absence of its ligand [12]. Thus, it is certainly possible to be facing a slower

degenerative progression in DRG neurons dependent of BDNF, for which it will be necessary to delay the measurements of axonal degeneration to later time points.

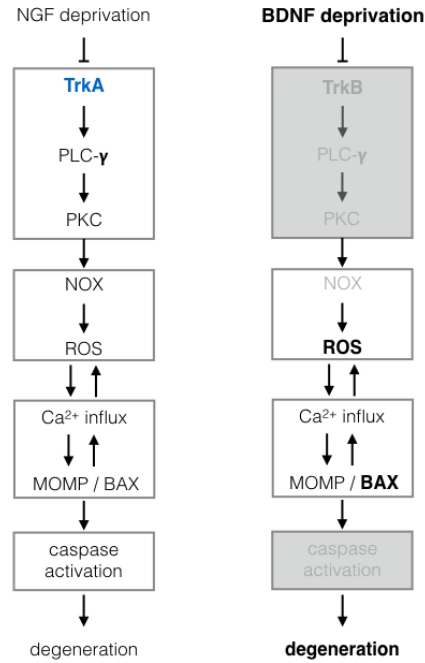
We have demonstrated that BDNF deprivation reduces the axonal area, causes blebbing and axonal fragmentation, but also decreases the amount Calcein-AM stained axons and increases Annexin-V levels and axoplasmic Ca^{2+} . However, we have not determined whether BDNF deprivation in DRG neurons causes cell death *in vivo*. In fact, the actual dependency of embryonic DRG neurons for survival based on BDNF is still quite controversial. While some studies have reported losses of DRG neurons in E13 BDNF-null mice embryos [588], more recent ones have shown that BDNF-deficiency does not alter the total number of DRG neurons at E12, E15 or P0 [599]. Coincidentally, no decrease in the number of DRG neurons is observed in TrkB-null mice [598], while the overexpression of BDNF at the skin increases the innervation to hair follicles, Meissner corpuscles and Merkel cells without altering the final number of DRG neurons [149]. Interestingly however, sensory neurons from petrose-nodosa, vestibular and geniculate ganglia, are almost completely lost in TrkB-null deficient animals [598], indicating that their survival highly depends on BDNF and NT4. It would be interesting to investigate whether other populations of sensory neurons respond in the same way to the pharmacological and genetic intervention applied in our study of BDNF-dependent DRG neurons.

The remodelling of the sensory innervation of the mammary gland (MMG) is a perfect example of axonal degeneration without cell death triggered by BDNF deprivation in DRG neurons. Liu et al. (2012) reported that BDNF produced in the MMG mesenchyme promotes the initial ingrowth and maintenance of TrkB positive sensory fibres. Male MMG innervation from early to late E13 is pruned due to the androgen-mediated expression of truncated TrkB (TrkB.T1) in the surrounding mesenchyme. Increase TrkB.T1 levels in males, neutralizes the BDNF-TrkB mediated trophic function in the sensory fibers, leading to their withdrawal from the MMG. This process is BAX independent, suggesting that axonal withdrawal from the MMG does not cause cell death [610]. Instead, the axonal degeneration we observed during global deprivation of BDNF-dependent explants is BAX dependent. A study of global versus distal BDNF deprivation in compartmentalized cultures would help resolve these differences.

Recently, Shalom et al. (2019) demonstrated that the genetic ablation of Plexin A4 delayed axonal degeneration in the MMG of male mouse embryos, while exogenous Sema3A application to BDNF-dependent DRG neurons *in vitro* induced growth cone collapse in a Plexin A4-dependent manner [159]. The absence of exogenous Semaphorin in our cultures reduces the possibility of an active role for Plexins in our model. However, it has been reported that Plexins could interact with Trk receptors [157], and more importantly, Plexins could function in a ligand-independent manner in the regulation of cell disassembly during apoptosis [611]. Perhaps the lack of BDNF primes the axons for degeneration and the action of Semaphorins and/or Plexins triggers the final signal that speeds up axonal remodeling in BDNF-dependent DRG neurons. These studies open a very interesting research avenue on the role of Plexins in the remodeling of BDNF-dependent sensory neurons.

In summary, the findings presented in the Chapter 3 of this thesis enrich our view of the diversity of the mechanisms employed by peripheral neurons to execute developmental neuronal remodelling. Undoubtedly, more research is needed to detail the exact cascade of events that lead to the degeneration of BDNF-dependent DRG neurons during development. The interest in knowing the effects and mechanisms triggered by the lack of BDNF in this population is not trivial. BDNF is a vital neurotrophin for the survival, growth and maintenance of neurons in key brain circuits involved in emotional and cognitive function [789]. Patients with psychiatric and neurodegenerative disorders often have reduced BDNF concentrations in their blood and brain [790] and the administration of BDNF have shown promising results in the fight against the cognitive decline that occurs during aging and AD [790-793]. Future therapeutic approaches could be revealed by understanding the sequence of molecular events culminating in the degeneration of BDNF-dependent neurons during development.

Figure 5.1. Summary of Study II (Chapter 3) major experimental outcomes



	E13.5 DRG cultures		Does it rescue degeneration?	
	Pathway	Inhibitor	NGF-deprivation	BDNF-deprivation
Figure 3.4	Trk receptors	K252a	✓	✗
Figure 3.4	p75NTR	genetic deletion	✗	✗
Figure 3.5	PKC	G66976	✓	✗
Figure 3.10	ROS	NAC	✓	✓
Figure 3.5	Ca ²⁺	EGTA	✓	✗*
Figure 3.7	BAX	genetic deletion	✓	✓
Figure 3.6	Protein translation	CHX	✓	✗
Figure 3.6	Autophagy	3MA	✓	✗
Figure 3.6	Necroptosis	NEC-1	✗	✗
Figure 3.6	Wallerian-like degeneration	NAD ⁺	✓	✗
Figure 3.8, 3.9	Caspases	zVAD-fmk / Boc-D-fmk	✓	✗

* Deprivation of NGF or BDNF significantly increases axoplasmic Ca²⁺ in DRG neurons but Ca²⁺ chelation with EGTA only rescues the axonal degeneration in DRGs deprived of NGF (Figures 3.3 and 3.5).

5.3 Study III: Modelling developmental axonal pruning *in vitro* using compartmentalized microfluidic devices

The culture of NGF-dependent embryonic DRG or postnatal SCG neurons in compartmentalized devices have been extensively used to model the process of developmental axonal pruning *in vitro*. The fundamental premise behind this technique is that the localized NGF deprivation in axons is sufficient to cause the degeneration of the axonal segment without causing cell death. In the Study III of this thesis we have presented preliminary data challenging this dogma. Our results show that the distal deprivation of embryonic DRG axons cause a significant decrease in the number of healthy neuronal cell bodies in the proximal compartment, suggesting that some neurons - instead of undergoing axonal pruning - fall into a cell death process. This effect is strongly attenuated in aged embryonic DRG cultures, which is coincident with the capacity of aged or mature neurons to restrict their cell death machinery [702].

These results are interesting, but they are preliminary and require some caution. Their validity was based on our capacity to track the health condition of axons and cell bodies over time using an imaging protocol that did not harm neurons *per se*. Through trial and error, we successfully optimized scanning conditions for that purpose, although further replication of these results is necessary. The optimization for tracking the healthy DRG cell bodies during the progression of the culture *in vitro* should also be pursued. We have suggested additional methods with that aim (see section 4.4 and Figure 4.5). In addition, it would be interesting to use labelling techniques to distinguish neurons that cross axons to the axonal compartment from those who do not, thus allowing us to calculate the cell body loss over the actual number of neurons that suffer distal deprivation. Alternatively, new designs of microfluidic devices could be pursued looking for the alignment of one cell body per microchannel. Experimenting and optimizing imaging techniques and designs will be definitely necessary for the future study of axonal pruning in microfluidic devices, as well as for those exploring local molecular events and the cellular communication between neuronal compartments.

The compartmentalization of the death stimulus is the main purpose behind the use of microfluidic devices to mimic axonal pruning *in vitro*. Axonal pruning constitutes

the localized response to a local stimulus and depends on the functional sub-compartmentalization of the apoptotic machinery to execute degeneration without affecting the neuronal survival. However, axonal pruning is not a compartment-autonomous process. Although the apoptotic machinery is present and functional in axons, it is not activated directly by distal trophic deprivation. Instead, for the axon to degenerate, the segment under trophic deprivation needs to maintain communication with the cell body to activate a transcriptional pro-apoptotic program in the soma, that then sends an anterograde pro-degenerative signal back to the axon [316, 322, 339, 663].

A localized response to a local extracellular stimulus requires the action of a compartmentalization mechanism, but the compartmentalization of the death stimulus does not imply - necessarily - that the neuron has born with the capacity to compartmentalize the response. Beyond the morphological polarization of neurons into very specific cellular compartments (cell body, axons, dendrites, synapse buttons or spines), it is becoming clear that neurons employ a diverse battery of functional sub-compartmentalization mechanisms, including the confinement of organelles, signal transduction molecules, Ca^{2+} transients and protein translation, to respond locally to local extracellular stimulus [794]. This means that to be able to model axonal pruning *in vitro* a conjunction of extrinsic and intrinsic factors is required: On one side, the compartmentalization of the extracellular death stimulus (extrinsic factor: NGF deprivation), on the other, the ability of neurons to execute the response locally (intrinsic factor: functional compartmentalization mechanisms).

Our results suggest that developing DRG neurons may not have those intrinsic factors fully developed but mature neurons do, in agreement with previous studies on SCG neurons [224]. Mature neurons differentiate from developing ones in their capacity to restrict cell death [702]. If the ability to restrict cell death increases with cell maturity in neurons, then the maturation of the compartmentalization processes underlying axonal pruning should be considered. However, this does not mean that developing neurons do not prune axons. Axonal pruning in developing DRG neurons takes place at the mammary gland of E13 male mice embryos [610]. Axonal pruning at the MMG is not driven by the lack of NGF but by the lack of BDNF, whose receptor TrkB, contrary to NGF receptor TrkA, is not able to induce cell death in the absence of its ligand [12]. In other words, the

nature of axonal pruning and the ultimate fate of a neuron also depends on the type of extrinsic death signal triggered during the pruning process.

Are there examples of NGF-dependent neurons undergoing developmental axonal pruning? The axonal competition among eye-projecting SCG neurons constitutes a prototypical example. Eye sympathetic innervation depends on NGF [735, 795]. These neurons initially extend axonal collaterals to both anterior and posterior eye compartments, but after a period of axonal competition only one of the two projections will survive. NGF and activity selectively confers a competitive growth advantage to stimulated axons by elevating local TrkA signaling pathways, promoting growth and branching. Concurrently, unstimulated competing axons deriving from the same and neighboring neurons acquire a growth disadvantage. This growth disadvantage is due to BDNF secreted from the unstimulated competing axons. BDNF binds and activates axonal p75NTR causing their degeneration. p75NTR, which is enriched in less stimulated axons, mediates this process by suppressing local NGF-TrkA signaling [189]. Interestingly, this axonal pruning event seems to take place during a protracted period of postnatal development after naturally occurring neuronal death has taken place [796]. In addition, p75NTR plays opposing role in SCG and DRG neuronal populations. While p75NTR genetic deletion rescues the loss of innervation in the eye and protects SCG neurons from NGF deprivation *in vitro*, its deficiency drastically decreases the number of DRG neurons *in vivo* and does not protect DRG neurons from NGF withdrawal *in vitro* [12, 194] (Figure 3.4). Thus, although both DRG and SCG neurons depend on NGF for survival, their intrinsic response to axonal pruning initiated by NGF deprivation is executed by different mechanisms.

Currently, there is no direct evidence of a specific *in vivo* pruning event in NGF-dependent DRG neurons during development. However, there is data suggesting that developmental axonal pruning on this particular subset of neurons could take place at the skin. The genetic deletion of the microtubule-destabilizing protein kinesin superfamily protein 2A (Kif2A), who manages the breakdown of microtubules during axonal degeneration, increases the sensory skin innervation in E15.5 mice embryos without affecting the total number of DRG neurons [797]. Similar findings *in vivo* were reported for the pro-apoptotic member of the Bcl-2 family PUMA [339]; distal NGF deprivation of

PUMA-null E13 DRG neurons does not induce axonal degeneration [316, 339]. In addition, the genetic deficiency of the endogenous caspase inhibitor XIAP decreases the skin innervation of E15.5 mice embryos without affecting the number of DRG neurons [225]. NGF-TrkA signaling is fundamental for cutaneous innervation [167] and although these studies do not delve into whether the changes observed in the skin persist in adult stages, their findings suggest that developmental axonal pruning of NGF-dependent DRG neurons may take place at the skin.

Assuming that, 1) DRG neurons are capable of axonal pruning triggered by the competition for limited amounts of NGF during development, 2) the compartmentalization of NGF deprivation in axons of embryonic DRG neurons causes a combinatory model of cell death and axonal pruning, and 3) neurons becomes more competent in their capacity to restrict the apoptotic machinery with age: what are the mechanisms explaining whether a DRG neuron dependent of NGF undergoes punning or cell death? The balance between the capacity to restrict cell death and the amount of retrograde death signal coming from distal axons may be an important factor [663]. The length of the axonal segment, or the number of axonal branches facing deprivation *in vitro*, or the balance between TrkA expression and NGF supply by target tissues, may be decisive in determining whether an NGF-dependent DRG neuron undergoes apoptosis or pruning during development. This may not be decisive in mature neurons, given their capacity to resist cell death, but it may be an important factor in the fate of this particular subset of developing neurons.

In summary, axonal pruning is the result of an intricate balance between extrinsic and intrinsic factors and of the complex coordination of molecular events among neuronal compartments. Axonal pruning is a complex process that is not only defined by the compartmentalization of the death stimulus, but by the nature and amount of this stimuli, the neuronal subtype and fundamentally, the capacity of the neuron to respond with a refined functional compartmentalization molecular mechanism. Our study using compartmentalized cultures of embryonic DRG neurons dependent on NGF demonstrates that researchers must carefully consider the age of these cultures before driving conclusion on underlying molecular mechanisms of axonal pruning. The Study III of this thesis also demonstrates the need to better understand the real scope that *in vitro*

models have in their ability to emulate axonal pruning. Hopefully, a deeper understating of these models would expand our knowledge on the actual axonal pruning itself.

5.4 Concluding remarks

Beyond the developmental stage, neuronal cells become a limited cellular resource. Their post-mitotic condition makes them almost irreplaceable. The factors that influence and trigger neuronal death are diverse, but a general consensus exist that the mechanisms that execute cell death are limited and conserved throughout life. The developmental stage is a period where neuronal cell death takes place naturally. More than six decades of studies proved that the death of peripheral neurons is a predictable and accessible system to characterize the conditions that triggers developmental neuronal cell death. In this thesis we have taken advantage of that property to explore the developmental neuronal degeneration of DRG sensory neurons at three different levels: 1) the role of the amyloid-precursor protein in the degeneration of NGF-dependent embryonic DRG sensory neurons, 2) the mechanisms of developmental cell death in BDNF-dependent DRG sensory neurons, and 3) the modelling of developmental axonal pruning *in vitro* using compartmentalized microfluidic cultures of NGF-dependent DRG neurons. Along the way, we were able to clarify controversial aspects, suggest new mechanism of actions, reveal unexplored cell death pathways and warn about the limitation of current *in vitro* models. The study of developmental neuronal degeneration is far from complete. The sequence of molecular event that govern, for example, the degeneration of NGF-dependent DRG neurons is incomplete and still not clear. Filling the missing pieces of this puzzle will be beneficial to understanding more complex pathological processes of the nervous system.

5.5 Major original contributions

This thesis contributes to the field of developmental neuronal remodelling on the following points:

- 1- We demonstrated a physiological role for the amyloid-precursor protein (APP) in Dorsal Root Ganglion neurons: APP promotes the degeneration of embryonic DRG sensory neurons during NGF deprivation. This helps to solve initial controversies about the role of APP in the developmental remodelling of DRG sensory neurons [331-333].
- 2- APP genetic deficiency decreases the content of Ca^{2+} in the ER, reduces the influx of Ca^{2+} via SOCE in NGF-dependent DRG neurons, and prevents the increase of axoplasmic Ca^{2+} during degeneration induced by NGF deprivation. The results presented in this thesis suggest that the APP pro-degenerative role in embryonic NGF-dependent DRG neurons might be related to its capacity to modulate the intracellular Ca^{2+} homeostasis.
- 3- For the first time, we characterize in detail the degeneration of Brain Derived Neurotrophic Factor (BDNF)-dependent DRG sensory neurons after BDNF withdrawal. We compared the signaling pathways implicated in NGF-deprivation and BDNF-deprivation. We discovered that beyond the shared role of BAX and ROS, NGF- and BDNF-dependent embryonic DRG sensory neurons deploy distinct degenerative signaling mechanisms in the absence of trophic support (summarized in Figure 5.1, page 204). These results emphasized the need to better characterized distinct ways neurons utilized to degenerate during the development of the nervous system.
- 4- We demonstrated that the use of microfluidic devices to compartmentalize the lack of trophic support (NGF deprivation) in axons, is not sufficient to mimic developmental axonal pruning in embryonic NGF-dependent DRG sensory neurons. Instead, we clearly observed that the use of this culture technique in this particular type of neurons induces a mix of cell death and axonal pruning.

References

1. Hempstead, B.L., *Dissecting the diverse actions of pro- and mature neurotrophins*. *Curr Alzheimer Res*, 2006. **3**(1): p. 19-24.
2. Gibon, J. and P.A. Barker, *Neurotrophins and Proneurotrophins: Focus on Synaptic Activity and Plasticity in the Brain*. *Neuroscientist*, 2017. **23**(6): p. 587-604.
3. Lee, R., et al., *Regulation of cell survival by secreted proneurotrophins*. *Science*, 2001. **294**(5548): p. 1945-8.
4. Squinto, S.P., et al., *trkB encodes a functional receptor for brain-derived neurotrophic factor and neurotrophin-3 but not nerve growth factor*. *Cell*, 1991. **65**(5): p. 885-93.
5. Harrington, A.W., et al., *Recruitment of actin modifiers to TrkA endosomes governs retrograde NGF signaling and survival*. *Cell*, 2011. **146**(3): p. 421-34.
6. Hempstead, B.L., et al., *High-affinity NGF binding requires coexpression of the trk proto-oncogene and the low-affinity NGF receptor*. *Nature*, 1991. **350**(6320): p. 678-83.
7. Barker, P.A. and E.M. Shooter, *Disruption of NGF binding to the low affinity neurotrophin receptor p75LNTFR reduces NGF binding to TrkA on PC12 cells*. *Neuron*, 1994. **13**(1): p. 203-15.
8. Jing, S., P. Tapley, and M. Barbacid, *Nerve growth factor mediates signal transduction through trk homodimer receptors*. *Neuron*, 1992. **9**(6): p. 1067-79.
9. Fenner, B.M., *Truncated TrkB: beyond a dominant negative receptor*. *Cytokine Growth Factor Rev*, 2012. **23**(1-2): p. 15-24.
10. Reichardt, L.F., *Neurotrophin-regulated signalling pathways*. *Philos Trans R Soc Lond B Biol Sci*, 2006. **361**(1473): p. 1545-64.
11. Arévalo, J.C., et al., *Cell survival through Trk neurotrophin receptors is differentially regulated by ubiquitination*. *Neuron*, 2006. **50**(4): p. 549-59.
12. Nikolettou, V., et al., *Neurotrophin receptors TrkA and TrkC cause neuronal death whereas TrkB does not*. *Nature*, 2010. **467**(7311): p. 59-63.
13. Nimnual, A.S., B.A. Yatsula, and D. Bar-Sagi, *Coupling of Ras and Rac guanosine triphosphatases through the Ras exchanger Sos*. *Science*, 1998. **279**(5350): p. 560-3.
14. Borasio, G.D., et al., *Involvement of ras p21 in neurotrophin-induced response of sensory, but not sympathetic neurons*. *J Cell Biol*, 1993. **121**(3): p. 665-72.
15. Klesse, L.J. and L.F. Parada, *p21 ras and phosphatidylinositol-3 kinase are required for survival of wild-type and NF1 mutant sensory neurons*. *J Neurosci*, 1998. **18**(24): p. 10420-8.
16. Mazzone, I.E., et al., *Ras regulates sympathetic neuron survival by suppressing the p53-mediated cell death pathway*. *J Neurosci*, 1999. **19**(22): p. 9716-27.
17. Carter, B.D., U. Zirrgiebel, and Y.A. Barde, *Differential regulation of p21ras activation in neurons by nerve growth factor and brain-derived neurotrophic factor*. *J Biol Chem*, 1995. **270**(37): p. 21751-7.
18. Sommerfeld, M.T., et al., *Down-regulation of the neurotrophin receptor TrkB following ligand binding. Evidence for an involvement of the proteasome and differential regulation of TrkA and TrkB*. *J Biol Chem*, 2000. **275**(12): p. 8982-90.

19. Haapasalo, A., et al., *Regulation of TRKB surface expression by brain-derived neurotrophic factor and truncated TRKB isoforms*. J Biol Chem, 2002. **277**(45): p. 43160-7.
20. Yu, T., et al., *In vivo regulation of NGF-mediated functions by Nedd4-2 ubiquitination of TrkA*. J Neurosci, 2014. **34**(17): p. 6098-106.
21. English, J.M., et al., *Contribution of the ERK5/MEK5 pathway to Ras/Raf signaling and growth control*. J Biol Chem, 1999. **274**(44): p. 31588-92.
22. Bartsch, D., et al., *CREB1 encodes a nuclear activator, a repressor, and a cytoplasmic modulator that form a regulatory unit critical for long-term facilitation*. Cell, 1998. **95**(2): p. 211-23.
23. Gao, Y., et al., *Activated CREB is sufficient to overcome inhibitors in myelin and promote spinal axon regeneration in vivo*. Neuron, 2004. **44**(4): p. 609-21.
24. Finkbeiner, S., et al., *CREB: a major mediator of neuronal neurotrophin responses*. Neuron, 1997. **19**(5): p. 1031-47.
25. Crowder, R.J. and R.S. Freeman, *Phosphatidylinositol 3-kinase and Akt protein kinase are necessary and sufficient for the survival of nerve growth factor-dependent sympathetic neurons*. J Neurosci, 1998. **18**(8): p. 2933-43.
26. Hetman, M., et al., *Neuroprotection by brain-derived neurotrophic factor is mediated by extracellular signal-regulated kinase and phosphatidylinositol 3-kinase*. J Biol Chem, 1999. **274**(32): p. 22569-80.
27. Vaillant, A.R., et al., *Depolarization and neurotrophins converge on the phosphatidylinositol 3-kinase-Akt pathway to synergistically regulate neuronal survival*. J Cell Biol, 1999. **146**(5): p. 955-66.
28. Rodriguez-Viciana, P., et al., *Phosphatidylinositol-3-OH kinase as a direct target of Ras*. Nature, 1994. **370**(6490): p. 527-32.
29. Korhonen, J.M., et al., *Gab1 mediates neurite outgrowth, DNA synthesis, and survival in PC12 cells*. J Biol Chem, 1999. **274**(52): p. 37307-14.
30. Zheng, W.H., S. Kar, and R. Quirion, *Insulin-like growth factor-1-induced phosphorylation of transcription factor FKHRL1 is mediated by phosphatidylinositol 3-kinase/Akt kinase and role of this pathway in insulin-like growth factor-1-induced survival of cultured hippocampal neurons*. Mol Pharmacol, 2002. **62**(2): p. 225-33.
31. Datta, S.R., et al., *Akt phosphorylation of BAD couples survival signals to the cell-intrinsic death machinery*. Cell, 1997. **91**(2): p. 231-41.
32. Foehr, E.D., et al., *NF-kappa B signaling promotes both cell survival and neurite process formation in nerve growth factor-stimulated PC12 cells*. J Neurosci, 2000. **20**(20): p. 7556-63.
33. Wooten, M.W., et al., *The atypical protein kinase C-interacting protein p62 is a scaffold for NF-kappaB activation by nerve growth factor*. J Biol Chem, 2001. **276**(11): p. 7709-12.
34. Atwal, J.K., et al., *The TrkB-Shc site signals neuronal survival and local axon growth via MEK and P13-kinase*. Neuron, 2000. **27**(2): p. 265-77.
35. Markus, A., J. Zhong, and W.D. Snider, *Raf and akt mediate distinct aspects of sensory axon growth*. Neuron, 2002. **35**(1): p. 65-76.

36. Zhou, F.Q., et al., *NGF-induced axon growth is mediated by localized inactivation of GSK-3beta and functions of the microtubule plus end binding protein APC*. *Neuron*, 2004. **42**(6): p. 897-912.
37. Chuang, H.H., et al., *Bradykinin and nerve growth factor release the capsaicin receptor from PtdIns(4,5)P2-mediated inhibition*. *Nature*, 2001. **411**(6840): p. 957-62.
38. Amaral, M.D. and L. Pozzo-Miller, *BDNF induces calcium elevations associated with IBDNF, a nonselective cationic current mediated by TRPC channels*. *J Neurophysiol*, 2007. **98**(4): p. 2476-82.
39. Choi, D.Y., et al., *Sustained signaling by phospholipase C-gamma mediates nerve growth factor-triggered gene expression*. *Mol Cell Biol*, 2001. **21**(8): p. 2695-705.
40. Minichiello, L., et al., *Essential role for TrkB receptors in hippocampus-mediated learning*. *Neuron*, 1999. **24**(2): p. 401-14.
41. Sciarretta, C., et al., *PLCγ-activated signalling is essential for TrkB mediated sensory neuron structural plasticity*. *BMC Dev Biol*, 2010. **10**: p. 103.
42. Lee, F.S. and M.V. Chao, *Activation of Trk neurotrophin receptors in the absence of neurotrophins*. *Proc Natl Acad Sci U S A*, 2001. **98**(6): p. 3555-60.
43. Lee, F.S., et al., *Activation of Trk neurotrophin receptor signaling by pituitary adenylate cyclase-activating polypeptides*. *J Biol Chem*, 2002. **277**(11): p. 9096-102.
44. Rodríguez-Tébar, A., G. Dechant, and Y.A. Barde, *Binding of brain-derived neurotrophic factor to the nerve growth factor receptor*. *Neuron*, 1990. **4**(4): p. 487-92.
45. Rodríguez-Tébar, A., et al., *Binding of neurotrophin-3 to its neuronal receptors and interactions with nerve growth factor and brain-derived neurotrophic factor*. *Embo j*, 1992. **11**(3): p. 917-22.
46. Arévalo, J.C. and S.H. Wu, *Neurotrophin signaling: many exciting surprises!* *Cell Mol Life Sci*, 2006. **63**(13): p. 1523-37.
47. Nykjaer, A., et al., *Sortilin is essential for proNGF-induced neuronal cell death*. *Nature*, 2004. **427**(6977): p. 843-8.
48. Chen, Z.Y., et al., *Sortilin controls intracellular sorting of brain-derived neurotrophic factor to the regulated secretory pathway*. *J Neurosci*, 2005. **25**(26): p. 6156-66.
49. Teng, H.K., et al., *ProBDNF induces neuronal apoptosis via activation of a receptor complex of p75^{NTR} and sortilin*. *J Neurosci*, 2005. **25**(22): p. 5455-63.
50. Wang, K.C., et al., *P75 interacts with the Nogo receptor as a co-receptor for Nogo, MAG and OMgp*. *Nature*, 2002. **420**(6911): p. 74-8.
51. Wong, S.T., et al., *A p75^{NTR} and Nogo receptor complex mediates repulsive signaling by myelin-associated glycoprotein*. *Nat Neurosci*, 2002. **5**(12): p. 1302-8.
52. Mi, S., et al., *LINGO-1 is a component of the Nogo-66 receptor/p75 signaling complex*. *Nat Neurosci*, 2004. **7**(3): p. 221-8.
53. Hamanoue, M., et al., *p75-mediated NF-kappaB activation enhances the survival response of developing sensory neurons to nerve growth factor*. *Mol Cell Neurosci*, 1999. **14**(1): p. 28-40.
54. Middleton, G., et al., *Cytokine-induced nuclear factor kappa B activation promotes the survival of developing neurons*. *J Cell Biol*, 2000. **148**(2): p. 325-32.
55. Yeiser, E.C., et al., *Neurotrophin signaling through the p75 receptor is deficient in traf6^{-/-} mice*. *J Neurosci*, 2004. **24**(46): p. 10521-9.

56. Khursigara, G., et al., *A prosurvival function for the p75 receptor death domain mediated via the caspase recruitment domain receptor-interacting protein 2*. J Neurosci, 2001. **21**(16): p. 5854-63.
57. Khursigara, G., J.R. Orlinick, and M.V. Chao, *Association of the p75 neurotrophin receptor with TRAF6*. J Biol Chem, 1999. **274**(5): p. 2597-600.
58. Mamidipudi, V., X. Li, and M.W. Wooten, *Identification of interleukin 1 receptor-associated kinase as a conserved component in the p75-neurotrophin receptor activation of nuclear factor-kappa B*. J Biol Chem, 2002. **277**(31): p. 28010-8.
59. Yoon, S.O., et al., *Competitive signaling between TrkA and p75 nerve growth factor receptors determines cell survival*. J Neurosci, 1998. **18**(9): p. 3273-81.
60. Carter, B.D., et al., *Selective activation of NF-kappa B by nerve growth factor through the neurotrophin receptor p75*. Science, 1996. **272**(5261): p. 542-5.
61. Ceni, C., et al., *The p75NTR intracellular domain generated by neurotrophin-induced receptor cleavage potentiates Trk signaling*. J Cell Sci, 2010. **123**(Pt 13): p. 2299-307.
62. Bui, N.T., et al., *p75 neurotrophin receptor is required for constitutive and NGF-induced survival signalling in PC12 cells and rat hippocampal neurones*. J Neurochem, 2002. **81**(3): p. 594-605.
63. Massa, S.M., et al., *Small, nonpeptide p75NTR ligands induce survival signaling and inhibit proNGF-induced death*. J Neurosci, 2006. **26**(20): p. 5288-300.
64. Roux, P.P., et al., *The p75 neurotrophin receptor activates Akt (protein kinase B) through a phosphatidylinositol 3-kinase-dependent pathway*. J Biol Chem, 2001. **276**(25): p. 23097-104.
65. Yamashita, T., K.L. Tucker, and Y.A. Barde, *Neurotrophin binding to the p75 receptor modulates Rho activity and axonal outgrowth*. Neuron, 1999. **24**(3): p. 585-93.
66. Bamji, S.X., et al., *The p75 neurotrophin receptor mediates neuronal apoptosis and is essential for naturally occurring sympathetic neuron death*. J Cell Biol, 1998. **140**(4): p. 911-23.
67. Volosin, M., et al., *Induction of proneurotrophins and activation of p75NTR-mediated apoptosis via neurotrophin receptor-interacting factor in hippocampal neurons after seizures*. J Neurosci, 2008. **28**(39): p. 9870-9.
68. Sedel, F., C. Béchade, and A. Triller, *Nerve growth factor (NGF) induces motoneuron apoptosis in rat embryonic spinal cord in vitro*. Eur J Neurosci, 1999. **11**(11): p. 3904-12.
69. Deppmann, C.D., et al., *A model for neuronal competition during development*. Science, 2008. **320**(5874): p. 369-73.
70. Dhanasekaran, D.N. and E.P. Reddy, *JNK signaling in apoptosis*. Oncogene, 2008. **27**(48): p. 6245-51.
71. Frisch, S.M., et al., *A role for Jun-N-terminal kinase in anoikis; suppression by bcl-2 and crmA*. J Cell Biol, 1996. **135**(5): p. 1377-82.
72. Herrmann, J.L., et al., *Regulation of lipid signaling pathways for cell survival and apoptosis by bcl-2 in prostate carcinoma cells*. Exp Cell Res, 1997. **234**(2): p. 442-51.
73. Coulson, E.J., K. Reid, and P.F. Bartlett, *Signaling of neuronal cell death by the p75NTR neurotrophin receptor*. Mol Neurobiol, 1999. **20**(1): p. 29-44.
74. Tabassum, A., F. Khwaja, and D. Djakiew, *The p75(NTR) tumor suppressor induces caspase-mediated apoptosis in bladder tumor cells*. Int J Cancer, 2003. **105**(1): p. 47-52.

75. Bhakar, A.L., et al., *Apoptosis induced by p75NTR overexpression requires Jun kinase-dependent phosphorylation of Bad*. J Neurosci, 2003. **23**(36): p. 11373-81.
76. Ambacher, K.K., et al., *The JNK- and AKT/GSK3 β - signaling pathways converge to regulate Puma induction and neuronal apoptosis induced by trophic factor deprivation*. PLoS One, 2012. **7**(10): p. e46885.
77. Salehi, A.H., S. Xanthoudakis, and P.A. Barker, *NRAGE, a p75 neurotrophin receptor-interacting protein, induces caspase activation and cell death through a JNK-dependent mitochondrial pathway*. J Biol Chem, 2002. **277**(50): p. 48043-50.
78. Pehar, M., et al., *Mitochondrial superoxide production and nuclear factor erythroid 2-related factor 2 activation in p75 neurotrophin receptor-induced motor neuron apoptosis*. J Neurosci, 2007. **27**(29): p. 7777-85.
79. Kenchappa, R.S., et al., *p75 neurotrophin receptor-mediated apoptosis in sympathetic neurons involves a biphasic activation of JNK and up-regulation of tumor necrosis factor-alpha-converting enzyme/ADAM17*. J Biol Chem, 2010. **285**(26): p. 20358-68.
80. Kenchappa, R.S., et al., *Ligand-dependent cleavage of the P75 neurotrophin receptor is necessary for NRIF nuclear translocation and apoptosis in sympathetic neurons*. Neuron, 2006. **50**(2): p. 219-32.
81. Ye, X., et al., *TRAF family proteins interact with the common neurotrophin receptor and modulate apoptosis induction*. J Biol Chem, 1999. **274**(42): p. 30202-8.
82. Gentry, J.J., et al., *A functional interaction between the p75 neurotrophin receptor interacting factors, TRAF6 and NRIF*. J Biol Chem, 2004. **279**(16): p. 16646-56.
83. Linggi, M.S., et al., *Neurotrophin receptor interacting factor (NRIF) is an essential mediator of apoptotic signaling by the p75 neurotrophin receptor*. J Biol Chem, 2005. **280**(14): p. 13801-8.
84. DeFreitas, M.F., P.S. McQuillen, and C.J. Shatz, *A novel p75NTR signaling pathway promotes survival, not death, of immunopurified neocortical subplate neurons*. J Neurosci, 2001. **21**(14): p. 5121-9.
85. McCollum, A.T. and S. Estus, *NGF acts via p75 low-affinity neurotrophin receptor and calpain inhibition to reduce UV neurotoxicity*. J Neurosci Res, 2004. **77**(4): p. 552-64.
86. MacPhee, I.J. and P.A. Barker, *Brain-derived neurotrophic factor binding to the p75 neurotrophin receptor reduces TrkA signaling while increasing serine phosphorylation in the TrkA intracellular domain*. J Biol Chem, 1997. **272**(38): p. 23547-51.
87. Le Pichon, C.E. and A.T. Chesler, *The functional and anatomical dissection of somatosensory subpopulations using mouse genetics*. Front Neuroanat, 2014. **8**: p. 21.
88. Montañó, J.A., et al., *Development and neuronal dependence of cutaneous sensory nerve formations: Lessons from neurotrophins*. Microsc Res Tech, 2010. **73**(5): p. 513-29.
89. McCoy, E.S., et al., *Peptidergic CGRP α primary sensory neurons encode heat and itch and tonically suppress sensitivity to cold*. Neuron, 2013. **78**(1): p. 138-51.
90. Abraira, V.E. and D.D. Ginty, *The sensory neurons of touch*. Neuron, 2013. **79**(4): p. 618-39.
91. Dong, X. and X. Dong, *Peripheral and Central Mechanisms of Itch*. Neuron, 2018. **98**(3): p. 482-494.
92. Bishop, G.H., *The skin as an organ of senses with special reference to the itching sensation*. J Invest Dermatol, 1948. **11**(2): p. 143-54.

93. Sharif, B., et al., *Differential Coding of Itch and Pain by a Subpopulation of Primary Afferent Neurons*. Neuron, 2020. **106**(6): p. 940-951.e4.
94. Sikand, P., et al., *Sensory responses to injection and punctate application of capsaicin and histamine to the skin*. Pain, 2011. **152**(11): p. 2485-94.
95. Roberson, D.P., et al., *Activity-dependent silencing reveals functionally distinct itch-generating sensory neurons*. Nat Neurosci, 2013. **16**(7): p. 910-8.
96. Han, L., et al., *A subpopulation of nociceptors specifically linked to itch*. Nat Neurosci, 2013. **16**(2): p. 174-82.
97. Castillo, K., et al., *Thermally activated TRP channels: molecular sensors for temperature detection*. Phys Biol, 2018. **15**(2): p. 021001.
98. Serbedzija, G.N., S.E. Fraser, and M. Bronner-Fraser, *Pathways of trunk neural crest cell migration in the mouse embryo as revealed by vital dye labelling*. Development, 1990. **108**(4): p. 605-12.
99. Lallemand, F. and P. Ernfors, *Molecular interactions underlying the specification of sensory neurons*. Trends Neurosci, 2012. **35**(6): p. 373-81.
100. ElShamy, W.M. and P. Ernfors, *A local action of neurotrophin-3 prevents the death of proliferating sensory neuron precursor cells*. Neuron, 1996. **16**(5): p. 963-72.
101. Ockel, M., et al., *Roles of neurotrophin-3 during early development of the peripheral nervous system*. Philos Trans R Soc Lond B Biol Sci, 1996. **351**(1338): p. 383-7.
102. Sieber-Blum, M., *Role of the neurotrophic factors BDNF and NGF in the commitment of pluripotent neural crest cells*. Neuron, 1991. **6**(6): p. 949-55.
103. Kalcheim, C., C. Carmeli, and A. Rosenthal, *Neurotrophin 3 is a mitogen for cultured neural crest cells*. Proc Natl Acad Sci U S A, 1992. **89**(5): p. 1661-5.
104. Pinco, O., et al., *Neurotrophin-3 affects proliferation and differentiation of distinct neural crest cells and is present in the early neural tube of avian embryos*. J Neurobiol, 1993. **24**(12): p. 1626-41.
105. Henion, P.D., et al., *trkC-mediated NT-3 signaling is required for the early development of a subpopulation of neurogenic neural crest cells*. Dev Biol, 1995. **172**(2): p. 602-13.
106. Rifkin, J.T., et al., *Dynamic expression of neurotrophin receptors during sensory neuron genesis and differentiation*. Dev Biol, 2000. **227**(2): p. 465-80.
107. Fariñas, I., et al., *Characterization of neurotrophin and Trk receptor functions in developing sensory ganglia: direct NT-3 activation of TrkB neurons in vivo*. Neuron, 1998. **21**(2): p. 325-34.
108. Bartkowska, K., et al., *Trk signaling regulates neural precursor cell proliferation and differentiation during cortical development*. Development, 2007. **134**(24): p. 4369-80.
109. Marmigère, F. and P. Ernfors, *Specification and connectivity of neuronal subtypes in the sensory lineage*. Nat Rev Neurosci, 2007. **8**(2): p. 114-27.
110. Pavan, W.J. and D.W. Raible, *Specification of neural crest into sensory neuron and melanocyte lineages*. Dev Biol, 2012. **366**(1): p. 55-63.
111. Ernsberger, U., *Role of neurotrophin signalling in the differentiation of neurons from dorsal root ganglia and sympathetic ganglia*. Cell Tissue Res, 2009. **336**(3): p. 349-84.
112. Memberg, S.P. and A.K. Hall, *Proliferation, differentiation, and survival of rat sensory neuron precursors in vitro require specific trophic factors*. Mol Cell Neurosci, 1995. **6**(4): p. 323-35.

113. Ernfors, P., et al., *Lack of neurotrophin-3 leads to deficiencies in the peripheral nervous system and loss of limb proprioceptive afferents*. Cell, 1994. **77**(4): p. 503-12.
114. Klein, R., et al., *Disruption of the neurotrophin-3 receptor gene *trkC* eliminates la muscle afferents and results in abnormal movements*. Nature, 1994. **368**(6468): p. 249-51.
115. Minichiello, L., et al., *Differential effects of combined *trk* receptor mutations on dorsal root ganglion and inner ear sensory neurons*. Development, 1995. **121**(12): p. 4067-75.
116. Davies, A.M., L. Minichiello, and R. Klein, *Developmental changes in NT3 signalling via *TrkA* and *TrkB* in embryonic neurons*. Embo j, 1995. **14**(18): p. 4482-9.
117. Huang, E.J., et al., *Expression of *Trk* receptors in the developing mouse trigeminal ganglion: in vivo evidence for NT-3 activation of *TrkA* and *TrkB* in addition to *TrkC**. Development, 1999. **126**(10): p. 2191-203.
118. ElShamy, W.M., L.K. Fridvall, and P. Ernfors, *Growth arrest failure, G1 restriction point override, and S phase death of sensory precursor cells in the absence of neurotrophin-3*. Neuron, 1998. **21**(5): p. 1003-15.
119. Fariñas, I., et al., *Lack of neurotrophin-3 results in death of spinal sensory neurons and premature differentiation of their precursors*. Neuron, 1996. **17**(6): p. 1065-78.
120. Liebl, D.J., et al., *Absence of sensory neurons before target innervation in brain-derived neurotrophic factor-, neurotrophin 3-, and *TrkC*-deficient embryonic mice*. J Neurosci, 1997. **17**(23): p. 9113-21.
121. Tessarollo, L., et al., *Targeted deletion of all isoforms of the *trkC* gene suggests the use of alternate receptors by its ligand neurotrophin-3 in neuronal development and implicates *trkC* in normal cardiogenesis*. Proc Natl Acad Sci U S A, 1997. **94**(26): p. 14776-81.
122. White, F.A., et al., *Synchronous onset of NGF and *TrkA* survival dependence in developing dorsal root ganglia*. J Neurosci, 1996. **16**(15): p. 4662-72.
123. Kramer, I., et al., *A role for *Runx* transcription factor signaling in dorsal root ganglion sensory neuron diversification*. Neuron, 2006. **49**(3): p. 379-93.
124. McMahon, S.B., et al., *Expression and coexpression of *Trk* receptors in subpopulations of adult primary sensory neurons projecting to identified peripheral targets*. Neuron, 1994. **12**(5): p. 1161-71.
125. Karchewski, L.A., et al., *Anatomical evidence supporting the potential for modulation by multiple neurotrophins in the majority of adult lumbar sensory neurons*. J Comp Neurol, 1999. **413**(2): p. 327-41.
126. Ernfors, P., K.F. Lee, and R. Jaenisch, *Target derived and putative local actions of neurotrophins in the peripheral nervous system*. Prog Brain Res, 1994. **103**: p. 43-54.
127. Abdo, H., et al., *Dependence on the transcription factor *Shox2* for specification of sensory neurons conveying discriminative touch*. Eur J Neurosci, 2011. **34**(10): p. 1529-41.
128. Scott, A., et al., *Transcription factor short stature homeobox 2 is required for proper development of tropomyosin-related kinase B-expressing mechanosensory neurons*. J Neurosci, 2011. **31**(18): p. 6741-9.
129. Ernfors, P., K.F. Lee, and R. Jaenisch, *Mice lacking brain-derived neurotrophic factor develop with sensory deficits*. Nature, 1994. **368**(6467): p. 147-50.
130. Jones, K.R., et al., *Targeted disruption of the *BDNF* gene perturbs brain and sensory neuron development but not motor neuron development*. Cell, 1994. **76**(6): p. 989-99.

131. Conover, J.C., et al., *Neuronal deficits, not involving motor neurons, in mice lacking BDNF and/or NT4*. Nature, 1995. **375**(6528): p. 235-8.
132. Erickson, J.T., et al., *Mice lacking brain-derived neurotrophic factor exhibit visceral sensory neuron losses distinct from mice lacking NT4 and display a severe developmental deficit in control of breathing*. J Neurosci, 1996. **16**(17): p. 5361-71.
133. Perez-Pinera, P., et al., *Characterization of sensory deficits in TrkB knockout mice*. Neurosci Lett, 2008. **433**(1): p. 43-7.
134. Bourane, S., et al., *Low-threshold mechanoreceptor subtypes selectively express MafA and are specified by Ret signaling*. Neuron, 2009. **64**(6): p. 857-70.
135. Marmigère, F. and P. Carroll, *Neurotrophin signalling and transcription programmes interactions in the development of somatosensory neurons*. Handb Exp Pharmacol, 2014. **220**: p. 329-53.
136. Wright, D.E. and W.D. Snider, *Neurotrophin receptor mRNA expression defines distinct populations of neurons in rat dorsal root ganglia*. J Comp Neurol, 1995. **351**(3): p. 329-38.
137. Phillips, H.S. and M.P. Armanini, *Expression of the trk family of neurotrophin receptors in developing and adult dorsal root ganglion neurons*. Philos Trans R Soc Lond B Biol Sci, 1996. **351**(1338): p. 413-6.
138. Luo, W., et al., *A hierarchical NGF signaling cascade controls Ret-dependent and Ret-independent events during development of nonpeptidergic DRG neurons*. Neuron, 2007. **54**(5): p. 739-54.
139. Bachy, I., et al., *The transcription factor Cux2 marks development of an A-delta sublineage of TrkA sensory neurons*. Dev Biol, 2011. **360**(1): p. 77-86.
140. Abdel Samad, O., et al., *Characterization of two Runx1-dependent nociceptor differentiation programs necessary for inflammatory versus neuropathic pain*. Mol Pain, 2010. **6**: p. 45.
141. Chen, C.L., et al., *Runx1 determines nociceptive sensory neuron phenotype and is required for thermal and neuropathic pain*. Neuron, 2006. **49**(3): p. 365-77.
142. Gascon, E., et al., *Hepatocyte growth factor-Met signaling is required for Runx1 extinction and peptidergic differentiation in primary nociceptive neurons*. J Neurosci, 2010. **30**(37): p. 12414-23.
143. Crowley, C., et al., *Mice lacking nerve growth factor display perinatal loss of sensory and sympathetic neurons yet develop basal forebrain cholinergic neurons*. Cell, 1994. **76**(6): p. 1001-11.
144. Smeyne, R.J., et al., *Severe sensory and sympathetic neuropathies in mice carrying a disrupted Trk/NGF receptor gene*. Nature, 1994. **368**(6468): p. 246-9.
145. Berg, J.S. and P.B. Farel, *Developmental regulation of sensory neuron number and limb innervation in the mouse*. Brain Res Dev Brain Res, 2000. **125**(1-2): p. 21-30.
146. Mu, X., et al., *Neurotrophin receptor genes are expressed in distinct patterns in developing dorsal root ganglia*. J Neurosci, 1993. **13**(9): p. 4029-41.
147. Huang, E.J. and L.F. Reichardt, *Neurotrophins: roles in neuronal development and function*. Annu Rev Neurosci, 2001. **24**: p. 677-736.
148. Albers, K.M., D.E. Wright, and B.M. Davis, *Overexpression of nerve growth factor in epidermis of transgenic mice causes hypertrophy of the peripheral nervous system*. J Neurosci, 1994. **14**(3 Pt 2): p. 1422-32.

149. LeMaster, A.M., et al., *Overexpression of brain-derived neurotrophic factor enhances sensory innervation and selectively increases neuron number*. J Neurosci, 1999. **19**(14): p. 5919-31.
150. Tucker, K.L., M. Meyer, and Y.A. Barde, *Neurotrophins are required for nerve growth during development*. Nat Neurosci, 2001. **4**(1): p. 29-37.
151. Fornaro, M., et al., *Role of neurotrophic factors in enhancing linear axonal growth of ganglionic sensory neurons in vitro*. Neural Regen Res, 2020. **15**(9): p. 1732-1739.
152. Runge, E.M., et al., *Neurotrophin-4 is more potent than brain-derived neurotrophic factor in promoting, attracting and suppressing geniculate ganglion neurite outgrowth*. Dev Neurosci, 2012. **34**(5): p. 389-401.
153. Minichiello, L., et al., *Point mutation in trkB causes loss of NT4-dependent neurons without major effects on diverse BDNF responses*. Neuron, 1998. **21**(2): p. 335-45.
154. Cao, X. and M.S. Shoichet, *Investigating the synergistic effect of combined neurotrophic factor concentration gradients to guide axonal growth*. Neuroscience, 2003. **122**(2): p. 381-9.
155. Gillespie, L.N., *Regulation of axonal growth and guidance by the neurotrophin family of neurotrophic factors*. Clin Exp Pharmacol Physiol, 2003. **30**(10): p. 724-33.
156. Paves, H. and M. Saarma, *Neurotrophins as in vitro growth cone guidance molecules for embryonic sensory neurons*. Cell Tissue Res, 1997. **290**(2): p. 285-97.
157. Yamashita, N., et al., *TrkA mediates retrograde semaphorin 3A signaling through plexin A4 to regulate dendritic branching*. J Cell Sci, 2016. **129**(9): p. 1802-14.
158. Tuttle, R. and D.D. O'Leary, *Neurotrophins rapidly modulate growth cone response to the axon guidance molecule, collapsin-1*. Mol Cell Neurosci, 1998. **11**(1-2): p. 1-8.
159. Sar Shalom, H., et al., *Balance between BDNF and Semaphorins gates the innervation of the mammary gland*. Elife, 2019. **8**.
160. Levi-Montalcini, R., *The nerve growth factor 35 years later*. Science, 1987. **237**(4819): p. 1154-62.
161. Oppenheim, R.W., *Cell death during development of the nervous system*. Annu Rev Neurosci, 1991. **14**: p. 453-501.
162. Thoenen, H. and Y.A. Barde, *Physiology of nerve growth factor*. Physiol Rev, 1980. **60**(4): p. 1284-335.
163. Miguel-Aliaga, I. and S. Thor, *Programmed cell death in the nervous system--a programmed cell fate? Curr Opin Neurobiol, 2009. 19(2): p. 127-33.*
164. Wang, Y., et al., *A cell fitness selection model for neuronal survival during development*. Nat Commun, 2019. **10**(1): p. 4137.
165. Ellis, H.M. and H.R. Horvitz, *Genetic control of programmed cell death in the nematode C. elegans*. Cell, 1986. **44**(6): p. 817-29.
166. Bibel, M. and Y.A. Barde, *Neurotrophins: key regulators of cell fate and cell shape in the vertebrate nervous system*. Genes Dev, 2000. **14**(23): p. 2919-37.
167. Patel, T.D., et al., *Development of sensory neurons in the absence of NGF/TrkA signaling in vivo*. Neuron, 2000. **25**(2): p. 345-57.
168. Ginty, D.D. and R.A. Segal, *Retrograde neurotrophin signaling: Trk-ing along the axon*. Curr Opin Neurobiol, 2002. **12**(3): p. 268-74.

169. Ito, K. and H. Enomoto, *Retrograde transport of neurotrophic factor signaling: implications in neuronal development and pathogenesis*. J Biochem, 2016. **160**(2): p. 77-85.
170. Tanaka, Y., et al., *The molecular motor KIF1A transports the TrkA neurotrophin receptor and is essential for sensory neuron survival and function*. Neuron, 2016. **90**(6): p. 1215-1229.
171. Mehlen, P. and D.E. Bredesen, *The dependence receptor hypothesis*. Apoptosis, 2004. **9**(1): p. 37-49.
172. Tauszig-Delamasure, S., et al., *The TrkC receptor induces apoptosis when the dependence receptor notion meets the neurotrophin paradigm*. Proc Natl Acad Sci U S A, 2007. **104**(33): p. 13361-6.
173. Matrone, C., et al., *Tyrosine kinase nerve growth factor receptor switches from pro-survival to pro-apoptotic activity via Abeta-mediated phosphorylation*. Proc Natl Acad Sci U S A, 2009. **106**(27): p. 11358-63.
174. Ichim, G., et al., *The dependence receptor TrkC triggers mitochondria-dependent apoptosis upon Cobra-1 recruitment*. Mol Cell, 2013. **51**(5): p. 632-46.
175. Feinberg, K., et al., *A neuroprotective agent that inactivates prodegenerative TrkA and preserves mitochondria*. J Cell Biol, 2017. **216**(11): p. 3655-3675.
176. Ménard, M., et al., *Hey1- and p53-dependent TrkC proapoptotic activity controls neuroblastoma growth*. PLoS Biol, 2018. **16**(5): p. e2002912.
177. Mukhopadhyay, A., et al., *HeyL regulates the number of TrkC neurons in dorsal root ganglia*. Dev Biol, 2009. **334**(1): p. 142-51.
178. Harel, L., B. Costa, and M. Fainzilber, *On the death Trk*. Dev Neurobiol, 2010. **70**(5): p. 298-303.
179. Rabizadeh, S., et al., *Induction of apoptosis by the low-affinity NGF receptor*. Science, 1993. **261**(5119): p. 345-8.
180. Barrett, G.L. and P.F. Bartlett, *The p75 nerve growth factor receptor mediates survival or death depending on the stage of sensory neuron development*. Proc Natl Acad Sci U S A, 1994. **91**(14): p. 6501-5.
181. Rabizadeh, S. and D.E. Bredesen, *Ten years on: mediation of cell death by the common neurotrophin receptor p75(NTR)*. Cytokine Growth Factor Rev, 2003. **14**(3-4): p. 225-39.
182. Yeo, T.T., et al., *Absence of p75NTR causes increased basal forebrain cholinergic neuron size, choline acetyltransferase activity, and target innervation*. J Neurosci, 1997. **17**(20): p. 7594-605.
183. Naumann, T., et al., *Complete deletion of the neurotrophin receptor p75NTR leads to long-lasting increases in the number of basal forebrain cholinergic neurons*. J Neurosci, 2002. **22**(7): p. 2409-18.
184. Barker, P.A., *p75NTR is positively promiscuous: novel partners and new insights*. Neuron, 2004. **42**(4): p. 529-33.
185. Lee, K.F., et al., *Targeted mutation of the gene encoding the low affinity NGF receptor p75 leads to deficits in the peripheral sensory nervous system*. Cell, 1992. **69**(5): p. 737-49.
186. Lee, K.F., A.M. Davies, and R. Jaenisch, *p75-deficient embryonic dorsal root sensory and neonatal sympathetic neurons display a decreased sensitivity to NGF*. Development, 1994. **120**(4): p. 1027-33.

187. Fan, G., R. Jaenisch, and J. Kucera, *A role for p75 receptor in neurotrophin-3 functioning during the development of limb proprioception*. *Neuroscience*, 1999. **90**(1): p. 259-68.
188. Agerman, K., et al., *Attenuation of a caspase-3 dependent cell death in NT4- and p75-deficient embryonic sensory neurons*. *Mol Cell Neurosci*, 2000. **16**(3): p. 258-68.
189. Singh, K.K., et al., *Developmental axon pruning mediated by BDNF-p75NTR-dependent axon degeneration*. *Nat Neurosci*, 2008. **11**(6): p. 649-58.
190. Buchman, V.L. and A.M. Davies, *Different neurotrophins are expressed and act in a developmental sequence to promote the survival of embryonic sensory neurons*. *Development*, 1993. **118**(3): p. 989-1001.
191. Hantzopoulos, P.A., et al., *The low affinity NGF receptor, p75, can collaborate with each of the Trks to potentiate functional responses to the neurotrophins*. *Neuron*, 1994. **13**(1): p. 187-201.
192. Makkerh, J.P., et al., *p75 neurotrophin receptor reduces ligand-induced Trk receptor ubiquitination and delays Trk receptor internalization and degradation*. *EMBO Rep*, 2005. **6**(10): p. 936-41.
193. Chen, Z., et al., *p75 Is Required for the Establishment of Postnatal Sensory Neuron Diversity by Potentiating Ret Signaling*. *Cell Rep*, 2017. **21**(3): p. 707-720.
194. Cheng, I., et al., *Temporally restricted death and the role of p75NTR as a survival receptor in the developing sensory nervous system*. *Dev Neurobiol*, 2018. **78**(7): p. 701-717.
195. Bergmann, I., et al., *Analysis of cutaneous sensory neurons in transgenic mice lacking the low affinity neurotrophin receptor p75*. *Eur J Neurosci*, 1997. **9**(1): p. 18-28.
196. Murray, S.S., P.F. Bartlett, and S.S. Cheema, *Differential loss of spinal sensory but not motor neurons in the p75NTR knockout mouse*. *Neurosci Lett*, 1999. **267**(1): p. 45-8.
197. Vaegter, C.B., et al., *Sortilin associates with Trk receptors to enhance anterograde transport and neurotrophin signaling*. *Nat Neurosci*, 2011. **14**(1): p. 54-61.
198. Yamaguchi, Y. and M. Miura, *Programmed cell death in neurodevelopment*. *Dev Cell*, 2015. **32**(4): p. 478-90.
199. Orrenius, S., V. Gogvadze, and B. Zhivotovsky, *Calcium and mitochondria in the regulation of cell death*. *Biochem Biophys Res Commun*, 2015. **460**(1): p. 72-81.
200. Fricker, M., et al., *Neuronal Cell Death*. *Physiol Rev*, 2018. **98**(2): p. 813-880.
201. Galluzzi, L., et al., *Molecular mechanisms of cell death: recommendations of the Nomenclature Committee on Cell Death 2018*. *Cell Death Differ*, 2018. **25**(3): p. 486-541.
202. Hollville, E., S.E. Romero, and M. Deshmukh, *Apoptotic cell death regulation in neurons*. *Febs j*, 2019. **286**(17): p. 3276-3298.
203. Galluzzi, L., et al., *Molecular definitions of cell death subroutines: recommendations of the Nomenclature Committee on Cell Death 2012*. *Cell Death Differ*, 2012. **19**(1): p. 107-20.
204. Galluzzi, L., et al., *Essential versus accessory aspects of cell death: recommendations of the NCCD 2015*. *Cell Death Differ*, 2015. **22**(1): p. 58-73.
205. Marsden, V.S., et al., *Apoptosis initiated by Bcl-2-regulated caspase activation independently of the cytochrome c/Apaf-1/caspase-9 apoptosome*. *Nature*, 2002. **419**(6907): p. 634-7.
206. Wheeler, M.A., et al., *TNF- α /TNFR1 signaling is required for the development and function of primary nociceptors*. *Neuron*, 2014. **82**(3): p. 587-602.

207. Brumatti, G., M. Salmanidis, and P.G. Ekert, *Crossing paths: interactions between the cell death machinery and growth factor survival signals*. Cell Mol Life Sci, 2010. **67**(10): p. 1619-30.
208. Czabotar, P.E., et al., *Control of apoptosis by the BCL-2 protein family: implications for physiology and therapy*. Nat Rev Mol Cell Biol, 2014. **15**(1): p. 49-63.
209. Pihán, P., A. Carreras-Sureda, and C. Hetz, *BCL-2 family: integrating stress responses at the ER to control cell demise*. Cell Death Differ, 2017. **24**(9): p. 1478-1487.
210. Cheng, E.H., et al., *BCL-2, BCL-X(L) sequester BH3 domain-only molecules preventing BAX- and BAK-mediated mitochondrial apoptosis*. Mol Cell, 2001. **8**(3): p. 705-11.
211. Wei, M.C., et al., *Proapoptotic BAX and BAK: a requisite gateway to mitochondrial dysfunction and death*. Science, 2001. **292**(5517): p. 727-30.
212. Jakobson, M., et al., *Multiple mechanisms repress N-Bak mRNA translation in the healthy and apoptotic neurons*. Cell death & disease, 2013. **4**(8): p. e777-e777.
213. Schoenmann, Z., et al., *Axonal degeneration is regulated by the apoptotic machinery or a NAD⁺-sensitive pathway in insects and mammals*. J Neurosci, 2010. **30**(18): p. 6375-86.
214. Simon, D.J., et al., *A caspase cascade regulating developmental axon degeneration*. J Neurosci, 2012. **32**(49): p. 17540-53.
215. Czabotar, P.E., et al., *Bax crystal structures reveal how BH3 domains activate Bax and nucleate its oligomerization to induce apoptosis*. Cell, 2013. **152**(3): p. 519-31.
216. Dewson, G., et al., *Bax dimerizes via a symmetric BH3:groove interface during apoptosis*. Cell Death Differ, 2012. **19**(4): p. 661-70.
217. Otera, H., et al., *Drp1-dependent mitochondrial fission via MiD49/51 is essential for apoptotic cristae remodeling*. J Cell Biol, 2016. **212**(5): p. 531-44.
218. Jiang, X., et al., *Activation of mitochondrial protease OMA1 by Bax and Bak promotes cytochrome c release during apoptosis*. Proc Natl Acad Sci U S A, 2014. **111**(41): p. 14782-7.
219. Tait, S.W. and D.R. Green, *Mitochondria and cell death: outer membrane permeabilization and beyond*. Nat Rev Mol Cell Biol, 2010. **11**(9): p. 621-32.
220. Tait, S.W. and D.R. Green, *Mitochondrial regulation of cell death*. Cold Spring Harb Perspect Biol, 2013. **5**(9).
221. Li, P., et al., *Cytochrome c and dATP-dependent formation of Apaf-1/caspase-9 complex initiates an apoptotic protease cascade*. Cell, 1997. **91**(4): p. 479-89.
222. Wright, K.M., et al., *Chromatin modification of Apaf-1 restricts the apoptotic pathway in mature neurons*. J Cell Biol, 2007. **179**(5): p. 825-32.
223. Madden, S.D., M. Donovan, and T.G. Cotter, *Key apoptosis regulating proteins are down-regulated during postnatal tissue development*. Int J Dev Biol, 2007. **51**(5): p. 415-23.
224. Cusack, C.L., et al., *Distinct pathways mediate axon degeneration during apoptosis and axon-specific pruning*. Nat Commun, 2013. **4**: p. 1876.
225. Unsain, N., et al., *XIAP regulates caspase activity in degenerating axons*. Cell Rep, 2013. **4**(4): p. 751-63.
226. Roy, N., et al., *The c-IAP-1 and c-IAP-2 proteins are direct inhibitors of specific caspases*. Embo j, 1997. **16**(23): p. 6914-25.
227. Eckelman, B.P., G.S. Salvesen, and F.L. Scott, *Human inhibitor of apoptosis proteins: why XIAP is the black sheep of the family*. EMBO Rep, 2006. **7**(10): p. 988-94.

228. Du, C., et al., *Smac, a mitochondrial protein that promotes cytochrome c-dependent caspase activation by eliminating IAP inhibition*. Cell, 2000. **102**(1): p. 33-42.
229. Salvesen, G.S. and C.S. Duckett, *IAP proteins: blocking the road to death's door*. Nat Rev Mol Cell Biol, 2002. **3**(6): p. 401-10.
230. Kouroku, Y., et al., *Detection of activated Caspase-3 by a cleavage site-directed antiserum during naturally occurring DRG neurons apoptosis*. Biochem Biophys Res Commun, 1998. **247**(3): p. 780-4.
231. Shacham-Silverberg, V., et al., *Phosphatidylserine is a marker for axonal debris engulfment but its exposure can be decoupled from degeneration*. Cell Death Dis, 2018. **9**(11): p. 1116.
232. Yong, Y., et al., *p75NTR and DR6 Regulate Distinct Phases of Axon Degeneration Demarcated by Spheroid Rupture*. J Neurosci, 2019. **39**(48): p. 9503-9520.
233. Galluzzi, L., J.M. Bravo-San Pedro, and G. Kroemer, *Organelle-specific initiation of cell death*. Nat Cell Biol, 2014. **16**(8): p. 728-36.
234. Zhang, Y., et al., *RIP1 autophosphorylation is promoted by mitochondrial ROS and is essential for RIP3 recruitment into necrosome*. Nat Commun, 2017. **8**: p. 14329.
235. Conrad, M., et al., *Regulated necrosis: disease relevance and therapeutic opportunities*. Nat Rev Drug Discov, 2016. **15**(5): p. 348-66.
236. Kaiser, W.J., et al., *RIP3 mediates the embryonic lethality of caspase-8-deficient mice*. Nature, 2011. **471**(7338): p. 368-72.
237. Oberst, A., et al., *Catalytic activity of the caspase-8-FLIP(L) complex inhibits RIPK3-dependent necrosis*. Nature, 2011. **471**(7338): p. 363-7.
238. Remijsen, Q., et al., *Dying for a cause: NETosis, mechanisms behind an antimicrobial cell death modality*. Cell Death Differ, 2011. **18**(4): p. 581-8.
239. Newton, K., et al., *Activity of protein kinase RIPK3 determines whether cells die by necroptosis or apoptosis*. Science, 2014. **343**(6177): p. 1357-60.
240. Fatokun, A.A., V.L. Dawson, and T.M. Dawson, *Parthanatos: mitochondrial-linked mechanisms and therapeutic opportunities*. Br J Pharmacol, 2014. **171**(8): p. 2000-16.
241. Zhivotovsky, B. and S. Orrenius, *Calcium and cell death mechanisms: a perspective from the cell death community*. Cell Calcium, 2011. **50**(3): p. 211-21.
242. Alano, C.C., et al., *NAD⁺ depletion is necessary and sufficient for poly(ADP-ribose) polymerase-1-mediated neuronal death*. J Neurosci, 2010. **30**(8): p. 2967-78.
243. Bonora, M., et al., *Molecular mechanisms of cell death: central implication of ATP synthase in mitochondrial permeability transition*. Oncogene, 2015. **34**(12): p. 1475-86.
244. Vanden Berghe, T., et al., *Regulated necrosis: the expanding network of non-apoptotic cell death pathways*. Nat Rev Mol Cell Biol, 2014. **15**(2): p. 135-47.
245. Schinzel, A.C., et al., *Cyclophilin D is a component of mitochondrial permeability transition and mediates neuronal cell death after focal cerebral ischemia*. Proc Natl Acad Sci U S A, 2005. **102**(34): p. 12005-10.
246. Mukherjee, R., et al., *Mechanism of mitochondrial permeability transition pore induction and damage in the pancreas: inhibition prevents acute pancreatitis by protecting production of ATP*. Gut, 2016. **65**(8): p. 1333-46.

247. Miura, T. and M. Tanno, *The mPTP and its regulatory proteins: final common targets of signalling pathways for protection against necrosis*. *Cardiovasc Res*, 2012. **94**(2): p. 181-9.
248. Karch, J., et al., *Bax and Bak function as the outer membrane component of the mitochondrial permeability pore in regulating necrotic cell death in mice*. *Elife*, 2013. **2**: p. e00772.
249. Whelan, R.S., et al., *Bax regulates primary necrosis through mitochondrial dynamics*. *Proc Natl Acad Sci U S A*, 2012. **109**(17): p. 6566-71.
250. Marzo, I., et al., *Bax and adenine nucleotide translocator cooperate in the mitochondrial control of apoptosis*. *Science*, 1998. **281**(5385): p. 2027-31.
251. Zamzami, N., et al., *Bid acts on the permeability transition pore complex to induce apoptosis*. *Oncogene*, 2000. **19**(54): p. 6342-50.
252. Xu, F., et al., *The mitochondrial division inhibitor Mdivi-1 rescues mammalian neurons from anesthetic-induced cytotoxicity*. *Mol Brain*, 2016. **9**: p. 35.
253. Vaseva, A.V., et al., *p53 opens the mitochondrial permeability transition pore to trigger necrosis*. *Cell*, 2012. **149**(7): p. 1536-48.
254. Morkuniene, R., et al., *Small A β 1-42 oligomer-induced membrane depolarization of neuronal and microglial cells: role of N-methyl-D-aspartate receptors*. *J Neurosci Res*, 2015. **93**(3): p. 475-86.
255. Kahraman, S., et al., *Permeability transition pore-dependent and PARP-mediated depletion of neuronal pyridine nucleotides during anoxia and glucose deprivation*. *J Bioenerg Biomembr*, 2015. **47**(1-2): p. 53-61.
256. Hara, T., et al., *Suppression of basal autophagy in neural cells causes neurodegenerative disease in mice*. *Nature*, 2006. **441**(7095): p. 885-9.
257. Inoue, K., et al., *Macroautophagy deficiency mediates age-dependent neurodegeneration through a phospho-tau pathway*. *Mol Neurodegener*, 2012. **7**: p. 48.
258. Anding, A.L. and E.H. Baehrecke, *Autophagy in Cell Life and Cell Death*. *Curr Top Dev Biol*, 2015. **114**: p. 67-91.
259. Goodall, M.L., et al., *The Autophagy Machinery Controls Cell Death Switching between Apoptosis and Necroptosis*. *Dev Cell*, 2016. **37**(4): p. 337-349.
260. Arakawa, S., et al., *Role of Atg5-dependent cell death in the embryonic development of Bax/Bak double-knockout mice*. *Cell Death Differ*, 2017. **24**(9): p. 1598-1608.
261. Arakawa, S., et al., *Molecular mechanisms and physiological roles of Atg5/Atg7-independent alternative autophagy*. *Proc Jpn Acad Ser B Phys Biol Sci*, 2017. **93**(6): p. 378-385.
262. Berridge, M.J., M.D. Bootman, and P. Lipp, *Calcium--a life and death signal*. *Nature*, 1998. **395**(6703): p. 645-8.
263. Berridge, M.J., *Inositol trisphosphate and calcium signalling*. *Nature*, 1993. **361**(6410): p. 315-25.
264. Berridge, M.J., P. Lipp, and M.D. Bootman, *The versatility and universality of calcium signalling*. *Nat Rev Mol Cell Biol*, 2000. **1**(1): p. 11-21.
265. Qian, T., B. Herman, and J.J. Lemasters, *The mitochondrial permeability transition mediates both necrotic and apoptotic death of hepatocytes exposed to Br-A23187*. *Toxicol Appl Pharmacol*, 1999. **154**(2): p. 117-25.

266. Cerella, C., M. Diederich, and L. Ghibelli, *The dual role of calcium as messenger and stressor in cell damage, death, and survival*. Int J Cell Biol, 2010. **2010**: p. 546163.
267. Richter, C., *Pro-oxidants and mitochondrial Ca²⁺: their relationship to apoptosis and oncogenesis*. FEBS Lett, 1993. **325**(1-2): p. 104-7.
268. Syntichaki, P., et al., *Specific aspartyl and calpain proteases are required for neurodegeneration in C. elegans*. Nature, 2002. **419**(6910): p. 939-44.
269. Neumar, R.W., et al., *Cross-talk between calpain and caspase proteolytic systems during neuronal apoptosis*. J Biol Chem, 2003. **278**(16): p. 14162-7.
270. Yousefi, S., et al., *Calpain-mediated cleavage of Atg5 switches autophagy to apoptosis*. Nat Cell Biol, 2006. **8**(10): p. 1124-32.
271. Xia, H.G., et al., *Control of basal autophagy by calpain1 mediated cleavage of ATG5*. Autophagy, 2010. **6**(1): p. 61-6.
272. Kass, G.E. and S. Orrenius, *Calcium signaling and cytotoxicity*. Environ Health Perspect, 1999. **107 Suppl 1**(Suppl 1): p. 25-35.
273. Pakos-Zebrucka, K., et al., *The integrated stress response*. EMBO Rep, 2016. **17**(10): p. 1374-1395.
274. Bahar, E., H. Kim, and H. Yoon, *ER Stress-Mediated Signaling: Action Potential and Ca(2+) as Key Players*. Int J Mol Sci, 2016. **17**(9).
275. Szegezdi, E., et al., *Mediators of endoplasmic reticulum stress-induced apoptosis*. EMBO Rep, 2006. **7**(9): p. 880-5.
276. Rutkowski, D.T., et al., *Adaptation to ER stress is mediated by differential stabilities of pro-survival and pro-apoptotic mRNAs and proteins*. PLoS Biol, 2006. **4**(11): p. e374.
277. Morishima, N., et al., *An endoplasmic reticulum stress-specific caspase cascade in apoptosis. Cytochrome c-independent activation of caspase-9 by caspase-12*. J Biol Chem, 2002. **277**(37): p. 34287-94.
278. Bravo, R., et al., *Endoplasmic reticulum and the unfolded protein response: dynamics and metabolic integration*. Int Rev Cell Mol Biol, 2013. **301**: p. 215-90.
279. Nishitoh, H., et al., *ASK1 is essential for endoplasmic reticulum stress-induced neuronal cell death triggered by expanded polyglutamine repeats*. Genes Dev, 2002. **16**(11): p. 1345-55.
280. Urra, H., et al., *When ER stress reaches a dead end*. Biochim Biophys Acta, 2013. **1833**(12): p. 3507-3517.
281. Haze, K., et al., *Mammalian transcription factor ATF6 is synthesized as a transmembrane protein and activated by proteolysis in response to endoplasmic reticulum stress*. Mol Biol Cell, 1999. **10**(11): p. 3787-99.
282. Harding, H.P., Y. Zhang, and D. Ron, *Protein translation and folding are coupled by an endoplasmic-reticulum-resident kinase*. Nature, 1999. **397**(6716): p. 271-4.
283. Vannuvel, K., et al., *Functional and morphological impact of ER stress on mitochondria*. J Cell Physiol, 2013. **228**(9): p. 1802-18.
284. Ameri, K. and A.L. Harris, *Activating transcription factor 4*. Int J Biochem Cell Biol, 2008. **40**(1): p. 14-21.
285. Han, J., et al., *ER-stress-induced transcriptional regulation increases protein synthesis leading to cell death*. Nat Cell Biol, 2013. **15**(5): p. 481-90.

286. McCullough, K.D., et al., *Gadd153 sensitizes cells to endoplasmic reticulum stress by down-regulating Bcl2 and perturbing the cellular redox state*. Mol Cell Biol, 2001. **21**(4): p. 1249-59.
287. Baffy, G., et al., *Apoptosis induced by withdrawal of interleukin-3 (IL-3) from an IL-3-dependent hematopoietic cell line is associated with repartitioning of intracellular calcium and is blocked by enforced Bcl-2 oncoprotein production*. J Biol Chem, 1993. **268**(9): p. 6511-9.
288. Lam, M., et al., *Evidence that BCL-2 represses apoptosis by regulating endoplasmic reticulum-associated Ca²⁺ fluxes*. Proc Natl Acad Sci U S A, 1994. **91**(14): p. 6569-73.
289. Annis, M.G., et al., *Endoplasmic reticulum localized Bcl-2 prevents apoptosis when redistribution of cytochrome c is a late event*. Oncogene, 2001. **20**(16): p. 1939-52.
290. Pinton, P., et al., *The Ca²⁺ concentration of the endoplasmic reticulum is a key determinant of ceramide-induced apoptosis: significance for the molecular mechanism of Bcl-2 action*. Embo j, 2001. **20**(11): p. 2690-701.
291. Rudner, J., et al., *Wild-type, mitochondrial and ER-restricted Bcl-2 inhibit DNA damage-induced apoptosis but do not affect death receptor-induced apoptosis*. J Cell Sci, 2001. **114**(Pt 23): p. 4161-72.
292. Nutt, L.K., et al., *Bax and Bak promote apoptosis by modulating endoplasmic reticular and mitochondrial Ca²⁺ stores*. J Biol Chem, 2002. **277**(11): p. 9219-25.
293. Zong, W.X., et al., *Bax and Bak can localize to the endoplasmic reticulum to initiate apoptosis*. J Cell Biol, 2003. **162**(1): p. 59-69.
294. Chami, M., et al., *Bcl-2 and Bax exert opposing effects on Ca²⁺ signaling, which do not depend on their putative pore-forming region*. J Biol Chem, 2004. **279**(52): p. 54581-9.
295. Shi, J., L.F. Parada, and S.G. Kernie, *Bax limits adult neural stem cell persistence through caspase and IP3 receptor activation*. Cell Death Differ, 2005. **12**(12): p. 1601-12.
296. Scorrano, L., et al., *BAX and BAK regulation of endoplasmic reticulum Ca²⁺: a control point for apoptosis*. Science, 2003. **300**(5616): p. 135-9.
297. Foskett, J.K., et al., *Inositol trisphosphate receptor Ca²⁺ release channels*. Physiol Rev, 2007. **87**(2): p. 593-658.
298. Zalk, R., S.E. Lehnart, and A.R. Marks, *Modulation of the ryanodine receptor and intracellular calcium*. Annu Rev Biochem, 2007. **76**: p. 367-85.
299. Pinton, P., et al., *Calcium and apoptosis: ER-mitochondria Ca²⁺ transfer in the control of apoptosis*. Oncogene, 2008. **27**(50): p. 6407-18.
300. Krebs, J., L.B. Agellon, and M. Michalak, *Ca(2+) homeostasis and endoplasmic reticulum (ER) stress: An integrated view of calcium signaling*. Biochem Biophys Res Commun, 2015. **460**(1): p. 114-21.
301. Rong, Y.P., et al., *Targeting Bcl-2-IP3 receptor interaction to reverse Bcl-2's inhibition of apoptotic calcium signals*. Mol Cell, 2008. **31**(2): p. 255-65.
302. Heath-Engel, H.M., N.C. Chang, and G.C. Shore, *The endoplasmic reticulum in apoptosis and autophagy: role of the BCL-2 protein family*. Oncogene, 2008. **27**(50): p. 6419-33.
303. Nakayama, T., et al., *The regulatory domain of the inositol 1,4,5-trisphosphate receptor is necessary to keep the channel domain closed: possible physiological significance of specific cleavage by caspase 3*. Biochem J, 2004. **377**(Pt 2): p. 299-307.

304. Assefa, Z., et al., *Caspase-3-induced truncation of type 1 inositol trisphosphate receptor accelerates apoptotic cell death and induces inositol trisphosphate-independent calcium release during apoptosis*. J Biol Chem, 2004. **279**(41): p. 43227-36.
305. Schulman, J.J., et al., *The Bcl-2 protein family member Bok binds to the coupling domain of inositol 1,4,5-trisphosphate receptors and protects them from proteolytic cleavage*. J Biol Chem, 2013. **288**(35): p. 25340-9.
306. Boehning, D., et al., *Cytochrome c binds to inositol (1,4,5) trisphosphate receptors, amplifying calcium-dependent apoptosis*. Nat Cell Biol, 2003. **5**(12): p. 1051-61.
307. Høyer-Hansen, M., et al., *Control of macroautophagy by calcium, calmodulin-dependent kinase kinase-beta, and Bcl-2*. Mol Cell, 2007. **25**(2): p. 193-205.
308. Vicencio, J.M., et al., *The inositol 1,4,5-trisphosphate receptor regulates autophagy through its interaction with Beclin 1*. Cell Death Differ, 2009. **16**(7): p. 1006-17.
309. Shlomovitz, I., M. Speir, and M. Gerlic, *Flipping the dogma - phosphatidylserine in non-apoptotic cell death*. Cell Commun Signal, 2019. **17**(1): p. 139.
310. Levi-Montalcini, R. and B. Booker, *DESTRUCTION OF THE SYMPATHETIC GANGLIA IN MAMMALS BY AN ANTISERUM TO A NERVE-GROWTH PROTEIN*. Proc Natl Acad Sci U S A, 1960. **46**(3): p. 384-91.
311. Johnstone, A.D., *Developmental neurodegeneration requires axoplasmic Ca²⁺ influx via Trpv1*, in *Integrated Program in Neuroscience*. 2018, McGill. p. 131.
312. Deckwerth, T.L. and E.M. Johnson, Jr., *Neurotrophic factor deprivation-induced death*. Ann N Y Acad Sci, 1993. **679**: p. 121-31.
313. Wang, J.T., Z.A. Medress, and B.A. Barres, *Axon degeneration: molecular mechanisms of a self-destruction pathway*. J Cell Biol, 2012. **196**(1): p. 7-18.
314. Kristiansen, M. and J. Ham, *Programmed cell death during neuronal development: the sympathetic neuron model*. Cell Death Differ, 2014. **21**(7): p. 1025-35.
315. Edwards, S.N., A.E. Buckmaster, and A.M. Tolkovsky, *The death programme in cultured sympathetic neurones can be suppressed at the posttranslational level by nerve growth factor, cyclic AMP, and depolarization*. J Neurochem, 1991. **57**(6): p. 2140-3.
316. Simon, D.J., et al., *Axon Degeneration Gated by Retrograde Activation of Somatic Pro-apoptotic Signaling*. Cell, 2016. **164**(5): p. 1031-45.
317. Brunet, A., et al., *Akt promotes cell survival by phosphorylating and inhibiting a Forkhead transcription factor*. Cell, 1999. **96**(6): p. 857-68.
318. Ngok-Ngam, P., et al., *Pharmacological inhibition of GSK3 attenuates DNA damage-induced apoptosis via reduction of p53 mitochondrial translocation and Bax oligomerization in neuroblastoma SH-SY5Y cells*. Cell Mol Biol Lett, 2013. **18**(1): p. 58-74.
319. Chen, M., et al., *Spatially coordinated kinase signaling regulates local axon degeneration*. J Neurosci, 2012. **32**(39): p. 13439-53.
320. Ghosh, A.S., et al., *DLK induces developmental neuronal degeneration via selective regulation of proapoptotic JNK activity*. J Cell Biol, 2011. **194**(5): p. 751-64.
321. Huntwork-Rodriguez, S., et al., *JNK-mediated phosphorylation of DLK suppresses its ubiquitination to promote neuronal apoptosis*. J Cell Biol, 2013. **202**(5): p. 747-63.
322. Larhammar, M., et al., *Dual leucine zipper kinase-dependent PERK activation contributes to neuronal degeneration following insult*. Elife, 2017. **6**.

323. Zareen, N., S.C. Biswas, and L.A. Greene, *A feed-forward loop involving Trib3, Akt and FoxO mediates death of NGF-deprived neurons*. Cell Death Differ, 2013. **20**(12): p. 1719-30.
324. Rajagopal, R. and M.V. Chao, *A role for Fyn in Trk receptor transactivation by G-protein-coupled receptor signaling*. Mol Cell Neurosci, 2006. **33**(1): p. 36-46.
325. Nishizuka, Y., *Intracellular signaling by hydrolysis of phospholipids and activation of protein kinase C*. Science, 1992. **258**(5082): p. 607-14.
326. Hansen, M., et al., *A role for phospholipase C activity but not ryanodine receptors in the initiation and propagation of intercellular calcium waves*. J Cell Sci, 1995. **108 (Pt 7)**: p. 2583-90.
327. Patterson, R.L., et al., *Phospholipase C-gamma: diverse roles in receptor-mediated calcium signaling*. Trends Biochem Sci, 2005. **30**(12): p. 688-97.
328. Land, M. and C.S. Rubin, *A Calcium- and Diacylglycerol-Stimulated Protein Kinase C (PKC), Caenorhabditis elegans PKC-2, Links Thermal Signals to Learned Behavior by Acting in Sensory Neurons and Intestinal Cells*. Mol Cell Biol, 2017. **37**(19).
329. Johnstone, A.D., et al., *Developmental Axon Degeneration Requires TRPV1-Dependent Ca(2+) Influx*. eNeuro, 2019. **6**(1).
330. Putney, J.W. and T. Tomita, *Phospholipase C signaling and calcium influx*. Adv Biol Regul, 2012. **52**(1): p. 152-64.
331. Nikolaev, A., et al., *APP binds DR6 to trigger axon pruning and neuron death via distinct caspases*. Nature, 2009. **457**(7232): p. 981-9.
332. Olsen, O., et al., *Genetic analysis reveals that amyloid precursor protein and death receptor 6 function in the same pathway to control axonal pruning independent of beta-secretase*. J Neurosci, 2014. **34**(19): p. 6438-47.
333. Nishimura, I., et al., *Upregulation and antiapoptotic role of endogenous Alzheimer amyloid precursor protein in dorsal root ganglion neurons*. Exp Cell Res, 2003. **286**(2): p. 241-51.
334. Matrone, C., et al., *APP is phosphorylated by TrkA and regulates NGF/TrkA signaling*. J Neurosci, 2011. **31**(33): p. 11756-61.
335. Triaca, V., et al., *NGF controls APP cleavage by downregulating APP phosphorylation at Thr668: relevance for Alzheimer's disease*. Aging Cell, 2016. **15**(4): p. 661-72.
336. Zeng, L., et al., *Death receptor 6 induces apoptosis not through type I or type II pathways, but via a unique mitochondria-dependent pathway by interacting with Bax protein*. J Biol Chem, 2012. **287**(34): p. 29125-33.
337. Martin, D.P., et al., *Inhibitors of protein synthesis and RNA synthesis prevent neuronal death caused by nerve growth factor deprivation*. J Cell Biol, 1988. **106**(3): p. 829-44.
338. Cosker, K.E., et al., *Target-derived neurotrophins coordinate transcription and transport of bclw to prevent axonal degeneration*. J Neurosci, 2013. **33**(12): p. 5195-207.
339. Maor-Nof, M., et al., *Axonal Degeneration Is Regulated by a Transcriptional Program that Coordinates Expression of Pro- and Anti-degenerative Factors*. Neuron, 2016. **92**(5): p. 991-1006.
340. Fuenzalida, K., et al., *Peroxisome proliferator-activated receptor gamma up-regulates the Bcl-2 anti-apoptotic protein in neurons and induces mitochondrial stabilization and protection against oxidative stress and apoptosis*. J Biol Chem, 2007. **282**(51): p. 37006-15.

341. Pazyra-Murphy, M.F., et al., *A retrograde neuronal survival response: target-derived neurotrophins regulate MEF2D and bcl-w.* J Neurosci, 2009. **29**(20): p. 6700-9.
342. Courchesne, S.L., et al., *Sensory neuropathy attributable to loss of Bcl-w.* J Neurosci, 2011. **31**(5): p. 1624-34.
343. Cosker, K.E., et al., *The RNA-binding protein SFPQ orchestrates an RNA regulon to promote axon viability.* Nat Neurosci, 2016. **19**(5): p. 690-696.
344. Honarpour, N., et al., *Embryonic neuronal death due to neurotrophin and neurotransmitter deprivation occurs independent of Apaf-1.* Neuroscience, 2001. **106**(2): p. 263-74.
345. Oppenheim, R.W., et al., *Developing postmitotic mammalian neurons in vivo lacking Apaf-1 undergo programmed cell death by a caspase-independent, nonapoptotic pathway involving autophagy.* J Neurosci, 2008. **28**(6): p. 1490-7.
346. Johnson, C.E., et al., *Differential Apaf-1 levels allow cytochrome c to induce apoptosis in brain tumors but not in normal neural tissues.* Proc Natl Acad Sci U S A, 2007. **104**(52): p. 20820-5.
347. Rudhard, Y., et al., *Identification of 12/15-lipoxygenase as a regulator of axon degeneration through high-content screening.* J Neurosci, 2015. **35**(7): p. 2927-41.
348. Vohra, B.P., et al., *Amyloid precursor protein cleavage-dependent and -independent axonal degeneration programs share a common nicotinamide mononucleotide adenylyltransferase 1-sensitive pathway.* J Neurosci, 2010. **30**(41): p. 13729-38.
349. Julien, O. and J.A. Wells, *Caspases and their substrates.* Cell Death Differ, 2017. **24**(8): p. 1380-1389.
350. Hertz, N.T., et al., *Neuronally Enriched RUFY3 Is Required for Caspase-Mediated Axon Degeneration.* Neuron, 2019. **103**(3): p. 412-422. e4.
351. Kato, M., et al., *Caspases cleave the amino-terminal calpain inhibitory unit of calpastatin during apoptosis in human Jurkat T cells.* The Journal of Biochemistry, 2000. **127**(2): p. 297-305.
352. Porn-Ares, M., Samali A, and Orrenius S. Cleavage of the calpain inhibitor, calpastatin, during apoptosis. Cell Death Differ, 1998. **5**: p. 1028-1033.
353. Wang, K.K., et al., *Caspase-mediated fragmentation of calpain inhibitor protein calpastatin during apoptosis.* Archives of biochemistry and biophysics, 1998. **356**(2): p. 187-196.
354. Yang, J., et al., *Regulation of axon degeneration after injury and in development by the endogenous calpain inhibitor calpastatin.* Neuron, 2013. **80**(5): p. 1175-1189.
355. Takano, J., et al., *Calpain Mediates Excitotoxic DNA Fragmentation via Mitochondrial Pathways in Adult Brains EVIDENCE FROM CALPASTATIN MUTANT MICE.* Journal of Biological Chemistry, 2005. **280**(16): p. 16175-16184.
356. Schlaepfer, W.W., *Calcium-induced degeneration of axoplasm in isolated segments of rat peripheral nerve.* Brain research, 1974. **69**(2): p. 203-215.
357. George, E.B., J.D. Glass, and J.W. Griffin, *Axotomy-induced axonal degeneration is mediated by calcium influx through ion-specific channels.* Journal of Neuroscience, 1995. **15**(10): p. 6445-6452.
358. LoPachin, R.M. and E.J. Lehning, *Mechanism of calcium entry during axon injury and degeneration.* Toxicology and applied pharmacology, 1997. **143**(2): p. 233-244.
359. Barrientos, S.A., et al., *Axonal degeneration is mediated by the mitochondrial permeability transition pore.* Journal of Neuroscience, 2011. **31**(3): p. 966-978.

360. Johnstone, A.D., et al., *A novel method for quantifying axon degeneration*. PLoS One, 2018. **13**(7): p. e0199570.
361. Vaughn, A.E. and M. Deshmukh, *Glucose metabolism inhibits apoptosis in neurons and cancer cells by redox inactivation of cytochrome c*. Nature cell biology, 2008. **10**(12): p. 1477-1483.
362. Kirkland, R.A. and J.L. Franklin, *Evidence for redox regulation of cytochrome C release during programmed neuronal death: antioxidant effects of protein synthesis and caspase inhibition*. J Neurosci, 2001. **21**(6): p. 1949-63.
363. Kirkland, R.A. and J.L. Franklin, *Bax, reactive oxygen, and cytochrome c release in neuronal apoptosis*. Antioxidants and Redox Signaling, 2003. **5**(5): p. 589-596.
364. Kirkland, R.A., et al., *A Bax-induced pro-oxidant state is critical for cytochrome c release during programmed neuronal death*. J Neurosci, 2002. **22**(15): p. 6480-90.
365. Greenlund, L.J., T.L. Deckwerth, and E.M. Johnson Jr, *Superoxide dismutase delays neuronal apoptosis: a role for reactive oxygen species in programmed neuronal death*. Neuron, 1995. **14**(2): p. 303-315.
366. Kristiansen, M., et al., *Global analysis of gene expression in NGF-deprived sympathetic neurons identifies molecular pathways associated with cell death*. BMC genomics, 2011. **12**(1): p. 551.
367. Potts, P.R., et al., *Critical function of endogenous XIAP in regulating caspase activation during sympathetic neuronal apoptosis*. J Cell Biol, 2003. **163**(4): p. 789-99.
368. Hiramatsu, N., et al., *Translational and posttranslational regulation of XIAP by eIF2 α and ATF4 promotes ER stress-induced cell death during the unfolded protein response*. Molecular biology of the cell, 2014. **25**(9): p. 1411-1420.
369. Chang, L.K. and E.M. Johnson, Jr., *Cyclosporin A inhibits caspase-independent death of NGF-deprived sympathetic neurons: a potential role for mitochondrial permeability transition*. J Cell Biol, 2002. **157**(5): p. 771-81.
370. Chang, L.K., R.E. Schmidt, and E.M. Johnson, Jr., *Alternating metabolic pathways in NGF-deprived sympathetic neurons affect caspase-independent death*. J Cell Biol, 2003. **162**(2): p. 245-56.
371. Goldgaber, D., et al., *Characterization and chromosomal localization of a cDNA encoding brain amyloid of Alzheimer's disease*. Science, 1987. **235**(4791): p. 877-80.
372. Kang, J., et al., *The precursor of Alzheimer's disease amyloid A4 protein resembles a cell-surface receptor*. Nature, 1987. **325**(6106): p. 733-6.
373. Tanzi, R.E., et al., *Amyloid beta protein gene: cDNA, mRNA distribution, and genetic linkage near the Alzheimer locus*. Science, 1987. **235**(4791): p. 880-884.
374. Hunter, S. and C. Brayne, *Understanding the roles of mutations in the amyloid precursor protein in Alzheimer disease*. Molecular Psychiatry, 2018. **23**(1): p. 81-93.
375. Yoshikai, S.-i., et al., *Genomic organization of the human amyloid beta-protein precursor gene*. Gene, 1990. **87**(2): p. 257-263.
376. Lamb, B.T., et al., *Introduction and expression of the 400 kilobase precursor amyloid protein gene in transgenic mice*. Nature genetics, 1993. **5**(1): p. 22-30.
377. Shariati, S.A.M. and B. De Strooper, *Redundancy and divergence in the amyloid precursor protein family*. FEBS letters, 2013. **587**(13): p. 2036-2045.
378. Barber, R.C., *The genetics of Alzheimer's disease*. Scientifica, 2012. **2012**.

379. Lorent, K., et al., *Expression in mouse embryos and in adult mouse brain of three members of the amyloid precursor protein family, of the alpha-2-macroglobulin receptor/low density lipoprotein receptor-related protein and of its ligands apolipoprotein E, lipoprotein lipase, alpha-2-macroglobulin and the 40,000 molecular weight receptor-associated protein*. Neuroscience, 1995. **65**(4): p. 1009-1025.
380. Sarasa, M., et al., *Alzheimer beta-amyloid precursor proteins display specific patterns of expression during embryogenesis*. Mech Dev, 2000. **94**(1-2): p. 233-6.
381. Ott, M.O. and S.L. Bullock, *A gene trap insertion reveals that amyloid precursor protein expression is a very early event in murine embryogenesis*. Dev Genes Evol, 2001. **211**(7): p. 355-7.
382. Gralle, M. and S.T. Ferreira, *Structure and functions of the human amyloid precursor protein: the whole is more than the sum of its parts*. Prog Neurobiol, 2007. **82**(1): p. 11-32.
383. Wasco, W., R. Tanzi, and J. Brook, *The amyloid precursor-like protein (APLP) gene maps to the long arm of human chromosome 19*. Genomics;(United States), 1993. **15**(1).
384. von der Kammer, H., et al., *The gene for the amyloid precursor-like protein APLP2 is assigned to human chromosome 11q23-q25*. Genomics, 1994. **20**(2): p. 308-311.
385. Sandbrink, R., C. Masters, and K. Beyreuther, *APP Gene Family Alternative Splicing Generates Functionally Related Isoforms a*. Annals of the New York Academy of Sciences, 1996. **777**(1): p. 281-287.
386. Daigle, I. and C.a.-. Li, *apl-1, a Caenorhabditis elegans gene encoding a protein related to the human beta-amyloid protein precursor*. Proceedings of the National Academy of Sciences, 1993. **90**(24): p. 12045-12049.
387. Walsh, D., et al., *The APP family of proteins: similarities and differences*. Biochemical Society Transactions, 2007. **35**(2): p. 416-420.
388. Cousins, S.L., W. Dai, and F.A. Stephenson, *APLP 1 and APLP 2, members of the APP family of proteins, behave similarly to APP in that they associate with NMDA receptors and enhance NMDA receptor surface expression*. Journal of neurochemistry, 2015. **133**(6): p. 879-885.
389. Slunt, H.H., et al., *Expression of a ubiquitous, cross-reactive homologue of the mouse beta-amyloid precursor protein (APP)*. J Biol Chem, 1994. **269**(4): p. 2637-44.
390. Botelho, M.G., et al., *Folding and stability of the extracellular domain of the human amyloid precursor protein*. Journal of Biological Chemistry, 2003. **278**(36): p. 34259-34267.
391. Gralle, M., et al., *Solution studies and structural model of the extracellular domain of the human amyloid precursor protein*. Biophysical journal, 2002. **83**(6): p. 3513-3524.
392. Khalifa, N.B., et al., *Structural features of the KPI domain control APP dimerization, trafficking, and processing*. The FASEB Journal, 2012. **26**(2): p. 855-867.
393. Sinha, S., et al., *The protease inhibitory properties of the Alzheimer's beta-amyloid precursor protein*. Journal of Biological Chemistry, 1990. **265**(16): p. 8983-8985.
394. Kerr, M.L. and D.H. Small, *Cytoplasmic domain of the β -amyloid protein precursor of Alzheimer's disease: Function, regulation of proteolysis, and implications for drug development*. Journal of neuroscience research, 2005. **80**(2): p. 151-159.

395. Baumkötter, F., et al., *Amyloid precursor protein dimerization and synaptogenic function depend on copper binding to the growth factor-like domain*. Journal of Neuroscience, 2014. **34**(33): p. 11159-11172.
396. Wang, Z., et al., *Presynaptic and postsynaptic interaction of the amyloid precursor protein promotes peripheral and central synaptogenesis*. Journal of Neuroscience, 2009. **29**(35): p. 10788-10801.
397. Muller, U.C. and H. Zheng, *Physiological functions of APP family proteins*. Cold Spring Harb Perspect Med, 2012. **2**(2): p. a006288.
398. Ling, Y., K. Morgan, and N. Kalsheker, *Amyloid precursor protein (APP) and the biology of proteolytic processing: relevance to Alzheimer's disease*. Int J Biochem Cell Biol, 2003. **35**(11): p. 1505-35.
399. Haass, C., et al., *Trafficking and proteolytic processing of APP*. Cold Spring Harb Perspect Med, 2012. **2**(5): p. a006270.
400. Agostinho, P., et al., *Localization and trafficking of amyloid- β protein precursor and secretases: Impact on Alzheimer's disease*. Journal of Alzheimer's Disease, 2015. **45**(2): p. 329-347.
401. Nunan, J. and D.H. Small, *Regulation of APP cleavage by α -, β - and γ -secretases*. FEBS letters, 2000. **483**(1): p. 6-10.
402. Koo, E.H. and P. Greengard, *Phorbol esters affect multiple steps in β -amyloid precursor protein trafficking and amyloid β -protein production*. Molecular Medicine, 1997. **3**(3): p. 204-211.
403. Buxbaum, J.D., et al., *Evidence that tumor necrosis factor α converting enzyme is involved in regulated α -secretase cleavage of the Alzheimer amyloid protein precursor*. Journal of Biological Chemistry, 1998. **273**(43): p. 27765-27767.
404. Kuhn, P.H., et al., *ADAM10 is the physiologically relevant, constitutive α -secretase of the amyloid precursor protein in primary neurons*. The EMBO journal, 2010. **29**(17): p. 3020-3032.
405. Zhu, G., et al., *Protein kinase C ϵ suppresses $A\beta$ production and promotes activation of α -secretase*. Biochemical and biophysical research communications, 2001. **285**(4): p. 997-1006.
406. Skovronsky, D.M., et al., *Protein kinase C-dependent α -secretase competes with β -secretase for cleavage of amyloid- β precursor protein in the trans-Golgi network*. Journal of Biological Chemistry, 2000. **275**(4): p. 2568-2575.
407. Parvathy, S., et al., *Cleavage of Alzheimer's amyloid precursor protein by α -secretase occurs at the surface of neuronal cells*. Biochemistry, 1999. **38**(30): p. 9728-9734.
408. Vassar, R., et al., *β -Secretase cleavage of Alzheimer's amyloid precursor protein by the transmembrane aspartic protease BACE*. science, 1999. **286**(5440): p. 735-741.
409. Dobrowolska, J.A., et al., *CNS amyloid- β , soluble APP- α and- β kinetics during BACE inhibition*. Journal of Neuroscience, 2014. **34**(24): p. 8336-8346.
410. LaFerla, F.M., K.N. Green, and S. Oddo, *Intracellular amyloid-beta in Alzheimer's disease*. Nat Rev Neurosci, 2007. **8**(7): p. 499-509.
411. Murphy, M.P. and H. LeVine III, *Alzheimer's disease and the amyloid- β peptide*. Journal of Alzheimer's disease, 2010. **19**(1): p. 311-323.

412. Kimberly, W.T., et al., *γ -Secretase is a membrane protein complex comprised of presenilin, nicastrin, aph-1, and pen-2*. Proceedings of the National Academy of Sciences, 2003. **100**(11): p. 6382-6387.
413. Wakabayashi, T. and B. De Strooper, *Presenilins: members of the γ -secretase quartets, but part-time soloists too*. Physiology, 2008. **23**(4): p. 194-204.
414. Thinakaran, G., et al., *Endoproteolysis of presenilin 1 and accumulation of processed derivatives in vivo*. Neuron, 1996. **17**(1): p. 181-190.
415. Dries, D.R. and G. Yu, *Assembly, maturation, and trafficking of the γ -secretase complex in Alzheimer's disease*. Current Alzheimer Research, 2008. **5**(2): p. 132-146.
416. Wolfe, M.S., et al., *Two transmembrane aspartates in presenilin-1 required for presenilin endoproteolysis and γ -secretase activity*. Nature, 1999. **398**(6727): p. 513-517.
417. Konietzko, U., *AICD nuclear signaling and its possible contribution to Alzheimer's disease*. Current Alzheimer research, 2012. **9**(2): p. 200-216.
418. Pardossi-Piquard, R. and F. Checler, *The physiology of the β -amyloid precursor protein intracellular domain AICD*. Journal of neurochemistry, 2012. **120**: p. 109-124.
419. Andrew, R.J., et al., *A Greek tragedy: the growing complexity of Alzheimer amyloid precursor protein proteolysis*. Journal of Biological Chemistry, 2016. **291**(37): p. 19235-19244.
420. Willem, M., et al., *η -Secretase processing of APP inhibits neuronal activity in the hippocampus*. Nature, 2015. **526**(7573): p. 443-447.
421. Pellegrini, L., et al., *Alternative, non-secretase processing of Alzheimer's β -amyloid precursor protein during apoptosis by caspase-6 and-8*. Journal of Biological Chemistry, 1999. **274**(30): p. 21011-21016.
422. Gervais, F.G., et al., *Involvement of caspases in proteolytic cleavage of Alzheimer's amyloid- β precursor protein and amyloidogenic A β peptide formation*. Cell, 1999. **97**(3): p. 395-406.
423. Weidemann, A., et al., *Proteolytic processing of the Alzheimer's disease amyloid precursor protein within its cytoplasmic domain by caspase-like proteases*. Journal of Biological Chemistry, 1999. **274**(9): p. 5823-5829.
424. Lu, D.C., et al., *A second cytotoxic proteolytic peptide derived from amyloid β -protein precursor*. Nature medicine, 2000. **6**(4): p. 397-404.
425. Xu, H., et al., *Generation of Alzheimer beta-amyloid protein in the trans-Golgi network in the apparent absence of vesicle formation*. Proc Natl Acad Sci U S A, 1997. **94**(8): p. 3748-52.
426. Thinakaran, G. and E.H. Koo, *Amyloid precursor protein trafficking, processing, and function*. Journal of Biological Chemistry, 2008. **283**(44): p. 29615-29619.
427. Lai, A., S.S. Sisodia, and I.S. Trowbridge, *Characterization of sorting signals in the β -amyloid precursor protein cytoplasmic domain*. Journal of Biological Chemistry, 1995. **270**(8): p. 3565-3573.
428. Marquez-Sterling, N.R., et al., *Trafficking of cell-surface β -amyloid precursor protein: evidence that a sorting intermediate participates in synaptic vesicle recycling*. Journal of Neuroscience, 1997. **17**(1): p. 140-151.
429. Schon, E.A. and E. Area-Gomez, *Mitochondria-associated ER membranes in Alzheimer disease*. Molecular and Cellular Neuroscience, 2013. **55**: p. 26-36.

430. Pera, M., et al., *Increased localization of APP-C99 in mitochondria-associated ER membranes causes mitochondrial dysfunction in Alzheimer disease*. The EMBO journal, 2017. **36**(22): p. 3356-3371.
431. Pavlov, P.F., et al., *Mitochondrial accumulation of APP and A β : significance for Alzheimer disease pathogenesis*. Journal of cellular and molecular medicine, 2009. **13**(10): p. 4137-4145.
432. Yamazaki, T., D.J. Selkoe, and E.H. Koo, *Trafficking of cell surface beta-amyloid precursor protein: retrograde and transcytotic transport in cultured neurons*. The Journal of cell biology, 1995. **129**(2): p. 431-442.
433. Kamenetz, F., et al., *APP processing and synaptic function*. Neuron, 2003. **37**(6): p. 925-937.
434. DeBoer, S.R., et al., *Differential release of beta-amyloid from dendrite- versus axon-targeted APP*. J Neurosci, 2014. **34**(37): p. 12313-27.
435. Brunholz, S., et al., *Axonal transport of APP and the spatial regulation of APP cleavage and function in neuronal cells*. Experimental brain research, 2012. **217**(3-4): p. 353-364.
436. Dickens, M., et al., *A cytoplasmic inhibitor of the JNK signal transduction pathway*. Science, 1997. **277**(5326): p. 693-696.
437. Fu, M.-m. and E.L. Holzbaur, *JIP1 regulates the directionality of APP axonal transport by coordinating kinesin and dynein motors*. Journal of Cell Biology, 2013. **202**(3): p. 495-508.
438. Szodorai, A., et al., *APP anterograde transport requires Rab3A GTPase activity for assembly of the transport vesicle*. Journal of Neuroscience, 2009. **29**(46): p. 14534-14544.
439. Goldsbury, C., et al., *Inhibition of APP trafficking by tau protein does not increase the generation of amyloid- β peptides*. Traffic, 2006. **7**(7): p. 873-888.
440. Lazarov, O., et al., *Axonal transport, amyloid precursor protein, kinesin-1, and the processing apparatus: revisited*. Journal of Neuroscience, 2005. **25**(9): p. 2386-2395.
441. Stokin, G.B., et al., *Axonopathy and transport deficits early in the pathogenesis of Alzheimer's disease*. Science, 2005. **307**(5713): p. 1282-8.
442. Muresan, V. and Z. Ladescu Muresan, *Amyloid-beta precursor protein: Multiple fragments, numerous transport routes and mechanisms*. Exp Cell Res, 2015. **334**(1): p. 45-53.
443. Bai, Y., et al., *The in vivo brain interactome of the amyloid precursor protein*. Molecular & Cellular Proteomics, 2008. **7**(1): p. 15-34.
444. Deyts, C., G. Thinakaran, and A.T. Parent, *APP Receptor? To Be or Not To Be*. Trends Pharmacol Sci, 2016. **37**(5): p. 390-411.
445. Perreau, V.M., et al., *A domain level interaction network of amyloid precursor protein and A β of Alzheimer's disease*. Proteomics, 2010. **10**(12): p. 2377-2395.
446. Müller, U.C., T. Deller, and M. Korte, *Not just amyloid: physiological functions of the amyloid precursor protein family*. Nature Reviews Neuroscience, 2017. **18**(5): p. 281-298.
447. Guo, Q., et al., *APP physiological and pathophysiological functions: insights from animal models*. Cell Res, 2012. **22**(1): p. 78-89.
448. Caldwell, J.H., et al., *Roles of the amyloid precursor protein family in the peripheral nervous system*. Mechanisms of development, 2013. **130**(6-8): p. 433-446.
449. Bittner, T., et al., *Gamma-secretase inhibition reduces spine density in vivo via an amyloid precursor protein-dependent pathway*. J Neurosci, 2009. **29**(33): p. 10405-9.

450. Priller, C., et al., *Synapse formation and function is modulated by the amyloid precursor protein*. J Neurosci, 2006. **26**(27): p. 7212-21.
451. Lee, K.J., et al., *Beta amyloid-independent role of amyloid precursor protein in generation and maintenance of dendritic spines*. Neuroscience, 2010. **169**(1): p. 344-56.
452. Southam, K.A., et al., *Knockout of amyloid β protein precursor (APP) expression alters synaptogenesis, neurite branching and axonal morphology of hippocampal neurons*. Neurochemical research, 2019. **44**(6): p. 1346-1355.
453. Müller, U., et al., *Behavioral and anatomical deficits in mice homozygous for a modified β -amyloid precursor protein gene*. Cell, 1994. **79**(5): p. 755-765.
454. Zheng, H., et al., *beta-Amyloid precursor protein-deficient mice show reactive gliosis and decreased locomotor activity*. Cell, 1995. **81**(4): p. 525-31.
455. Ring, S., et al., *The secreted β -amyloid precursor protein ectodomain APP_s is sufficient to rescue the anatomical, behavioral, and electrophysiological abnormalities of APP-deficient mice*. Journal of Neuroscience, 2007. **27**(29): p. 7817-7826.
456. Magara, F., et al., *Genetic background changes the pattern of forebrain commissure defects in transgenic mice underexpressing the β -amyloid-precursor protein*. Proceedings of the National Academy of Sciences, 1999. **96**(8): p. 4656-4661.
457. Smith, K.D., et al., *Increased human wildtype tau attenuates axonal transport deficits caused by loss of APP in mouse models*. Magnetic resonance insights, 2010. **4**: p. MRI. S5237.
458. Smith, K.D.B., et al., *In vivo axonal transport rates decrease in a mouse model of Alzheimer's disease*. Neuroimage, 2007. **35**(4): p. 1401-1408.
459. Goldstein, L.S., *Axonal transport and neurodegenerative disease: can we see the elephant?* Prog Neurobiol, 2012. **99**(3): p. 186-90.
460. White, A.R., et al., *Copper levels are increased in the cerebral cortex and liver of APP and APLP2 knockout mice*. Brain research, 1999. **842**(2): p. 439-444.
461. Grimm, M.O., et al., *Regulation of cholesterol and sphingomyelin metabolism by amyloid- β and presenilin*. Nature cell biology, 2005. **7**(11): p. 1118-1123.
462. Needham, B., et al., *Identification of the Alzheimer's disease amyloid precursor protein (APP) and its homologue APLP2 as essential modulators of glucose and insulin homeostasis and growth*. The Journal of Pathology: A Journal of the Pathological Society of Great Britain and Ireland, 2008. **215**(2): p. 155-163.
463. Lyckman, A.W., et al., *Post-translational processing and turnover kinetics of presynaptically targeted amyloid precursor superfamily proteins in the central nervous system*. Journal of Biological Chemistry, 1998. **273**(18): p. 11100-11106.
464. Sisodia, S.S., et al., *Identification and transport of full-length amyloid precursor proteins in rat peripheral nervous system*. Journal of Neuroscience, 1993. **13**(7): p. 3136-3142.
465. Xu, D.-E., et al., *Amyloid precursor protein at node of Ranvier modulates nodal formation*. Cell adhesion & migration, 2014. **8**(4): p. 396-403.
466. Truong, P.H., et al., *Amyloid precursor protein and amyloid precursor-like protein 2 have distinct roles in modulating myelination, demyelination, and remyelination of axons*. Glia, 2019. **67**(3): p. 525-538.

467. Shukla, M., R. Quirion, and W. Ma, *Reduced expression of pain mediators and pain sensitivity in amyloid precursor protein over-expressing CRND8 transgenic mice*. Neuroscience, 2013. **250**: p. 92-101.
468. Zheng, H., et al., *APP Knockout and APP Over-Expression in Transgenic Mice*, in *Alzheimer Disease*. 1997, Springer. p. 133-136.
469. Heber, S., et al., *Mice with combined gene knock-outs reveal essential and partially redundant functions of amyloid precursor protein family members*. Journal of Neuroscience, 2000. **20**(21): p. 7951-7963.
470. Von Koch, C., et al., *Generation of APLP2 KO mice and early postnatal lethality in APLP2/APP double KO mice*. Neurobiology of aging, 1997. **18**(6): p. 661-669.
471. Herms, J., et al., *Cortical dysplasia resembling human type 2 lissencephaly in mice lacking all three APP family members*. EMBO J, 2004. **23**(20): p. 4106-15.
472. Salbaum, J.M. and F.H. Ruddle, *Embryonic expression pattern of amyloid protein precursor suggests a role in differentiation of specific subsets of neurons*. J Exp Zool, 1994. **269**(2): p. 116-27.
473. Ma, Q.H., et al., *A TAG1-APP signalling pathway through Fe65 negatively modulates neurogenesis*. Nat Cell Biol, 2008. **10**(3): p. 283-94.
474. Zhang, W., et al., *Amyloid precursor protein regulates neurogenesis by antagonizing miR-574-5p in the developing cerebral cortex*. Nat Commun, 2014. **5**: p. 3330.
475. Rice, H.C., et al., *Pancortins interact with amyloid precursor protein and modulate cortical cell migration*. Development, 2012. **139**(21): p. 3986-3996.
476. Hayashi, Y., et al., *Alzheimer amyloid protein precursor enhances proliferation of neural stem cells from fetal rat brain*. Biochem Biophys Res Commun, 1994. **205**(1): p. 936-43.
477. Ohsawa, I., et al., *Amino-terminal region of secreted form of amyloid precursor protein stimulates proliferation of neural stem cells*. European Journal of Neuroscience, 1999. **11**(6): p. 1907-1913.
478. Caillé, I., et al., *Soluble form of amyloid precursor protein regulates proliferation of progenitors in the adult subventricular zone*. Development, 2004. **131**(9): p. 2173-2181.
479. Demars, M.P., et al., *Soluble amyloid precursor protein: a novel proliferation factor of adult progenitor cells of ectodermal and mesodermal origin*. Stem cell research & therapy, 2011. **2**(4): p. 1-15.
480. Zhang, Y.-w., et al., *Presenilin/γ-secretase-dependent processing of β-amyloid precursor protein regulates EGF receptor expression*. Proceedings of the National Academy of Sciences, 2007. **104**(25): p. 10613-10618.
481. Ayuso-Sacido, A., et al., *Activated EGFR signaling increases proliferation, survival, and migration and blocks neuronal differentiation in post-natal neural stem cells*. Journal of neuro-oncology, 2010. **97**(3): p. 323-337.
482. Ghosal, K., A. Stathopoulos, and S.W. Pimplikar, *APP intracellular domain impairs adult neurogenesis in transgenic mice by inducing neuroinflammation*. PloS one, 2010. **5**(7): p. e11866.
483. Ma, Q.H., et al., *A TAG on to the neurogenic functions of APP*. Cell Adh Migr, 2008. **2**(1): p. 2-8.

484. Coronel, R., et al., *Neuronal and glial differentiation of human neural stem cells is regulated by amyloid precursor protein (APP) levels*. *Molecular neurobiology*, 2019. **56**(2): p. 1248-1261.
485. Coronel, R., et al., *Role of amyloid precursor protein (APP) and its derivatives in the biology and cell fate specification of neural stem cells*. *Molecular neurobiology*, 2018. **55**(9): p. 7107-7117.
486. Lee, I.-S., et al., *Amyloid- β oligomers regulate the properties of human neural stem cells through GSK-3 β signaling*. *Experimental & molecular medicine*, 2013. **45**(11): p. e60-e60.
487. Fonseca, M.B., et al., *Amyloid β peptides promote autophagy-dependent differentiation of mouse neural stem cells*. *Molecular neurobiology*, 2013. **48**(3): p. 829-840.
488. Chen, Y. and C. Dong, *Abeta40 promotes neuronal cell fate in neural progenitor cells*. *Cell Death Differ*, 2009. **16**(3): p. 386-94.
489. López-Toledano, M.A. and M.L. Shelanski, *Neurogenic effect of β -amyloid peptide in the development of neural stem cells*. *Journal of Neuroscience*, 2004. **24**(23): p. 5439-5444.
490. Young-Pearse, T.L., et al., *Secreted APP regulates the function of full-length APP in neurite outgrowth through interaction with integrin beta1*. *Neural development*, 2008. **3**(1): p. 1-14.
491. Milward, E.A., et al., *The amyloid protein precursor of Alzheimer's disease is a mediator of the effects of nerve growth factor on neurite outgrowth*. *Neuron*, 1992. **9**(1): p. 129-137.
492. Hoareau, C., et al., *Amyloid precursor protein cytoplasmic domain antagonizes reelin neurite outgrowth inhibition of hippocampal neurons*. *Neurobiology of aging*, 2008. **29**(4): p. 542-553.
493. Sabo, S.L., et al., *The amyloid precursor protein and its regulatory protein, FE65, in growth cones and synapses in vitro and in vivo*. *Journal of Neuroscience*, 2003. **23**(13): p. 5407-5415.
494. Cheung, H.N., et al., *FE65 interacts with ADP-ribosylation factor 6 to promote neurite outgrowth*. *Faseb j*, 2014. **28**(1): p. 337-49.
495. Magdesian, M.H., et al., *Secreted human amyloid precursor protein binds semaphorin 3a and prevents semaphorin-induced growth cone collapse*. *PLoS One*, 2011. **6**(7): p. e22857.
496. Västrik, I., et al., *Sema3A-induced growth-cone collapse is mediated by Rac1 amino acids 17–32*. *Current Biology*, 1999. **9**(18): p. 991-998.
497. Hasebe, N., et al., *Soluble beta-amyloid Precursor Protein Alpha binds to p75 neurotrophin receptor to promote neurite outgrowth*. *PLoS One*, 2013. **8**(12): p. e82321.
498. Lourenco, F., et al., *Netrin-1 interacts with amyloid precursor protein and regulates amyloid- β production*. *Cell Death & Differentiation*, 2009. **16**(5): p. 655-663.
499. Rama, N., et al., *Amyloid precursor protein regulates netrin-1-mediated commissural axon outgrowth*. *J Biol Chem*, 2012. **287**(35): p. 30014-23.
500. Wang, B., et al., *The amyloid precursor protein is a conserved receptor for slit to mediate axon guidance*. *eNeuro*, 2017. **4**(3).
501. Cuello, A.C. and M.A. Bruno, *The failure in NGF maturation and its increased degradation as the probable cause for the vulnerability of cholinergic neurons in Alzheimer's disease*. *Neurochem Res*, 2007. **32**(6): p. 1041-5.

502. Bruno, M.A., et al., *Amyloid beta-induced nerve growth factor dysmetabolism in Alzheimer disease*. J Neuropathol Exp Neurol, 2009. **68**(8): p. 857-69.
503. Cuello, A.C., et al., *Cholinergic involvement in Alzheimer's disease. A link with NGF maturation and degradation*. J Mol Neurosci, 2010. **40**(1-2): p. 230-5.
504. Bryson, J.B., et al., *Amyloid precursor protein (APP) contributes to pathology in the SOD1(G93A) mouse model of amyotrophic lateral sclerosis*. Hum Mol Genet, 2012. **21**(17): p. 3871-82.
505. Kuester, M., et al., *The crystal structure of death receptor 6 (DR6): a potential receptor of the amyloid precursor protein (APP)*. J Mol Biol, 2011. **409**(2): p. 189-201.
506. Ponomarev, S.Y. and J. Audie, *Computational prediction and analysis of the DR6–NAPP interaction*. Proteins: Structure, Function, and Bioinformatics, 2011. **79**(5): p. 1376-1395.
507. Rabizadeh, S. and D.E. Bredesen, *Is p75NGFR involved in developmental neural cell death?* Dev Neurosci, 1994. **16**(3-4): p. 207-11.
508. Yaar, M., et al., *Binding of beta-amyloid to the p75 neurotrophin receptor induces apoptosis. A possible mechanism for Alzheimer's disease*. J Clin Invest, 1997. **100**(9): p. 2333-40.
509. Sothibundhu, A., et al., *Beta-amyloid(1-42) induces neuronal death through the p75 neurotrophin receptor*. J Neurosci, 2008. **28**(15): p. 3941-6.
510. Knowles, J.K., et al., *The p75 neurotrophin receptor promotes amyloid-beta(1-42)-induced neuritic dystrophy in vitro and in vivo*. J Neurosci, 2009. **29**(34): p. 10627-37.
511. Yu, H., et al., *p75NTR is mainly responsible for A β toxicity but not for its internalization: a primary study*. Neurological Sciences, 2012. **33**(5): p. 1043-1050.
512. Hu, Y., et al., *A DR6/p75(NTR) complex is responsible for beta-amyloid-induced cortical neuron death*. Cell Death Dis, 2013. **4**: p. e579.
513. Xu, Y., et al., *Beta amyloid-induced upregulation of death receptor 6 accelerates the toxic effect of N-terminal fragment of amyloid precursor protein*. Neurobiol Aging, 2015. **36**(1): p. 157-68.
514. Akar, C.A. and W.C. Wallace, *Amyloid precursor protein modulates the interaction of nerve growth factor with p75 receptor and potentiates its activation of trkA phosphorylation*. Brain Res Mol Brain Res, 1998. **56**(1-2): p. 125-32.
515. Tarr, P.E., et al., *Tyrosine phosphorylation of the beta-amyloid precursor protein cytoplasmic tail promotes interaction with Shc*. J Biol Chem, 2002. **277**(19): p. 16798-804.
516. Zambrano, N., et al., *The β -amyloid precursor protein APP is tyrosine-phosphorylated in cells expressing a constitutively active form of the Abl protooncogene*. Journal of Biological Chemistry, 2001. **276**(23): p. 19787-19792.
517. Russo, C., et al., *Signal transduction through tyrosine-phosphorylated C-terminal fragments of amyloid precursor protein via an enhanced interaction with Shc/Grb2 adaptor proteins in reactive astrocytes of Alzheimer's disease brain*. J Biol Chem, 2002. **277**(38): p. 35282-8.
518. Tamayev, R., D. Zhou, and L. D'Adamio, *The interactome of the amyloid β precursor protein family members is shaped by phosphorylation of their intracellular domains*. Molecular neurodegeneration, 2009. **4**(1): p. 1-14.
519. Basso, E.M., C., *NGF and APP Interplay: Focus on YENPTY Motif of Amyloid Precursor Protein and Y682 Residue*. Cell Biology: Research and Therapy, 2013. **2**(2): p. 11.

520. Zhang, Y.W., et al., *APP regulates NGF receptor trafficking and NGF-mediated neuronal differentiation and survival*. PLoS One, 2013. **8**(11): p. e80571.
521. Canu, N., et al., *Association of TrkA and APP is promoted by NGF and reduced by cell death-promoting agents*. Frontiers in Molecular Neuroscience, 2017. **10**: p. 15.
522. Scheuermann, S., et al., *Homodimerization of amyloid precursor protein and its implication in the amyloidogenic pathway of Alzheimer's disease*. Journal of Biological Chemistry, 2001. **276**(36): p. 33923-33929.
523. Shaked, G., et al., *A β induces cell death by direct interaction with its cognate extracellular domain on APP (APP 597–624)*. The FASEB journal: official publication of the Federation of American Societies for Experimental Biology, 2006. **20**(8): p. 1254.
524. Munter, L.M., et al., *GxxxG motifs within the amyloid precursor protein transmembrane sequence are critical for the etiology of A β 42*. The EMBO journal, 2007. **26**(6): p. 1702-1712.
525. So, P.P., et al., *Lowering of amyloid beta peptide production with a small molecule inhibitor of amyloid- β precursor protein dimerization*. American journal of neurodegenerative disease, 2012. **1**(1): p. 75.
526. Barbagallo, A.P., et al., *Tyr(682) in the intracellular domain of APP regulates amyloidogenic APP processing in vivo*. PLoS One, 2010. **5**(11): p. e15503.
527. Matrone, C., *A new molecular explanation for age-related neurodegeneration: the Tyr682 residue of amyloid precursor protein*. Bioessays, 2013. **35**(10): p. 847-52.
528. La Rosa, L.R., et al., *Y682G Mutation of Amyloid Precursor Protein Promotes Endo-Lysosomal Dysfunction by Disrupting APP-SorLA Interaction*. Front Cell Neurosci, 2015. **9**: p. 109.
529. Matrone, C., et al., *Tyr682 in the Abeta-precursor protein intracellular domain regulates synaptic connectivity, cholinergic function, and cognitive performance*. Aging Cell, 2012. **11**(6): p. 1084-93.
530. Slomnicki, L.P. and W. Lesniak, *A putative role of the Amyloid Precursor Protein Intracellular Domain (AICD) in transcription*. Acta Neurobiol Exp (Wars), 2008. **68**(2): p. 219-28.
531. Schettini, G., et al., *Phosphorylation of APP-CTF-AICD domains and interaction with adaptor proteins: signal transduction and/or transcriptional role—relevance for Alzheimer pathology*. Journal of neurochemistry, 2010. **115**(6): p. 1299-1308.
532. Chang, K.A., et al., *Phosphorylation of amyloid precursor protein (APP) at Thr668 regulates the nuclear translocation of the APP intracellular domain and induces neurodegeneration*. Mol Cell Biol, 2006. **26**(11): p. 4327-38.
533. Iijima, K., et al., *Neuron-specific phosphorylation of Alzheimer's beta-amyloid precursor protein by cyclin-dependent kinase 5*. J Neurochem, 2000. **75**(3): p. 1085-91.
534. Standen, C.L., et al., *Phosphorylation of thr668 in the cytoplasmic domain of the Alzheimer's disease amyloid precursor protein by stress-activated protein kinase 1b (Jun N-terminal kinase-3)*. Journal of neurochemistry, 2001. **76**(1): p. 316-320.
535. Liu, F., et al., *Regulation of amyloid precursor protein (APP) phosphorylation and processing by p35/Cdk5 and p25/Cdk5*. FEBS letters, 2003. **547**(1-3): p. 193-196.
536. Colombo, A., et al., *JNK regulates APP cleavage and degradation in a model of Alzheimer's disease*. Neurobiol Dis, 2009. **33**(3): p. 518-25.

537. Sclip, A., et al., *c-Jun N-terminal kinase regulates soluble Abeta oligomers and cognitive impairment in AD mouse model*. J Biol Chem, 2011. **286**(51): p. 43871-80.
538. Wang, X., et al., *FoxO mediates APP-induced AICD-dependent cell death*. Cell Death Dis, 2014. **5**: p. e1233.
539. Logue, S.E., et al., *New directions in ER stress-induced cell death*. Apoptosis, 2013. **18**(5): p. 537-46.
540. Nicotera, P. and S. Orrenius, *The role of calcium in apoptosis*. Cell calcium, 1998. **23**(2-3): p. 173-180.
541. Copanaki, E., et al., *The amyloid precursor protein potentiates CHOP induction and cell death in response to ER Ca²⁺ depletion*. Biochimica et Biophysica Acta (BBA)-Molecular Cell Research, 2007. **1773**(2): p. 157-165.
542. Takahashi, K., et al., *Amyloid precursor protein promotes endoplasmic reticulum stress-induced cell death via C/EBP homologous protein-mediated pathway*. J Neurochem, 2009. **109**(5): p. 1324-37.
543. O'Connor, T., et al., *Phosphorylation of the translation initiation factor eIF2 α increases BACE1 levels and promotes amyloidogenesis*. Neuron, 2008. **60**(6): p. 988-1009.
544. Ferreira, E., C.R. Oliveira, and C.M. Pereira, *The release of calcium from the endoplasmic reticulum induced by amyloid-beta and prion peptides activates the mitochondrial apoptotic pathway*. Neurobiol Dis, 2008. **30**(3): p. 331-42.
545. Moccia, F., et al., *Stim and Orai proteins in neuronal Ca²⁺ signaling and excitability*. Frontiers in cellular neuroscience, 2015. **9**: p. 153.
546. Hogan, P.G. and A. Rao, *Store-operated calcium entry: Mechanisms and modulation*. Biochemical and biophysical research communications, 2015. **460**(1): p. 40-49.
547. Putney Jr, J.W., *Capacitative calcium entry in the nervous system*. Cell calcium, 2003. **34**(4-5): p. 339-344.
548. Emptage, N.J., C.A. Reid, and A. Fine, *Calcium stores in hippocampal synaptic boutons mediate short-term plasticity, store-operated Ca²⁺ entry, and spontaneous transmitter release*. Neuron, 2001. **29**(1): p. 197-208.
549. Baba, A., et al., *Activity-evoked capacitative Ca²⁺ entry: implications in synaptic plasticity*. Journal of Neuroscience, 2003. **23**(21): p. 7737-7741.
550. Gemes, G., et al., *Store-operated Ca²⁺ entry in sensory neurons: functional role and the effect of painful nerve injury*. Journal of Neuroscience, 2011. **31**(10): p. 3536-3549.
551. Wei, D., et al., *Orai1 and Orai3 mediate store-operated calcium entry contributing to neuronal excitability in dorsal root ganglion neurons*. Frontiers in cellular neuroscience, 2017. **11**: p. 400.
552. Linde, C.I., et al., *Dysregulation of Ca²⁺ signaling in astrocytes from mice lacking amyloid precursor protein*. American Journal of Physiology-Cell Physiology, 2011. **300**(6): p. C1502-C1512.
553. Rojas, G., et al., *Effect of the knockdown of amyloid precursor protein on intracellular calcium increases in a neuronal cell line derived from the cerebral cortex of a trisomy 16 mouse*. Experimental neurology, 2008. **209**(1): p. 234-242.
554. Schuchmann, S., W. Müller, and U. Heinemann, *Altered Ca²⁺ signaling and mitochondrial deficiencies in hippocampal neurons of trisomy 16 mice: a model of Down's syndrome*. Journal of Neuroscience, 1998. **18**(18): p. 7216-7231.

555. Niu, Y., et al., *Effect of amyloid β on capacitive calcium entry in neural 2a cells*. Brain research bulletin, 2009. **78**(4-5): p. 152-157.
556. Hamid, R., et al., *Amyloid precursor protein intracellular domain modulates cellular calcium homeostasis and ATP content*. Journal of neurochemistry, 2007. **102**(4): p. 1264-1275.
557. Gazda, K., J. Kuznicki, and T. Wegierski, *Knockdown of amyloid precursor protein increases calcium levels in the endoplasmic reticulum*. Scientific reports, 2017. **7**(1): p. 1-10.
558. Ma, T., et al., *Mitochondrial modulation of store-operated Ca^{2+} entry in model cells of Alzheimer's disease*. Biochemical and biophysical research communications, 2012. **426**(2): p. 196-202.
559. Wegierski, T., K. Gazda, and J. Kuznicki, *Microscopic analysis of Orai-mediated store-operated calcium entry in cells with experimentally altered levels of amyloid precursor protein*. Biochemical and biophysical research communications, 2016. **478**(3): p. 1087-1092.
560. Oakes, S.A., et al., *Proapoptotic BAX and BAK regulate the type 1 inositol trisphosphate receptor and calcium leak from the endoplasmic reticulum*. Proceedings of the National Academy of Sciences, 2005. **102**(1): p. 105-110.
561. Grimm, S., *The ER-mitochondria interface: the social network of cell death*. Biochim Biophys Acta, 2012. **1823**(2): p. 327-34.
562. Montagna, E., et al., *In vivo Ca^{2+} imaging of astrocytic microdomains reveals a critical role of the amyloid precursor protein for mitochondria*. Glia, 2019. **67**(5): p. 985-998.
563. Agarwal, A., et al., *Transient opening of the mitochondrial permeability transition pore induces microdomain calcium transients in astrocyte processes*. Neuron, 2017. **93**(3): p. 587-605. e7.
564. Grosche, J., et al., *Microdomains for neuron–glia interaction: parallel fiber signaling to Bergmann glial cells*. Nature neuroscience, 1999. **2**(2): p. 139-143.
565. Srinivasan, R., et al., *Ca^{2+} signaling in astrocytes from *Ip3r2*^{-/-} mice in brain slices and during startle responses in vivo*. Nature neuroscience, 2015. **18**(5): p. 708-717.
566. Sheng, B., et al., *Inhibition of γ -secretase activity reduces $A\beta$ production, reduces oxidative stress, increases mitochondrial activity and leads to reduced vulnerability to apoptosis: Implications for the treatment of Alzheimer's disease*. Free Radical Biology and Medicine, 2009. **46**(10): p. 1362-1375.
567. Pan, J.-X., et al., *APP promotes osteoblast survival and bone formation by regulating mitochondrial function and preventing oxidative stress*. Cell death & disease, 2018. **9**(11): p. 1-18.
568. Anandatheerthavarada, H.K., et al., *Mitochondrial targeting and a novel transmembrane arrest of Alzheimer's amyloid precursor protein impairs mitochondrial function in neuronal cells*. Journal of Cell Biology, 2003. **161**(1): p. 41-54.
569. Devi, L., et al., *Accumulation of amyloid precursor protein in the mitochondrial import channels of human Alzheimer's disease brain is associated with mitochondrial dysfunction*. J Neurosci, 2006. **26**(35): p. 9057-68.
570. Wang, Y., et al., *Lost region in amyloid precursor protein (APP) through TALEN-mediated genome editing alters mitochondrial morphology*. Scientific reports, 2016. **6**: p. 22244.

571. Pavlov, P.F., et al., *Mitochondrial γ -secretase participates in the metabolism of mitochondria-associated amyloid precursor protein*. The FASEB Journal, 2011. **25**(1): p. 78-88.
572. Du, H., et al., *Cyclophilin D deficiency attenuates mitochondrial and neuronal perturbation and ameliorates learning and memory in Alzheimer's disease*. Nature medicine, 2008. **14**(10): p. 1097-1105.
573. Lustbader, J.W., et al., *ABAD directly links A β to mitochondrial toxicity in Alzheimer's Disease*. Science, 2004. **304**(5669): p. 448-452.
574. Area-Gomez, E., et al., *Presenilins are enriched in endoplasmic reticulum membranes associated with mitochondria*. Am J Pathol, 2009. **175**(5): p. 1810-6.
575. Schreiner, B., et al., *Amyloid-beta peptides are generated in mitochondria-associated endoplasmic reticulum membranes*. J Alzheimers Dis, 2015. **43**(2): p. 369-74.
576. Calvo-Rodriguez, M., et al., *Increased mitochondrial calcium levels associated with neuronal death in a mouse model of Alzheimer's disease*. Nature Communications, 2020. **11**(1): p. 1-17.
577. Calvo-Rodriguez, M., et al., *Amyloid β oligomers increase ER-mitochondria Ca $^{2+}$ cross talk in young hippocampal neurons and exacerbate aging-induced intracellular Ca $^{2+}$ remodeling*. Frontiers in cellular neuroscience, 2019. **13**: p. 22.
578. Cardoso, S.M., R.H. Swerdlow, and C.R. Oliveira, *Induction of cytochrome c-mediated apoptosis by amyloid β 25-35 requires functional mitochondria*. Brain research, 2002. **931**(2): p. 117-125.
579. Ward, M.W., et al., *The amyloid precursor protein intracellular domain (AICD) disrupts actin dynamics and mitochondrial bioenergetics*. Journal of neurochemistry, 2010. **113**(1): p. 275-284.
580. Barde, Y.-A., D. Edgar, and H. Thoenen, *Purification of a new neurotrophic factor from mammalian brain*. The EMBO journal, 1982. **1**(5): p. 549-553.
581. Lindsay, R.M., H. Thoenen, and Y.-A. Barde, *Placode and neural crest-derived sensory neurons are responsive at early developmental stages to brain-derived neurotrophic factor*. Developmental biology, 1985. **112**(2): p. 319-328.
582. Davies, A.M., H. Thoenen, and Y.-A. Barde, *The response of chick sensory neurons to brain-derived neurotrophic factor*. Journal of Neuroscience, 1986. **6**(7): p. 1897-1904.
583. Rodriguez-Tébar, A., et al., *The survival of chick retinal ganglion cells in response to brain-derived neurotrophic factor depends on their embryonic age*. Developmental biology, 1989. **136**(2): p. 296-303.
584. Acheson, A., Y.-A. Barde, and H. Thoenen, *High K $^{+}$ -mediated survival of spinal sensory neurons depends on developmental stage*. Experimental cell research, 1987. **170**(1): p. 56-63.
585. Hamburger, V., J. Brunso-Bechtold, and J. Yip, *Neuronal death in the spinal ganglia of the chick embryo and its reduction by nerve growth factor*. Journal of Neuroscience, 1981. **1**(1): p. 60-71.
586. Hofer, M. and Y.-A. Barde, *Brain-derived neurotrophic factor prevents neuronal death in vivo*. Nature, 1988. **331**(6153): p. 261-262.
587. Kalchauer, C., et al., *In vivo effect of brain-derived neurotrophic factor on the survival of developing dorsal root ganglion cells*. Embo j, 1987. **6**(10): p. 2871-3.

588. Liebl, D.J., et al., *Loss of brain-derived neurotrophic factor-dependent neural crest-derived sensory neurons in neurotrophin-4 mutant mice*. Proceedings of the National Academy of Sciences, 2000. **97**(5): p. 2297-2302.
589. Klein, R., et al., *Targeted disruption of the *trkB* neurotrophin receptor gene results in nervous system lesions and neonatal death*. Cell, 1993. **75**(1): p. 113-122.
590. Albers, K.M., et al., *Cutaneous overexpression of NT-3 increases sensory and sympathetic neuron number and enhances touch dome and hair follicle innervation*. The Journal of Cell Biology, 1996. **134**(2): p. 487-497.
591. Lopresti, P. and S.A. Scottt, *Target specificity and size of avian sensory neurons supported in vitro by nerve growth factor, brain-derived neurotrophic factor, and neurotrophin-3*. Journal of neurobiology, 1994. **25**(12): p. 1613-1624.
592. Krimm, R.F., et al., *Overexpression of neurotrophin 4 in skin enhances myelinated sensory endings but does not influence sensory neuron number*. Journal of Comparative Neurology, 2006. **498**(4): p. 455-465.
593. Liu, X., et al., *Sensory but not motor neuron deficits in mice lacking NT4 and BDNF*. Nature, 1995. **375**(6528): p. 238-241.
594. Fan, G., et al., *Knocking the NT4 gene into the BDNF locus rescues BDNF deficient mice and reveals distinct NT4 and BDNF activities*. Nature neuroscience, 2000. **3**(4): p. 350-357.
595. Acheson, A., et al., *A BDNF autocrine loop in adult sensory neurons prevents cell death*. Nature, 1995. **374**(6521): p. 450-453.
596. Huber, K., et al., *TrkB expression and early sensory neuron survival are independent of endogenous BDNF*. J Neurosci Res, 2000. **59**(3): p. 372-8.
597. Baudet, C., et al., *Positive and negative interactions of GDNF, NTN and ART in developing sensory neuron subpopulations, and their collaboration with neurotrophins*. Development, 2000. **127**(20): p. 4335-4344.
598. Silos-Santiago, I., et al., *Severe sensory deficits but normal CNS development in newborn mice lacking TrkB and TrkC tyrosine protein kinase receptors*. European Journal of Neuroscience, 1997. **9**(10): p. 2045-2056.
599. Valdés-Sánchez, T., et al., *BDNF is essentially required for the early postnatal survival of nociceptors*. Dev Biol, 2010. **339**(2): p. 465-76.
600. Ernfors, P., J.P. Merlio, and H. Persson, *Cells expressing mRNA for neurotrophins and their receptors during embryonic rat development*. European Journal of Neuroscience, 1992. **4**(11): p. 1140-1158.
601. Schecterson, L.C. and M. Bothwell, *Novel roles for neurotrophins are suggested by BDNF and NT-3 mRNA expression in developing neurons*. Neuron, 1992. **9**(3): p. 449-463.
602. Krimm, R.F., B.M. Davis, and K.M. Albers, *Cutaneous overexpression of neurotrophin-3 (NT3) selectively restores sensory innervation in NT3 gene knockout mice*. Journal of neurobiology, 2000. **43**(1): p. 40-49.
603. Krimm, R.F., et al., *NT3 expressed in skin causes enhancement of SA1 sensory neurons that leads to postnatal enhancement of Merkel cells*. Journal of Comparative Neurology, 2004. **471**(3): p. 352-360.
604. Iwakura, Y., et al., *Dopamine D1 receptor-induced signaling through TrkB receptors in striatal neurons*. Journal of Biological Chemistry, 2008. **283**(23): p. 15799-15806.

605. Puehringer, D., et al., *EGF transactivation of Trk receptors regulates the migration of newborn cortical neurons*. *Nature neuroscience*, 2013. **16**(4): p. 407-415.
606. Sasi, M., et al., *Neurobiology of local and intercellular BDNF signaling*. *Pflügers Archiv-European Journal of Physiology*, 2017. **469**(5-6): p. 593-610.
607. Rajagopal, R., et al., *Transactivation of Trk neurotrophin receptors by G-protein-coupled receptor ligands occurs on intracellular membranes*. *Journal of Neuroscience*, 2004. **24**(30): p. 6650-6658.
608. Wiese, S., et al., *Adenosine receptor A2A-R contributes to motoneuron survival by transactivating the tyrosine kinase receptor TrkB*. *Proceedings of the National Academy of Sciences*, 2007. **104**(43): p. 17210-17215.
609. Pradhan, J., P.G. Noakes, and M.C. Bellingham, *The role of altered BDNF/TrkB signalling in amyotrophic lateral sclerosis*. *Frontiers in cellular neuroscience*, 2019. **13**: p. 368.
610. Liu, Y., et al., *Sexually dimorphic BDNF signaling directs sensory innervation of the mammary gland*. *Science*, 2012. **338**(6112): p. 1357-60.
611. Atkin-Smith, G.K., et al., *Plexin B2 is a regulator of monocyte apoptotic cell disassembly*. *Cell Reports*, 2019. **29**(7): p. 1821-1831. e3.
612. Yu, L.-y., M. Saarma, and U. Arumäe, *Death receptors and caspases but not mitochondria are activated in the GDNF-or BDNF-deprived dopaminergic neurons*. *Journal of Neuroscience*, 2008. **28**(30): p. 7467-7475.
613. Hellard, D., et al., *Cranial sensory neuron development in the absence of brain-derived neurotrophic factor in BDNF/Bax double null mice*. *Dev Biol*, 2004. **275**(1): p. 34-43.
614. Smith, E.D., et al., *Rapamycin and interleukin-1 β impair brain-derived neurotrophic factor-dependent neuron survival by modulating autophagy*. *Journal of Biological Chemistry*, 2014. **289**(30): p. 20615-20629.
615. Nikolettou, V., et al., *Modulation of autophagy by BDNF underlies synaptic plasticity*. *Cell metabolism*, 2017. **26**(1): p. 230-242. e5.
616. O'Leary, D.D. and S.E. Koester, *Development of projection neuron types, axon pathways, and patterned connections of the mammalian cortex*. *Neuron*, 1993. **10**(6): p. 991-1006.
617. Low, L.K., et al., *Plexin signaling selectively regulates the stereotyped pruning of corticospinal axons from visual cortex*. *Proc Natl Acad Sci U S A*, 2008. **105**(23): p. 8136-41.
618. Hashimoto, K. and M. Kano, *Synapse elimination in the developing cerebellum*. *Cellular and molecular life sciences*, 2013. **70**(24): p. 4667-4680.
619. Bagri, A., et al., *Stereotyped pruning of long hippocampal axon branches triggered by retraction inducers of the semaphorin family*. *Cell*, 2003. **113**(3): p. 285-99.
620. Gonçalves, J.T., et al., *In vivo imaging of dendritic pruning in dentate granule cells*. *Nature neuroscience*, 2016. **19**(6): p. 788-791.
621. Bishop, D.L., et al., *Axon branch removal at developing synapses by axosome shedding*. *Neuron*, 2004. **44**(4): p. 651-661.
622. Riccomagno, M.M. and A.L. Kolodkin, *Sculpting neural circuits by axon and dendrite pruning*. *Annu Rev Cell Dev Biol*, 2015. **31**: p. 779-805.
623. Thomas, M.S., et al., *The over-pruning hypothesis of autism*. *Developmental Science*, 2016. **19**(2): p. 284-305.

624. Amaral, D.G. and J.A. Dent, *Development of the mossy fibers of the dentate gyrus: I. A light and electron microscopic study of the mossy fibers and their expansions*. Journal of Comparative Neurology, 1981. **195**(1): p. 51-86.
625. Liu, X.B., et al., *Stereotyped axon pruning via plexin signaling is associated with synaptic complex elimination in the hippocampus*. J Neurosci, 2005. **25**(40): p. 9124-34.
626. Cheng, H.-J., et al., *Plexin-A3 mediates semaphorin signaling and regulates the development of hippocampal axonal projections*. Neuron, 2001. **32**(2): p. 249-263.
627. Sahay, A., et al., *Semaphorin 3F is critical for development of limbic system circuitry and is required in neurons for selective CNS axon guidance events*. Journal of Neuroscience, 2003. **23**(17): p. 6671-6680.
628. Low, L.K. and H.J. Cheng, *Axon pruning: an essential step underlying the developmental plasticity of neuronal connections*. Philos Trans R Soc Lond B Biol Sci, 2006. **361**(1473): p. 1531-44.
629. Williams, D.W. and J.W. Truman, *Cellular mechanisms of dendrite pruning in Drosophila: insights from in vivo time-lapse of remodeling dendritic arborizing sensory neurons*. Development, 2005. **132**(16): p. 3631-3642.
630. Yu, F. and O. Schuldiner, *Axon and dendrite pruning in Drosophila*. Current opinion in neurobiology, 2014. **27**: p. 192-198.
631. Schuldiner, O. and A. Yaron, *Mechanisms of developmental neurite pruning*. Cell Mol Life Sci, 2015. **72**(1): p. 101-19.
632. Kanamori, T., et al., *Local endocytosis triggers dendritic thinning and pruning in Drosophila sensory neurons*. Nature communications, 2015. **6**(1): p. 1-14.
633. Lee, H.-H., L.Y. Jan, and Y.-N. Jan, *Drosophila IKK-related kinase Ik2 and Katanin p60-like 1 regulate dendrite pruning of sensory neuron during metamorphosis*. Proceedings of the National Academy of Sciences, 2009. **106**(15): p. 6363-6368.
634. Han, C., L.Y. Jan, and Y.-N. Jan, *Enhancer-driven membrane markers for analysis of nonautonomous mechanisms reveal neuron–glia interactions in Drosophila*. Proceedings of the National Academy of Sciences, 2011. **108**(23): p. 9673-9678.
635. Kuo, C.T., L.Y. Jan, and Y.N. Jan, *Dendrite-specific remodeling of Drosophila sensory neurons requires matrix metalloproteases, ubiquitin-proteasome, and ecdysone signaling*. Proceedings of the National Academy of Sciences, 2005. **102**(42): p. 15230-15235.
636. Kuo, C.T., et al., *Identification of E2/E3 ubiquitinating enzymes and caspase activity regulating Drosophila sensory neuron dendrite pruning*. Neuron, 2006. **51**(3): p. 283-90.
637. Williams, D.W., et al., *Local caspase activity directs engulfment of dendrites during pruning*. Nat Neurosci, 2006. **9**(10): p. 1234-6.
638. Conforti, L., J. Gilley, and M.P. Coleman, *Wallerian degeneration: an emerging axon death pathway linking injury and disease*. Nature Reviews Neuroscience, 2014. **15**(6): p. 394-409.
639. Coleman, M.P. and A. Höke, *Programmed axon degeneration: from mouse to mechanism to medicine*. Nature Reviews Neuroscience, 2020: p. 1-14.
640. Hoopfer, E.D., et al., *Wlds protection distinguishes axon degeneration following injury from naturally occurring developmental pruning*. Neuron, 2006. **50**(6): p. 883-95.
641. MacDonald, J.M., et al., *The Drosophila cell corpse engulfment receptor Draper mediates glial clearance of severed axons*. Neuron, 2006. **50**(6): p. 869-881.

642. Tao, J. and M.M. Rolls, *Dendrites have a rapid program of injury-induced degeneration that is molecularly distinct from developmental pruning*. Journal of Neuroscience, 2011. **31**(14): p. 5398-5405.
643. Low, L.K. and H.J. Cheng, *A little nip and tuck: axon refinement during development and axonal injury*. Curr Opin Neurobiol, 2005. **15**(5): p. 549-56.
644. Luo, L. and D.D. O'Leary, *Axon retraction and degeneration in development and disease*. Annu Rev Neurosci, 2005. **28**: p. 127-56.
645. Saxena, S. and P. Caroni, *Mechanisms of axon degeneration: from development to disease*. Prog Neurobiol, 2007. **83**(3): p. 174-91.
646. Stanfield, B.B., D.D. O'Leary, and C. Fricks, *Selective collateral elimination in early postnatal development restricts cortical distribution of rat pyramidal tract neurones*. Nature, 1982. **298**(5872): p. 371-373.
647. O'Leary, D., et al. *Target selection by cortical axons: alternative mechanisms to establish axonal connections in the developing brain*. in *Cold Spring Harbor symposia on quantitative biology*. 1990. Cold Spring Harbor Laboratory Press.
648. Nakamura, H. and D.D. O'Leary, *Inaccuracies in initial growth and arborization of chick retinotectal axons followed by course corrections and axon remodeling to develop topographic order*. J Neurosci, 1989. **9**(11): p. 3776-95.
649. McLaughlin, T., et al., *Retinotopic map refinement requires spontaneous retinal waves during a brief critical period of development*. Neuron, 2003. **40**(6): p. 1147-1160.
650. Watts, R.J., E.D. Hoopfer, and L. Luo, *Axon pruning during Drosophila metamorphosis: evidence for local degeneration and requirement of the ubiquitin-proteasome system*. Neuron, 2003. **38**(6): p. 871-85.
651. Schubiger, M., et al., *Drosophila EcR-B ecdysone receptor isoforms are required for larval molting and for neuron remodeling during metamorphosis*. Development, 1998. **125**(11): p. 2053-2062.
652. Technau, G. and M. Heisenberg, *Neural reorganization during metamorphosis of the corpora pedunculata in Drosophila melanogaster*. Nature, 1982. **295**(5848): p. 405-407.
653. Lee, T., et al., *Cell-autonomous requirement of the USP/EcR-B ecdysone receptor for mushroom body neuronal remodeling in Drosophila*. Neuron, 2000. **28**(3): p. 807-818.
654. Watts, R.J., et al., *Glia engulf degenerating axons during developmental axon pruning*. Current Biology, 2004. **14**(8): p. 678-684.
655. Yaron, A. and O. Schuldiner, *Common and divergent mechanisms in developmental neuronal remodeling and dying back neurodegeneration*. Current Biology, 2016. **26**(13): p. R628-R639.
656. Kuranaga, E. and M. Miura, *Nonapoptotic functions of caspases: caspases as regulatory molecules for immunity and cell-fate determination*. Trends in cell biology, 2007. **17**(3): p. 135-144.
657. Awasaki, T., et al., *Essential role of the apoptotic cell engulfment genes draper and ced-6 in programmed axon pruning during Drosophila metamorphosis*. Neuron, 2006. **50**(6): p. 855-867.
658. Zhai, Q., et al., *Involvement of the ubiquitin-proteasome system in the early stages of wallerian degeneration*. Neuron, 2003. **39**(2): p. 217-25.

659. Kanamori, T., et al., *Compartmentalized calcium transients trigger dendrite pruning in Drosophila sensory neurons*. *Science*, 2013. **340**(6139): p. 1475-1478.
660. Geden, M.J., S.E. Romero, and M. Deshmukh, *Apoptosis versus axon pruning: Molecular intersection of two distinct pathways for axon degeneration*. *Neurosci Res*, 2019. **139**: p. 3-8.
661. Campenot, R.B., *Development of sympathetic neurons in compartmentalized cultures. II. Local control of neurite survival by nerve growth factor*. *Dev Biol*, 1982. **93**(1): p. 13-21.
662. Campenot, R.B., K. Lund, and S.-A. Mok, *Production of compartmented cultures of rat sympathetic neurons*. *Nature protocols*, 2009. **4**(12): p. 1869-1887.
663. Mok, S.A., K. Lund, and R.B. Campenot, *A retrograde apoptotic signal originating in NGF-deprived distal axons of rat sympathetic neurons in compartmented cultures*. *Cell Res*, 2009. **19**(5): p. 546-60.
664. Taylor, A.M., et al., *A microfluidic culture platform for CNS axonal injury, regeneration and transport*. *Nature methods*, 2005. **2**(8): p. 599-605.
665. Whitesides, G.M., *The origins and the future of microfluidics*. *Nature*, 2006. **442**(7101): p. 368-373.
666. Taylor, A. and N.L. Jeon, *Microfluidic and compartmentalized platforms for neurobiological research*. *Critical Reviews™ in Biomedical Engineering*, 2011. **39**(3).
667. Yong, Y., C. Hughes, and C. Deppmann, *A Microfluidic Culture Platform to Assess Axon Degeneration*, in *Axon Degeneration*. 2020, Springer. p. 83-96.
668. Osaki, T., et al., *In vitro microfluidic models for neurodegenerative disorders*. *Advanced healthcare materials*, 2018. **7**(2): p. 1700489.
669. Delcroix, J.D., et al., *NGF signaling in sensory neurons: evidence that early endosomes carry NGF retrograde signals*. *Neuron*, 2003. **39**(1): p. 69-84.
670. Matusica, D. and E.J. Coulson. *Local versus long-range neurotrophin receptor signalling: endosomes are not just carriers for axonal transport*. in *Seminars in cell & developmental biology*. 2014. Elsevier.
671. Cox, L.J., et al., *Intra-axonal translation and retrograde trafficking of CREB promotes neuronal survival*. *Nature cell biology*, 2008. **10**(2): p. 149-159.
672. Willis, D., et al., *Differential transport and local translation of cytoskeletal, injury-response, and neurodegeneration protein mRNAs in axons*. *Journal of Neuroscience*, 2005. **25**(4): p. 778-791.
673. Willis, D.E., et al., *Axonal localization of transgene mRNA in mature PNS and CNS neurons*. *Journal of Neuroscience*, 2011. **31**(41): p. 14481-14487.
674. Cosker, K.E., S.L. Courchesne, and R.A. Segal, *Action in the axon: generation and transport of signaling endosomes*. *Current opinion in neurobiology*, 2008. **18**(3): p. 270-275.
675. Galehdar, Z., et al., *Neuronal apoptosis induced by endoplasmic reticulum stress is regulated by ATF4-CHOP-mediated induction of the Bcl-2 homology 3-only member PUMA*. *Journal of Neuroscience*, 2010. **30**(50): p. 16938-16948.
676. Yu, J. and L. Zhang, *PUMA, a potent killer with or without p53*. *Oncogene*, 2008. **27**(1): p. S71-S83.
677. Kole, A., R. Annis, and M. Deshmukh, *Mature neurons: equipped for survival*. *Cell death & disease*, 2013. **4**(6): p. e689-e689.

678. Kuranaga, E., et al., *Drosophila IKK-related kinase regulates nonapoptotic function of caspases via degradation of IAPs*. Cell, 2006. **126**(3): p. 583-596.
679. Hammond, S.M., *An overview of microRNAs*. Advanced drug delivery reviews, 2015. **87**: p. 3-14.
680. Kole, A.J., et al., *miR-29b is activated during neuronal maturation and targets BH3-only genes to restrict apoptosis*. Genes Dev, 2011. **25**(2): p. 125-30.
681. Calin, G.A., et al., *Frequent deletions and down-regulation of micro-RNA genes miR15 and miR16 at 13q14 in chronic lymphocytic leukemia*. Proceedings of the national academy of sciences, 2002. **99**(24): p. 15524-15529.
682. Cimmino, A., et al., *miR-15 and miR-16 induce apoptosis by targeting BCL2*. Proceedings of the National Academy of Sciences, 2005. **102**(39): p. 13944-13949.
683. Wang, J.-X., et al., *Oxidative modification of miR-184 enables it to target Bcl-xL and Bcl-w*. Molecular cell, 2015. **59**(1): p. 50-61.
684. Kaplan, B.B., et al., *Axonal protein synthesis and the regulation of local mitochondrial function*, in *Cell biology of the axon*. 2009, Springer. p. 1-25.
685. Gummy, L.F., et al., *Transcriptome analysis of embryonic and adult sensory axons reveals changes in mRNA repertoire localization*. Rna, 2011. **17**(1): p. 85-98.
686. Hancock, M.L., et al., *MicroRNA-132 is enriched in developing axons, locally regulates Rasa1 mRNA, and promotes axon extension*. Journal of Neuroscience, 2014. **34**(1): p. 66-78.
687. Kim, S. and K.C. Martin, *Neuron-wide RNA transport combines with netrin-mediated local translation to spatially regulate the synaptic proteome*. Elife, 2015. **4**: p. e04158.
688. Cusack, C.L., *The molecular intersection between axon-specific pruning and neuronal apoptosis*. 2014, University of North Carolina at Chapel Hill.
689. Andreassi, C., et al., *An NGF-responsive element targets myo-inositol monophosphatase-1 mRNA to sympathetic neuron axons*. Nature neuroscience, 2010. **13**(3): p. 291.
690. Price, T., et al., *The RNA binding and transport proteins stau1 and fragile X mental retardation protein are expressed by rat primary afferent neurons and localize to peripheral and central axons*. Neuroscience, 2006. **141**(4): p. 2107-2116.
691. Price, T.J., et al., *Decreased nociceptive sensitization in mice lacking the fragile X mental retardation protein: role of mGluR1/5 and mTOR*. Journal of Neuroscience, 2007. **27**(51): p. 13958-13967.
692. Wang, B., et al., *FMRP-mediated axonal delivery of miR-181d regulates axon elongation by locally targeting Map1b and Calm1*. Cell reports, 2015. **13**(12): p. 2794-2807.
693. Tessier, C.R. and K. Broadie, *Drosophila fragile X mental retardation protein developmentally regulates activity-dependent axon pruning*. Development, 2008. **135**(8): p. 1547-1557.
694. Lee, E.K., et al., *hnRNP C promotes APP translation by competing with FMRP for APP mRNA recruitment to P bodies*. Nature structural & molecular biology, 2010. **17**(6): p. 732.
695. Gatto, C.L. and K. Broadie, *Fragile X mental retardation protein is required for programmed cell death and clearance of developmentally-transient peptidergic neurons*. Developmental biology, 2011. **356**(2): p. 291-307.

696. Cheng, Y., J.G. Corbin, and R.J. Levy, *Programmed cell death is impaired in the developing brain of FMR1 mutants*. *Developmental neuroscience*, 2013. **35**(4): p. 347-358.
697. Steinberg, J. and C. Webber, *The roles of FMRP-regulated genes in autism spectrum disorder: single-and multiple-hit genetic etiologies*. *The American Journal of Human Genetics*, 2013. **93**(5): p. 825-839.
698. Hu, B.R., et al., *Involvement of caspase-3 in cell death after hypoxia–ischemia declines during brain maturation*. *Journal of Cerebral Blood Flow & Metabolism*, 2000. **20**(9): p. 1294-1300.
699. Yakovlev, A.G., et al., *Differential expression of apoptotic protease-activating factor-1 and caspase-3 genes and susceptibility to apoptosis during brain development and after traumatic brain injury*. *Journal of Neuroscience*, 2001. **21**(19): p. 7439-7446.
700. Wright, K.M., et al., *Decreased apoptosome activity with neuronal differentiation sets the threshold for strict IAP regulation of apoptosis*. *The Journal of cell biology*, 2004. **167**(2): p. 303-313.
701. Zhu, C., et al., *The influence of age on apoptotic and other mechanisms of cell death after cerebral hypoxia–ischemia*. *Cell Death & Differentiation*, 2005. **12**(2): p. 162-176.
702. Annis, R.P., et al., *Mature neurons dynamically restrict apoptosis via redundant premitochondrial brakes*. *The FEBS journal*, 2016. **283**(24): p. 4569-4582.
703. Vogelbaum, M.A., et al., *Transfection of C6 glioma cells with the bax gene and increased sensitivity to treatment with cytosine arabinoside*. *Journal of neurosurgery*, 1998. **88**(1): p. 99-105.
704. Polster, B., et al., *Postnatal brain development and neural cell differentiation modulate mitochondrial Bax and BH3 peptide-induced cytochrome c release*. *Cell Death & Differentiation*, 2003. **10**(3): p. 365-370.
705. Putcha, G.V., M. Deshmukh, and E.M. Johnson, Jr., *Inhibition of apoptotic signaling cascades causes loss of trophic factor dependence during neuronal maturation*. *J Cell Biol*, 2000. **149**(5): p. 1011-8.
706. Walsh, G.S., et al., *The invulnerability of adult neurons: a critical role for p73*. *J Neurosci*, 2004. **24**(43): p. 9638-47.
707. Deckwerth, T.L., et al., *BAX is required for neuronal death after trophic factor deprivation and during development*. *Neuron*, 1996. **17**(3): p. 401-411.
708. Tsui-Pierchala, B.A. and D.D. Ginty, *Characterization of an NGF–P-TrkA retrograde-signaling complex and age-dependent regulation of TrkA phosphorylation in sympathetic neurons*. *Journal of Neuroscience*, 1999. **19**(19): p. 8207-8218.
709. Neukomm, L.J. and M.R. Freeman, *Diverse cellular and molecular modes of axon degeneration*. *Trends Cell Biol*, 2014. **24**(9): p. 515-23.
710. Cashman, C.R. and A. Hoke, *Mechanisms of distal axonal degeneration in peripheral neuropathies*. *Neurosci Lett*, 2015. **596**: p. 33-50.
711. Liu, J., et al., *Enhanced CD4+ T cell proliferation and Th2 cytokine production in DR6-deficient mice*. *Immunity*, 2001. **15**(1): p. 23-34.
712. Acheson, A., et al., *Detection of brain-derived neurotrophic factor-like activity in fibroblasts and Schwann cells: inhibition by antibodies to NGF*. *Neuron*, 1991. **7**(2): p. 265-75.

713. Nakamura, S., et al., *Dynamic regulation of the expression of neurotrophin receptors by Runx3*. *Development*, 2008. **135**(9): p. 1703-1711.
714. Lauria, G., et al., *EFNS guidelines on the use of skin biopsy in the diagnosis of peripheral neuropathy*. *European journal of neurology*, 2005. **12**(10): p. 747-758.
715. Koivisto, A., et al., *Inhibiting TRPA1 ion channel reduces loss of cutaneous nerve fiber function in diabetic animals: sustained activation of the TRPA1 channel contributes to the pathogenesis of peripheral diabetic neuropathy*. *Pharmacological Research*, 2012. **65**(1): p. 149-158.
716. Lalancette-Hebert, M., et al., *Gamma motor neurons survive and exacerbate alpha motor neuron degeneration in ALS*. *Proceedings of the National Academy of Sciences*, 2016. **113**(51): p. E8316-E8325.
717. Renier, N., et al., *iDISCO: a simple, rapid method to immunolabel large tissue samples for volume imaging*. *Cell*, 2014. **159**(4): p. 896-910.
718. Gibon, J., P. Tu, and A. Bouron, *Store-depletion and hyperforin activate distinct types of Ca²⁺-conducting channels in cortical neurons*. *Cell Calcium*, 2010. **47**(6): p. 538-543.
719. Lipp, P. and G. Reither, *Protein kinase C: the "masters" of calcium and lipid*. *Cold Spring Harbor perspectives in biology*, 2011. **3**(7): p. a004556.
720. Marik, S.A., et al., *Physiological role for amyloid precursor protein in adult experience-dependent plasticity*. *Proceedings of the National Academy of Sciences*, 2016. **113**(28): p. 7912-7917.
721. Wang, P., et al., *Defective neuromuscular synapses in mice lacking amyloid precursor protein (APP) and APP-Like protein 2*. *Journal of Neuroscience*, 2005. **25**(5): p. 1219-1225.
722. Vanderhaeghen, P. and H.-J. Cheng, *Guidance molecules in axon pruning and cell death*. *Cold Spring Harbor perspectives in biology*, 2010. **2**(6): p. a001859.
723. Pinton, P. and R. Rizzuto, *Bcl-2 and Ca²⁺ homeostasis in the endoplasmic reticulum*. *Cell Death & Differentiation*, 2006. **13**(8): p. 1409-1418.
724. Walsh, C., et al., *Modulation of calcium signalling by mitochondria*. *Biochimica et Biophysica Acta (BBA)-Bioenergetics*, 2009. **1787**(11): p. 1374-1382.
725. Kerkhofs, M., et al., *Emerging molecular mechanisms in chemotherapy: Ca²⁺ signaling at the mitochondria-associated endoplasmic reticulum membranes*. *Cell death & disease*, 2018. **9**(3): p. 1-15.
726. Buss, R.R., W. Sun, and R.W. Oppenheim, *Adaptive roles of programmed cell death during nervous system development*. *Annu Rev Neurosci*, 2006. **29**: p. 1-35.
727. Burek, M.J. and R.W. Oppenheim, *Programmed cell death in the developing nervous system*. *Brain Pathol*, 1996. **6**(4): p. 427-46.
728. Kirkland, R.A. and J.L. Franklin, *Bax, reactive oxygen, and cytochrome c release in neuronal apoptosis*. *Antioxid Redox Signal*, 2003. **5**(5): p. 589-96.
729. Fischer, L.R. and J.D. Glass, *Axonal degeneration in motor neuron disease*. *Neurodegener Dis*, 2007. **4**(6): p. 431-42.
730. Vickers, J.C., et al., *Axonopathy and cytoskeletal disruption in degenerative diseases of the central nervous system*. *Brain Res Bull*, 2009. **80**(4-5): p. 217-23.
731. Kanaan, N.M., et al., *Axonal degeneration in Alzheimer's disease: when signaling abnormalities meet the axonal transport system*. *Exp Neurol*, 2013. **246**: p. 44-53.

732. Barde, Y.A., *Trophic factors and neuronal survival*. Neuron, 1989. **2**(6): p. 1525-34.
733. DOLKART, P. and E. JOHNSON. *AUTO-IMMUNE APPROACH TO THE STUDY OF THE ROLE OF NERVE GROWTH-FACTOR (NGF) IN THE PERIPHERAL NERVOUS-SYSTEM*. in *FEDERATION PROCEEDINGS*. 1979. FEDERATION AMER SOC EXP BIOL 9650 ROCKVILLE PIKE, BETHESDA, MD 20814-3998 USA.
734. Kirstein, M. and I. Fariñas, *Sensing life: regulation of sensory neuron survival by neurotrophins*. Cell Mol Life Sci, 2002. **59**(11): p. 1787-802.
735. Glebova, N.O. and D.D. Ginty, *Growth and survival signals controlling sympathetic nervous system development*. Annu Rev Neurosci, 2005. **28**: p. 191-222.
736. Unsain, N., et al., *Production and isolation of axons from sensory neurons for biochemical analysis using porous filters*. J Vis Exp, 2014(89).
737. Knudson, C.M., et al., *Bax-deficient mice with lymphoid hyperplasia and male germ cell death*. Science, 1995. **270**(5233): p. 96-9.
738. Kirkland, R.A. and J.L. Franklin, *Bax affects production of reactive oxygen by the mitochondria of non-apoptotic neurons*. Exp Neurol, 2007. **204**(1): p. 458-61.
739. Kirkland, R.A., et al., *Bax regulates production of superoxide in both apoptotic and nonapoptotic neurons: role of caspases*. J Neurosci, 2010. **30**(48): p. 16114-27.
740. Johnson, J.E., et al., *Brain-derived neurotrophic factor supports the survival of cultured rat retinal ganglion cells*. J Neurosci, 1986. **6**(10): p. 3031-8.
741. Borasio, G.D., et al., *ras p21 protein promotes survival and fiber outgrowth of cultured embryonic neurons*. Neuron, 1989. **2**(1): p. 1087-96.
742. Wakatsuki, S. and T. Araki, *Specific phospholipid scramblases are involved in exposure of phosphatidylserine, an "eat-me" signal for phagocytes, on degenerating axons*. Commun Integr Biol, 2017. **10**(2): p. e1296615.
743. Roux, P.P. and P.A. Barker, *Neurotrophin signaling through the p75 neurotrophin receptor*. Prog Neurobiol, 2002. **67**(3): p. 203-33.
744. Wilson, C., E. Muñoz-Palma, and C. González-Billault, *From birth to death: A role for reactive oxygen species in neuronal development*. Semin Cell Dev Biol, 2018. **80**: p. 43-49.
745. Kalkavan, H. and D.R. Green, *MOMP, cell suicide as a BCL-2 family business*. Cell Death Differ, 2018. **25**(1): p. 46-55.
746. Deshmukh, M., K. Kuida, and E.M. Johnson, Jr., *Caspase inhibition extends the commitment to neuronal death beyond cytochrome c release to the point of mitochondrial depolarization*. J Cell Biol, 2000. **150**(1): p. 131-43.
747. Lang-Rollin, I.C., et al., *Mechanisms of caspase-independent neuronal death: energy depletion and free radical generation*. J Neurosci, 2003. **23**(35): p. 11015-25.
748. Jiang, J., et al., *Interplay between bax, reactive oxygen species production, and cardiolipin oxidation during apoptosis*. Biochem Biophys Res Commun, 2008. **368**(1): p. 145-50.
749. Garcia-Perez, C., et al., *Bid-induced mitochondrial membrane permeabilization waves propagated by local reactive oxygen species (ROS) signaling*. Proc Natl Acad Sci U S A, 2012. **109**(12): p. 4497-502.
750. Lamarche, F., et al., *Mitochondrial permeability transition pore inhibitors prevent ethanol-induced neuronal death in mice*. Chem Res Toxicol, 2013. **26**(1): p. 78-88.

751. Lazarus, K.J., et al., *Adaptive survival of rat sympathetic neurons cultured without supporting cells or exogenous nerve growth factor*. Brain Res, 1976. **113**(1): p. 159-64.
752. Easton, R.M., et al., *Analysis of the mechanism of loss of trophic factor dependence associated with neuronal maturation: a phenotype indistinguishable from Bax deletion*. J Neurosci, 1997. **17**(24): p. 9656-66.
753. Maor-Nof, M. and A. Yaron, *Neurite pruning and neuronal cell death: spatial regulation of shared destruction programs*. Curr Opin Neurobiol, 2013. **23**(6): p. 990-6.
754. Tong, J.X., M.E. Eichler, and K.M. Rich, *Intracellular calcium levels influence apoptosis in mature sensory neurons after trophic factor deprivation*. Experimental neurology, 1996. **138**(1): p. 45-52.
755. Lee, M.S., et al., *APP processing is regulated by cytoplasmic phosphorylation*. J Cell Biol, 2003. **163**(1): p. 83-95.
756. Cruz, J.C., et al., *p25/cyclin-dependent kinase 5 induces production and intraneuronal accumulation of amyloid β in vivo*. Journal of Neuroscience, 2006. **26**(41): p. 10536-10541.
757. Cruz, J.C. and L.-H. Tsai, *Cdk5 deregulation in the pathogenesis of Alzheimer's disease*. Trends in molecular medicine, 2004. **10**(9): p. 452-458.
758. Bukhari, H., et al., *Small things matter: Implications of APP intracellular domain AICD nuclear signaling in the progression and pathogenesis of Alzheimer's disease*. Progress in neurobiology, 2017. **156**: p. 189-213.
759. Ferreiro, E., C.R. Oliveira, and C. Pereira, *Involvement of endoplasmic reticulum Ca^{2+} release through ryanodine and inositol 1, 4, 5-triphosphate receptors in the neurotoxic effects induced by the amyloid- β peptide*. Journal of neuroscience research, 2004. **76**(6): p. 872-880.
760. Gentile, M.T., et al., *Mechanisms of soluble β -amyloid impairment of endothelial function*. Journal of Biological Chemistry, 2004. **279**(46): p. 48135-48142.
761. Kim, H.-S., J.-H. Lee, and Y.-H. Suh, *C-terminal fragment of Alzheimer's amyloid precursor protein inhibits sodium/calcium exchanger activity in SK-N-SH cell*. Neuroreport, 1999. **10**(1): p. 113-116.
762. Kawahara, M. and Y. Kuroda, *Molecular mechanism of neurodegeneration induced by Alzheimer's β -amyloid protein: channel formation and disruption of calcium homeostasis*. Brain research bulletin, 2000. **53**(4): p. 389-397.
763. Lin, H., R. Bhatia, and R. Lal, *Amyloid β protein forms ion channels: implications for Alzheimer's disease pathophysiology*. The FASEB Journal, 2001. **15**(13): p. 2433-2444.
764. Bode, D.C., M.D. Baker, and J.H. Viles, *Ion channel formation by amyloid- β 42 oligomers but not amyloid- β 40 in cellular membranes*. Journal of Biological Chemistry, 2017. **292**(4): p. 1404-1413.
765. MacManus, A., et al., *enhancement of Ca^{2+} influx and voltage-dependent Ca^{2+} channel activity by β -amyloid-(1-40) in rat cortical synaptosomes and cultured cortical neurons modulation by the proinflammatory cytokine interleukin- 1β* . Journal of Biological Chemistry, 2000. **275**(7): p. 4713-4718.
766. Liu, C., et al., *Amyloid precursor protein enhances Nav1.6 sodium channel cell surface expression*. Journal of Biological Chemistry, 2015. **290**(19): p. 12048-12057.

767. Yang, L., et al., *Amyloid precursor protein regulates Cav1. 2 L-type calcium channel levels and function to influence GABAergic short-term plasticity*. Journal of Neuroscience, 2009. **29**(50): p. 15660-15668.
768. Santos, S.F., et al., *Inhibition of neuronal calcium oscillations by cell surface APP phosphorylated on T668*. Neurobiology of aging, 2011. **32**(12): p. 2308-2313.
769. Beckett, C., et al., *Nuclear signalling by membrane protein intracellular domains: the AICD enigma*. Cellular signalling, 2012. **24**(2): p. 402-409.
770. Pousinha, P.A., et al., *The amyloid precursor protein C-terminal domain alters CA1 neuron firing, modifying hippocampus oscillations and impairing spatial memory encoding*. Cell reports, 2019. **29**(2): p. 317-331. e5.
771. Pousinha, P.A., et al., *Physiological and pathophysiological control of synaptic GluN2B-NMDA receptors by the C-terminal domain of amyloid precursor protein*. Elife, 2017. **6**: p. e25659.
772. Dedov, V. and B. Roufogalis, *Mitochondrial Ca21 accumulation in DRG neurons following activation of capsaicin receptors in DRG neurons*. Neuroscience, 2000. **95**: p. 183-188.
773. Jackson, J.G. and S.A. Thayer, *Mitochondrial modulation of Ca2+-induced Ca2+-release in rat sensory neurons*. Journal of neurophysiology, 2006. **96**(3): p. 1093-1104.
774. Chalmers, S. and J.G. McCarron, *Inhibition of mitochondrial calcium uptake rather than efflux impedes calcium release by inositol-1, 4, 5-trisphosphate-sensitive receptors*. Cell calcium, 2009. **46**(2): p. 107-113.
775. Ben-Kasus Nissim, T., et al., *Mitochondria control store-operated Ca2+ entry through Na+ and redox signals*. The EMBO journal, 2017. **36**(6): p. 797-815.
776. Favaro, G., et al., *DRP1-mediated mitochondrial shape controls calcium homeostasis and muscle mass*. Nature communications, 2019. **10**(1): p. 1-17.
777. Goiran, T., et al., *b-Amyloid Precursor Protein Intracellular Domain Controls Mitochondrial Function by Modulating Phosphatase and Tensin Homolog–Induced Kinase Mice Models*. 2017.
778. Yu, W., et al., *The PINK1/Parkin pathway regulates mitochondrial dynamics and function in mammalian hippocampal and dopaminergic neurons*. Human molecular genetics, 2011. **20**(16): p. 3227-3240.
779. Matsuda, N., et al., *PINK1 stabilized by mitochondrial depolarization recruits Parkin to damaged mitochondria and activates latent Parkin for mitophagy*. Journal of Cell Biology, 2010. **189**(2): p. 211-221.
780. Bezprozvanny, I. and M.P. Mattson, *Neuronal calcium mishandling and the pathogenesis of Alzheimer's disease*. Trends in neurosciences, 2008. **31**(9): p. 454-463.
781. Green, K.N. and F.M. LaFerla, *Linking calcium to A β and Alzheimer's disease*. Neuron, 2008. **59**(2): p. 190-194.
782. Kuchibhotla, K.V., et al., *A β plaques lead to aberrant regulation of calcium homeostasis in vivo resulting in structural and functional disruption of neuronal networks*. Neuron, 2008. **59**(2): p. 214-225.
783. Tong, B.C.-K., et al., *Calcium signaling in Alzheimer's disease & therapies*. Biochimica et Biophysica Acta (BBA)-Molecular Cell Research, 2018. **1865**(11): p. 1745-1760.

784. Popugaeva, E., E. Pchitskaya, and I. Bezprozvanny, *Dysregulation of Intracellular Calcium Signaling in Alzheimer's Disease*. *Antioxidants & redox signaling*, 2018. **29**(12): p. 1176-1188.
785. Cuello, A.C., R. Pentz, and H. Hall, *The brain NGF metabolic pathway in health and in Alzheimer's pathology*. *Frontiers in neuroscience*, 2019. **13**: p. 62.
786. Gupta, V.K., et al., *TrkB receptor signalling: implications in neurodegenerative, psychiatric and proliferative disorders*. *International journal of molecular sciences*, 2013. **14**(5): p. 10122-10142.
787. Moubarak, R.S., et al., *Sequential activation of poly (ADP-ribose) polymerase 1, calpains, and Bax is essential in apoptosis-inducing factor-mediated programmed necrosis*. *Molecular and cellular biology*, 2007. **27**(13): p. 4844-4862.
788. Cabon, L., et al., *BID regulates AIF-mediated caspase-independent necroptosis by promoting BAX activation*. *Cell Death & Differentiation*, 2012. **19**(2): p. 245-256.
789. Phillips, C., *Brain-derived neurotrophic factor, depression, and physical activity: making the neuroplastic connection*. *Neural plasticity*, 2017. **2017**.
790. Giacobbo, B.L., et al., *Brain-derived neurotrophic factor in brain disorders: focus on neuroinflammation*. *Molecular neurobiology*, 2019. **56**(5): p. 3295-3312.
791. Allen, S.J., et al., *GDNF, NGF and BDNF as therapeutic options for neurodegeneration*. *Pharmacology & therapeutics*, 2013. **138**(2): p. 155-175.
792. Buchman, A.S., et al., *Higher brain BDNF gene expression is associated with slower cognitive decline in older adults*. *Neurology*, 2016. **86**(8): p. 735-741.
793. Jiao, S., et al., *Brain-derived neurotrophic factor protects against tau-related neurodegeneration of Alzheimer's disease*. *Translational psychiatry*, 2016. **6**(10): p. e907-e907.
794. Donato, A., et al., *Neuronal sub-compartmentalization: a strategy to optimize neuronal function*. *Biological Reviews*, 2019. **94**(3): p. 1023-1037.
795. Glebova, N.O. and D.D. Ginty, *Heterogeneous requirement of NGF for sympathetic target innervation in vivo*. *Journal of Neuroscience*, 2004. **24**(3): p. 743-751.
796. Davies, A.M., *Neurotrophins giveth and they taketh away*. *Nature neuroscience*, 2008. **11**(6): p. 627-628.
797. Maor-Nof, M., et al., *Axonal pruning is actively regulated by the microtubule-destabilizing protein kinesin superfamily protein 2A*. *Cell Rep*, 2013. **3**(4): p. 971-7.